High-Oxidation-State Molybdenum and Tungsten Monoalkoxide Pyrrolide Alkylidenes as Catalysts for Olefin Metathesis
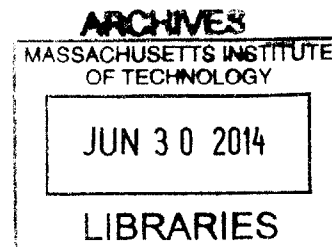
by

Erik Matthew Townsend

B.S. (*summa cum laude*) in Chemistry (2009)
Rensselaer Polytechnic Institute, Troy, NY

Submitted to the Department of Chemistry
in Partial Fulfillment of the Requirements for the Degree of

Doctor of Philosophy

at the
Massachusetts Institute of Technology
June 2014

Signature of Author _ Signature redacted

Department of Chemistry
May 5, 2014

Certified by Signature redacted

Richard R. Schrock
Frederick G. Keyes Professor of Chemistry
Thesis Supervisor

Accepted by Signature redacted

Robert W. Field
Haslam and Dewey Professor of Chemistry
Chairman, Departmental Committee on Graduate Students

1

This doctoral thesis has been examined by a Committee of the Department of Chemistry as follows:

Signature redacted

Professor Mircea Dincă

Chairman

Signature redacted

Professor Richard R. Schrock

Thesis Supervisor

Signature redacted

Professor Christopher C. Cummins

3

High-Oxidation-State Molybdenum and Tungsten Monoalkoxide Pyrrolide Alkylidenes as Catalysts for Olefin Metathesis

by

Erik Matthew Townsend

Submitted to the Department of Chemistry on May 5, 2014
in Partial Fulfillment of the Requirements for the
Degree of Doctor of Philosophy in Chemistry

ABSTRACT

Chapter 1 describes work toward solid-supported W olefin metathesis catalysts. Attempts to tether derivatives of the known Z-selective catalyst $W(NAr)(C_3H_6)(pyr)(OHIPT)$ (Ar = 2,6-diisopropylphenyl, pyr = pyrrolide; HIPT = 2,6-bis-(2,4,6-triisopropylphenyl)phenyl) to a modified silica surface by covalent linkages are unsuccessful due to destructive interactions between W precursors and silica. $W(NAr)(C_3H_6)(pyr)(OHIPT)$ and $W(NAr)(CHCMe_2Ph)(pyr)(OHIPT-NMe_2)$ (HIPT-NMe$_2$ = 2,6-bis-(2,4,6-triisopropylphenyl)-4-dimethylaminophenyl) are adsorbed onto calcined alumina. $W(NAr)(C_3H_6)(pyr)(OHIPT)$ is destroyed upon binding to alumina, while $W(NAr)(CHCMe_2Ph)(pyr)(OHIPT-NMe_2)$ appears to bind through a non-destructive interaction between the dimethylamino group and an acidic surface site. The heterogeneous catalysts perform non-stereoselective metathesis of terminal olefins, and $W(NAr)(CHCMe_2Ph)(pyr)(OHIPT-NMe_2)$ can be washed off the surface with polar solvent and perform solution-phase Z-selective metathesis.

Chapter 2 details selective metathesis homocoupling of 1,3-dienes with Mo and W monoalkoxide pyrrolide (MAP) catalysts. A catalytically relevant vinylalkylidene complex, $Mo(NAr)(CHCHCH(CH_3)_2)(Me_2pyr)(OHMT)$ (HMT = 2,6-bis(2,4,6-trimethylphenyl)phenyl; Me$_2$pyr = 2,5-dimethylpyrrolide), is isolated. A series of Mo and W MAP catalysts is synthesized and tested for activity, stereoselectivity, and chemoselectivity in 1,3-diene metathesis homocoupling. Catalysts containing the OHIPT ligand display excellent selectivity in general, and W catalysts are less active but more selective than their Mo counterparts.

Chapter 3 recounts the synthesis and characterization of several heteroatom-substituted alkylidene complexes with the formula $Mo(NAr)(CHER)(Me_2pyr)(OTPP)$ (TPP = 2,3,5,6-tetraphenylphenyl; ER = OPr, N-pyrrolidinonyl, N-carbazolyl, pinacolborato, trimethylsilyl, SPh, or PPh$_2$). Synthesis proceeds via alkylidene exchange between $Mo(NAr)(CHR)(Me_2pyr)(OTPP)$ (R = H, CMe$_2$Ph) and a CH$_2$CHER precursor. Each complex behaves similarly to known MAP complexes in olefin metathesis processes; the electronic identity of ER has little effect on catalytic properties. Distinctive features of alkylidene isomerism and catalyst resting state are examined.

Chapter 4 contains synthetic and catalytic studies of thiolate-containing Mo and W imido alkylidene complexes. The species $M(NAr)(CHCMe_2Ph)(pyr)(SHMT)$ (M = Mo or W), $Mo(NAr)(CHCMe_2Ph)(Me_2pyr)(STPP)$, and $Mo(NAr)(CHCMe_2Ph)(STPP)_2$ are synthesized by

substitution of the appropriate thiol or thiolate ligands for pyrrolide or triflate ligands in metal precursors. These complexes show similar structural and spectral characteristics to alkoxide-containing species. The thiolate complexes and their alkoxide analogues are compared for activity and selectivity in metathesis homocoupling and ring-opening metathesis polymerization processes. In general, thiolate catalysts are slower and less selective than alkoxide catalysts.

Thesis Supervisor: Richard R. Schrock
Title: Frederick G. Keyes Professor of Chemistry

Table of Contents

8

9

List of Figures

GENERAL INTRODUCTION

CHAPTER 1

CHAPTER 2

CHAPTER 4

List of Schemes

GENERAL INTRODUCTION

CHAPTER 1

CHAPTER 2

CHAPTER 3

List of Tables

16

List of Abbreviations

°C	degrees Celsius
Ad	1-adamantyl
Anal. Calcd	analysis calculated
anti	isomer in which alkylidene substituent points away from imido ligand
Ar	2,6-diisopropylphenyl
Ar'	2,6-dimethylphenyl
atm	atmospheres
BPin	pinacolborate
bpy	2,2'-bipyridine
Carbaz	*N*-carbazolyl
Cy	cyclohexyl
d	days or doublet
dba	dibenzylideneacetone
DCMNBD	2,3-dicarbomethoxynorbornadiene
DCPD	*endo*-dicyclopentadiene
DFT	density functional theory
DMA	N,N-dimethylacetamide
dme	1,2-dimethoxyethane
ee	enantiomeric excess
Et	ethyl
GC/MS	gas chromatography/mass spectrometry
h	hours
hex-silica	SBA-15 silica with 5-hexenyl pendent groups
HIPT	2,6-bis-(2,4,6-triisopropylphenyl)phenyl
HMT	2,6-bis-(2,4,6-trimethylphenyl)phenyl
HRMS	high-resolution mass spectrometry
hyd-silica	SBA-15 silica with hydrogenated hexenyl (hexyl) pendent groups
Hz	hertz
IMes	(1,3-bis(2,4,6-trimethylphenyl)dihydroimidazolyl

i-Pr	isopropyl
$^n J_{AB}$	the coupling constant between atoms A and B through n bonds
k	rate constant
k_b	Boltzmann constant ($1.38 \times 10\text{-}23$ J/K)
m	multiplet
M	molar
MAP	monoalkoxide pyrrolide
Me	methyl
Me_2pyr	2,5-dimethylpyrrolide
min	minutes
mL	milliliters
mmol	millimoles
mol	moles
MOM	methoxymethyl
MTP	monothiolate pyrrolide
NBO	Natural Bond Orbital
NCO-silica	SBA-15 silica with 3-(isocyanato)propyl pendent groups
neophyl	2-methyl-2-phenylpropyl
NLMO	Natural Localized Molecular Orbital
NMR	nuclear magnetic resonance
Np	2,2-dimethylpropyl
NVC	*N*-vinylcarbazole
NVP	*N*-vinylpyrrolidinone
Ph	phenyl
ppm	parts per million
Pr	*n*-propyl
PVP	*para*-vinylphenyl
pyr	pyrrolide
Pyrrol	*N*-vinylpyrrolidinonyl
q	quartet
R	Gas constant (8.314 J/mol*K)

ROMP	ring-opening metathesis polymerization
RT	room temperature
sept	septet
SBA-15	mesoporous silica made from tetraethoxysilane and Surfactant P_{123}
syn	isomer in which alkylidene substituent points toward the imido ligand
t	triplet
T	temperature
t-Bu	tertiary butyl
THF	tetrahydrofuran
TMS	trimethylsilyl
TPP	2,3,5,6-tetraphenylphenyl
trip	1,3,5-triisopropylphenyl
Z4O	Z-4-octene
δ	chemical shift
$\Delta H^{\ddagger}$	enthalpy of activation
$\Delta S^{\ddagger}$	entropy of activation
μL	microliter

General Introduction

Since its development over fifty years ago, transition-metal-catalyzed olefin metathesis has become a powerful and versatile tool for organic synthesis and polymer chemistry.[1] An olefin metathesis reaction between two molecules is characterized by the exchange of substituents on carbon-carbon double bonds (Scheme 1).
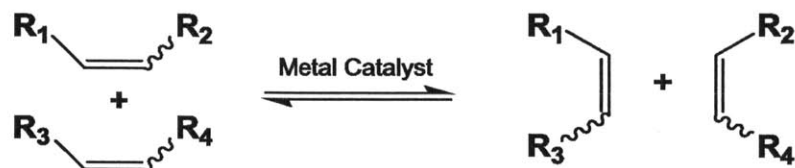
Scheme 1: The olefin metathesis reaction

Olefin metathesis reactions can be categorized according to the types of substrates and products that are involved. An overview of the common types of olefin metathesis reactions can be seen in Scheme 2.
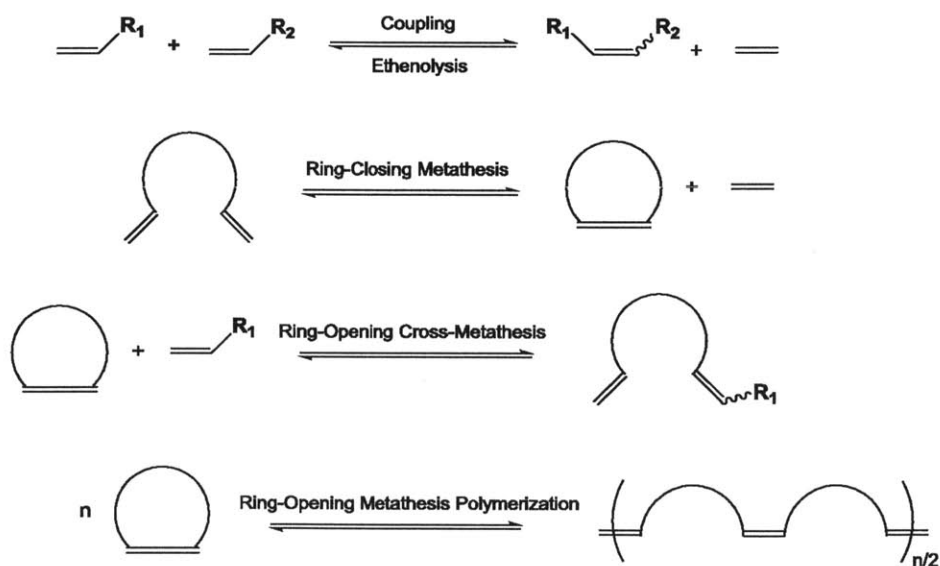
Scheme 2: Common types of olefin metathesis reactions

Coupling reactions and ring-closing metathesis reactions are characterized by the conversion of two terminal olefin functionalities into an internal olefin. Loss of ethylene provides a driving force for these processes, which would otherwise produce a thermodynamic mixture of olefins at equilibrium. Ring-opening cross-metathesis and ring-opening metathesis polymerization (ROMP) generally rely on release of ring strain in their substrates as the driving force for conversion to product. All olefin metathesis reactions have a high activation barrier under normal conditions and thus require an organometallic catalyst to proceed.

21

An ever-increasing understanding of the fundamental organometallic principles involved in catalytic olefin metathesis reactions has proven to be crucial to the advancement of the field. Olefin metathesis activity was first reported in the patent literature by Eleuterio in 1960,[2] and in the chemical literature by Banks and Bailey in 1964[3], but the mechanism of the process was yet unknown. It was not until 1971 that the currently accepted mechanism was proposed by Hérrison and Chauvin[4] (Scheme 3).
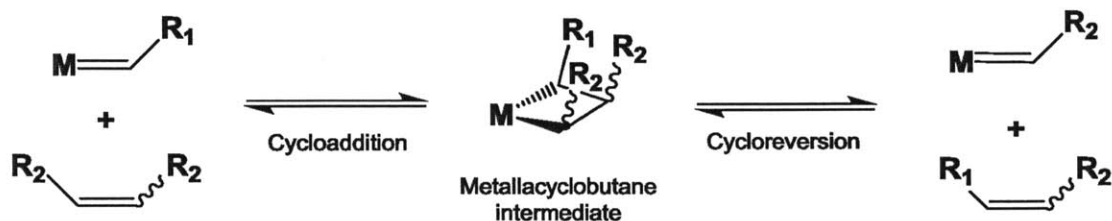
Scheme 3: Accepted mechanism for metal-catalyzed olefin metathesis

A metal center possessing a double bond to a carbon atom of an alkyl group is approached by an olefin, and the two molecules undergo a [2 + 2] cycloaddition step to form a metallacyclobutane intermediate. Subsequently, the metallacyclobutane breaks up, releasing an olefin molecule and regenerating a metal-carbon double bond. In this way, a new olefin can be generated while the metal is again ready to undergo cycloaddition with an olefin and close the catalytic cycle.

The above mechanism inspired research into organometallic compounds with metal-carbon double bonds as possible catalysts. Some such compounds of titanium that performed Wittig-like chemistry were obtained by Tebbe[5] and Grubbs[6] (each with coworkers), but these were stoichiometric reagents and showed no catalytic activity. A particularly interesting example was reported by Schrock: during an attempt to form pentakis(neopentyl)tantalum, it was discovered that the stable 10-electron tantalum alkylidene complex $Ta(CHCMe_3)(CH_2CMe_3)_3$ was obtained instead.[7] This discovery eventually led to the first well-defined complex with olefin metathesis activity, $Ta(CHCMe_3)Cl(PMe_3)(OCMe_3)_2$.[8]

Early in the search for metathesis catalysts, it was learned that only specific types of metal-carbon double bonds are likely to react with olefins to form metallacycles. A distinction must be drawn between complexes in which the carbon attached to the metal is nucleophilic (Schrock carbenes or alkylidenes) and those in which it is electrophilic (Fischer carbenes) (Figure 1).[9]

22
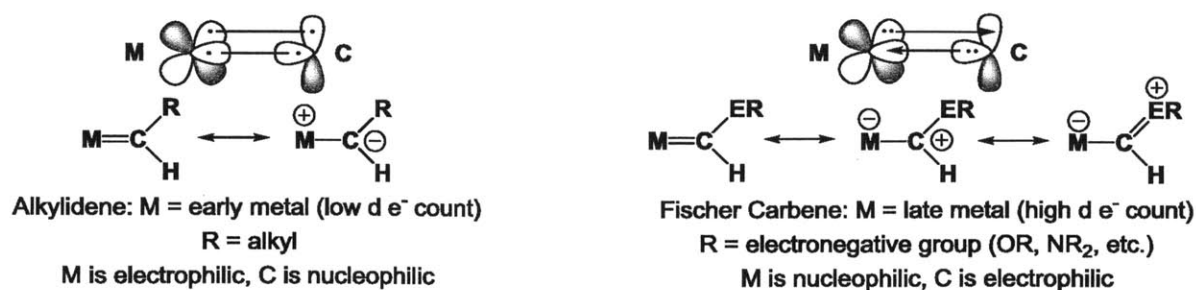
Figure 1: Electronic structure of alkylidenes and Fischer carbenes

The bonding electrons in an alkylidene bond have more ligand character than metal character due to the high energies of the empty d orbitals on the metal, meaning that the electron density of the bond is primarily located near the carbon atom. The opposite is true of Fischer carbenes, which have metals with low-energy, filled d orbitals as well as acceptor substituents that can stabilize a partial positive charge on the carbon atom. The reactivity modes of the two types of complexes differ accordingly. Fischer carbenes often react analogously to carbonyl compounds, with nucleophiles attacking the carbon atom and performing substitutions. Alkylidenes attract nucleophiles to the metal center; for instance, an approaching olefin can bind to the metal and subsequently undergo cycloaddition to form a metallacycle. For this reason, alkylidenes specifically (rather than all metal-carbon double-bonded complexes) are of primary interest for olefin metathesis.

The first class of synthetically relevant molecular olefin metathesis catalysts was made up of Mo and W imido alkylidene bisalkoxide complexes reported by Schrock and coworkers in the late 1980s.[10] Many variations of these complexes can be synthesized from simple metal starting materials in a 4-step route (Scheme 4).[11]
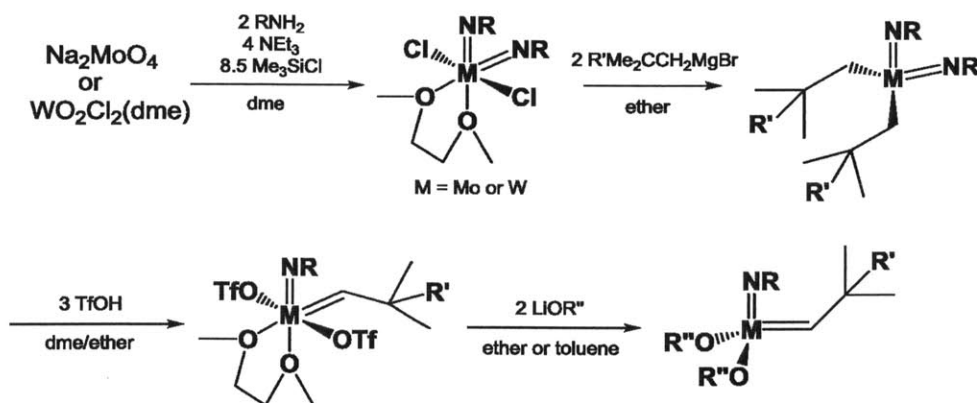
Scheme 4: Synthesis of Mo/W imido alkylidene bisalkoxide catalysts for olefin metathesis

23

One advantage of this synthetic route is its modularity: a wide variety of imido groups and alkoxides can be employed, and the effects of these ligands on metathesis activity can therefore be studied. The basic components of an effective catalyst, aside from the essential alkylidene ligand, are steric bulk to prevent bimolecular decomposition and an electropositive metal to increase reactivity with olefins.[1a] Some 2,6-disubstituted phenyl groups on the imido ligand (especially the widely-used NAr ligand; Ar = 2,6-diisopropylphenyl) are effective in protecting the metal center from decomposition processes. Bulky electron-withdrawing alkoxide ligands, such as hexafluoro-*t*-butoxide, also provide protection while increasing the Lewis acidity of the metal center; complexes bearing fluorinated *t*-butoxide ligands perform metathesis significantly faster than the analogous *t*-butoxide complexes.[12]

A fundamentally interesting and important feature of $M(NR)(CHCMe_2R')(OR'')_2$ complexes is the rotational isomerism displayed by the alkylidene ligand. Due to the electronic structure of the metal-ligand bonds, the alkyl substituent on the alkylidene carbon will be oriented either toward the imido group (a *syn* alkylidene) or away from the imido group (an *anti* alkylidene) (Figure 2).

syn alkylidene
(C-H agostic interaction pictured)
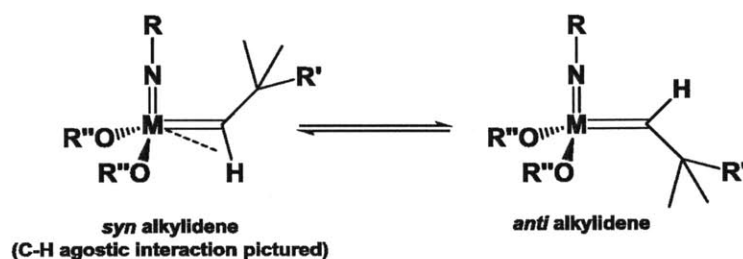
anti alkylidene

Figure 2: *Syn* and *anti* alkylidene isomers in $M(NR)(CHCMe_2R')(OR'')_2$ complexes

These isomers are observable because the pseudo-triple bond between the metal and the imido group occupies the metal π orbital that would otherwise stabilize the alkylidene rotation transition state.[13] Agostic donation of the alkylidene C-H bond into an empty metal orbital is thought to increase the stability of the *syn* isomer, and often the *syn* is the only observable form.[14] The isomers can be differentiated in ^{1}H NMR spectra by the alkylidene $^1J_{CH}$ coupling constants: *syn* alkylidenes have $^1J_{CH}$ of 120-130 Hz, while *anti* alkylidenes are generally in the region of 140 Hz.[13] To avoid confusion, it should be noted that the proton signal observed in a *syn* alkylidene arises from the proton pointing <u>away</u> from the imido group, as the orientation of the alkyl group is what determines the isomer designation.

Active and efficient alkylidene catalysts are not limited to Mo and W systems. A very successful class of ruthenium phosphine dichloride alkylidene catalysts was introduced by Grubbs in 1992.[15] Since that time, hundreds of derivatives with varying activity and selectivity have been prepared.[16] The original catalyst and its most popular derivative (Grubbs I and Grubbs II, respectively) are shown in Figure 3.

Grubbs I   Grubbs II

Cy = cyclohexyl   Mes = mesityl
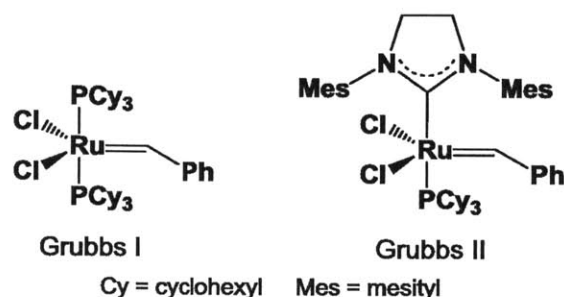
Figure 3: Ruthenium-based olefin metathesis catalysts

The pictured ruthenium catalysts are 16e complexes that must lose a phosphine ligand in order to bind an olefin and perform metathesis. Grubbs catalysts are a popular choice among synthetic chemists because of their stability to protic functional groups; Mo and W catalysts are generally not stable in the presence of water or alcohols. However, Mo and W catalysts are more resilient to phosphorus-, nitrogen-, and sulfur-containing functional groups, and are often more active overall than their Ru counterparts.[17]
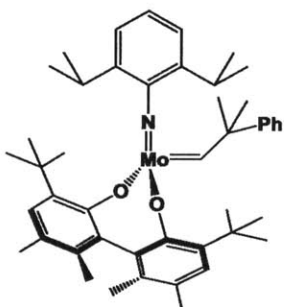
Figure 4: An enantioselective olefin metathesis catalyst

Further improvements to the Mo/W imido alkylidene system continued throughout the 1990s, including the introduction of chiral diolate ligands that enabled enantioselective metathesis processes. For instance, the catalyst pictured in Figure 4 is able to perform ring-closing metathesis on a variety of racemic substrates to produce product mixtures with >90% ee.[18] Furthermore, ROMP of substituted norbornenes and norbornadienes with similar chiral Mo catalysts resulted in *cis*, isotactic polymer.[19] In each case, the enantiomorphic reaction site enforced by the chiral ligand is responsible for the observed selectivity.

The success of the imido alkylidene framework for Mo and W metathesis catalysts led to an interest in heterogeneous versions, particularly those attached to a silica surface. Precursors of the type $M(NAr)(CHCMe_2R)(X)_2$ (M = Mo, W; R = H, Me; X = alkoxide, amide, pyrrolide,

alkyl) can be treated with specially prepared silica surfaces, resulting in well-defined surface species with the general formula $M(NAr)(CHCMe_2R)(X)(O_{silica})$.[20] Such catalysts are highly active for simple metathesis processes in many cases, but the use of the surface as a ligand makes it more difficult to predict and achieve selectivity.[21]

The most significant advance in Mo/W catalyst technology in the past decade was the discovery of monoalkoxide pyrrolide (MAP) imido alkylidene complexes.[22] MAPs can be synthesized in two steps from the bistriflate precursors pictured in Scheme 4. Replacement of the triflates with pyrrolide ligands by addition of lithium pyrrolide produces imido alkylidene bispyrrolide complexes.[23] The bispyrrolides can then be converted either into bisalkoxides/diolates by addition of two alcohol equivalents[24], or into MAPs by addition of just one equivalent of alcohol ligand (Scheme 5).[22]
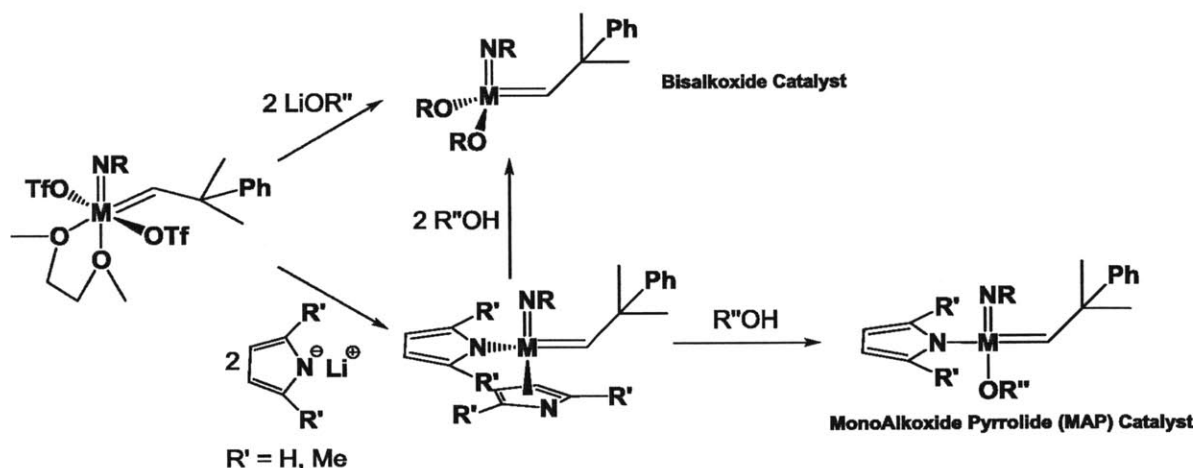
Scheme 5: Synthesis of bispyrrolides and MAP complexes

The metathesis reactivity of MAP species often exceeds that of both bisalkoxides and bispyrrolides. Given the previous observations that more electron-withdrawing ligands increased catalyst activity, this initially came as a surprise (pyrrolides being stronger donors than alkoxides in general). However, some theoretical studies by Eisenstein and coworkers revealed that $M(NR)(CHCMe_2R')(X)(Y)$ complexes in which X and Y are of differing donor abilities are optimal for rapid metathesis turnover (for more details, see Chapter 3 of this work).[25] MAP catalysts showed the ability to perform a number of ring-closing metathesis reactions that were slow or impossible with bisalkoxides, including examples of enyne metathesis[26] and some

enantioselective ring-closings achieved using MAPs bearing monofunctional chiral alkoxide ligands.[27]

In addition to their superior reactivity, MAP catalysts have allowed for great strides in the area of stereoselective olefin metathesis. Specifically, MAPs with sterically bulky alkoxide ligands and comparatively small imido groups are able to carry out metathesis processes with high selectivity for the formation of Z double bonds (Scheme 6).
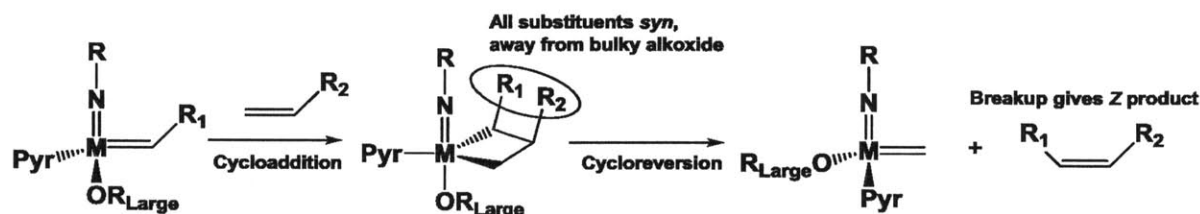
Scheme 6: Origin of Z selectivity in MAP catalysts with bulky alkoxides

When a trigonal bipyramidal metallacycle complex is formed as part of the metathesis cycle, each substituent on the metallacycle can be oriented either toward the imido group or toward the alkoxide. According to the currently held theory of Z selectivity, in the case that the alkoxide is sterically demanding, the substituents preferentially point towards the smaller imido group. Productive breakup of the metallacycle releases a product olefin in which the substituents on the double bond are oriented in the same direction; in other words, a Z olefin.

There are many recent examples of Z-selective metathesis employing MAP catalysts. Polymerization of substituted norbornadienes with $Mo(NAd)(CHCMe_2Ph)(pyr)(OHIPT)$ (Ad = 1-adamantyl, pyr = pyrrolide, HIPT = 2,6-bis-(2,4,6-triisopropylphenyl)phenyl) led to *cis*, syndiotactic polymer, which was a previously unknown structure.[28] Studies of the polymerization of 3-substituted cyclooctenes using MAP catalysts of the type M(N-*t*-Bu)$(CHCMe_3)$(pyr)(OHMT) (M = Mo, W; HMT = 2,6-bis-(2,4,6-trimethylphenyl)phenyl) resulted in polymer with all *cis* linkages as well.[29] In the realm of coupling reactions, W MAPs in particular have shown the ability to carry out homocoupling of terminal olefins with exceptional Z selectivity.[30] Examples of each of the above reactions are shown in Scheme 7.
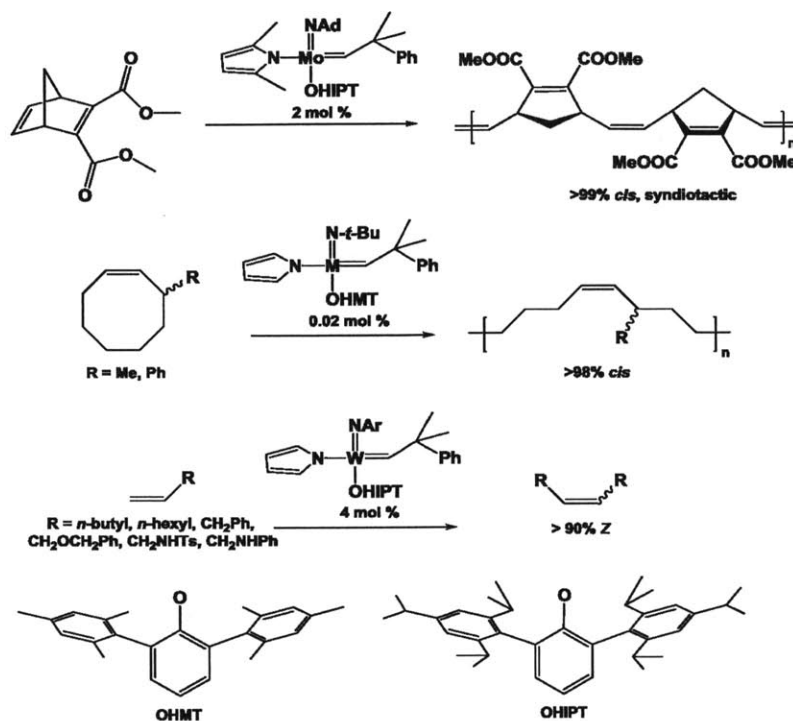
Scheme 7: Examples of MAP-catalyzed Z-selective metathesis reactions

MAP complexes have also been utilized in Z-selective ring-opening cross-metathesis reactions,[31] terminal olefin cross-metathesis,[32] and ethenolysis of Z internal olefins.[33]

The versatility and selectivity of Mo and W MAP catalysts inspired the studies that make up the body of this work. Chapter 1 treats efforts towards Z-selective MAP-based heterogeneous catalysts based on silica and alumina. In contrast to the aforementioned heterogeneous catalysts in which the surface itself serves as a ligand,[20] the experiments are focused on creating systems in which the steric ligand environment of a known Z-selective MAP is conserved while the entire complex is covalently tethered to silica or adsorbed onto alumina via a Lewis acid-base interaction. Chapter 2 contains an examination of 1,3-diene metathesis by MAP catalysts. The stability of the necessary vinyl-substituted alkylidene intermediates is established, and the effects of metal identity and ligand sterics on chemoselectivity, stereoselectivity, and overall reactivity are analyzed. Chapter 3 is primarily focused on broadening our understanding of substituent effects on the alkylidene ligand in MAP complexes. A variety of new heteroatom-substituted alkylidene complexes are synthesized and characterized, and the unusual behavior of some of these species is studied in detail. Furthermore, basic tests of the effect of a heteroatom alkylidene substituent on metathesis activity are performed. Finally, Chapter 4 deals with thiolate analogues

of MAP and bisalkoxide compounds. The possible electronic effects of replacing oxygen donors with sulfur donors are discussed within the mechanistic framework of olefin metathesis. Several comparisons between imido alkylidene thiolate complexes and their direct alkoxide analogues are explored, and the overall ligand effects on metathesis capabilities are determined.

REFERENCES

[1] (a) Schrock, R. R. *Chem. Rev.* **2009**, *109*, 3211. (b) Schrock, R. R. *Chem. Commun.* **2005**, 2773. (c) Schrock, R. R. *Chem. Rev.* **2002**, *102*, 45. (d) Ivin, K. J.; Mol, J. C. *Olefin Metathesis and Metathesis Polymerization*, Academic Press: San Diego, CA, **1997**. (e) Grubbs, R. H. *Handbook of Metathesis, vols. 1-3*, Wiley-VCH: Wenheim **2003**.

[2] Eleuterio, H. S. *J. Molec. Catal.* **1991**, *65*, 55.

[3] Banks, R. L.; Bailey, G. C. *I & EC Product Research and Development* **1964**, *3*, 170.

[4] Hérrison, J. L.; Chauvin, Y. *Makromol. Chem.* **1971**, *141*, 161.

[5] Tebbe, F. N.; Parshall, G. W.; Reddy, G. S. *J. Am. Chem. Soc.* **1978**, *100*, 3611.

[6] Howard, T. R.; Lee, J. R.; Grubbs, R. H. *J. Am. Chem. Soc.* **1980**, *102*, 6876.

[7] (a) Schrock, R. R. *J. Am. Chem. Soc.* **1974**, *96*, 6796. (b) Schrock, R. R.; Fellmann, J. D. *J. Am. Chem. Soc.* **1978**, *100*, 3359.

[8] (a) Schrock, R. R.; Rocklage, S. M.; Wengrovius, J. H.; Rupprecht, G.; Fellmann, J. D. *J. Mol. Catal.* **1980**, *8*, 73. (b) Rocklage, S. M.; Fellmann, J. D.; Rupprecht, G. A.; Messerle, L. W.; Schrock, R. R. *J. Am. Chem. Soc.* **1981**, *103*, 1440.

[9] Hartwig, J. H. *Organotransition Metal Chemistry: From Bonding to Catalysis*, University Science Books: Herndon, VA, **2010**.

[10] Murdzek, J. S.; Schrock, R. R. *Organometallics* **1987**, *6*, 1373.

[11] Schrock, R. R.; Murdzek, J. S.; Bazan, G. C.; Robbins, J.; DiMare, M.; O'Regan, M. *J. Am. Chem. Soc.* **1990**, *112*, 3875.

[12] Schrock, R. R.; DePue, R. T.; Feldman, J.; Schaverien, C. J.; Dewan, J. C.; Liu, A. H. *J. Am. Chem. Soc.* **1988**, *110*, 1423.

[13] Oskam, J. H.; Schrock, R. R. *J. Am. Chem. Soc.* **1993**, *115*, 11831.

[14] Poater, A.; Solans-Monfort, X.; Clot, E.; Copéret, C.; Eisenstein, O. *Dalton Trans.* **2006**, 3077.

[15] Nguyen, S. T.; Johnson, L. K.; Grubbs, R. H.; Ziller, J. W. *J. Am. Chem. Soc.* **1992**, *114*, 3974.

[16] Vougioukalakis, G. C.; Grubbs, R. H. *Chem. Rev.* **2010**, *110*, 1746.

[17] Astruc, D. *New J. Chem.* **2005**, *29*, 42.

[18] (a) Alexander, J. B.; La, D. S.; Cefalo, D. R.; Hoveyda, A. H.; Schrock, R. R. *J. Am. Chem. Soc.* **1998**, *120*, 4041. (b) La, D. S.; Alexander, J. B.; Cefalo, D. R.; Graf, D. D.; Hoveyda, A. H.; Schrock, R. R. *J. Am. Chem. Soc.* **1998**, *120*, 9720.

[19] (a) McConville, D. H.; Wolf, J. R.; Schrock, R. R. *J. Am. Chem. Soc.* **1993**, *115*, 4413. (b) O'Dell, R.; McConville, D. H.; Hofmeister, G. E.; Schrock, R. R. *J. Am. Chem. Soc.* **1994**, *116*, 3414.

[20] a) Rendón, N.; Berthoud, R.; Blanc, F.; Gajan, D.; Maishal, T.; Basset, J.-M.; Copéret, C.; Lesage, A.; Emsley, L.; Marinescu, S. C.; Singh, R.; Schrock, R. R. *Chem. Eur. J.* **2009**, *15*, 5083. b) Blanc, F.; Thivolle-Cazat, J.; Copéret, C.; Hock, A. S.; Tonzetich, Z. J.; Schrock, R. R. *J. Am. Chem. Soc.* **2007**, *129*, 1044. c) Rhers, B.; Salameh, A.; Baudouin, A.; Quadrelli, E. A.; Taoufik, M.; Copéret, C.; Lefebvre, F.; Basset, J.-M.; Solans-Monfort, X.; Eisenstein, O.; Lukens, W. W.; Lopez, L. P. H.; Sinha, A.; Schrock, R. R. *Organometallics* **2006**, *25*, 3554.

[21] Copéret, C.; Basset, J.-M. *Adv. Synth. Catal.* **2007**, *349*, 78.

[22] Marinescu, S. C.; Singh, R.; Hock, A. S.; Wampler, K. M.; Schrock, R. R.; Müller, P. *Organometallics* **2008**, *27*, 6570.

[23] Hock, A. S.; Schrock, R. R.; Hoveyda, A. H. *J. Am. Chem. Soc.* **2006**, *128*, 16373.

[24] Singh, R.; Czekelius, C.; Schrock, R. R.; Müller, P. *Organometallics* **2007**, *26*, 2528.

[25] Poater, A.; Solans-Monfort, X.; Clot, E.; Copéret, C.; Eisenstein, O. *J. Am. Chem. Soc.* **2007**, *129*, 8207.

[26] Singh, R.; Schrock, R. R.; Müller, P.; Hoveyda, A. H. *J. Am. Chem. Soc.* **2007**, *129*, 12654.

[27] (a) Malcolmson, S. J.; Meek, S. J.; Sattely, E. S.; Schrock, R. R.; Hoveyda, A. H. *Nature* **2008**, *456*, 933. (b) Sattely, E. S.; Meek, S. J.; Malcolmson, S. J.; Schrock, R. R.; Hoveyda, A. H. *J. Am. Chem. Soc.* **2009**, *131*, 943.

[28] (a) Flook, M. M.; Jiang, A. J.; Schrock, R. R.; Müller, P.; Hoveyda, A. H. *J. Am. Chem. Soc.* **2009**, *131*, 7962. (b) Flook, M. M.; Gerber, L. C. H.; Debelouchina, G. T.; Schrock, R. R. *Macromolecules* **2010**, *43*, 7515.

[29] Jeong, H.; Kozera, D. J.; Schrock, R. R.; Smith, S. J.; Zhang, J.; Ren, N.; Hillmyer, M. A. *Organometallics* **2013**, *32*, 4843.

[30] (a) Jiang, A. J.; Zhao, Y.; Schrock, R. R.; Hoveyda, A. H. *J. Am. Chem. Soc.* **2009**, *131*, 16330. (b) Marinescu, S. C.; Schrock, R. R.; Müller, P.; Takase, M. K.; Hoveyda, A. H. *Organometallics* **2011**, *30*, 1780. (c) Peryshkov, D. V.; Schrock, R. R.; Takase, Müller, P.; Hoveyda, A. H. *J. Am. Chem. Soc.* **2011**, *133*, 20754.

[31] (a) Ibrahem, I.; Yu. M.; Schrock, R. R.; Hoveyda, A. H. *J. Am. Chem. Soc.* **2009**, *131*, 3844. (b) Yu, M.; Ibrahem, I.; Hasegawa, M.; Schrock, R. R.; Hoveyda, A. H. *J. Am. Chem. Soc.* **2012**, *134*, 2788.

[32] Meek, S. J.; O'Brien, R. V.; Llaveria, J.; Schrock, R. R.; Hoveyda, A. H. *Nature* **2011**, *471*, 461.

[33] Marinescu, S. C.; Levine, D.; Zhao, Y.; Schrock, R. R.; Hoveyda, A. H. *J. Am. Chem. Soc.* **2011**, *133*, 11512.

Chapter 1

Investigations of Solid-Supported Olefin Metathesis Catalysts

INTRODUCTION

The field of high-oxidation-state Mo and W imido alkylidene olefin metathesis catalysts has been shown to be a rich area of chemistry, with new developments continuing to emerge in the areas of reactivity and selectivity.[1] One exciting recent advance has been the rise of Mo and W monoaryloxide pyrrolide (MAP) complexes that perform Z-selective olefin metathesis, both for polymerization[2] and for coupling of terminal olefins.[3] With MAP catalysts come new opportunities for application; for instance, the synthesis of a heterogeneous version of a Z-selective catalyst is of great interest. Heterogeneous metathesis catalysts provide advantages such as facile separation of products and decreased chance of bimolecular catalyst decomposition.[1] Furthermore, an eventual goal is the creation of a flow reactor system wherein the substrate would have a shortened catalyst contact time, lessening the chances of secondary isomerization from Z product to E product.[3]

Previous heterogeneous manifestations of Mo and W imido alkylidene complexes have focused either on using a surface oxygen site of an inorganic oxide as a ligand[4] or on covalent attachment of one of the ligands to an organic polymer.[5] In the former case, use of the surface as a ligand may afford an active metathesis catalyst, but the steric restrictions of the ligand environment are drastically changed from those of the homogeneous complex, which can inhibit selectivity.[6] In the latter case, enantioselective polymer-supported catalysts have been synthesized, but problems such as swelling and fragmentation of the polymer support preclude such systems from use in simple flow reactors.[5] With these limitations in mind, we have turned our focus toward systems in which a molecular Z-selective metathesis catalyst is attached to a hard inorganic support via a functional group on its ligand periphery. Specifically, efforts have focused on synthesizing variants of the OHIPT ligand in complex **1** (W(NAr)(CHCMe₂Ph)(pyr)(OHIPT) (Ar = 2,6-diisopropylphenyl; HIPT = 2,6-bis-(2,4,6-triisopropylphenyl)phenyl; pyr = η^1 N-pyrrolide)

1   Modification site

Figure 1: W(NAr)(CHCMe₂Ph)(pyr)(OHIPT) **(1) and site of functional group installation for attachment to surfaces**

with a functional group in the *para* position (Figure 1). The steric environment at the reaction site of **1** is known to be key to Z selectivity,[3] and since the proposed interactions with the surface

happen at a site remote from the metal center, it is reasonable to expect the heterogenized versions to retain selectivity.

The first plan was to create a structurally intact version of complex **1** covalently linked to a silica surface (Scheme 1).
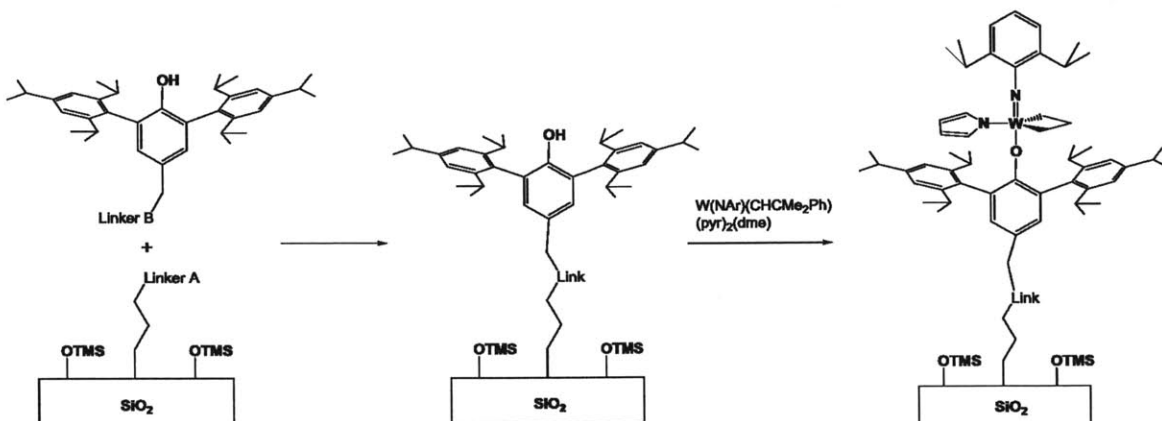
Scheme 1: General strategy for tethering of 1 to silica

The primary strategy would begin with the synthesis of both a passivated silica derivative with pendant functional groups and a HOHIPT derivative that has a functional group in the *para*
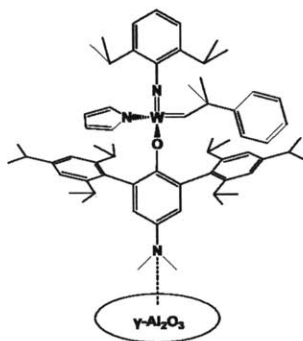
Figure 2: General strategy for immobilization of 1 on alumina

position. Reaction between these functional groups would form the all-important linkage, and addition of W(NAr)(CHCMe$_2$Ph)(pyr)$_2$(dme)[7] (dme = 1,2-dimethoxyethane) (the direct precursor of **1**) would then complete the tethered catalyst system. A similar approach was employed previously by van Koten and coworkers, who used *para*-functionalized pincer ligands and modified silica to create triazole- and carbamate-linked immobilized versions of homogeneous Pd pincer complexes.[8]

The second approach to solid-supported catalysis involved the functionalization of HOHIPT with a dimethylamino group in the *para* position (Figure 2). This group could serve as a Lewis-basic binding site for the ligand or complexes thereof with calcined γ-alumina, which has Lewis-acidic surface Al sites.[9] Inspiration for this approach came from the recent work of Goldman, Brookhart and coworkers, who found that a *para*-dimethylamino group on the pincer ligand of their Ir hydrogenation catalyst allowed the catalyst to remain supported on the calcined γ-alumina surface.[10]

The efforts toward a silica-based heterogeneous Z-selective metathesis system, along with investigations of the problems encountered therewith, will be detailed in Part I of this chapter. Part II will describe the studies of the more successful alumina-based system, including an in-depth look at the effect of solvent polarity on the catalytic reactions.

RESULTS AND DISCUSSION

I. Efforts toward silica-supported Z-selective MAP catalysts

The general strategy in Figure 1 was pursued through two routes. The first route involved the creation of isocyanate-functionalized silica and subsequent reaction with amino-substituted HOHIPT to form a urea linkage; this path will be described in Section I-A below. The second route, detailed in Section I-B, was designed to create a hydrocarbon linkage between the ligand and the surface through the use of olefin metathesis. While neither of these routes was ultimately successful in creating a solid-supported Z-selective metathesis catalyst, the results of the involved experiments still provided substantial information on the pitfalls of this linking strategy.

I-A. Urea linkage

Formation of the urea linkage required a reaction between an isocyanate group attached to the silica surface and an amino group on the HOHIPT ligand. To this end, silica bearing pendent isocyanate groups (NCO-silica) was synthesized as shown in Scheme 2 (this synthesis was carried out along with Dr. Yu Zhao).
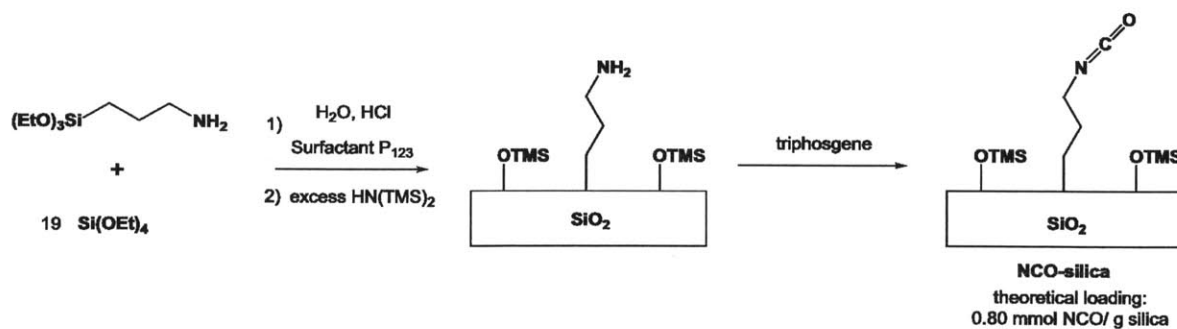
Scheme 2: Synthesis of isocyanate-functionalized silica (NCO-silica).

Condensation of a 19:1 mixture of tetraethoxysilane and 3-triethoxysilylpropylamine under acidic conditions with the polymer templating agent P_{123} formed amino-functionalized mesoporous SBA-15 silica as described in a previous report.[11] Subsequently, the free Si-OH

groups on the surface were protected with trimethylsilyl (TMS) groups by refluxing overnight with Li(N(TMS)$_2$) in hexanes.[12] Finally, the amino groups were converted to isocyanates by reaction with triphosgene.[8] The IR stretch for the isocyanate group was visible in the 2100-2200 cm^{-1} region. An attempt to directly synthesize NCO-silica by condensation of tetraethoxysilane and 3-triethoxysilylpropylisocyanate resulted in a product whose IR spectrum was largely void of the isocyanate stretch. This outcome was probably due to hydrolysis of the isocyanate groups under the acidic conditions of the synthesis.

The remaining piece of the desired urea linkage would come from a derivative of the HOHIPT with an amino group in the para position (henceforth referred to as HOHIPT-NH$_2$). HOHIPT-NH$_2$ was synthesized as shown in Scheme 3.
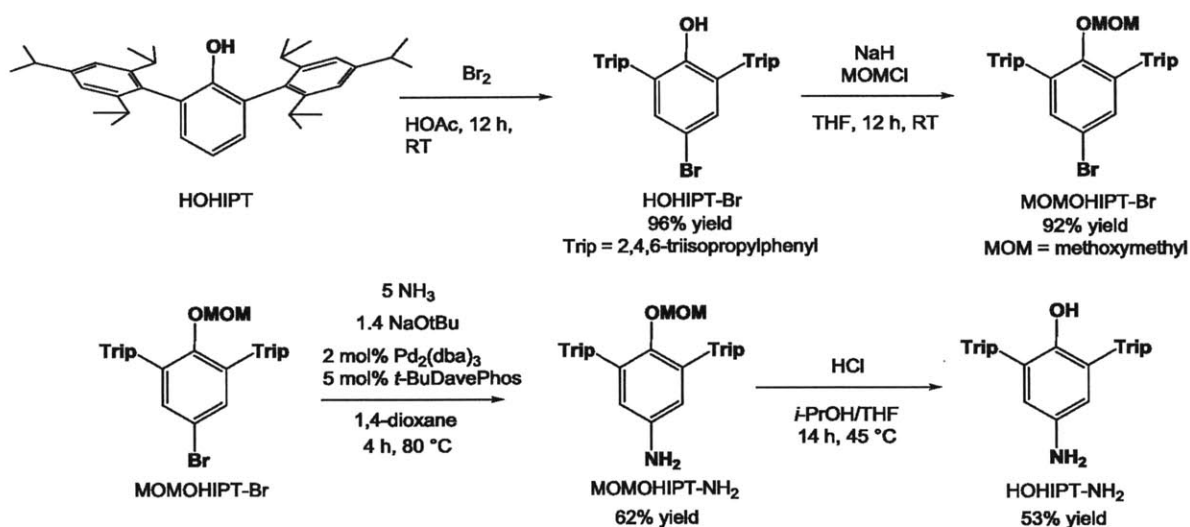
Scheme 3: Synthesis of HOHIPT-NH$_2$ from HOHIPT

The first step was to synthesize HOHIPT by literature methods.[13] Functionalization of the *para* position was achieved by treatment with bromine in acetic acid to give the brominated product in 96% yield. Next, the phenol group was protected by deprotonation with sodium hydride followed by reaction with methoxymethyl chloride (MOMCl). The protection was necessary for the clean execution of the next step, which involved a palladium-catalyzed coupling with ammonia.[14] Finally, deprotection with hydrochloric acid afforded the free phenol ligand HOHIPT-NH$_2$ in 53% yield.

The reaction between NCO-silica and HOHIPT-NH$_2$ was carried out in refluxing toluene over a period of 3 days. Disappearance of the ^{1}H NMR signals for HOHIPT-NH$_2$ with respect to an internal standard (anthracene) was interpreted as attachment of the ligand to the surface. The

reaction appeared to proceed to 27% conversion of HOHIPT-NH$_2$, which corresponded to a loading of 0.133 mmol of surface-bound HOHIPT per gram of silica (this silica sample will be referred to as **2**). This coupling step and the subsequent metallation are shown in Scheme 4.
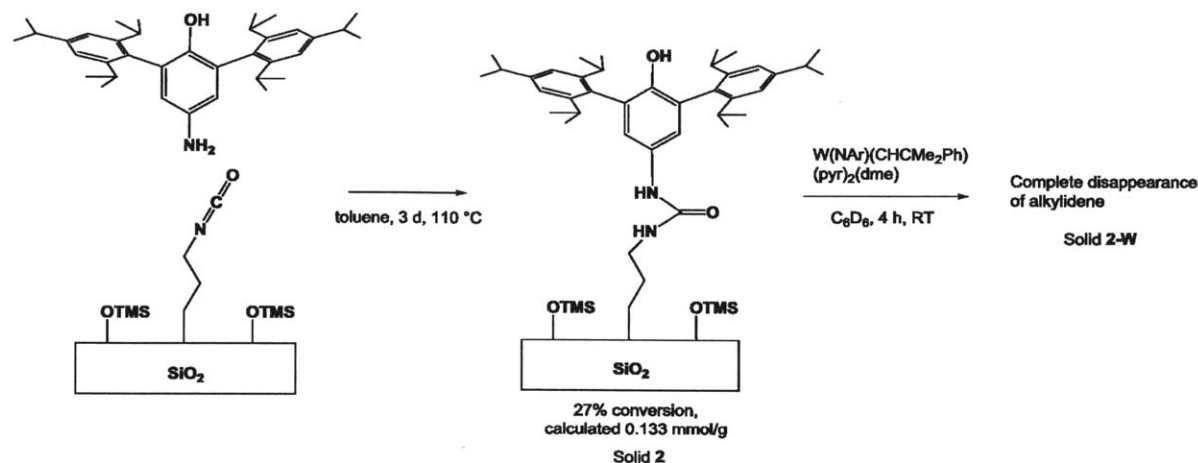
Scheme 4: Synthesis of 2 (HOHIPT-urea-silica) and 2-W

Following the general strategy in Scheme 1, the final step in the surface catalyst synthesis was the addition of the catalyst precursor W(NAr)(CHCMe$_2$Ph)(pyr)$_2$(dme). It was presumed that the phenol functionality on the surface-tethered HOHIPT ligand would react with the W center and result in the desired heterogeneous version of **1** along with free pyrrole and dimethoxyethane. When this reaction was carried out, all of the signals from the W precursor disappeared, so it was assumed that a surface-bound catalyst had been formed (**2-W**).

In order to test the effects of the urea moiety on the MAP formation reaction, two homogeneous model ligands were synthesized. HOHIPT-NH$_2$ was coupled with phenyl isocyanate to create a ligand with urea functionality but no silicon-containing groups (**3-OH**). Also synthesized was the methyl-protected version of this molecule (**3-OMe**), wherein the phenol functionality is sealed off. Each of these test ligands was combined with W(NAr)(CHCMe$_2$Ph)(pyr)$_2$(dme) to give mixtures of alkylidenes (**3-OH-W** and **3-OMe-W**, respectively) that appeared almost identical to each other by ^{1}H NMR.
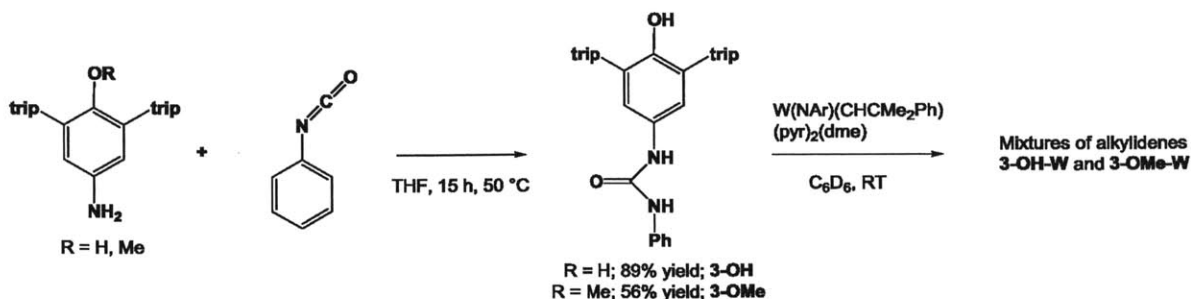
Scheme 5: Synthesis of test ligands 3-OH and 3-OMe. Reactions with W(NAr)(CHCMe₂Ph)(pyr)₂(dme) to form mixtures of alkylidenes

The structures of the alkylidene species in **2-W**, **3-OH-W**, and **3-OMe-W** were unknown at this point, but it was hypothesized that clean formation of MAP complexes had not taken place, based on comparisons with ^{1}H NMR spectra of existing MAPs. As Z selectivity in terminal olefin homocoupling is known to be dependent on specific structural features of MAP complexes, experiments involving the homocoupling of 1-octene to (Z/E)-7-tetradecene were carried out as structural probes. In these reactions, high Z selectivity would be interpreted as evidence that W-OHIPT species were being formed, and poor selectivity would signify that W(NAr)(CHCMe₂Ph)(pyr)₂(dme) had undergone side reactions.

The homocoupling trials were run with 5 mol% catalyst in C_6D_6, and the results are shown in Table 1.

Catalyst (5 mol%)	Time	% Conversion	% Z
2-W	4 h	10	51
3-OH-W	3 h	9	46
3-OMe-W	3 h	9	49

Table 1: Homocoupling of 1-octene with silica-based catalyst 2-W and homogeneous models 3-OH-W and 3-OMe-W

In each case the Z content was around 50%—nowhere near the 90+% found in the homogeneous MAP systems.[3] Furthermore, the conversion was similarly low for each catalyst system. We postulate that the urea functionality interferes with the formation of MAP species by binding to the metal center of the bispyrrolide and forming one or more unwanted alkylidene complexes. These complexes clearly participate in the homocoupling of 1-octene as shown. Since the conversions and selectivities were poor in each application of a urea-linker-based

system, it was decided that the urea linker approach was not feasible for the creation of supported MAP species.

I-B. Hydrocarbon linkage via olefin metathesis

Since the problems with the urea group seemed to stem from the donor properties of its heteroatoms, a hydrocarbon linker was a logical alternative. To this end, the next approach was to synthesize an olefinic linker via terminal olefin cross-metathesis between hexenyl groups pendent from silica and a *para*-vinylphenyl derivative of HOHIPT (HOHIPT-PVP, Scheme 6). A similar strategy was reported in the literature for attachment of organic moieties to vinyl-functionalized silsesquioxanes.[15]
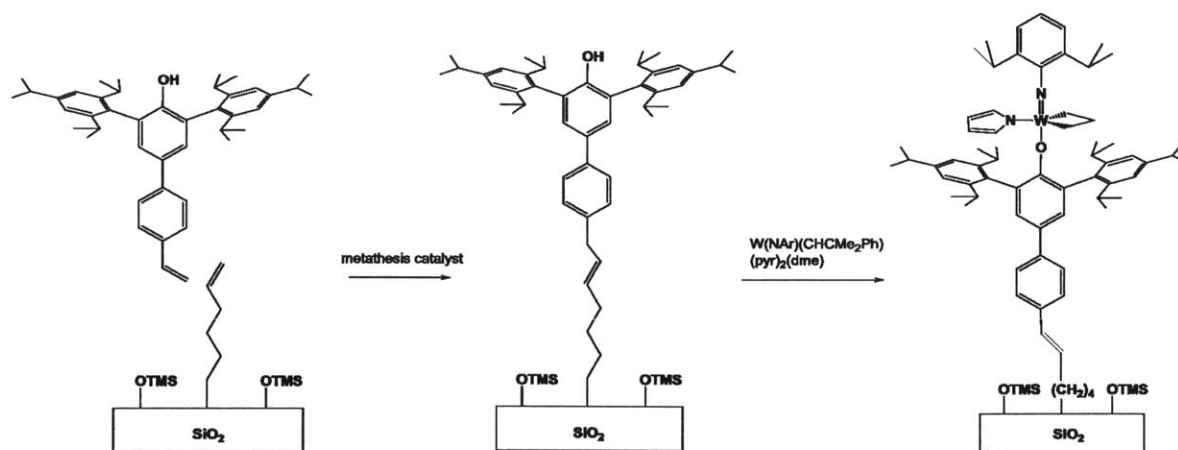
Scheme 6: General strategy for olefin metathesis linkage

Hexenyl-functionalized silica (hex-silica) was synthesized as shown in Scheme 7. Also pictured in Scheme 7 is the subsequent treatment with hydrogen and Wilkinson's catalyst to form hexyl-functionalized silica (hyd-silica), which was used in control reactions that are described later in this section. HOHIPT-PVP was synthesized from HOHIPT-Br in a Suzuki coupling reaction with *para*-vinylphenylboronic acid according to a previous report.[16]
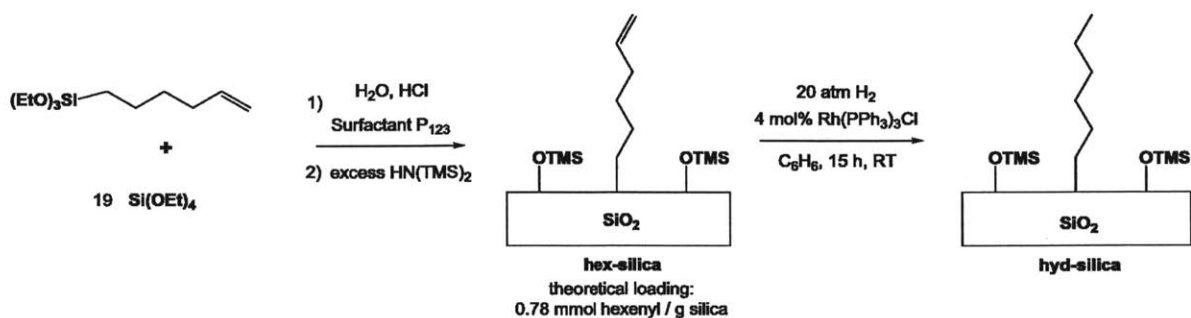
Scheme 7: Synthesis of hex-silica and hyd-silica

A variety of Mo and Ru metathesis catalysts were used in attempts to link the HOHIPT-PVP to the hex-silica, but in each case there was little to no evidence for successful coupling. For some catalysts, including $Mo(NAr)(CHCMe_2Ph)(OC(CF_3)_2CH_3)_2$ and $Ru(CHPh)Cl_2(PCy_3)_2$ (Grubbs I), there was no consumption of HOHIPT-PVP as quantified by ^{1}H NMR with respect to an internal standard. Some other catalysts, such as $Mo(NAr)(CHCMe_2Ph)(Me_2pyr)(OTPP)$ (Me_2pyr = 2,5-dimethylpyrrolide; TPP = 2,3,5,6-tetraphenylphenyl) and $Ru(CHPh)Cl_2(PCy_3)(IMes)$ (Grubbs II; IMes = 1,3-bis(2,4,6-trimethylphenyl)-2-imidazolidinylidene) were able to effect some metathesis homocoupling of HOHIPT-PVP, but no surface attachment. The solid resulting from the Grubbs II surface coupling attempt (referred to as solid **4**) was treated with $W(NAr)(CHCMe_2Ph)(pyr)_2(dme)$. This reaction resulted in disappearance of the alkylidene signal and formation of 0.83 equivalents of free pyrrole, which was interpreted to mean that a surface-bound W-complex (**4-W**) had formed (Scheme 8).
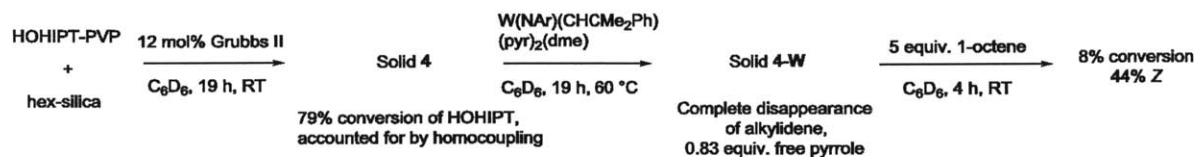
Scheme 8: Synthesis and homocoupling trial with 4-W

The homocoupling of 1-octene with 20 mol% **4-W** resulted in low conversion and poor Z-selectivity, similarly to the species studied in Section I-A. Since **4** did not appear to contain any HOHIPT moiety, the metathesis activity of **4-W** was attributed to one or more silica-bound W alkylidenes of unknown structure.

Taking stock of these results, it was clear that some W alkylidene was attached to the surface in each case that $W(NAr)(CHCMe_2Ph)(pyr)_2(dme)$ was added to a silica derivative, but

40

these surface species were only capable of low conversion and ~1:1 $Z:E$ selectivity in the homocoupling of 1-octene. To further investigate the surface interactions, a series of control experiments was carried out by treating hex-silica, hyd-silica, and unfunctionalized TMS-capped silica (synthesized using pure tetraethoxysilane)[11] with W(NAr)(CHCMe$_2$Ph)(pyr)$_2$(dme) in C$_6$D$_6$. The amount of unreacted alkylidene, the amount of free pyrrole, and the presence of the metathesis cleavage product 3,3-dimethyl-3-phenylpropene (signifying reaction at the alkylidene site of W(NAr)(CHCMe$_2$Ph)(pyr)$_2$(dme)) were observed by ^{1}H NMR spectroscopy (Table 2).

Silica	Remaining Alkylidene	Free Pyrrole	Cleavage Product?
Hex-silica	8%	.86 eq.	Yes
Hyd-silica	25%	.66 eq.	No
TMS-capped	29%	.94 eq.	No

Table 2: Stability of W(NAr)(CHCMe$_2$Ph)(pyr)$_2$(dme) when exposed to silica surfaces Experimental conditions: .025 mmol W complex and 32 mg silica in 1 mL C$_6$D$_6$, stirred for 8 h at room temperature.

The fact that the majority of the alkylidene signal is gone in all three cases strongly suggests that the TMS-protected surface reacts with W(NAr)(CHCMe$_2$Ph)(pyr)$_2$(dme), either by action of residual silanol groups or through silyl ether binding. The surface reaction releases pyrrole into solution and, based on prior observations, creates one or more W species that can carry out homocoupling of 1-octene slowly and with poor selectivity. Furthermore, a second reaction mode exists in the case of hex-silica, where the presence of 3,3-dimethyl-3-phenylpropene indicates that metathesis between the surface hexenyl groups and the starting W neophylidene has taken place. Hydrogenation shuts down this mode of reactivity, but many surface sites remain active. Exposure of the Mo metathesis catalysts Mo(NAr)(CHCMe$_2$Ph)(OC(CF$_3$)$_2$CH$_3$)$_2$ and Mo(NAr)(CHCMe$_2$Ph)(Me$_2$pyr)(OTPP) to the same three silica variants shown in Table 2 resulted in similar findings: the alkylidene signals largely disappeared and there was evidence for ligand dissociation from each complex.

Any further attempts at tethering W- or Mo-based metathesis catalysts to silica should begin with a new surface system—either a different silica variant, a new protection scheme, or both—because the TMS-protected SBA-15 system explored above has substantial deleterious effects on the desired catalysts and their precursors.

II. Alumina-supported MAP catalysts

As the silica systems explored above proved to be problematic, attention shifted to the use of alumina as the support for Z-selective MAP metathesis catalysts. (It should be noted that

some of the work in this area was done in conjunction with Dr. Jian Yuan, as will be indicated later). The chosen method in this case was to adsorb a variant of **1** with a dimethylamino group in the *para* position of the HOHIPT ligand onto calcined alumina through a Lewis acid-base interaction with a surface Al site. A similar approach to heterogenized molecular catalysts had been previously reported by Goldman and Brookhart, who made use of a Lewis acid-base interaction between a dimethylamino group and calcined γ-alumina in the immobilization of Ir pincer complexes.[10] Unlike in the silica case, the MAP variant (**1-NMe₂**) would be completely synthesized in the homogeneous phase prior to surface attachment (Scheme 9).
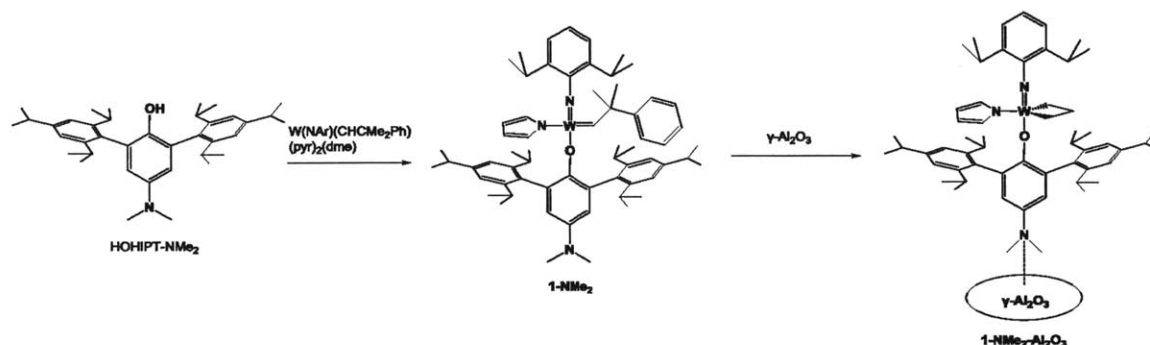
Scheme 9: Strategy for synthesis of an alumina-supported MAP catalyst

II-A. Synthesis of catalysts

The synthesis of the dimethylamino-functionalized HOHIPT ligand (HOHIPT-NMe₂) was developed in conjunction with Dr. Jian Yuan. The route was very similar to that shown previously for HOHIPT-NH₂ (Scheme 3), but with different coupling conditions at the amine installation step (Scheme 10).
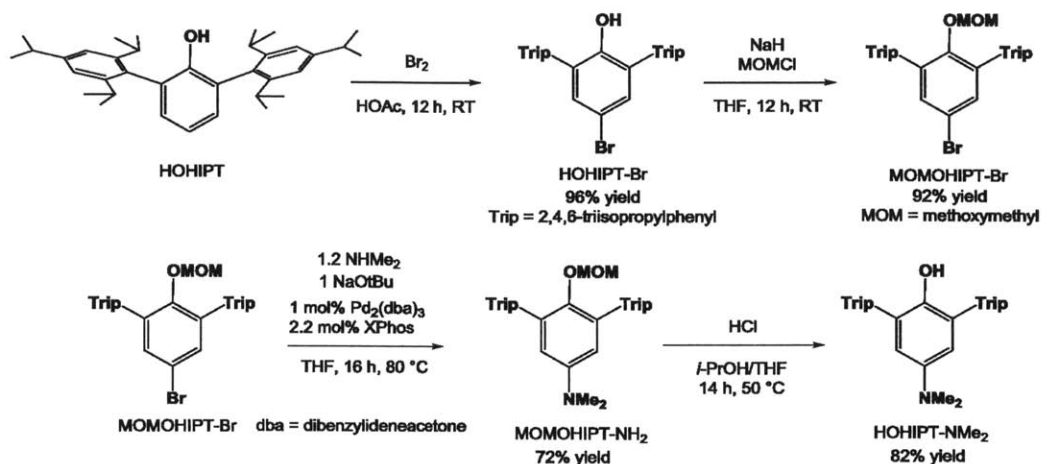
Scheme 10: Synthesis of HOHIPT-NMe₂ (with Dr. Jian Yuan)

With HOHIPT-NMe$_2$ in hand, the next step was to synthesize the homogeneous MAP catalyst (**1-NMe$_2$**) in preparation for immobilization on alumina. In order to make direct comparisons to the parent MAP system and isolate the effects of the dimethylamino group, the unsubstituted metallacyclobutane form of **1** (called **1-C$_3$H$_6$**) was also synthesized according to literature procedures. (The neophylidene complex **1** is very difficult to isolate during workup, while **1-C$_3$H$_6$** readily precipitates from pentane). **1-NMe$_2$** and **1-C$_3$H$_6$** were each treated with calcined (heated to 500 °C under a flow of oxygen) γ-alumina in a pentane suspension to obtain the alumina-bound catalysts **1-NMe$_2$-Al$_2$O$_3$** and **1-C$_3$H$_6$-Al$_2$O$_3$**, respectively. The syntheses of the four catalysts are outlined in Scheme 11.
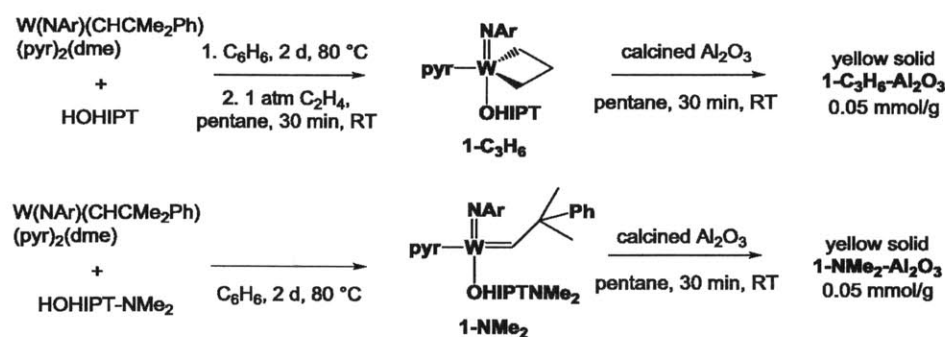
Scheme 11: Syntheses of 1-C$_3$H$_6$, 1-NMe$_2$, 1-C$_3$H$_6$-Al$_2$O$_3$, and 1-NMe$_2$-Al$_2$O$_3$

II-B. Initial homocoupling studies

The four catalysts shown above were used for the metathesis homocoupling of an array of terminal olefin substrates: 1-octene, vinylboronic acid pinacol ester (vinylBpin), allyl benzyl ether, and allylbenzene. These substrates were chosen because they had been studied previously as substrates for Z-selective homocoupling by 1-C$_3$H$_6$ and related complexes.[3] The following reactions were carried out in 1 mL pentane at room temperature for 16 h using 0.025 mmol substrate and 4 mol% catalyst. The results are displayed in Table 3.

	1-C$_3$H$_6$		1-C$_3$H$_6$/Al$_2$O$_3$		1-NMe$_2$		1-NMe$_2$-Al$_2$O$_3$	
Substrate	*% Z*	*% conv.*	*% Z*	*% conv.*	*% Z*	*% conv.*	*% Z*	*% conv.*
1-Octene[a]	94	69	0	0	93	57	30	47
VinylBpin[a]	96	33	78	14	93	42	91[b]	23[b]
Allyl benzyl ether	93	3	83	5	95	4	94	3
Allylbenzene	93	93	31	94	91	66	31	62

Table 3: Homocoupling of various substrates with homogeneous and heterogeneous catalyst systems. [a]Screening by Dr. Jian Yuan. [b]Average of four independent runs

As expected, the homogeneous catalysts 1-C$_3$H$_6$ and 1-NMe$_2$ were able to achieve decent conversion and high levels of Z selectivity in most cases (allyl benzyl ether showed low conversion across the board, perhaps due to substrate oxygen binding to the metal). The alumina-supported versions, however, showed some deviance from expected behavior. In the cases of the nonpolar substrates (1-octene, allylbenzene), the alumina-supported catalysts 1-C$_3$H$_6$-Al$_2$O$_3$ and 1-NMe$_2$-Al$_2$O$_3$ failed to retain any substantial Z selectivity. On the other hand, these catalysts were able to maintain moderate (for 1-C$_3$H$_6$-Al$_2$O$_3$) to good (for 1-NMe$_2$-Al$_2$O$_3$) Z selectivity for the substrates containing polar functional groups (allyl benzyl ether, allylboronic acid pinacol ester). A possible explanation for this phenomenon involves a scenario in which the alumina-bound catalysts are active for metathesis, but are not nearly as Z-selective as their solution analogues. In the presence of polar substrates, some of these surface-bound catalysts may be washed into solution, where they are much more reactive and Z-selective. This leaching would be much less prevalent in systems with nonpolar substrates due to the solubility properties of the catalysts.

II-C. Investigation of catalyst leaching effects

Experiments were performed to determine how much, if any, intact catalyst is released from the alumina surface into solution when the systems were subjected to washes with pentane, diethyl ether, and dichloromethane (see Experimental for details). The washings were analyzed by ^{1}H NMR and the amounts of leached catalyst recovered versus an internal standard were quantified as shown in Table 4.

Solvent	1-C$_3$H$_6$/Al$_2$O$_3$	1-NMe$_2$/Al$_2$O$_3$
Pentane	0% recovered[a]	0% recovered[c]
Diethyl ether	0% recovered[b]	91% recovered[c]
Dichloromethane	0% recovered[b]	93% recovered[c]

Table 4: Catalyst recovery upon washing of supported catalysts with solvents [a] ~0.6 equiv. free HOHIPT observed. [b] ~1.0 equiv. free HOHIPT observed. [c] Screening by Dr. Jian Yuan

These results show that **1-NMe$_2$** is able to bind to alumina as an intact unit that can be washed off and recovered with polar solvent. This is consistent with the theory that the dimethylamino group serves as a primary binding site for the complex on alumina, and that this binding mode is much preferred over possibly destructive modes. **1-C$_3$H$_6$**, on the other hand, undergoes decomposition on the alumina surface, as evidenced by the fact that none of the starting complex could be recovered after washing **1-C$_3$H$_6$-Al$_2$O$_3$** with any of the solvents. Large amounts of free HOHIPT ligand could be observed in the washings of **1-C$_3$H$_6$-Al$_2$O$_3$**, which is further evidence that the covalent structure of **1-C$_3$H$_6$** is altered upon surface binding.

In order to further explore the solvent effects on catalyst behavior, a series of 1-octene and allylbenzene homocouplings were run with the four catalyst systems using different amounts of ether added to the pentane medium. Each reaction was carried out in 1 mL solvent at room temperature for 16 h using 0.025 mmol substrate and 4 mol% catalyst. The results are displayed in Table 5.

45

Entry	Catalyst	Solvent	1-Octene		Allylbenzene	
			%Z	% conv.	%Z	% conv.
1	1-C$_3$H$_6$	Pentane	94	69	93	93
2	1-C$_3$H$_6$	Pentane (1 eq. ether)	95	98	93	41
3	1-C$_3$H$_6$	Pentane (10 eq. ether)	95	48	94	27
4	1-C$_3$H$_6$	Pentane (50 eq. ether)	80	55	82	26
5	1-C$_3$H$_6$	Ether	67	59	42	16
6	1-C$_3$H$_6$-Al$_2$O$_3$	Pentane	N/A	0	31	94
7	1-C$_3$H$_6$-Al$_2$O$_3$	Pentane (1 eq. ether)	47	12	35	1
8	1-C$_3$H$_6$-Al$_2$O$_3$	Pentane (10 eq. ether)	49	42	34	9
9	1-C$_3$H$_6$-Al$_2$O$_3$	Pentane (50 eq. ether)	57	20	37	5
10	1-C$_3$H$_6$-Al$_2$O$_3$	Ether	72	3	N/A	0
11	1-NMe$_2$	Pentane	93	57	91	66
12	1-NMe$_2$	Pentane (1 eq. ether)	90	92	93	53
13	1-NMe$_2$	Pentane (10 eq. ether)	93	87	91	49
14	1-NMe$_2$	Pentane (50 eq. ether)	87	68	87	41
15	1-NMe$_2$	Ether	85	64	77	20
16	1-NMe$_2$-Al$_2$O$_3$	Pentane	30	47	31	62
17	1-NMe$_2$-Al$_2$O$_3$	Pentane (1 eq. ether)	38	70	39	26
18	1-NMe$_2$-Al$_2$O$_3$	Pentane (10 eq. ether)	50	87	49	66
19	1-NMe$_2$-Al$_2$O$_3$	Pentane (50 eq. ether)	67	71	59	33
20	1-NMe$_2$-Al$_2$O$_3$	Ether	92	61	91	72

Table 5: Homocoupling of 1-octene and allylbenzene in pentane/diethyl ether mixtures

The data match fairly well with what would be expected based on the previous observations and hypotheses. For instance, entries 16-20 (1-NMe$_2$-Al$_2$O$_3$) on Table 5 show how the Z content starts at ~30% in pure pentane and rises with the ether concentration to reach a final point of ~90% (in the case of 1-octene) in pure ether, reinforcing the idea that a polar environment causes active and selective 1-NMe$_2$ to be released into solution. The trend is less clear for the cases involving 1-C$_3$H$_6$-Al$_2$O$_3$: entries 6-10 show a more marginal improvement as ether is added for the 1-octene reactions, and the activity and selectivity both remain quite low for allylbenzene. These results are not surprising based on the conclusions from the washing experiments: most or all of the catalyst in 1-C$_3$H$_6$-Al$_2$O$_3$ has undergone decomposition at the surface and is therefore unlikely to regain high Z selectivity even if washed into solution.

A more unexpected trend can be seen upon inspection of the homogeneous trials (entries 1-5 and 11-15): the Z selectivities of both 1-C$_3$H$_6$ and 1-NMe$_2$ decrease as the amount of ether

present in the mixture increases. Because the solvent dependence of Z-selective metathesis processes has not been examined, further study would be needed to make strong claims about the origin of this effect.
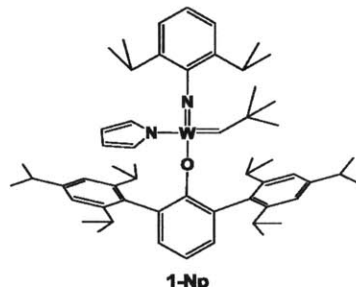
Figure 3:
W(NAr)(CHCMe3)(pyr)(OHIPT)
(1-Np)

One concern that arose during the above studies was that the comparison between **1-C$_3$H$_6$** and **1-NMe$_2$** (and subsequently the comparison between their alumina-supported versions) may be weakened by the difference in hydrocarbyl ligand: **1-C$_3$H$_6$** is a metallacycle, while **1-NMe$_2$** is an alkylidene. To ensure that this distinction was negligible in the context of the above experiments, an analogue of **1-C$_3$H$_6$** with a neopentylidene ligand in place of the metallacycle was synthesized (W(NAr)(CHCMe$_3$)(pyr)(OHIPT), **1-Np**, Figure 3). **1-Np** was synthesized directly from **1-C$_3$H$_6$** and *t*-butylethylene. The alumina-supported version (**1-Np-Al$_2$O$_3$**) was next synthesized using an analogous procedure as for the previous alumina-supported catalysts (Scheme 11). Homocoupling of 1-octene with **1-Np-Al$_2$O$_3$** in pentane (analogous to the experiments in Table 3) gave 15% conversion and 47% Z. Homocoupling of 1-octene with **1-Np-Al$_2$O$_3$** in pentane with 50 equivalents of ether (analogous to entry 9 of Table 5) gave 13% conversion and 64% Z. These results did not differ significantly from the analogous results with **1-C$_3$H$_6$**, indicating that the difference in hydrocarbyl ligand has a minimal effect on the system. Additionally, the washing experiments were repeated (using pentane and ether) on **1-Np-Al$_2$O$_3$**, with almost identical results as for **1-C$_3$H$_6$-Al$_2$O$_3$** (Table 4): no catalyst leaching with either solvent, 0.6 equivalents HOHIPT washed through with pentane, and 1.0 equivalents HOHIPT washed through with ether. The close matching of the behavior between **1-C$_3$H$_6$-Al$_2$O$_3$** and **1-Np-Al$_2$O$_3$** supports the assumption that the comparison of **1-C$_3$H$_6$-Al$_2$O$_3$** and **1-NMe$_2$-Al$_2$O$_3$** is valid despite the difference in hydrocarbyl ligand.

The preponderance of the data and observations lead to the following conclusions. First, **1-NMe$_2$** behaves in a similar manner (with regard to activity and Z selectivity) to **1-C$_3$H$_6$** for the homogeneous homocoupling metathesis of selected substrates. The behavior of these catalysts when adsorbed to alumina, on the other hand, differs substantially. While **1-NMe$_2$** appears to bind to alumina while remaining structurally intact, **1-C$_3$H$_6$** undergoes decomposition on the surface, releasing HOHIPT. **1-NMe$_2$-Al$_2$O$_3$** and **1-C$_3$H$_6$-Al$_2$O$_3$** both show poor Z-selectivity in

nonpolar environments, with increasing selectivity in gradually more polar environments. This trend is attributed to leaching of intact catalyst from the surface back into solution, especially in the case of **1-NMe₂-Al₂O₃**, where nearly all of the catalyst could be washed off and recovered by polar solvent. The difference in leaching behavior between **1-NMe₂-Al₂O₃** and **1-C₃H₆-Al₂O₃** suggests that the dimethylamino group of **1-NMe₂** plays a role in the complex's binding to alumina, making the binding reversible and non-destructive. **1-C₃H₆**, with no convenient Lewis basic group for alumina binding, instead undergoes destructive decomposition on the surface. Ultimately, the strictly surface-bound form of each catalyst is incapable of retaining the Z selectivity displayed by its homogeneous parent. Thus, while alumina-supported olefin metathesis catalysts were formed, the original goal of heterogeneous Z-selective MAP catalysts remains unmet.

CONCLUSIONS

While MAP complexes have repeatedly shown the ability to perform Z-selective metathesis in solution, the above studies show that there are numerous complicating factors associated with the creation of solid-supported analogues. Attempts to immobilize a functionalized version of **1** via covalent tethering to silica with pendant functional groups were largely unsuccessful. In one case, the urea linking strategy was found to be problematic due to side reactions between the W catalyst precursor and the urea functionality. An attempt to circumvent this problem by forming an all-carbon linker via olefin metathesis also met with problems. Control experiments revealed that the passivated silica surface still retained enough reactivity to destroy catalyst precursors and even MAPs themselves, creating reactive but non-selective surface species.

The use of alumina as a support for MAP catalysts met with more success. The previously studied interaction between a dimethylamino group on the ligand periphery and Lewis acidic sites on calcined γ-alumina allowed for **1-NMe₂** to bind to alumina in a non-destructive manner. **1-C₃H₆**, which has no Lewis basic binding site, was largely destroyed upon treatment with alumina, as evidenced by the presence of free HOHIPT ligand in solution afterward. The binding of **1-NMe₂** to alumina was shown to be reversible, as nearly all of the homogeneous catalyst could be recovered by washing with polar solvents. Despite the desirable binding properties, however, the surface-bound catalysts did not show the ability to maintain high Z

selectivity for homocoupling of terminal olefins. Homocoupling studies in solvent media of varying polarity revealed that more polar environments led to increased Z selectivity, but this trend was ascribed to washing of surface MAP catalysts into solution, where they are known to be selective.

These studies have made clear some important issues to be considered when attempting to synthesize functional solid-supported organometallic catalysts. First, careful control experiments should be performed to ensure that the catalyst precursor reacts exclusively with desired surface sites. The choice of support and passivation method becomes crucial, and each type of organometallic precursor may require different decisions on this front. The reactivity of our W precursors with the supposedly passivated silica surface and the destruction of $1\text{-}C_3H_6$ on alumina reinforce this concept. Second, it cannot be assumed that the reactivity and selectivity profiles of an organometallic catalyst will be preserved in a solid-supported analogue. The comparison between the high Z selectivity of $1\text{-}NMe_2$ and the low Z selectivity of $1\text{-}NMe_2\text{-}Al_2O_3$ is an excellent example: although the structure of $1\text{-}NMe_2$ is not destroyed upon alumina binding, the metathesis reactions that take place at the surface-bound catalyst are still affected. Finally, any catalytic results from a heterogeneous system must be scrutinized to ensure that the reactions are actually happening on the surface rather than in solution by leached catalyst. Our homocoupling studies in varying solvent environments demonstrate this concept well: the observed increases in Z selectivity could reasonably be attributed to conditions in which more catalyst could be washed off of the surface and into solution.

The advantages of heterogeneous catalysts are great: ease of product separation, construction of flow reactors, catalyst reusability, and decreased bimolecular decomposition are all of substantial value to researchers on large and small scales. Therefore, creating solid-supported versions of reactive and selective organometallic catalysts remains of great interest. The results presented here provide both some promising avenues and some cautionary insight in the areas of silica- and alumina-supported olefin metathesis catalysts. It is our hope that these studies will help to lay the groundwork for more successful endeavors in the future.

EXPERIMENTAL

General Comments

All manipulations of air- and moisture-sensitive materials were performed in oven-dried (200 °C) or flame-dried glassware on a dual-manifold Schlenk line or a Vacuum Atmospheres glovebox with nitrogen atmosphere. NMR measurements of air- and moisture-sensitive materials were carried out in Teflon-valve-sealed J. Young-type NMR tubes. Anhydrous ether, pentane, toluene, THF, benzene, and CH_2Cl_2 were sparged with nitrogen and passed through activated alumina prior to use. Chloroform-d was stored over molecular sieves. 1,4-dioxane was dried over sodium/benzophenone ketyl, degassed twice by freeze-pump-thaw cycle, vacuum transferred, degassed by freeze-pump-thaw once more, and finally stored over molecular sieves. Allyl tosyl amide was prepared from allyl amine and tosyl chloride, and recrystallized from a concentrated solution of hexanes and diethyl ether. 1-Octene, allylbenzene, and allylboronic acid pinacol ester, were dried over CaH_2 and vacuum transferred. 5-Hexenyltri(ethoxy)silane was purchased from Gelest and used as received. Allyl benzyl ether was dried over CaH_2 and distilled. $HN(TMS)_2$, phenyl isocyanate, 3-(triethoxysilyl)propyl isocyanate, tetraethoxysilane, anthracene, Surfactant P_{123}, CH_3OCH_2Cl, 2.0 M $HNMe_2$ in THF, 4,4'-t-butyl-biphenyl, and 0.5 M NH_3 in 1,4-dioxane were purchased from Aldrich and used as received. XPhos, SPhos, t-BuDavePhos, Pd_2dba_3, $Pd(OAc)_2$, 1.6M n-BuLi in hexanes, Grubbs I, Grubbs II, and $Rh(PPh_3)_3Cl$ were purchased from Strem and used as received. The following compounds were prepared according to literature procedures: HOHIPT,[13] $W(NAr)(CHCMe_2Ph)(pyr)_2(dme)$,[7] $Mo(NAr)(CHCMe_2Ph)(OR_{F6})_2$,[17] $Mo(NAr)(CHCMe_2Ph)(Me_2pyr)(OTPP)$,[18] $W(NAr)(C_3H_6)(pyr)(OHIPT)$ (1),[2] MeOHIPT-Br[19] and HOHIPT-PVP.[16] 3-(isocyanato)propyl silica (NCO-silica) was synthesized from 3-aminopropylsilica according to a literature procedure.[8] 3-amino-propylsilica was synthesized according to a separate literature procedure.[11] γ-alumina was purchased from Strem and calcined as described below. NMR spectra were obtained on Varian spectrometers operating at either 300 MHz or 500 MHz. NMR chemical shifts are reported as ppm relative to tetramethylsilane, and are referenced to the residual proton or ^{13}C signal of the solvent (^1H $CDCl_3$: 7.27 ppm, ^1H C_6D_6: 7.16 ppm, ^{13}C $CDCl_3$: 77.16 ppm, ^{13}C C_6D_6, 128.06 ppm).

Experimental procedures for ligand synthesis

HOHIPT-Br

HOHIPT (10.2 g, 20.4 mmol) was dissolved in acetic acid (200 mL). Bromine (1.57 mL, 30.7 mmol) was added at room temperature. A yellow precipitate formed in a few minutes. After 16 h, Na_2SO_3 solution (10%, 200 mL) was added to quench excess Br_2. The off-white solid was filtered off and washed with water (3 mL). The solid was dissolved in Et_2O (300 mL) and the solution was washed with water and dried with $MgSO_4$. The $MgSO_4$ was filtered off and the ether removed to give the product as an off-white solid. The product was recrystallized from Et_2O/hexane to give white crystals; yield: 11.28 g (96%). ^1H NMR (500 MHz, $CDCl_3$, 20 °C): δ [ppm] 7.23 (s, 2H, ArH of phenol ring), 7.10 (s, 4H, ArH of Trip), 4.57 (s, 1H, OH), 2.95 (sept, J_{HH} = 7 Hz, 2H, p-CHMe$_2$), 2.70 (sept, J_{HH} = 7 Hz, 4H, o-CHMe$_2$),1.30 (d, J_{HH} = 7 Hz, 12H, CHMe_2), 1.17 (d, J_{HH} = 7 Hz, 12H, CHMe_2), 1.09 (d, J_{HH} = 7 Hz, 12H, CHMe_2); ^{13}C NMR (125 MHz, $CDCl_3$, 20 °C): δ [ppm] 150.46, 149.43, 147.72, 132.54, 129.65, 128.83, 121.42, 112.23, 34.51, 30.92, 24.47 24.21; HR-MS: m/z = 577.3040, calcd for $C_{36}H_{50}OBr$ [M+H]$^+$: 577.3045.

MOMOHIPT-Br

A 250-mL round bottom flask was charged with a stir bar and brought into a glovebox along with a septum. To the flask was added 0.787 g (31.2 mmol, 1.8 equiv.) 95% NaH and 20 mL anhydrous THF. The flask was sealed with the septum and brought out of the glovebox. A separate dried 250-mL round-bottom flask was cooled under N_2, charged with 10.0 g HOHIPT-Br (17.3 mmol, 1.0 equiv.) and 120 mL anhydrous THF, and swirled until the HOHIPT-Br dissolved. The HOHIPT-Br solution was transferred into the flask containing NaH via syringe under N_2. This mixture was stirred under N_2 at room temperature for 22 h (12 h should be sufficient, however). The solution changed to reddish during this time. After the stirring time, 2.37 mL CH_3OCH_2Cl (MOMCl, 31.2 mmol, 1.8 equiv.) was added by syringe. The solution changed to light yellow. The solution was stirred at room temperature for 3 h, then quenched with 200 mL water. Next, 150 mL CH_2Cl_2 was added, and the solution was shaken and separated in a separatory funnel. The aqueous layer was extracted with 2 x 125 mL CH_2Cl_2. The combined organic layer was washed with 2 x 200 mL water and 200 mL brine. The organic layer was dried over $MgSO_4$, filtered and evaporated in $vacuo$ to obtain 9.96 g (92.6%) product. ^1H NMR (500

MHz, CDCl$_3$, 20°C): δ [ppm] 7.31 (s, 2H, (Trip)$_2$BrC$_6$$H_2$OMOM), 7.04 (s, 4H, ((i-Pr)$_3$C$_6$$H_2$)$_2$), 4.16 (s, 2H, OC$H_2OCH_3$), 2.91 (sept, 2H, 4', 4''-CH(CH$_3$)$_2$, J$_{HH}$ = 7 Hz), 2.68 (sept, 4H, 2', 6', 2'', 6''-CH(CH$_3$)$_2$, J$_{HH}$ = 7 Hz), 2.39 (s, 3H, OCH$_2$OCH_3), 1.27 (d, 12H, i-Pr-CH_3, J$_{HH}$ = 7 Hz), 1.19 (d, 12H, i-Pr-CH_3, J$_{HH}$ = 7 Hz), 1.14 (d, 12H, i-Pr-CH_3, J$_{HH}$ = 7 Hz). ^{13}C{^{1}H} NMR (125 MHz, CDCl$_3$, 20°C): δ [ppm] 151.87, 148.99, 147.15, 136.80, 133.55, 132.07, 121.06, 116.20, 97.25, 55.47, 34.65, 31.21, 25.81, 24.46, 23.54. HR-MS (ESI): m/z = 638.3567, calcd for C$_{38}$H$_{57}$NO$_2$Br [M + NH$_4$]$^+$: 638.3573.

MOMOHIPT-NH$_2$

The following synthesis is based on a literature report.[14] A 300-mL Schlenk bomb, a stir bar, a graduated cylinder, and 2.49 g (4.0 mmol, 1.0 equiv.) MOMOHIPT-Br were brought into a glovebox. To the bomb was added the MOMOHIPT-Br, 36.6 mg Pd$_2$dba$_3$ (0.04 mmol, 2 mol% Pd), 68.2 mg t-BuDavePhos (0.20 mmol, 5 mol%), 0.538 g sodium t-butoxide (5.6 mmol, 1.4 equiv.), 64 mL 1,4-dioxane and the stir bar. The bomb was sealed and brought out of the glovebox. While flushing with N$_2$, 40 mL 0.5 M NH$_3$ in 1,4-dioxane was added to the bomb by syringe. The bomb was sealed and heated at 80 °C with stirring in an oil bath for 4 h. It was then cooled to room temperature and 100 mL ethyl acetate was added. The solution was filtered through a plug of silica and the solvent was removed in vacuo. The crude residue was dry-loaded onto a silica column, and the column was run using 2.5% ethyl acetate in hexanes as the eluent. The second major compound to elute was the product; 1.37 g (61.4%) was isolated. ^{1}H NMR (500 MHz, CDCl$_3$, 20 °C,): δ [ppm] 7.02 (s, 4H, ((i-Pr)$_3$C$_6$$H_2$)$_2$), 6.51 (s, 2H, (Trip)$_2NH_2C_6$$H_2$OMOM), 4.09, (s, 2H, OC$H_2OCH_3$), 3.55 (br s, 2H, N$H_2$), 2.90, (sept, 2H, 4', 4''-CH(CH$_3$)$_2$, J$_{HH}$ = 7 Hz), 2.80 (sept, 4H, 2', 6', 2'', 6''-CH(CH$_3$)$_2$, J$_{HH}$ = 7 Hz), 2.36 (s, 3H, OCH$_2$OCH_3), 1.26 (d, 12H, i-Pr-CH_3, J$_{HH}$ = 7 Hz), 1.19 (d, 12H, i-Pr-CH_3, J$_{HH}$ = 7 Hz), 1.13 (d, 12H, i-Pr-CH_3, J$_{HH}$ = 7 Hz). ^{13}C{^{1}H} NMR (125 MHz, CDCl$_3$, 20°C): δ [ppm] 148.29, 147.15, 144.92, 141.60, 135.52, 133.45, 120.84, 117.67, 97.23, 55.20, 34.61, 31.03, 26.02, 24.49, 23.61. HRMS: found [M + H]$^+$: 558.4311. calcd for C$_{38}$H$_{56}$NO$_2$ [M + H]$^+$: 558.4306.

HOHIPT-NH$_2$

This synthesis is based on a literature report.[20] 2.37 g MOMOHIPT-NH$_2$ (4.25 mmol, 1.0 equiv.) was placed in a 150-mL screw-cap bomb with stir bar. To the bomb was added 35 mL isopropanol, 35 mL THF, and 20 mL concentrated HCl. The bomb was sealed, stirred, and

heated at 45 °C in an oil bath for 14 h. The solution was allowed to cool to room temperature and the solvents removed *in vacuo* until only some water and crude solid remained. To this residue was added 75 mL H$_2$O and 75 mL CH$_2$Cl$_2$. The aqueous layer was neutralized to about pH 7 with solid NaHCO$_3$. The mixture was then added to a separatory funnel, shaken and separated. The aqueous layer was extracted with 2 x 75 mL CH$_2$Cl$_2$. The combined organic layer was washed with 2 x 100 mL H$_2$O and 100 mL brine. The organic layer was dried over MgSO$_4$, filtered, and evaporated *in vacuo*. The residue still contained a small amount of high-boiling liquid impurity, but the bulk was a tan solid. The residue was prepared as a dry-load for a silica column. The column was run using 4% ethyl acetate in hexanes as the eluent. The second major compound to elute was the product; 1.16 g (53% yield) was isolated. ^{1}H NMR (500 MHz, CDCl$_3$, 20°C): δ [ppm] 7.10 (s, 4H, ((*i*-Pr)$_3$C$_6$*H$_2$*)$_2$), 6.51 (s, 2H, (Trip)$_2$NH$_2$C$_6$*H$_2$*OH), 4.15 (br s, 1H, O*H*), 3.45, (br s, 2H, N*H$_2$*), 2.95, (sept, 2H, 4', 4''-C*H*(CH$_3$)$_2$, J$_{HH}$ = 7 Hz), 2.84 (sept, 4H, 2', 6', 2'', 6''-C*H*(CH$_3$)$_2$, J$_{HH}$ = 7 Hz), 1.32, (d, 12H, *i*-Pr-C*H$_3$*, J$_{HH}$ = 7 Hz), 1.17 (d, 12H, *i*-Pr-C*H$_3$*, J$_{HH}$ = 7 Hz), 1.10 (d, 12H, *i*-Pr-C*H$_3$*, J$_{HH}$ = 7 Hz). ^{13}C{^{1}H} NMR (125 MHz, CDCl$_3$, 20°C): δ [ppm] 148.83, 147.84, 144.50, 138.82, 131.40, 127.35, 121.31, 117.48, 34.58, 30.86, 24.65, 24.41, 24.35. HRMS: found [M + H]$^+$: 514.4043. Calcd for C$_{36}$H$_{52}$NO [M + H]$^+$: 514.4043.

MeOHIPT-NH$_2$

To a 100 mL Schlenk bomb in a glovebox were added a magnetic stir, 1.78 g MeOHIPT-Br[19] (3.00 mmol, 1.00 equiv.), 0.404 g sodium t-butoxide (4.2 mmol, 1.4 equiv.), 27.5 mg Pd$_2$dba$_3$ (0.03 mmol, 2 mol% Pd) , 51.2 mg *t*-BuDavePhos (0.15 mmol, 5 mol%) , and 48 mL 1,4-dioxane. The bomb was sealed and brought outside the glovebox, where 30 mL of a 0.5 M solution of NH$_3$ in 1,4-dioxane (15.0 mmol, 5.0 equiv.) was added to the bomb under a flow of N$_2$. The bomb was resealed and stirred in an oil bath at 80 °C for 4 h. At this point the solution was a brownish green color. The bomb was then opened in air, and the contents diluted by half with ethyl acetate. The resulting solution was filtered through a plug of silica and the filtrate concentrated down to a brown oil. This oil was purified by flash column chromatography using silica gel (3% ethyl acetate in hexanes). The first fraction (red) is diarylated side product, and the second fraction is the desired product. Yield: 0.99 g (62%) ^{1}H NMR (500 MHz, CDCl$_3$, 20 °C): δ [ppm] 7.04 (s, 4H, ((*i*-Pr)$_3$C$_6$*H$_2$*)$_2$), 6.45 (s, 2H, (Trip)$_2$(OCH$_3$)(NH$_2$)C$_6$*H$_2$*), 3.50 (br s, 2H, N*H$_2$*), 2.98 (s, 3H, OC*H$_3$*), 2.93 (sept, 2H, 4', 4''-C*H*(CH$_3$)$_2$), 2.83 (sept, 4H, 2', 6', 2'', 6''-

CH(CH$_3$)$_2$), 1.30 (d, 12H, i-Pr-CH_3), 1.16 (d, 12H, i-Pr-CH_3), 1.14 (d, 12H, i-Pr-CH_3). ^{13}C{^{1}H} NMR (125 MHz, CDCl$_3$, 20°C): δ [ppm] 148.87, 147.73, 146.65, 140.69, 134.10, 133.64, 120.66, 117.70, 59.60, 34.28, 30.77, 25.53, 24.22, 23.61.

MOMOHIPT-NMe$_2$

This synthesis was first developed by Dr. Jian Yuan. Pd$_2$dba$_3$ (124.5 mg, 0.136 mmol, 4% mol) and X-Phos (129 mg, 0.271 mmol, 8 mol%) were dissolved in THF (4 mL) and the mixture was stirred for 1 h. MOMOHIPT-Br (2.11 g, 3.39 mmol, 1.0 equiv.) and sodium t-butoxide (423.1 mg, 4.41 mmol, 1.3 equiv.) were suspended in THF (10 mL) in a Schlenk bomb. The Pd solution was added to this mixture to give a purple solution. Dimethylamine (2.04 mL, 2 M in THF, 4.08 mmol) was added and the mixture was heated to 80 °C. A white precipitate formed after a few minutes. After 1 d, the solution was cooled to room temperature and filtered through a silica gel and washed with ethyl acetate to give an orange solution. All volatiles were removed from the filtrate to yield a light orange oil product. Chromatographic separation (1% ethyl acetate in hexanes, silica column) gave a pure off-white solid product; yield: 1.442 g (72%). ^{1}H NMR (500 MHz, CDCl$_3$, 20 °C): δ [ppm] 7.04 (s, 4H, ArH of trip), 6.54 (s, 2H, ArH of phenol ring), 4.11 (s, 2H, OCH$_2$O), 2.92 (sept, J$_{HH}$ = 7 Hz, 2H, p-CHMe$_2$), 2.91 (s, 6H, NMe_2), 2.82 (sept, J$_{HH}$ = 7 Hz, 4H, o-CHMe$_2$), 2.38 (s, 3H, OCH_3), 1.28 (d, J$_{HH}$ = 7 Hz, 12H, CHMe_2), 1.20 (d, J$_{HH}$ = 7 Hz, 12H, CHMe_2), 1.16 (d, J$_{HH}$ = 7 Hz, 12H, CHMe_2); ^{13}C NMR (125 MHz, CDCl$_3$, 20 °C): δ [ppm] 147.9, 147.0, 146.1, 143.3, 134.7, 134.0, 120.7, 115.0, 97.1 (OCH$_2$-O), 54.9 (MeO), 41.2 (NMe$_2$), 34.4, 30.9, 25.9, 24.3, 23.4; HRMS: Found m/z = 586.4623, calcd for C$_{40}$H$_{60}$NO$_2$ [M+H]$^+$: 586.4624.

HOHIPT-NMe$_2$

This synthesis was first developed by Dr. Jian Yuan. MOMOHIPT-NMe$_2$ (5.00 g, 8.55 mmol) was dissolved in THF (40 mL). Isopropyl alcohol (20 mL) and HCl (30 mL) were added at room temperature. The mixture was heated to 50 °C in a Schlenk bomb. A precipitate formed in a few minutes. After 12 h, the mixture became a clear solution and the solvent was removed under vacuum. Dichloromethane (200 mL) and water (200 mL) were added. The organic layer was separated and washed with water until the pH reached 5–6. The organic part was washed with brine and dried with MgSO$_4$. After filtration, removal of solvent gave an off-white solid. Chromatographic separation (silica column) gave a pure off-white solid product; yield: 3.81 g

(82%). ^{1}H NMR (500 MHz, CDCl$_3$, 20 °C): δ [ppm] 7.10 (s, 4H, ArH of trip), 6.55 (s, 2H, ArH of phenol ring), 4.05 (s, 1H, HO), 2.95 (sept, J$_{HH}$ = 7 Hz, 2H, p-CHMe$_2$), 2.88 (s, 6H, NMe$_2$), 2.82 (sept, J$_{HH}$ = 7 Hz, 4H, o-CHMe2), 1.32 (d, J$_{HH}$ = 7 Hz, 12H, CHMe$_2$), 1.17 (d, J = 7 Hz, 12H, CHMe$_2$), 1.10 (d, J$_{HH}$ = 7 Hz, 12H, CHMe$_2$); ^{13}C NMR (125 MHz, CDCl$_3$, 20 °C): δ [ppm] 148.6, 147.0, 144.4, 143.3, 131.87, 121.2, 115.2, 41.7 (NMe$_2$), 34.4, 30.8, 24.6, 24.4, 24.2; Anal. Calcd for C$_{38}$H$_{55}$NO: C 84.23, H 10.23, N 2.58; found: C 84.19, H 9.96, N 2.70.

HOHIPT-urea-phenyl (3-OH)

A 50-mL oven-dried Schlenk bomb was cooled under N$_2$ and charged with 100 mg HOHIPT-NH$_2$ (0.195 mmol), 26.5 μL phenylisocyanate (0.243 mmol), a stir bar, and 20 mL anhydrous THF. The bomb was sealed and heated with stirring at 50 °C in an oil bath for 15 h. The solution was allowed to cool to room temperature and the solvent was evaporated *in vacuo* to leave residue, which was prepared as a silica dry-load for a column. The column was run with 8% ethyl acetate in hexanes as the eluent. The second major compound to elute was the product. 0.109 g product (89%) was isolated. ^{1}H NMR (500 MHz, C$_6$D$_6$, 20 °C): δ [ppm] 7.34-7.26 (m, 11H, ArH, partly obscured by solvent peak), 6.46 (br s, 1H, HIPT-NHC(O)NHPh), 6.33 (br s, 1H, HIPT-NHC(O)NHPh), 4.58 (s, 1H, OH), 2.94 (sept, 2H, 4', 4''-CH(CH$_3$)$_2$, J$_{HH}$ = 7 Hz), 2.74 (sept, 4H, 2', 6', 2'', 6''-CH(CH$_3$)$_2$, J$_{HH}$ = 7 Hz), 1.30 (d, 12H, *i*-Pr-CH$_3$, J$_{HH}$ = 7 Hz), 1.16 (d, 12H, *i*-Pr-CH$_3$, J$_{HH}$ = 7 Hz), 1.11 (d, 12H, iPr-CH$_3$, J$_{HH}$ = 7 Hz).

MeOHIPT-urea-phenyl (3-OMe)

A 50-mL oven-dried Schlenk bomb was cooled under N$_2$ and charged with 200 mg MeOHIPT-NH$_2$ (0.38 mmol), 51.6 μL phenylisocyanate (0.47 mmol), a stir bar, and 25 mL anhydrous THF. The bomb was sealed and heated with stirring at 50 °C in an oil bath for 3 h. The solution was allowed to cool to room temperature and the solvent was evaporated *in vacuo* to leave residue, which was prepared as a silica dry-load for a column. The column was run with 8% ethyl acetate in hexanes as the eluent. The second major compound to elute was the product. 0.138 g product (56%) was isolated. ^{1}H NMR (500 MHz, C$_6$D$_6$, 20°C): δ [ppm] 7.32-7.29 (m, 4H, ArH), 7.11-7.07 (m, 3H, ArH), 7.05 (s, 4H ((*i*-Pr)$_3$C$_6$H$_2$)$_2$), 6.44 (br s, 1H, HIPT-NHC(O)NHPh), 6.40 (br s, 1H, HIPT-NHC(O)NHPh), 3.08 (s, 1H, OH), 2.94 (sept, 2H, 4', 4''-CH(CH$_3$)$_2$, J$_{HH}$ = 7 Hz), 2.76 (sept, 4H, 2', 6', 2'', 6''-CH(CH$_3$)$_2$, J$_{HH}$ = 7 Hz), 1.30 (d, 12H, *i*-Pr-CH$_3$, J$_{HH}$ = 7 Hz), 1.18 (d, 12H, *i*-Pr-CH$_3$, J$_{HH}$ = 7 Hz), 1.14 (d, 12H, *i*-Pr-CH$_3$, J$_{HH}$ = 7 Hz).

Experimental procedures for catalysts and silica/alumina-based species

HOHIPT-urea-silica (2)

In a dried 50-mL round bottom flask under N_2 were combined 200 mg HOHIPT-NH$_2$ (0.39 mmol), 0.557 g 3-(isocyanato)propyl-silica (0.39 mmol NCO), ~70 mg anthracene (int. std.), and 25 mL anhydrous toluene. An aliquot for initial ratio against internal standard by ^{1}H NMR was taken. The mixture was refluxed under N_2 at 110 °C for 66 h. An aliquot taken for ^{1}H NMR showed 27% disappearance of HOHIPT-NH$_2$; this was interpreted as 27% conversion into product. The product was isolated by filtration, washing several times with CH$_2$Cl$_2$ and hexanes. The product was dried under vacuum. Estimated loading of HOHIPT: 0.175 mmol/g (was combined with another batch to make loading 0.133 mmol/g overall).

2-W

In a vial in the glovebox was placed 35.9 mg W(NAr)(CHCMe$_2$Ph)(pyr)$_2$(dme) (0.05 mmol), ~5 mg anthracene (internal standard), a stir bar, and 2 mL C$_6$D$_6$. An initial NMR ratio aliquot was taken. To the vial was added 376 mg 2 (0.05 mmol HOHIPT). The mixture was stirred for 4 h at room temperature. ^{1}H NMR spectroscopy of the mixture showed disappearance of all alkylidene; this was interpreted as 100% conversion to surface species. The solution was filtered to get orange-colored solid, which was washed with alternating portions of ether and pentane. The solid was dried to obtain 304 mg (75%) product. Estimated loading: 0.124 mmol W/g.

Observation of 3-OH-W

To a vial in the glovebox were added a stir bar, 35.9 mg W(NAr)(CHCMe$_2$Ph)(pyr)$_2$(dme) (0.05 mmol), 31.6 mg 3-OH (0.05 mmol), and 1 mL C$_6$D$_6$. The mixture was allowed to stir at room temperature for 38 h, after which time the ^{1}H NMR spectrum showed the presence of new alkylidene peaks at 12.075 ppm, 11.992 ppm, 11.941 ppm, and 10.836 ppm, with broad minor signals at 9.882 ppm and 9.204 ppm.

Observation of 3-OMe-W

To a vial in the glovebox were added a stir bar, 35.9 mg W(NAr)(CHCMe$_2$Ph)(pyr)$_2$(dme) (0.05 mmol), 32.3 mg 3-OMe (0.05 mmol), and 1 mL C$_6$D$_6$.

The mixture was allowed to stir at room temperature for 2.5 h, after which time the ^{1}H NMR spectrum showed the presence of new alkylidene peaks at 12.087 ppm, 12.011 ppm, 11.937 ppm, and 11.034 ppm, with broad signals at 9.983 ppm and 9.398 ppm.

TMS-capped 5-hexenyl-silica SBA-15 (hex-silica)

This procedure was based on a literature report.[11] To a 350-ml screw-cap bomb were added a stir bar, 300 mL 1.6M HCl solution in water, 1.0 g 5-hexenyltri(ethoxy)silane (4.0 mmol, 1.0 equiv), 16.9 mL tetra(ethoxy)silane (76.0 mmol, 19.0 equiv.), and 8.0 g Surfactant P_{123}. The bomb was sealed and stirred at 35 °C in an oil bath for 24 h, after which time the heat was increased to 100 °C. After 24 h of stirring at 100 °C, the solution was allowed to cool to room temperature and filtered, washing with water and ethanol. The solid was further washed in a thimble in a Soxhlet setup with refluxing ethanol for 2 d. After cooling to room temperature, the mixture was filtered and the solid washed with hexanes. The solid was then placed in a 100-mL round-bottom flask with 60 mL hexanes and a stir bar. To this flask was added 5.0 mL HN(TMS)$_2$ (23.9 mmol). The flask was equipped with a water-cooled reflux condenser and the mixture was refluxed under N$_2$ for 24 h. The contents of the flask were cooled to room temperature and filtered, washing with ethanol, CH$_2$Cl$_2$, and pentane. The resulting solid was dried *in vacuo* with heating. Estimated loading of hexenyl groups: 0.778 mmol/g.

TMS-Capped hydrogenated hexenyl-silica SBA-15 (hyd-silica)

Into a vial in a glovebox were placed 250 mg hex-silica (0.195 mmol), 5 mL benzene, a stir bar, and 7.2 mg Rh(PPh$_3$)$_3$Cl (0.0078 mmol). This vial was placed into a Parr bomb, which was sealed and brought out of the glovebox. The bomb was attached through a Schlenk line to a tank of H$_2$. The contents of the bomb were stirred at RT for 15 h under 20 atm of H$_2$. After this time, the bomb was opened, the contents filtered, and the resulting solid washed with CH$_2$Cl$_2$, toluene, methanol, and ether until it appeared white. The product was dried *in vacuo*.

TMS-capped silica SBA-15 (TMS-capped silica)

This synthesis followed exactly the synthesis of hex-silica, except pure tetra(ethoxy)silane was used instead of the mixture of silanes. The product was dried *in vacuo* at 80 °C.

General procedure for cross-metathesis screening for attachment of HOHIPT-PVP to hex-silica

Into a vial in the glovebox was placed 30.0 mg HOHIPT-PVP (.05 mmol), a stir bar, ~5 mg anthracene (int. std.), and 2 mL C_6D_6. An initial ^1H NMR spectrum of ratios was taken. To the vial was added 64.3 mg hex-silica (0.05 mmol olefin) and .0025 mmol catalyst (as solid or stock solution). The contents of the vial were then stirred at room temperature for the allotted time, after which a ^1H NMR spectrum was taken to quantify conversion.

4

The above general procedure for cross-metathesis screening was carried out using Grubbs II as the catalyst. The conversion of HOHIPT-PVP was 79%, but this could be accounted for by the presence of the metathesis homocoupled product rather than by surface attachment. After 19 h, 6.25 µL 1-hexene was added to cleave any surface-bound alkylidenes. The mixture was filtered and the solid washed with ether and pentane before drying to obtain 43.3 mg product.

4-W

Into a vial in the glovebox was placed 20.0 mg W(NAr)(CHCMe$_2$Ph)(pyr)$_2$(dme) (0.028 mmol) and ~5 mg anthracene (int. std.). An initial ^1H NMR spectrum was taken. The contents of the vial were added to a Schlenk tube along with 43.3 mg **5** and a stir bar. The tube was sealed, brought out of the glovebox, and the contents stirred and heated to 60 °C in an oil bath for 20 h. ^1H NMR of the supernatant showed a complete absence of alkylidenes: total loading onto surface was assumed. After this time, the tube was cooled to room temperature and the contents filtered. The resulting yellow solid was washed with pentane and ether and subsequently dried in vacuo to obtain 36.5 mg product. The metal loading was an estimated 0.550 mmol W/g.

W(NAr)(CHCMe$_2$Ph)(pyr)(OHIPT-NMe$_2$)

This synthesis was first developed by Dr. Jian Yuan. W(NAr)(CHCMe$_2$Ph)(pyr)$_2$(dme) (260 mg, 0.366 mmol, 1.0 equiv) was dissolved in benzene (~25 mL) in a Schlenk bomb. HO-HIPTNMe$_2$ (198 mg, 0.366 mmol, 1.0 equiv.) was added at room temperature. The mixture was heated at 80 °C for two days. The solvent was removed under vacuum and the residue was extracted into pentane. The solvent was removed under vacuum to give a yellow foam. Recrystallization of the crude product from pentane gave an analytically pure orange product;

yield: 225 mg (56%). ^{1}H NMR (500 MHz, C$_6$D$_6$, 20 °C): δ [ppm] 9.90 (s, 1H, W=CH), 7.36 (s, 2H, Ar-H), 7.24 (s, 2H, Ar-H), 7.16–7.12 (m, 4H, Ar-H), 7.01–6.92 (m, 4H, Ar-H), 6.39 (s, 2H, Ar-H), 6.10 (s, 2H, Pyr-H), 5.91 (s, 2H, Pyr-H), 3.13 (sept, 2H, J$_{HH}$ = 7 Hz, CHMe$_2$), 3.07 (sept, 2H, J$_{HH}$ = 7 Hz, CHMe$_2$), 2.89 (sept, 2H, J$_{HH}$ = 7 Hz, CHMe$_2$), 2.85 (sept, 2H, J$_{HH}$ = 7 Hz, CHMe$_2$), 2.36 (s, 6H, NMe_2), 1.31 (d, 6H, J$_{HH}$ = 7 Hz, CH$Me2$), 1.28 (d, 6H, J$_{HH}$ = 7 Hz, CH$Me2$), 1.20–1.12 (m, 30 H), 1.07 (d, 12H, J$_{HH}$ = 7 Hz, CHMe_2); ^{13}C NMR (125 MHz, C$_6$D$_6$, 20 °C): δ [ppm] 262.9 (Mo=C), 152.2, 151.1, 150.7, 148.5, 147.6, 147.3, 145.8, 134.7, 131.9, 128.4, 126.3, 126.1, 125.0, 122.9, 122.4, 121.7, 120.9, 115.4, 52.4, 34.7, 33.5 (br), 32.0 (br), 31.0 (br), 28.1 (br), 26.2, 25.6, 24.6, 24.3, 23.8, 23.2; anal. calcd for C$_{64}$H$_{87}$N$_3$OW: C 69.99, H 7.98, N 3.83; found: C 69.85, H 7.91, N 3.59.

Calcined γ-alumina

A quartz furnace tube was charged with γ-Al$_2$O$_3$ and evacuated for 2 h. Oxygen was passed through the tube while heating to 500°C overnight. Then, the apparatus was cooled to 135 °C under oxygen and afterwards to room temperature under high vacuum. The calcined γ-Al$_2$O$_3$ was stored under vacuum in the glovebox.

1-C$_3$H$_6$-Al$_2$O$_3$

In a vial in the glovebox, 200 mg calcined γ-Al$_2$O$_3$ was suspended in 2 mL pentane. In a separate vial, 10 mg 1-C$_3$H$_6$ was dissolved in 5 mL pentane to make a light yellow solution. The solution of 1-C$_3$H$_6$ was added to the γ-Al$_2$O$_3$ suspension along with a stir bar. The resulting suspension was stirred at room temperature for 3 h. After this time, the suspension was filtered to give a clear filtrate and yellow solid. The solid was washed with pentane and dried *in vacuo*. The catalyst loading of the product was 0.05 mmol/g. An analogous procedure was used to synthesize 1-Np-Al$_2$O$_3$ from 1-Np.

1-NMe$_2$-Al$_2$O$_3$

In a vial in the glovebox, 200 mg calcined γ-Al$_2$O$_3$ was suspended in 2 mL pentane. In a separate vial, 10 mg 1-NMe$_2$ was dissolved in 5 mL pentane to make a yellow solution. The solution of 1-NMe$_2$ was added to the γ-Al$_2$O$_3$ suspension along with a stir bar. The resulting suspension was stirred at room temperature for 3 h. After this time, the suspension was filtered to

give a clear filtrate and yellow solid. The solid was washed with pentane and dried *in vacuo*. The catalyst loading of the product was 0.05 mmol/g.

Synthesis of 1-Np from 1-C$_3$H$_6$

To a 50-mL round-bottom flask in the glovebox were added 60 mg of **1-C$_3$H$_6$** (0.062 mmol), 5 mL benzene, and 80 μL *t*-butylethylene (0.620 mmol, 10 equiv.). This mixture was allowed to stir for 1 hour, after which time the solvent was removed under vacuum. To the flask were added 5 mL pentane and 80 μL *t*-butylethylene. This mixture was allowed to stir for 1 hour, after which time the solvent was removed under vacuum. This process was repeated seven more times (using pentane as solvent). ^{1}H NMR after the nine addition cycles showed that 40% of the original **1-C$_3$H$_6$** had been converted into **1-Np** (alkylidene proton signal at 9.557 ppm in C$_6$D$_6$). The remaining 60% of **1-C$_3$H$_6$** appeared to have decomposed as suggested by the presence of free HOHIPT and the absence of the metallacycle proton signals. It is possible that fewer than nine addition cycles would be sufficient for full conversion, provided a high concentration of *t*-butylethylene is used and the solution is taken to dryness under vacuum each time.

General procedures for metathesis homocoupling reactions and catalyst leaching experiments

General procedure for screening catalysts for homocoupling of 1-octene (in Part I)

Into a vial in the glovebox were placed a stir bar, 15.7 μL 1-octene (0.100 mmol), and 0.005 mmol catalyst (as solid or stock solution). The solution was then diluted to 1 mL with C$_6$D$_6$ and allowed to stir at room temperature in the closed vial for the allotted time. Any aliquots taken were diluted with CDCl$_3$ before their NMR spectra were recorded.

General procedure for control reactions involving a metal complex and a silica variant

Into a vial in the glovebox were placed 0.025 mmol metal complex, ~5 mg anthracene (int. std.) and 1 mL C$_6$D$_6$. An initial ^{1}H NMR spectrum to obtain the ratio of complex to anthracene was taken. To the vial was then added 32.1 mg silica variant. The contents of the closed vial were allowed to stir at room temperature for the allotted time, with aliquots taken for ^{1}H NMR as needed.

General procedure for screening catalysts for homocoupling of 1-octene (for Part II)

In a vial in the glovebox were placed a stir bar, 0.001 mmol catalyst (as solid or stock solution), and 0.025 mmol substrate. In the case of allyl tosyl amide, a few drops of benzene were added to dissolve the substrate as well. The solution was then diluted with 1 mL pentane (or pentane/ether mixture, in the case of Table 5) and allowed to stir at room temperature for the allotted time. After this time, the solution was exposed to air, filtered through Celite if heterogeneous, and the solvent evaporated under a stream of N_2. The residue was dissolved in $CDCl_3$ for ^1H NMR analysis.

General procedure for catalyst leaching experiments

Freshly made supported catalyst (~200 mg) was suspended in solvent (~10 mL). After stirring for 10 min, the mixture was filtered and the filtrate collected. This process was repeated twice more. The filtrates were combined and the solvent was evaporated to give a residue. The amount of extracted catalyst (**1-C_3H_6, 1-NMe$_2$, or 1-Np**) was calculated by ^1H NMR integration of alkylidene peak versus an internal standard. Percentage of alkylidene washed through was calculated by comparison to a stock solution identical to that used in the original synthesis of the supported catalyst.

REFERENCE

[1] Schrock, R. R. *Chem. Rev.* **2009**, *109*, 3211.

[2] Flook, M. M.; Jiang, A. J.; Schrock, R. R.; Müller, P.; Hoveyda, A. H. *J. Am. Chem. Soc.* **2009**, *131*, 7962.

[3] Jiang, A. J.; Zhao, Y.; Schrock, R. R.; Hoveyda, A.H. *J. Am. Chem. Soc.* **2009**, *131*, 16330.

[4] a) Rendón, N.; Berthoud, R.; Blanc, F.; Gajan, D.; Maishal, T.; Basset, J.-M.; Copéret, C.; Lesage, A.; Emsley, L.; Marinescu, S. C.; Singh, R.; Schrock, R. R. *Chem. Eur. J.* **2009**, *15*, 5083. b) Blanc, F.; Thivolle-Cazat, J.; Copéret, C.; Hock, A. S.; Tonzetich, Z. J.; Schrock, R. R. *J. Am. Chem. Soc.* **2007**, *129*, 1044. c) Rhers, B.; Salameh, A.; Baudouin, A.; Quadrelli, E. A.; Taoufik, M.; Copéret, C.; Lefebvre, F.; Basset, J.-M.; Solans-Monfort, X.; Eisenstein, O.; Lukens, W. W.; Lopez, L. P. H.; Sinha, A.; Schrock, R. R. *Organometallics* **2006**, *25*, 3554. d) Buffon, R.; Wolke, S. I. *J Mol. Catal. A* **2000**, 160, 181.

[5] a) Hultzsch, K. C.; Jernelius, J. A.; Hoveyda, A. H.; Schrock, R. R. *Angew. Chem.* **2002**, *114*, 609. b) Dolman, S. J.; Hultzsch, K. C.; Pezet, F.; Teng, X.; Hoveyda, A. H.; Schrock, R. R. *J. Am. Chem. Soc.* **2004**, *126*, 10945. c) Wang, D.; Kröll, R.; Mayr, M.; Wurst, K.; Buchmeiser, M.

R. *Adv. Synth. Catal.* **2006**, *348*, 1567. d) Wampler, K. M. Synthetic Investigations of Molybdenum Pyrrolide and Related Complexes. Ph.D. Thesis, Massachusetts Institute of Technology, Cambridge, MA, May 2010.

[6] Copéret, C.; Basset, J.-M. *Adv. Synth. Catal.* **2007**, *349*, 78.

[7] Krieckmann, T; Arndt, S.; Schrock, R. R.; Müller, P. *Organometallics* **2007**, *26*, 5702.

[8] Mcdonald, A. R.; Dijkstra, H. P.; Suijkerbuijk, B. M. J. M.; van Klink, G. P. M.; van Koten, G. *Organometallics* **2009**, *28*, 4689.

[9] Knözinger, H.; Ratnasamy, P. *Cat. Rev.- Sci. Eng.* **1978**, *17*, 31.

[10] a) Huang, Z.; Brookhart, M.; Goldman, A. S.; Kundu, S.; Ray, A.; Scott, S. L.; Vicente, B. C. *Adv. Synth. Catal.* **2009**, *351*, 188. b) Huang, Z.; Rolfe, E.; Carson, E. C.; Brookhart, M., Goldman, A. S.; El-Khalafy, S. H.; MacArthur, A. H. R. *Adv. Synth. Catal.* **2010**, *352*, 125.

[11] Nakazawa, J.; Stack, T. D. P. *J. Am. Chem. Soc.* **2008**, *130*, 14360.

[12] Anwander, R.; Nagl, I.; Widenmayer, M. *J. Phys. Chem. B* **2000**, *104*, 3532.

[13] (a) Schiemenz, B.; Power, P. P. *Organometallics* **1996**, *15*, 958. (b) Stanciu, C.; Olmstead, M. M.; Phillips, A. D.; Stender, M.; Power, P. P. *Eur. J. Inorg. Chem.* **2003**, 3495.

[14] Surry, D. S.; Buchwald, S. L. *J. Am. Chem. Soc.* **2007**, *129*, 10354.

[15] Feher, F. J.; Soulivong, D.; Eklund, A. G.; Wyndham, K. D. *Chem. Commun.* **1997**, *13*, 1185.

[16] Wampler, K. M. Synthetic Investigations of Molybdenum Pyrrolide and Related Complexes. Ph. D. Thesis, Massachusetts Institute of Technology, Cambridge, MA, May 2010.

[17] Bazan, G. C.; Oskam, J. H.; Cho, H. N.; Park, L. Y.; Schrock, R. R. *J. Am. Chem. Soc.* **1991**, *113*, 6899.

[18] Lee, Y.-J.; Schrock, R. R.; Hoveyda, A. H. *J. Am. Chem. Soc.* **2009**, *131*, 10652.

[19] Hanna, B. S. Semi-Annual Report 4. Schrock Group, Massachusetts Institute of Technology, January 2008

[20] Guo, Q.-S.; Du, D.-M.; Xu, J. *Angew. Chem. Int. Ed.* **2008**, *47*, 759.

Chapter 2

Selective Metathesis of 1,3-Dienes with Molybdenum and Tungsten Monoalkoxide Pyrrolide (MAP) Complexes

INTRODUCTION

The scope of olefin metathesis reactions that are possible with high-oxidation-state Group VI alkylidene catalysts has steadily grown due to innovations in synthesis and catalytic methodology. A wide variety of substrates with synthetically useful functional groups can be employed in coupling or polymerization reactions with selective and high-yielding results.[1] Despite this growth, many challenges pertaining to functional group tolerance and product selectivity remain unmet. For instance, the selective metathesis coupling of 1,3-diene substrates was not reported until recently. The difficulty in this area was in part due to the ambiguity and complexity generated by the presence of two different olefin functionalities in each substrate molecule.
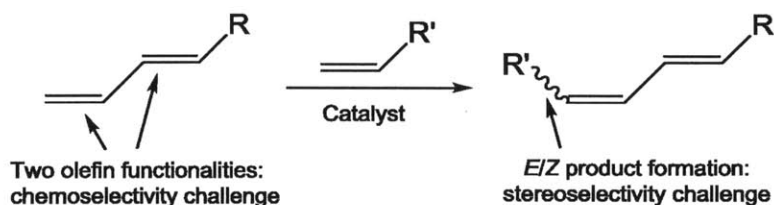
Figure 1: Selectivity challenges in 1,3-diene metathesis

Diene substrates offer two possible sites for catalyst attack (Figure 1). The terminal double bond is presumably the desired reaction site in many cases, as reaction at the internal double bond would split the substrate moiety and lead to a mixture of products. Thus, an ideal catalyst should show high chemoselectivity for the terminal double bond. Furthermore, most coupling reactions create the opportunity for *E/Z* isomerism, so in order to achieve a uniform product, the metathesis catalyst should also enforce stereoselectivity. Even before our exploration of 1,3-diene metathesis, it seemed plausible that Mo and W imido alkylidene monoalkoxide pyrrolide (MAP) complexes could perform well in these roles for reasons that will be explained below.

Yet another pitfall of 1,3-diene metathesis concerns the stability of the intermediate vinylalkylidene species formed upon reaction between the catalyst and the substrate. In previous studies within high-oxidation-state Mo alkylidene systems, it was found that vinylalkylidenes were only stable as 16e base adducts, as opposed to the four-coordinate, 14e species typically found in the catalytic cycle of metathesis (Scheme 1)[2]. Furthermore, no metathesis coupling products were observed in the trials. There are a few other examples of high-oxidation-state Mo

vinylalkylidenes, but they either do not have a proton on the alkylidene carbon[3a], are bimetallic[3b], or are proposed intermediates in polymerization of 1,6-heptadiyne derivatives[3c-f].
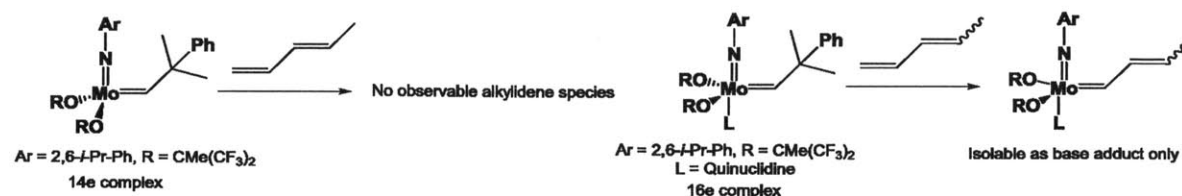
Scheme 1: Previous studies of vinylalkylidene intermediates

For a catalyst to be effective in reactions involving 1,3-diene substrates, it should be able to support the vinylalkylidene moiety without rapid decomposition. Base-free, 14e vinylalkylidene systems are of utmost interest because they closely resemble the successful metathesis catalyst framework that has been developed in our group over the past decades. It is thought that the bulky ligand framework attainable in MAP species could provide steric protection to prevent interference of the vinyl substituent on the alkylidene with the metal center, which is a logical decomposition pathway in the absence of a base adduct. To this end, a model complex is pursued in order to prove that the MAP framework can bear a vinylalkylidene ligand and still remain active for metathesis. These efforts are detailed in Part I of this chapter.

Once it is proven that MAP vinylalkylidenes are viable and stable, focus may turn towards their use for selective metathesis of 1,3-dienes. Despite the long history of olefin metathesis in the literature, metathesis of 1,3-dienes appears to be an underexplored area. Grubbs[4] and Blechert[5] (along with coworkers) have each published a report in which 1,3-dienes can be coupled to other alkenes with Ru catalysts, but the conversion and stereoselectivity is unimpressive in most of the reactions discussed. Furthermore, Grubbs has cited vinylalkylidene intermediates as problematic species due to possible cyclization concerns[6]. Other reports by the groups of Snapper[7] and Grimaud[8] discuss enyne cross-metatheses that invoke diene-to-alkene coupling as an intermediate reaction step. Finally, there exists a report from Mol[9] and coworkers that discusses the non-selective metathesis of dienes with a heterogeneous Re catalyst to form a statistical mixture of products.

As discussed above, the selectivity challenge presented by 1,3-dienes is twofold: it is preferable that reaction occurs at the terminal double bond of the substrate (chemoselectivity) and that the newly formed double bond is predominantly either the E or the Z isomer (stereoselectivity). Fortunately, Mo and W MAP complexes in which the alkoxide is large and

sterically demanding have shown excellent Z selectivity by virtue of their ability to direct all substituents of intermediate metallacyclobutanes away from the alkoxide and toward the imido ligand (see General Introduction)[10]. Furthermore, certain MAP species are slow to carry out secondary metathesis isomerization of internal olefin coupling products, which bodes well for their ability to avoid attack on internal double bonds of dienes.

With these precedents in mind, a metathesis homocoupling study using a select number of 1,3-diene substrates with a systematic series of Mo and W MAP catalysts is undertaken. Part II of this chapter discusses the rationale behind the choices of catalysts and substrates, as well as the synthesis and identification of all catalysts, substrates, and desired products. Part III builds on this foundation and details the full range of the catalytic runs, along with the trends in reactivity and selectivity that could be identified from them.

RESULTS AND DISCUSSION

I. Synthesis of MAP vinylalkylidene complexes

A general strategy for the synthesis of a vinylalkylidene from a diene and a Mo alkylidene MAP species is shown in Scheme 2. The ability to remove excess diene precursor and metathesis cleavage product by vacuum is especially important.
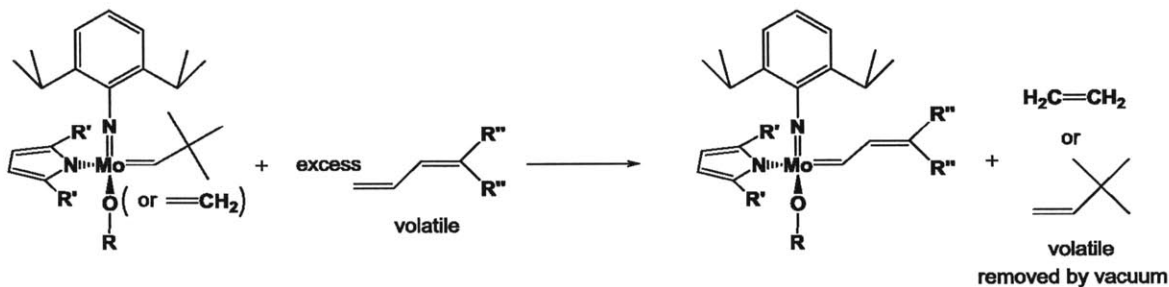
Scheme 2: General strategy for synthesis and isolation of a MAP vinylalkylidene complex

Given the large variety of ligands from which to choose, rational design was crucial in the selection of MAP precursors. Crystallinity of the final complex was a primary concern, as a crystalline product would allow for easy isolation and unambiguous characterization by X-ray crystallography. A bulky ligand environment would also be beneficial, as it would help to prevent cyclization of the vinylalkylidene ligand and stabilize the complex. Finally, given that the easiest route to vinylalkylidenes is via olefin exchange with an existing

alkylidene/metallacycle, a starting complex with a volatile metathesis cleavage product (such as ethylene or *t*-butylethylene) was desirable.

Another important factor in the design of a stable, base-free vinylalkylidene is the choice of diene precursor. Because evacuation plays a large role in the proposed isolation of the final complex, a volatile diene would be optimal. In this way, both the excess diene and the cleavage product from the starting complex are removed under vacuum, leaving only the vinylalkylidene complex behind. Furthermore, a simple diene that contains only one terminal double bond and has no *E/Z* isomerism would be preferred for simplicity's sake.

With these considerations in mind, the synthetic efforts toward a four-coordinate, 14e vinylalkylidene complex began. Section I-A below discusses the synthesis of the precursors to such a complex, while Section I-B treats the final alkylidene exchange step and the resulting desired species.

I-A. Synthesis of vinylalkylidene precursors

The chosen diene precursor was 4-methyl-1,3-pentadiene. It is volatile, has no *E/Z* isomerism, has only one terminal double bond, and is unlikely to cyclize at the metal due to steric hindrance. Unfortunately, this diene was not commercially available for a reasonable price, so it was prepared using Wittig chemistry[11] (Scheme 3).
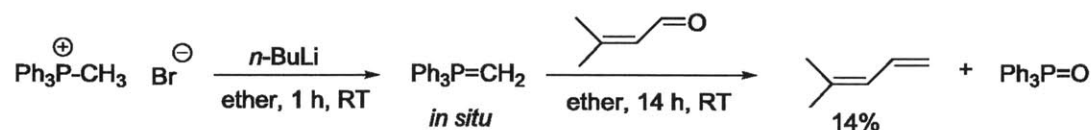
Scheme 3: Wittig synthesis of 4-methyl-1,3-pentadiene

Addition of *n*-butyllithium to a slurry of methyltriphenylphosphonium bromide created the triphenylmethylenephosphorane *in situ*. Subsequent addition of commercially available 3-methyl-2-butenal gave 4-methyl-1,3-pentadiene in 14% yield. The ^{1}H NMR spectrum of the product matched a previous literature report.[12]

The unbranched diene precursor (*E*)-1,3-pentadiene was also synthesized in order to test the stability of vinylalkylidenes with minimal protection on the internal double bond (Scheme 4).
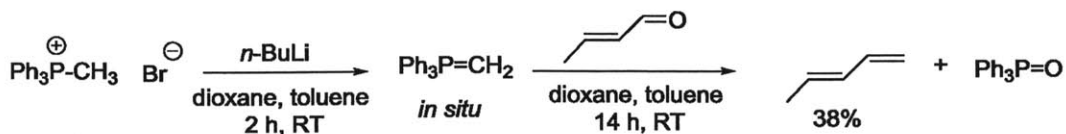
Scheme 4: Wittig synthesis of (*E*)-1,3-pentadiene

Addition of *n*-butyllithium in toluene to a slurry of methyltriphenylphosphonium bromide in 1,4-dioxane generated the triphenylmethylenephosphorane *in situ*. Subsequent addition of trans-2-butenal gave trans-1,3-pentadiene in 38% yield. The ^{1}H NMR spectrum of the product matched a previously reported spectrum.[13]
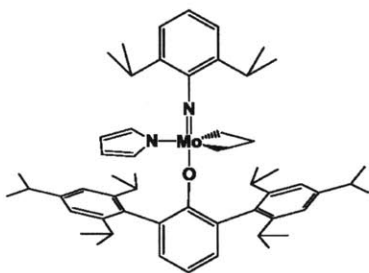
Figure 2:
Mo(NAr)(C₃H₆)(pyr)(OHIPT) (1)

The first metal complex precursor synthesized was the previously reported $Mo(NAr)(C_3H_6)(pyr)(OHIPT)$ (Ar = 2,6-diisopropylphenyl; OHIPT = 2,6-bis(2,4,6-triisopropylphenyl)phenoxide; pyr = pyrrolide.)[14] (**1**, Figure 2). It was chosen because of its bulky ligand environment and the fact that it is an easily isolable metallacycle. Although clean conversion to vinylalkylidene was observed for **1** upon treatment with 4-methyl-1,3-pentadiene, the target complex could not be isolated due to its extreme solubility (see Section I-B).

In order to avoid the problems associated with excessive solubility, focus was shifted toward a metal complex precursor with a ligand environment that would render it more crystalline and less soluble in nonpolar solvents. To this end, the a solution of the previously reported complex $Mo(NAr)(CHCMe_2Ph)(Me_2pyr)(OTPP)$[15] (OTPP = 2,3,5,6-tetraphenylphenoxide; Me_2pyr = 2,5-dimethylpyrrolide) was degassed and subjected to 1 atm ethylene in an attempt to make a metallacycle (analogous to **1**). The red-orange solid that resulted was not a metallacycle, but rather the methylidene complex $Mo(NAr)(CH_2)(Me_2pyr)$ (OTPP) (**2**, Scheme 5).

1 atm C$_2$H$_4$

pentane, 3 h, RT

2
79% yield

Scheme 5: Synthesis of Mo(NAr)(CH$_2$)(Me$_2$pyr)(OTPP) (2)

As will be described in Section I-B, **2** proved not to have the requisite chemoselectivity to form a pure vinylalkylidene species. In order to find a middle ground between the too-soluble OHIPT complexes and the non-selective OTPP complexes, it was decided that 2,6-bis(2,4,6-trimethylphenyl)phenoxide (OHMT) would make a good ligand. However, attempts to obtain a metallacycle or methylidene complex from complexes of the type Mo(NAr)(CHCMe$_2$Ph)(R$_2$pyr)(OHMT) (R = H, Me) and ethylene proved unsuccessful. Thus, some previously unreported analogous neopentylidene MAP complexes were pursued in order to get a precursor with a volatile metathesis cleavage product (Scheme 6).

2 LiMe$_2$Pyr

ether, 2.5 h, -25 °C to RT

3
59% yield

HOHMT

benzene, 22 h, 65 °C

4
73% yield
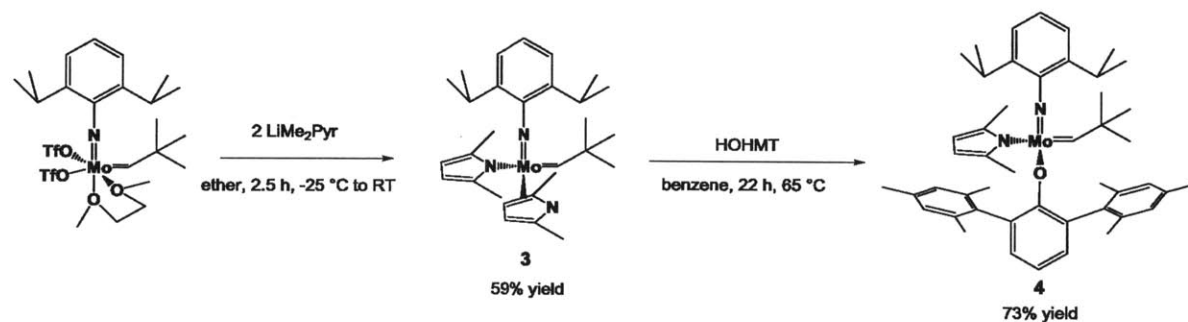
Scheme 6: Synthetic route to Mo(NAr)(CHCMe$_3$)(Me$_2$pyr)(OHMT) (4)

Mo(NAr)(CHCMe$_3$)(OTf)$_2$(dme) was prepared according to a literature procedure.[16] Mo(NAr)(CHCMe$_3$)(OTf)$_2$(dme) was then treated with 2 equivalents of Li(Me$_2$pyr) in ether to form Mo(NAr)(CHCMe$_3$)(Me$_2$pyr)$_2$ (**3**). **3** was combined with 1 equivalent of HOHMT in benzene to form Mo(NAr)(CHCMe$_3$)(Me$_2$pyr)(OHMT) (**4**) in 73% yield.

69

I-B. Synthesis of MAP vinylalkylidene complexes

The first attempt at the synthesis of a MAP vinylalkylidene involved reaction of **1** with 10 equivalents of 4-methyl-1,3-pentadiene in toluene (Scheme 7). Evacuation of the solution to dryness resulted in one major vinylalkylidene product: $Mo(NAr)(CHCHC(CH_3)_2)(OHIPT)(pyr)$ (**1a**), as observed by ^1H NMR spectroscopy. Also present in the product mixture was roughly 1 equivalent of 2,7-dimethyl-2,4,6-octatriene, which is the logical metathesis homocoupling product of 4-methyl-1,3-pentadiene. Attempts to recrystallize **1a** from pentane and tetramethylsilane failed.
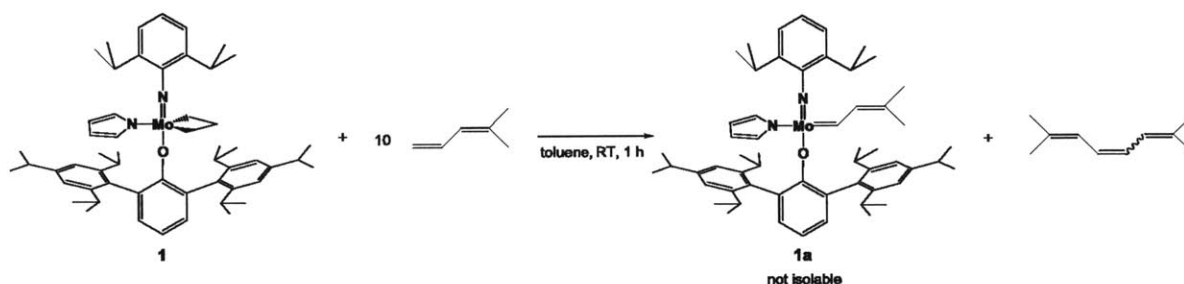
Scheme 7: Reaction of 1 with 4-methyl-1,3-pentadiene

Since excessive solubility prevented isolation of **1a**, focus shifted to **2** as a precursor in the hopes of forming a vinylalkylidene complex that would be easier to isolate. Treatment of **2** with 10 equivalents of 4-methyl-1,3-pentadiene led to a mixture of products arising from the attack of the methylidene complex on both the terminal *and* the internal double bonds of the diene (Scheme 8).
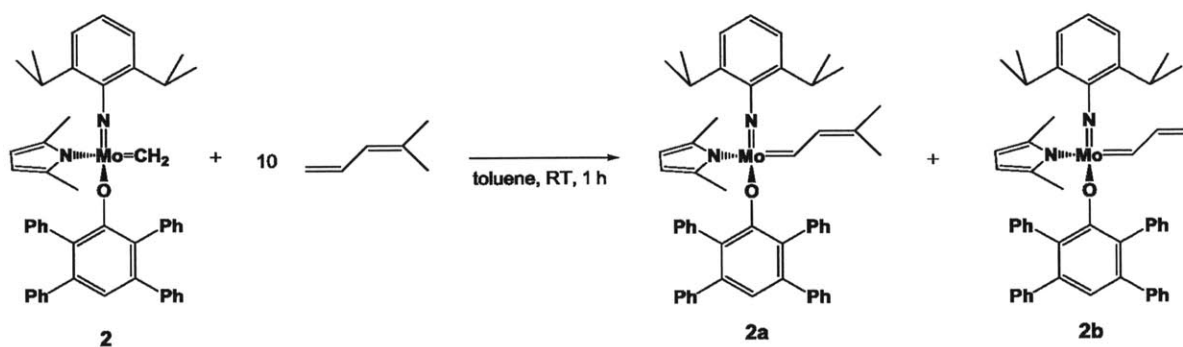
Scheme 8: Reaction of 2 with 4-methyl-1,3-pentadiene

A mixture of **2a** and **2b** could be isolated from this reaction as a red powder, and characteristic alkylidene signatures for each component could be observed in the ^1H NMR spectrum. This result signified that the ligand framework of **2** was not well equipped to enforce

chemoselectivity in diene metathesis, as **2b** came from undesirable attack on the internal double bond of 4-methyl-1,3-pentadiene.

Next, **4** was employed as the starting MAP complex in the hopes that the OHMT ligand would provide enough steric protection to enforce chemoselectivity while keeping the product insoluble enough for easy isolation. Reaction of **4** with 10 equivalents of 4-methyl-1,3-pentadiene in pentane for 4 h at RT followed by evacuation to dryness led to the vinylalkylidene complex Mo(NAr)(CHCHC(CH$_3$)$_2$)(Me$_2$pyr)(OHMT) in 59% yield (**4a**, Scheme 9).
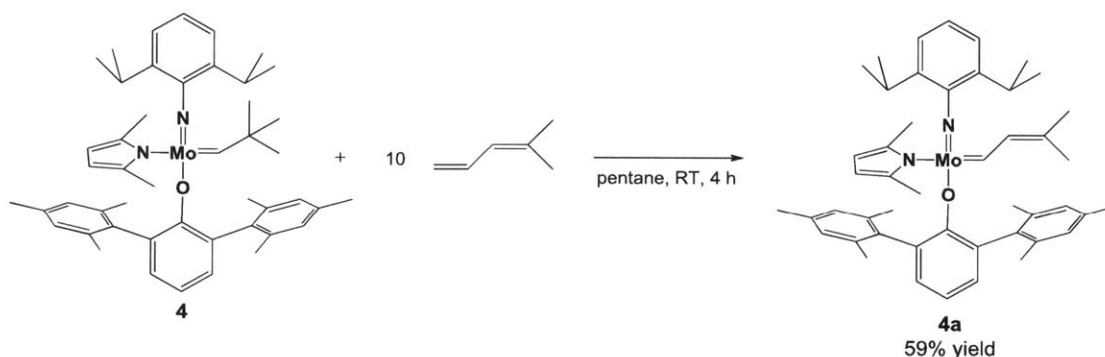
Scheme 9: Synthesis of Mo(NAr)(CHCHC(CH$_3$)$_2$)(Me$_2$pyr)(OHMT) (4a)

The ^{1}H NMR spectrum of **4a** showed a pattern characteristic of the vinylalkylidene moiety. The alkylidene resonance (red), which is normally a singlet in MAP species (no adjacent protons), appears as a doublet (12.91 ppm, J_{HH} = 10 Hz). The resonance for the vinyl proton (blue) is also a doublet (7.72 ppm, J_{HH} = 10 Hz), confirming the presence of the vinylalkylidene fragment. These resonances are shown in Figure 3.
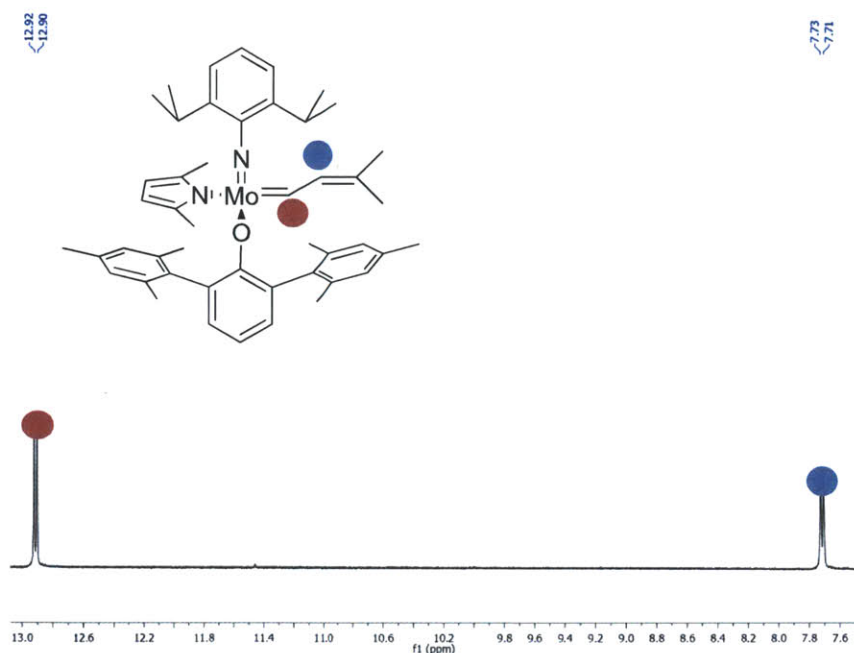
Figure 3: Alkylidene region of ^{1}H NMR spectrum (C_6D_6, 500 MHz) for 4a

4a was recrystallized from ether to give orange-red crystals, and the X-ray crystal structure was obtained in order to confirm the presence of the vinylalkylidene moiety (Figure 4).
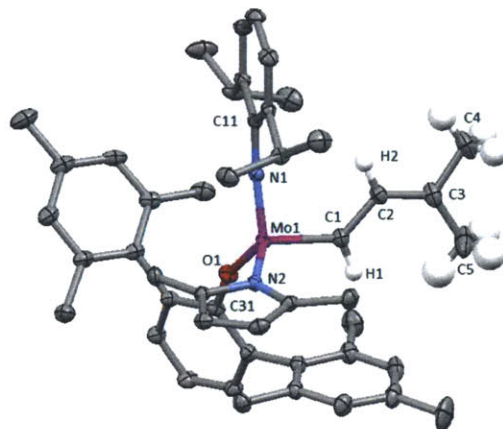
Figure 4: Thermal ellipsoid drawing of Mo(NAr)(CHCHC(CH$_3$)$_2$)(Me$_2$pyr)(OHMT) (4a) (50 % probability ellipsoids). Selected distances (Å) and angles (deg): Mo(1)-C(1) = 1.9120(14), C(1)-C(2) = 1.447(2), C(2)-C(3) = 1.351(2), Mo(1)-C(1)-C(2) = 131.57(11), C(1)-C(2)-C(3) = 127.77(15), C(2)-C(3)-C(4) = 120.41(16).

The planar configuration about C1, C2, and C3, along with the bond distance of 1.351 Å between C2 and C3, confirms that **4a** is an authentic vinylalkylidene complex. All other distances and angles are consistent with other MAP complexes. The alkylidene also displays the

syn configuration (substituent oriented toward the imido group), which is typical for MAP complexes.

Even after the isolation of **4a**, there remained some doubt as to the ability of MAP complexes to form stable vinylalkylidenes when the diene precursor has no branching or protection on its internal double bond. A simple experiment (Scheme 10) showed that an unbranched vinylalkylidene could be formed in much the same way as the dimethylvinylalkylidene of **4a**, putting to rest some concerns that cyclization to form a metallacyclobutene would be a spoiling factor.
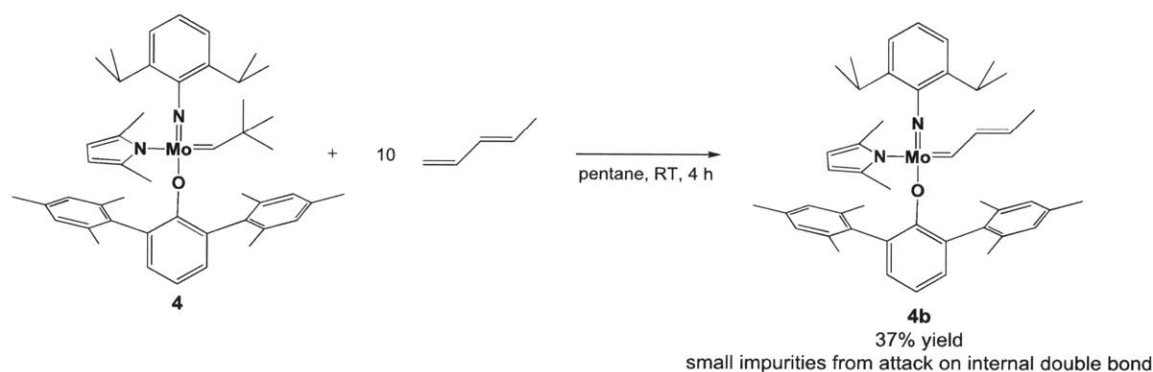
Scheme 10: Synthesis of an unbranched vinylalkylidene complex (4b)

In this experiment, **4** was subjected to an excess of (*E*)-1,3-pentadiene in pentane. Subsequent removal of the solvent *in vacuo* yielded an orange-red powder that contained mainly the species $Mo(NAr)(CHCHCHCH_3)(Me_2pyr)(OHMT)$ (**4b**) by ^1H NMR spectroscopy. Compound **4b** could not be isolated as an analytically pure compound due to small impurities from internal double bond cleavage.

Compound **4b** displayed an interesting ^1H NMR pattern that resulted from coupling along the vinylalkylidene ligand (Figure 5). The alkylidene proton (red) appears as a doublet (12.08 ppm, J_{HH} = 10 Hz), similar to that found in the spectrum of **4a** (Figure 4). The adjacent proton (blue) appears as a doublet of doublet of quartets (7.73 ppm) with 10 Hz coupling to each of its neighbors and 2 Hz coupling to the methyl protons that are four bonds away. Finally, the last olefinic resonance (green) has coupling to both the blue proton and the adjacent methyl protons.
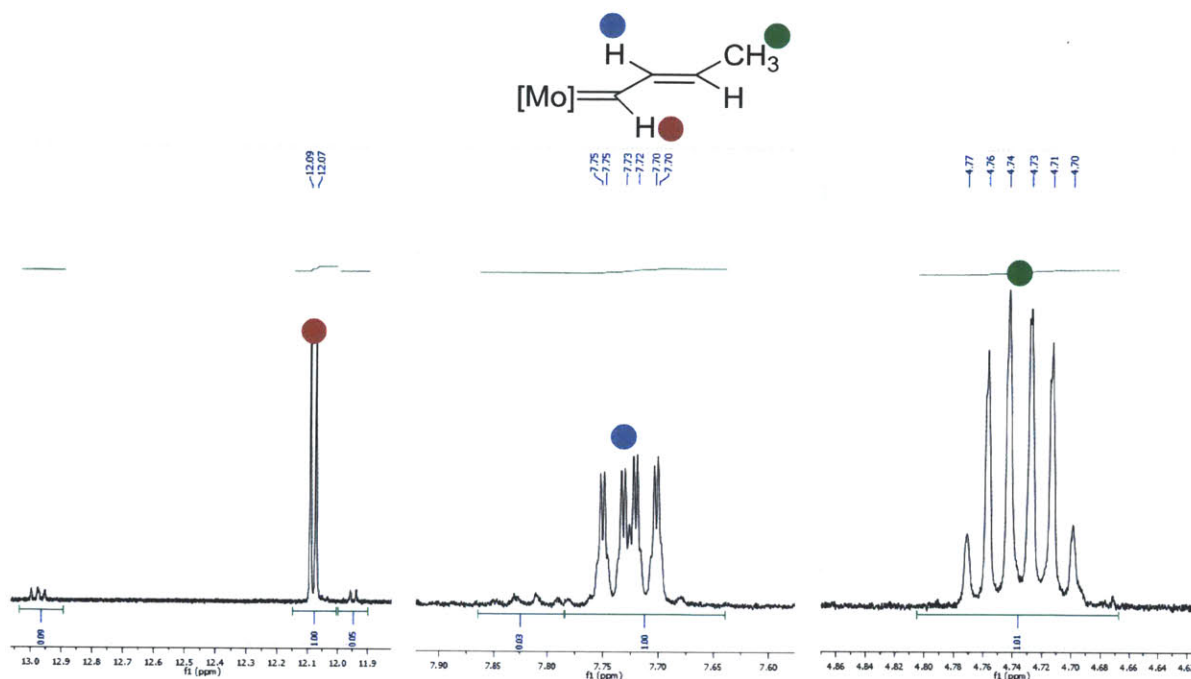
Figure 5: Vinylalkylidene resonances in the ^{1}H NMR spectrum (C$_6$D$_6$, 500 MHz) of 4b

The results of these synthetic efforts were very encouraging in our search for 1,3-diene metathesis catalysts: not only did vinylalkylidene MAP species prove stable and active for metathesis, but reasonable chemoselectivity for terminal double bonds was observed. It was these preliminary findings that opened the door to the detailed study of 1,3-diene homocoupling found in Parts II and III of this chapter.

II. Synthesis and identification of catalysts, substrates and products for homocoupling of 1,3-dienes

With the promising results from Part I as inspiration, we next undertook a systematic study of Mo and W MAP complexes in 1,3-diene metathesis homocoupling. This effort required a rationally assembled and well-characterized library of catalysts and substrates, as well as clearly identifiable products. Section II-A will discuss the selection and synthesis of the catalyst series. Section II-B gives a similar treatment of the chosen substrates, while Section II-C details the efforts to identify the relevant conjugated triene products.

74

II-A. Synthesis of catalysts for 1,3-diene homocoupling

The general structures of the catalysts chosen for metathesis homocoupling of 1,3-dienes were based on those of MAP complexes that had shown high stereoselectivity and chemoselectivity in previous coupling and polymerization studies. The full array of catalysts is shown in Figure 6.
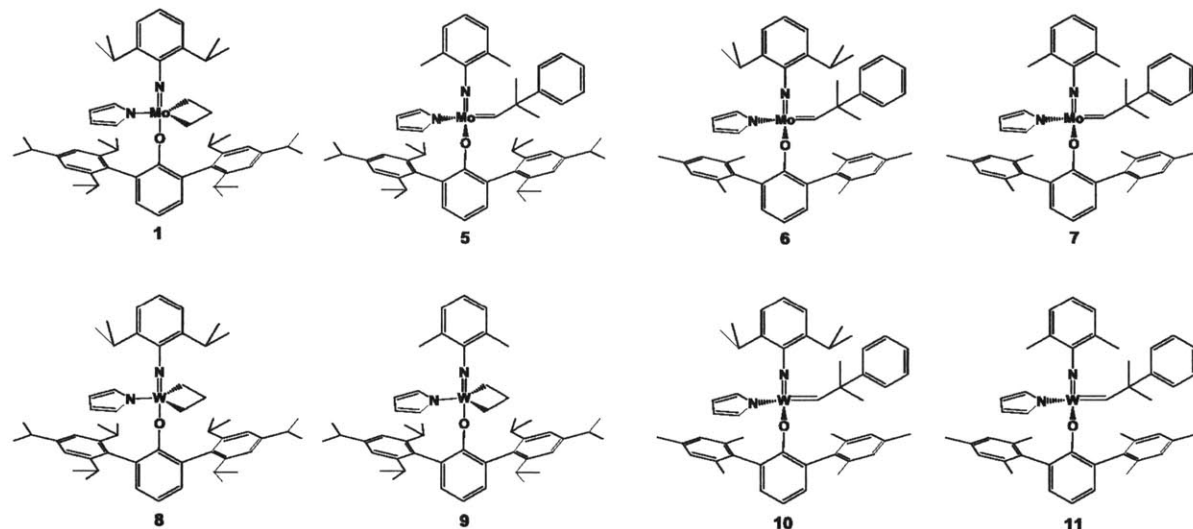
Figure 6: Catalysts for 1,3-diene homocoupling

The similarities between the catalyst complexes are evident: each has an unsubstituted pyrrolide ligand, along with either a neophylidene or an unsubstituted metallacycle (which should be equivalent once the catalytic cycle begins). In each case, the imido group is either the well-studied NAr group or the less bulky analogue NAr′ (Ar′ = 2,6-dimethylphenyl). The steric profile of the alkoxide group is varied between OHMT and OHIPT across the series, and both Mo and W were utilized as the metal center. These eight catalysts represent a systematic steric and electronic series based around the principles of Z-selective metathesis outlined in the General Introduction. Studying the trends in reactivity, stereoselectivity and chemoselectivity for diene homocoupling by this series should allow us to isolate some steric and/or electronic factors that affect catalyst effectiveness.

Catalysts **1**[14], **6**[17], **7**[17], **8**[10b], and **9**[10d] were synthesized according to literature procedures or received as gifts from members of the group. This left catalysts **5**, **10**, and **11** as remaining targets to complete the series.

Synthesis of **5** was achieved by treating Mo(NAr')(CHCMe$_2$Ph)(pyr)$_2$(bpy) with 0.5 equivalents of HOHIPT and 1 equivalent of ZnCl$_2$(dioxane) under sonication overnight (Scheme 8). This method is very similar to one described in a literature report[17].
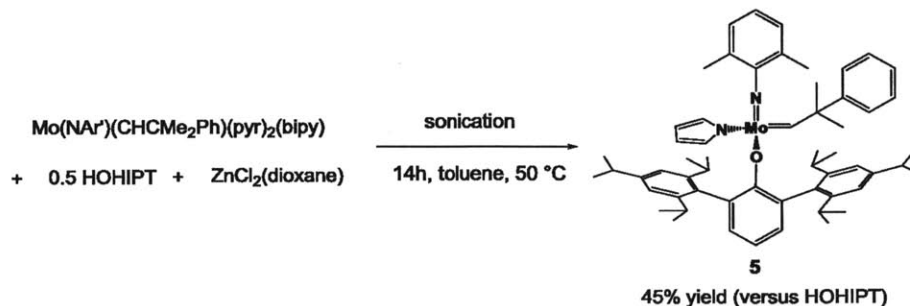
Scheme 11: Synthesis of Mo(N')(CHCMe$_2$Ph)(pyr)(OHIPT) (5)

In this reaction, the ZnCl$_2$(dioxane) acts as a "bipyridine sponge", freeing the Mo dipyrrolide complex for reaction with HOHIPT to generate the MAP. Filtration followed by drying of the filtrate yielded analytically pure product.

Catalysts **10** and **11** were synthesized in similar ways, each starting from its corresponding W dipyrrolide precursor (Scheme 12).
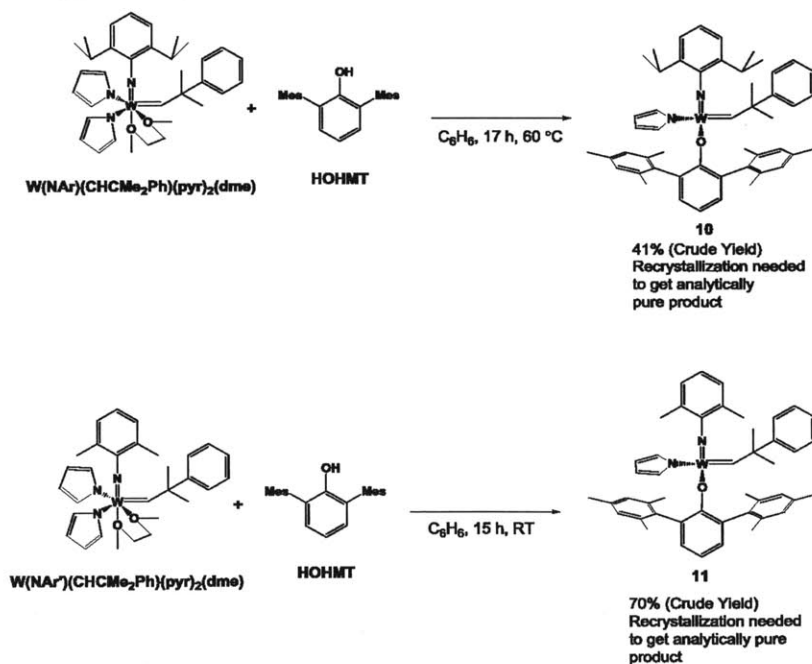
Scheme 12: Syntheses of W(NAr)(CHCMe$_2$Ph)(pyr)(OHMT) (10) and W(NAr)(CHCMe$_2$Ph)(pyr)(OHMT) (11)

W(NAr)(CHCMe$_2$Ph)(pyr)$_2$(dme) was treated with 1 equivalent of HOHMT in benzene for 17 h at 60 °C. Filtration and recrystallization led to a 41% yield of **10**, with further recrystallization needed to obtain analytically pure product. Likewise, W(NAr')(CHCMe$_2$Ph)(pyr)$_2$(dme) was treated with 1 equivalent of HOHMT in benzene at room temperature for 15 h. Filtration and recrystallization led to a 71% yield of **11**, with further recrystallization needed to obtain analytically pure product.

II-B. Synthesis of 1,3-diene substrates

Four substrates were selected for use in the metathesis homocoupling studies: 4-methyl-1,3-pentadiene (**A**), (*E*)-1,3-pentadiene (**B**), (*E*)-1-phenylbutadiene (**C**), and (*E*)-1,3-decadiene (**D**) (Figure 7).

A   **B**   **C**   **D**
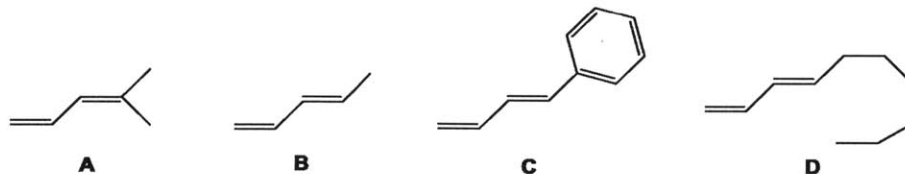
Figure 7: Substrates for 1,3-diene homocoupling

The differing structures of the four substrates give rise to some interesting effects on the homocoupling reactions. **A** and **C** have some steric protection around the internal double bond, which could help to deter unwanted reaction at that position. Substrates **B** and **D**, on the other hand, have unsubstituted internal double bonds, which should provide a tougher chemoselectivity challenge for the catalysts. Furthermore, the volatility of substrates **A** and **B** forced catalytic runs involving them to be run in sealed vessels, which prevented the escape of by-product ethylene and stunted the progress of the reactions (see Part III). Non-volatile substrates **C** and **D** allowed for open-vessel procedures, which generally produced better results.

The syntheses of substrates **A** and **B** are shown and discussed above in Section I-A (Scheme 3 and Scheme 4, respectively).

Substrate **C** was made in a similar manner to **A** and **B** (Scheme 13).
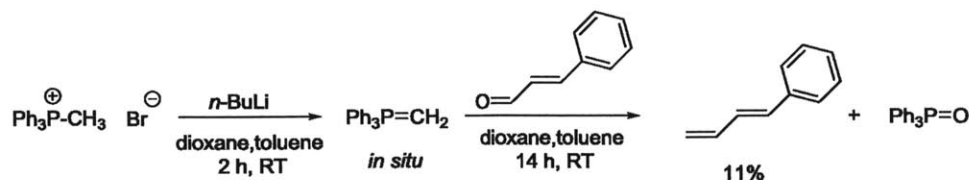
Scheme 13: Wittig synthesis of (*E*)-1-phenylbutadiene (C)

Addition of *n*-butyllithium in hexanes to a slurry of methyltriphenylphosphonium bromide in ether generated the triphenylmethylenephosphorane *in situ*. Subsequent addition of cinnamaldehyde (trans-3-phenyl-2-propenal) gave **C** in 11% yield. The ¹H NMR spectrum of **C** matched with one in a previous literature report.[18]

Substrate **D** was made in a similar manner to **A**, **B**, and **C** (Scheme 14).
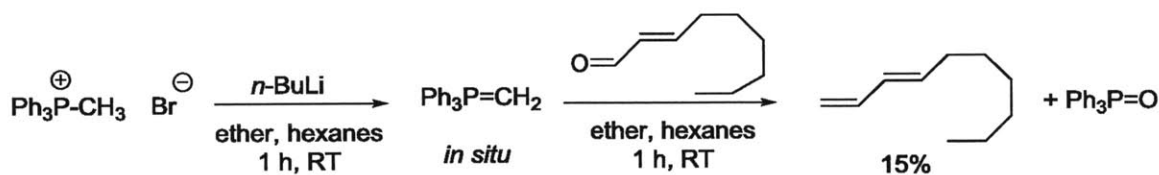
Scheme 14: Wittig synthesis of (*E*)-1,3-decadiene (D)

Addition of *n*-butyllithium in hexanes to a slurry of methyltriphenylphosphonium bromide in ether generated the triphenylmethylenephosphorane *in situ*. Subsequent addition of trans-2-nonenal gave **D** in 15% yield. The ¹H NMR spectrum of **D** matched that of a literature report.[19]

II-C. Identification of conjugated triene products

The metathesis homocoupling reactions of **A**, **B**, **C**, and **D** produce conjugated triene products. These trienes may have either *E* or *Z* configuration at the newly formed central double bond, leading to a total of eight possible homocoupling products (Figure 8).

78
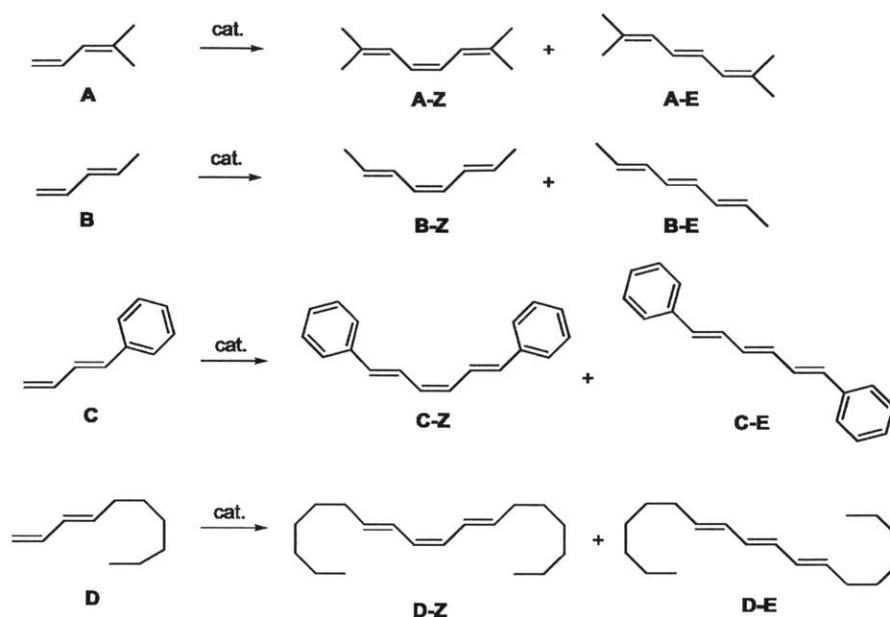
Figure 8: Diene substrates and homocoupling products

Since the homocoupling reactions to come would be monitored predominantly by ^{1}H NMR spectroscopy, it was important to clearly assign the diagnostic peaks for each of the eight substrates above to ensure that accurate values for conversion and *E:Z* ratio could be obtained. This identification was done by a number of methods, including comparison of reaction mixtures to reported spectra as well as independent synthesis of a triene product.

The *Z* and *E* homocoupled products derived from **A** (**A-Z** and **A-E**, respectively) were identified from reaction mixtures. Figure 9 shows two new products from the homocoupling of **A**. There are complex multiplets in the olefinic region of the ^{1}H NMR spectrum of the reaction mixture. At first, it was not known which of these products was **A-Z** and which was **A-E**, but they were eventually assigned by comparison to some calculated and observed spectra from a literature report.[20]
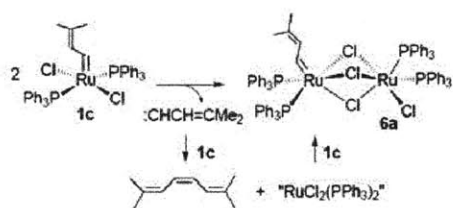
Scheme 3. Solution dimerization of 1c to 6a.
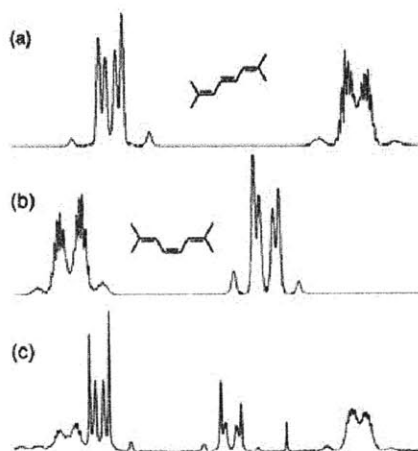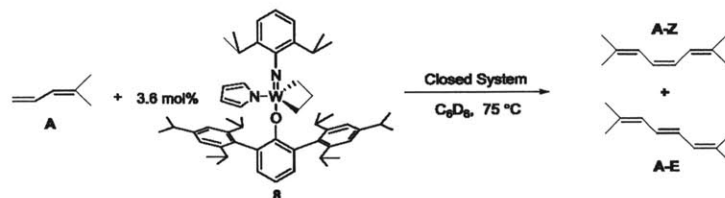
Figure 1. Olefinic AA'BB' signals for 2,7-dimethylocta-2,4,6-triene. (a) calcd., *E*-isomer; (b) calcd., *Z*-isomer; (c) experimentally observed.
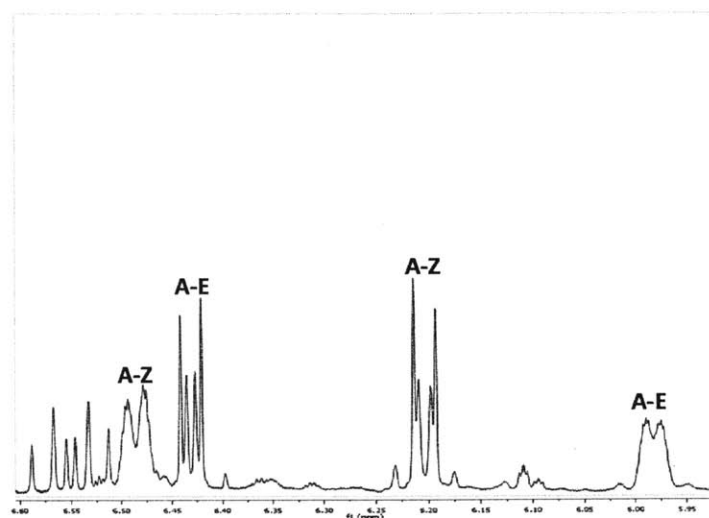
Figure 9: ^{1}H NMR assignment of products A-Z and A-E (in C$_6$D$_6$)
Panel on left from Amoroso, D.; Snelgrove, J. L.; Conrad, J. C.; Drouin S. D.; Yap, G. P. A.; Fogg D. E. *Adv. Synth. Catal.* **2002**, *344*, 757.

The left panel of Figure 9 describes the efforts of Fogg and coworkers to identify the isomers of 2,7-dimethyl-2,4,6-octatriene (**A-Z** and **A-E**). Items (a) and (b) are calculated spectra of the two isomers, and comparison of these to item (c) clearly shows that the isomers can easily be distinguished by ^{1}H NMR spectroscopy. The spectrum in item (c) is nearly identical to the one in the lower right panel, which itself comes from the non-stereoselective homocoupling reaction shown in the upper right panel. This direct comparison revealed clear diagnostic resonances for identification of **A-Z** and **A-E** in future reactions. GC/MS (m/z = 136) and ^{13}C NMR data of a sample of pure **A-Z** (obtained from a highly selective homocoupling with catalyst **1**) were also consistent with the assignments.

Product **B-Z** was identified from the product mixture (after column purification) of the reaction displayed in Figure 10. Also in Figure 10 is the olefinic portion of the ^{1}H NMR spectrum of **B-Z** in C$_6$D$_6$.

80
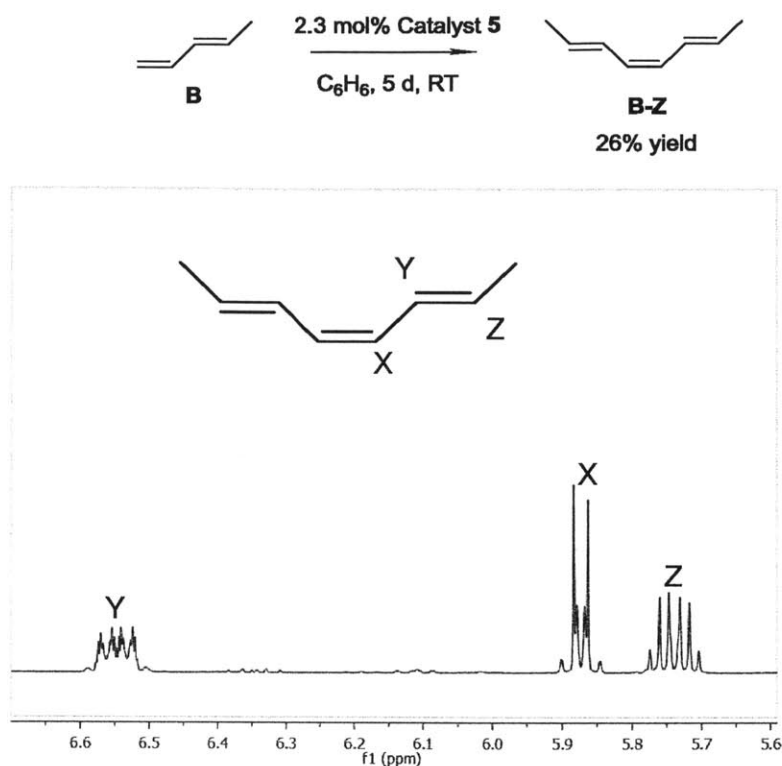
Figure 10: ^{1}H NMR assignment of B-Z (CDCl$_3$, 500 MHz)

The olefinic signals above were compared to literature reports of ^{1}H NMR spectra of **B-Z**[21] and **B-E**[22] from the literature. The literature report for **B-Z** denoted multiplets at 5.7 ppm, 5.83 ppm, and 6.5 ppm; this matched well with the experimental spectrum in Figure 10. The literature report for **B-E**, on the other hand, noted that the most downfield olefinic signal came at 6.2 ppm, further suggesting that the above reaction produced solely **B-Z**. GC/MS (m/z =108) and ^{13}C NMR data were collected and found to be consistent with this assignment. A ^{1}H NMR spectrum of **B-Z** in C$_6$D$_6$ was also collected so that the signature therein could be used in assigning yield and Z content for homocoupling reactions involving **B**.

In order to properly assign yield and Z content, however, it was also necessary to recognize the ^{1}H NMR signature of **B-E**. Unfortunately, a catalyst that would give a clean mixture of **B-Z** and **B-E** was not found. Each of the catalysts gave either clean conversion to **B-Z** or a mixture containing olefinic side products. This made it difficult to pick out the signals for **B-E**. Thus, it was determined that an alternate synthetic route was needed to make and identify **B-E** in the absence of side products.

81

The first attempt of this nature was a Wittig procedure based on a literature report (Scheme 15).[23]
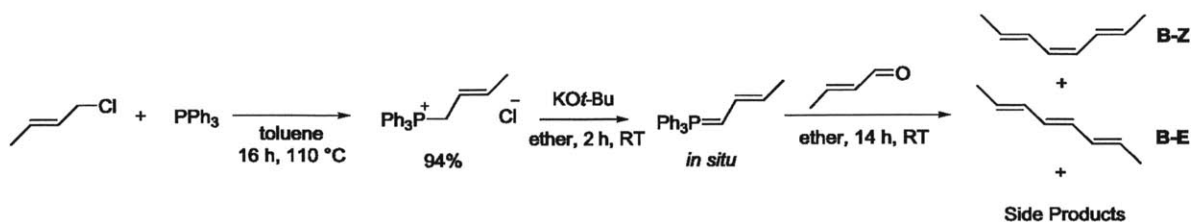
Scheme 15: Wittig synthesis of mixture of B-Z and B-E

Crotyl chloride was combined with triphenylphosphine in refluxing toluene to give crotyltriphenylphosphonium chloride as a white solid in high yield. This reagent was treated with potassium *t*-butoxide in ether to form crotylenetriphenylphosphorane *in situ*. To the solution was added crotonaldehyde, and the subsequent Wittig reaction gave a mixture of **B-Z**, **B-E**, and some other olefinic side products. Unfortunately, these products were not easily separable by column or distillation (the trienes decompose after prolonged air exposure and cyclize if heated). The ^{1}H NMR spectra of each of the column fractions was still too crowded in the olefinic region to make reliable peak assignments for **B-E**.

An alternative route was investigated in order to selectively synthesize **B-E**. This route is shown in Scheme 16 and the reactions therein were based on literature reports.[24,25,26,27]
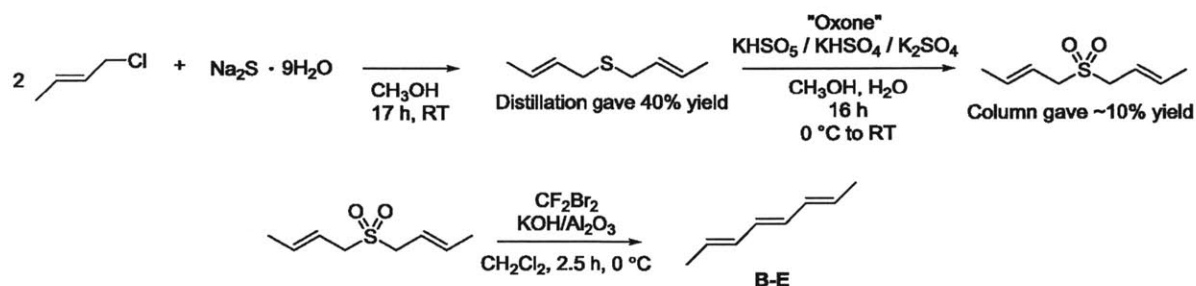
Scheme 16: Ramberg-Bäcklund sulfone elimination route to B-E

Two equivalents of crotyl chloride react with sodium sulfide nonahydrate in methanolic solution to form the symmetrical dicrotyl sulfide, which is isolated by fractional distillation (55 °C to 60 °C at 7 torr). The distillate contained some small isomeric impurities, but the ^{1}H NMR spectrum and GC/MS analysis (m/z = 142) were consistent with the reported data.[28] The dicrotyl sulfide was then oxidized with "Oxone" (potassium hydrogen persulfate) in methanol/water

solution at 0 °C to the dicrotyl sulfone. Subjecting the sulfone to Ramberg-Bäcklund conditions furnished pure **B-E**, which was characterized by GC/MS (m/z = 108) and NMR spectroscopy (^{1}H and ^{13}C). Figure 11 shows the olefinic region of the ^{1}H NMR spectrum of **B-E** in C_6D_6.
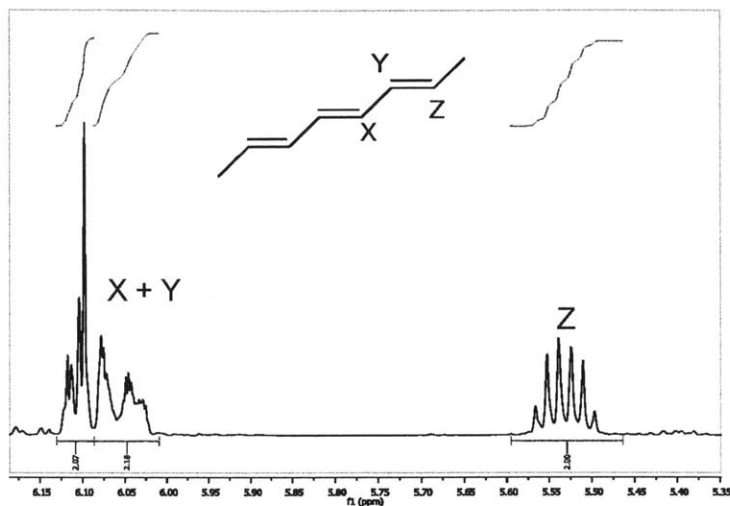
Figure 11: Olefinic region of ^{1}H NMR spectrum of B-E (C_6D_6, 500 MHz).

Product **C-Z** was identified as a clean product from the reaction shown below in Figure 12.

83
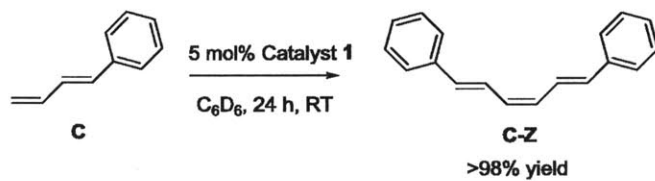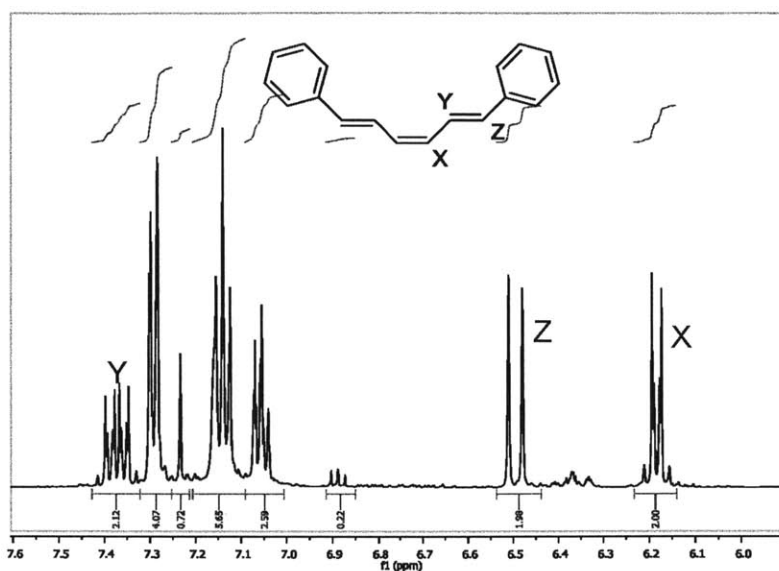
Figure 12: Homocoupling to form product C-Z and olefinic/aryl region of the ^{1}H NMR spectrum (C$_6$D$_6$, 500 MHz)

The above peaks (particularly the olefinic signals at 7.38 ppm, 6.51 ppm, and 6.19 ppm) were integrated in the product mixtures of homocouplings involving **C** in order to ascertain yield and Z content. The identity of **C-Z** was confirmed by taking a ^{1}H NMR spectrum of the product in CDCl$_3$ and comparing to a literature report.[29]

Product **C-E** was identified by direct comparison of the ^{1}H NMR spectrum in C$_6$D$_6$ with the spectrum of a pure sample purchased from Sigma Aldrich (Figure 13).
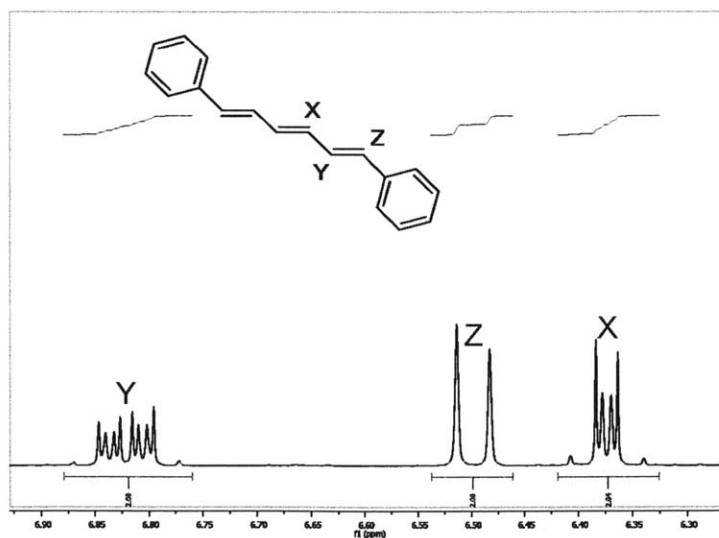
Figure 13: Olefinic region of ^{1}H NMR spectrum of C-E (C$_6$D$_6$, 500 MHz)

84

The olefinic ^{1}H NMR signals for products **D-Z** and **D-E** were identified from product mixtures of homocouplings involving **D** and assigned based largely on comparison to the olefinic ^{1}H NMR signals from the closely related compounds **B-Z** and **B-E**. Figure 14 and Figure 15 show the similarities between the spectra of these compounds and how the comparisons were used to assign the peaks of **D-Z** and **D-E**.
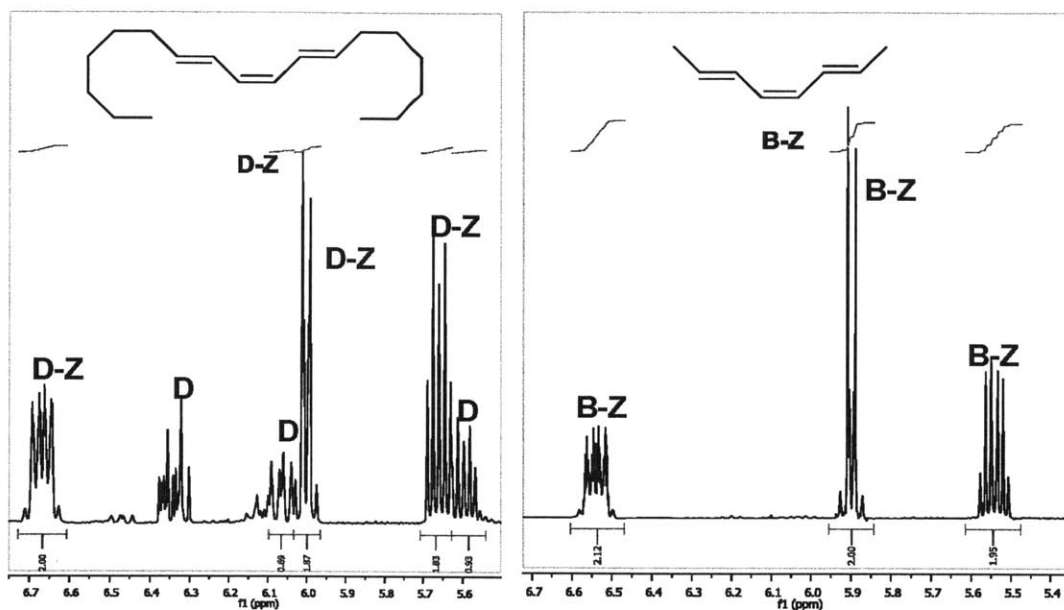
Figure 14: Comparison of olefinic regions of ^{1}H NMR spectra of D-Z and B-Z (C$_6$D$_6$, 500 MHz)

As seen above, there are striking similarities in the olefinic signals for these products. This is not surprising, given their highly similar structures. The integrations and peak shapes are nearly identical, and the chemical shifts are off by about 0.1 ppm. Thus, it was relatively easy to assign the ^{1}H NMR signature for **D-Z**.
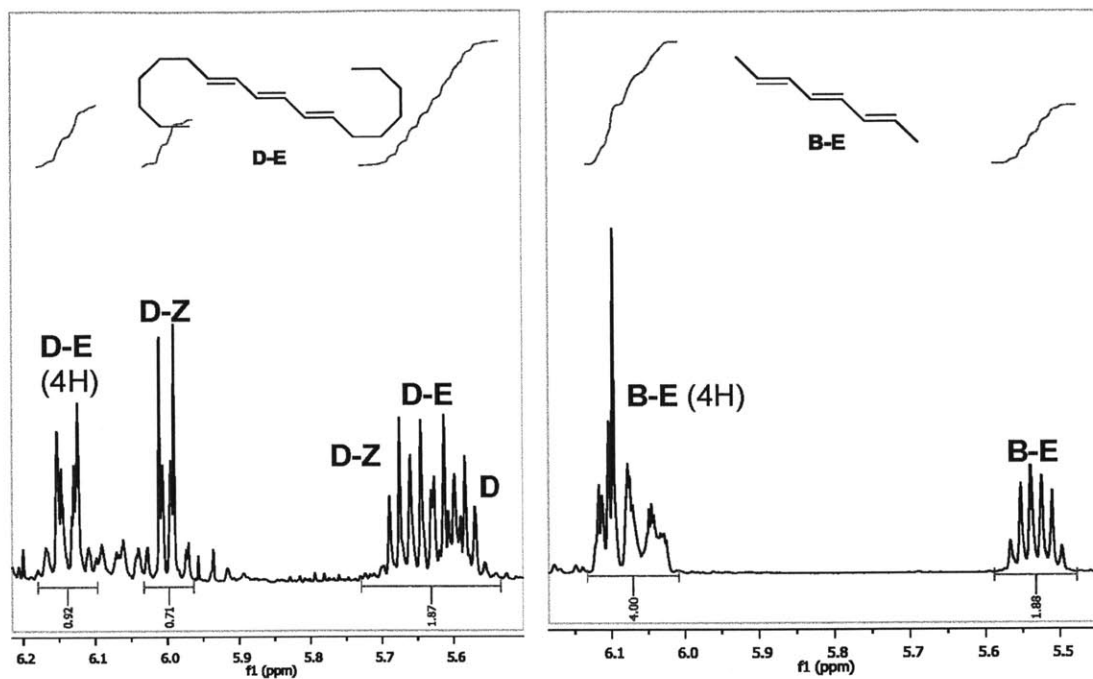
Figure 15: Comparison of olefinic regions of ^{1}H NMR spectra of D-E and B-E (C$_6$D$_6$, 500 MHz)

Assigning the ^{1}H NMR signature for **D-E** was somewhat more difficult. Similarly to the case of **B-E**, it was difficult to get a clean spectrum of the product because the homocouplings either gave predominantly **D-Z** or a mixture containing significant olefinic side products. A thorough inspection of the spectra of the product mixtures, along with comparison to the signature for **B-E**, led to the assignment of the olefinic signals detailed in Figure 15. The apparent sextet near 5.65 ppm is obscured by the signals of **D** and **D-Z**, so the complex signal spanning approximately from 6.19 ppm to 6.11 ppm was invoked as the main diagnostic signal for **D-E**. This signal bears a likeness to the complex signal spanning approximately from 6.12 ppm to 6.02 ppm in the spectrum for **B-E.** Thus, the complex signal in the spectrum for **D-E** was assigned to represent 4 protons per molecule (two sets of olefinic protons), stemming both from similarity to its counterpart in the spectrum for **B-E** and from the lack of other consistent signals in the olefinic region that could have been attributed to a set of olefinic protons from **D-E** (this judgment was based on inspection of spectra from multiple product mixtures). The above assignments for the ^{1}H NMR signatures of **D-Z** and **D-E** were used in determining yield and Z content for homocouplings involving **D**.

86

III. Metathesis homocoupling of 1,3-dienes

III-A. Catalytic trials

The final step was to test the activity and selectivity of the catalysts in metathesis homocoupling reactions of the 1,3-diene substrates. An overview of the compounds involved and the catalytic conditions is shown in Scheme 17.
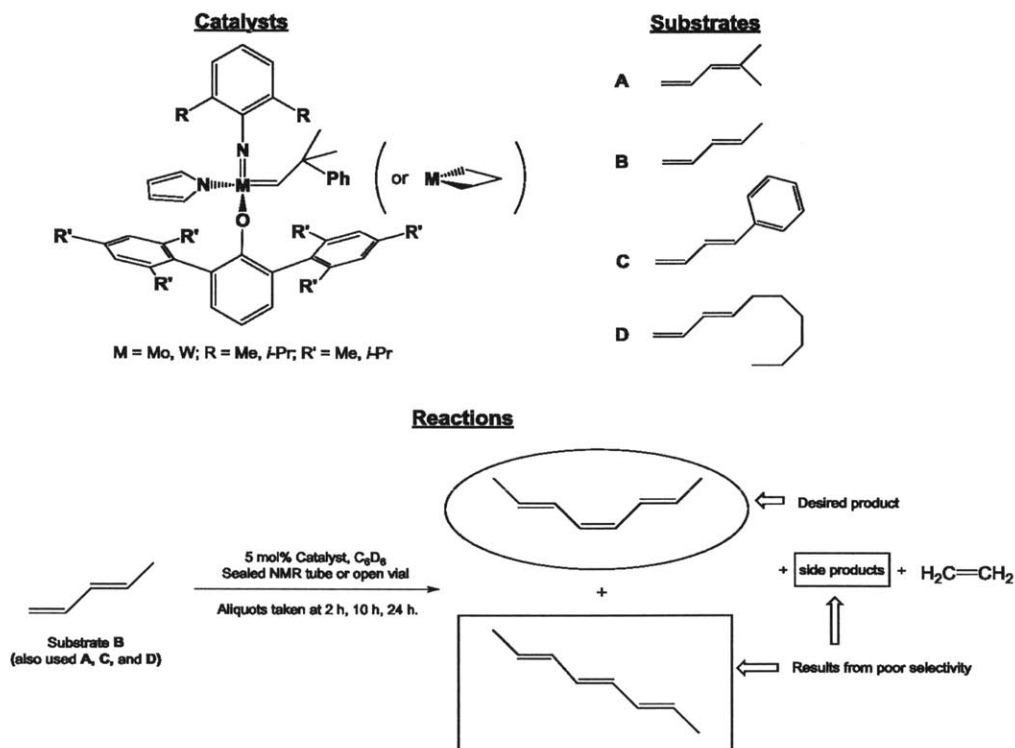
Scheme 17: Overview of catalysts, substrates and reactions for homocoupling of 1,3-dienes

Catalysts **1** and **5-11** (see Figure 6) made up the catalyst library, providing variation in the sterics of the imido and aryloxide groups across both Mo and W complexes. Substrates **A**, **B**, **C**, and **D** were subjected to conditions involving 5 mol% catalyst in C_6D_6 in either a sealed NMR tube (in the cases of **A** and **B**) or a loosely capped vial (in the cases of **C** and **D**). Measurements of the reaction solution were taken at reaction times of 2 h, 10 h, and 24 h in each case. At each time point, the conversion of substrate and yield of product was determined by integration of the ^{1}H NMR signals of interest. The Z content of the product was also identified from the ^{1}H NMR spectrum, utilizing the diagnostic resonances detailed in Section II-C. Finally, the amount of olefinic side products resulting from metathesis of substrate internal double bonds (if any) was

determined by comparison of total product and substrate concentration to that of an internal standard (4,4'-di-t-butylbiphenyl) by ^{1}H NMR spectroscopy. These data will be displayed in table form and discussed accordingly below.

Table 1 shows the results from the first set of homocoupling reactions. The catalysts used in this set (**1**, **5**, **8**, and **9**) each had the very bulky OHIPT aryloxide ligand, which was expected to enforce Z selectivity. As substrates **A** and **B** were featured in these trials, the reactions were run in sealed NMR tubes.

Catalyst	Substrate	Time (h)	% Conv	% Yield	Product	% Side Prd
1	A	2/10/24	50/59/59	50/59/59	>98/97/96	<2/<2/<2
1	B	2/10/24	60/62/65	43/43/40	84/87/88	17/19/25
5	A	2/10/24	60/65/65	60/65/65	>98/97/97	<2/<2/<2
5	B	2/10/24	56/58/58	47/50/49	89/87/87	9/8/9
8	A	2/10/24	7/14/20	7/14/20	>98/>98/96	<2/<2/<2
8	B	2/10/24	7/21/32	7/21/32	>98/97/98	<2/<2/<2
9	A	2/10/24	17/28/35	17/28/35	>98/98/98	<2/<2/<2
9	B	2/10/24	24/38/42	24/38/42	>98/>98/>98	<2/<2/<2

Table 1: Homocoupling of volatile substrates A and B in sealed vessels with OHIPT catalysts

The catalysts in Table 1 were generally successful at homocoupling **A** and **B** to the Z triene products with minimal side products. Mo OHIPT catalysts (**1** and **5**) gave high Z selectivity and little to no side products for the branched substrate **A**. For the unbranched substrate **B**, however, Mo catalysts were prone to more significant side product formation. W OHIPT catalysts (**8** and **9**) gave high Z selectivity and little to no side products for all substrates. Catalyst **8** was slower to turn over than catalyst **9**, perhaps due to the greater steric bulk on its imido group, but otherwise they were quite similar in their performance.

While the selectivity displayed in these trials was high, the product yields were unimpressive. Buildup of ethylene in the system was the likely cause of this. It is known that high ethylene concentration can accelerate decomposition of Mo catalysts[30], and this effect can be seen in our results: the Mo catalysts appeared to become deactivated between 2 h and 10 h. Studies have also shown that unsubstituted W MAP tungstacyclobutanes are quite stable with respect to loss of ethylene, which could explain the low rate and yields seen with the W catalysts in this system[14,31]. A separate experiment showed that **8** was visible in its unsubstituted metallacycle form in a sealed-vessel homocoupling run of **A** for at least 14 days, with conversion to product slowly and steadily increasing over that time.

In order to bypass the deleterious effects of ethylene buildup, the next set of experiments was run with non-volatile substrates **C** and **D** in loosely capped vials. The same four OHIPT catalysts were employed. Table 2 summarizes the results from these trials.

Catalyst	Substrate	Time (h)	%Conv	%Yield	%Z Product	%Side Prd
1	C	2/10/24	87/98/>98	87/98/>98	>98/>98/>98	<2/<2/<2
1	D	2/10/24	83/91/91	77/85/85	92/92/91	6/6/6
5	C	2/10/24	85/96/96	72/89/89	>98/>98/>98	13/7/7
5	D	2/10/24	82/94/96	65/72/72	89/83/81	17/22/24
8	C	2/10/24	33/93/98	33/93/98	>98/>98/93	<2/<2/<2
8	D	2/10/24	37/74/75	37/74/75	n.d.*/98/97	<2/<2/<2
9	C	2/10/24	72/97/98	72/97/98	>98/>98/>98	<2/<2/<2
9	D	2/10/24	72/88/88	72/88/88	96/97/96	<2/<2/<2

Table 2: Homocoupling of non-volatile substrates C and D in open vessels with OHIPT catalysts

The stereoselectivity and chemoselectivity of the reactions in Table 2 were quite similar to the results in Table 1: the W catalysts produced high Z content and negligible side products across the board, and the Mo catalysts performed well with **A**, but the unbranched **B** presented some selectivity problems.

A large improvement in both reaction rate and overall yield was seen as a result of allowing ethylene to escape the solution. All reactions reached high levels of substrate conversion, and some displayed nearly quantitative conversion of substrate to Z product. The top row of Table 2 represents perhaps the best result of all: **C** is completely converted into **C-Z** with no side products within 2 h.

It was clear at this point that the OHIPT catalysts **1, 5, 8,** and **9** were generally capable of achieving high chemoselectivity and stereoselectivity for diene homocoupling. The steric profile of the imido group appeared to have a slight effect on rate and selectivity in some cases (a smaller imido can mean faster, less chemoselective reactions), but was not too important on the whole. It remained to be seen, however, if the significant bulk of the OHIPT ligand was required to maintain selectivity; it remained plausible that some OHMT catalysts might be able to maintain selectivity while operating at a faster pace due to their decreased steric size.

To test this hypothesis, a set of homocoupling reactions were run using the OHMT-bearing catalysts (**6, 7, 10,** and **11**). The improved, open-vessel conditions were employed along with the non-volatile substrates **C** and **D**. Table 3 displays the results of these trials.

Catalyst	Substrate	Time (h)	%Conv	%Yield	%Z Product	%Side Prd
6	C	2/10/24	86/95/>98	75/89/94	64/64/59	11/6/6
6	D	2/10/24	85/96/97	47/52/52	47/41/42	38/44/45
7	C	2/10/24	81/91/91	73/84/84	83/80/84	8/7/7
7	D	2/10/24	84/89/95	55/59/60	61/58/52	29/30/35
10	C	2/10/24	66/80/83	66/80/83	>98/85/75	<2/<2/<2
10	D	2/10/24	36/36/38	36/36/38	92/91/91	<2/<2/<2
11	C	2/10/24	91/97/97	84/90/89	57/57/57	7/7/8
11	D	2/10/24	78/78/78	56/53/51	88/87/87	22/25/27

Table 3: Homocoupling of non-volatile substrates C and D in open vessels with OHMT catalysts

As demonstrated in Table 3, catalysts with OHMT generally gave poorer Z selectivity and more side products. The Mo catalysts (**6** and **7**) gave poor Z selectivity (40%-80%) and minor side products for the protected substrate **C**. For the unbranched substrate **D**, the Mo catalysts were prone to more significant side product formation with no improvement in Z selectivity. The W diisopropylphenylimido catalyst **10** gave moderate (75%-90%) Z selectivity and negligible side products for both substrates. For its dimethylphenylimido counterpart **11**, the Z selectivity was also mediocre and the amount of side products was much higher. The reaction rate and substrate conversion of these catalytic runs were quite high, as would be expected given the decreased catalyst bulk, but the price paid in selectivity was great.

Some overarching trends that relate catalyst structure to reactivity and selectivity can be identified from the observations above. Mo catalysts are generally more active (provide higher yield after a given time) than their W counterparts; however, with this increased activity comes a higher propensity to form side products, presumably through attack on internal double bonds. Some Mo catalysts (the OHIPT-containing species in particular) are quite successful in homocoupling the bulkier substrates (**A** and **C**) with minimal side product formation, but ran into side reactivity problems when faced with linear substrates (**B** and **D**). The linear substrates are better suited by the "gentler touch" of the W-based catalysts, especially those bearing OHIPT ligands. Decreasing the steric bulk of the ligand environment, whether by changing from OHIPT to OHMT or by substituting 2,6-dimethylphenylimido for 2,6-diisopropylphenylimido, appears to increase both the reaction rate and the amount of side products formed in general (in some cases there is no visible change). These observations are summarized in visual form in Figure 16.
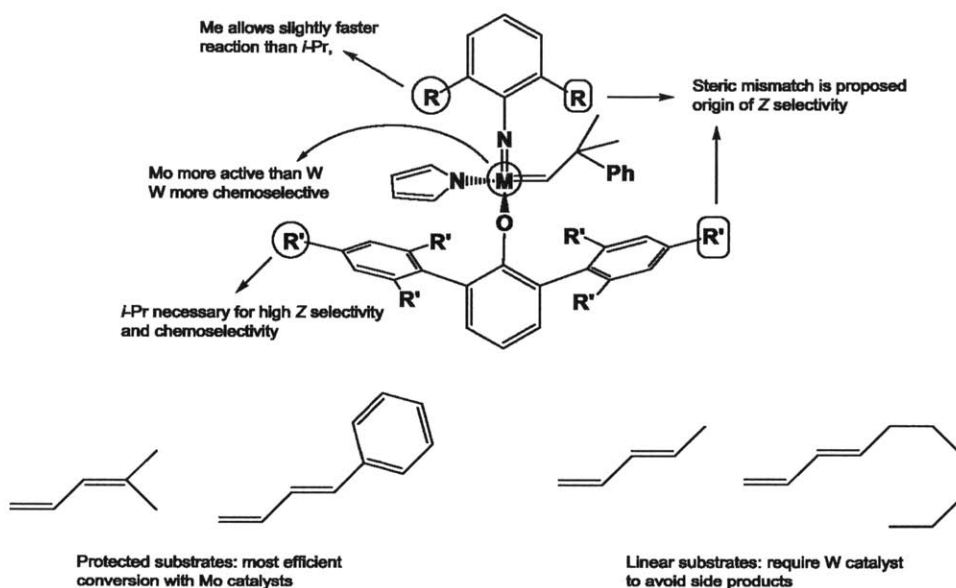
Figure 16: Catalytic trends for 1,3-diene homocoupling

III-B. Scaled-up isolation of a triene product

In order to prove that the diene homocoupling reactions above could be applied in a synthetically useful way, a larger-scale homocoupling of **C** was run in an attempt to isolate the triene product (Scheme 18).
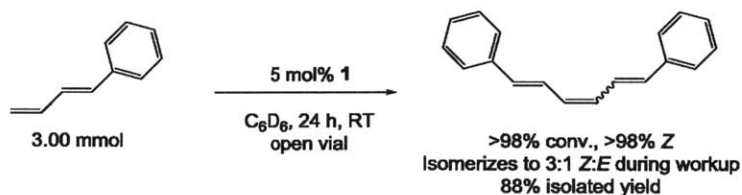
Scheme 18: Scaled-up homocoupling of substrate C with 1

The homocoupling reaction was allowed to proceed at room temperature for 24 h, at which point a ^{1}H NMR aliquot showed complete conversion to **C-Z**. The reaction mixture was brought out of the glovebox and quenched with methanol. A silica column was run in order to obtain 88% yield (308 mg) of product, which had isomerized into a 3:1 mixture of **C-Z:C-E**. A previous literature report suggests that isomerization of **C-Z** can be a result of exposure to light[32].

CONCLUSIONS

Mo and W MAP complexes have proven to be valuable tools for the study and execution of 1,3-diene metathesis. The vinylalkylidene model complexes in Part I serve as solid proof that the MAP framework can support reaction with dienes without decomposition, something that was not true of previous iterations of metathesis catalysts. MAP vinylalkylidenes are also well-behaved intermediates for the metathesis homocoupling of 1,3-dienes. This was proven for a series of Mo and W MAP catalysts and diene substrates, which are enumerated in Part II. Furthermore, some of the catalysts studied showed the ability enforce high levels of chemoselectivity (attack on terminal rather than internal double bonds) and stereoselectivity (preferential formation of Z product over E product). As described in Part III, the catalysts that contain the OHIPT ligand are consistently more selective. Other differences in catalyst makeup can also change their catalytic effectiveness; for instance, Mo catalysts are faster but less chemoselective than their W counterparts, especially for substrates in which the internal double bond is relatively unprotected. Reactions that were run in open vessels in order to avoid ethylene buildup went to much higher conversions than those run in sealed tubes. With the proper choice of catalyst and conditions, a given substrate can be selectively converted into its corresponding Z triene homocoupling product in very high yield. This represents an advance in the area of diene metathesis, as previous systems encountered problems with some combination of intermediate stability, chemoselectivity, and/or stereoselectivity.

EXPERIMENTAL

General Details

All manipulations of air- and moisture-sensitive materials were performed in oven-dried (175 °C) or flame-dried glassware on a dual-manifold Schlenk line or a Vacuum Atmospheres glovebox with nitrogen atmosphere. NMR measurements of air- and moisture-sensitive materials were carried out in Teflon-valve-sealed J. Young-type NMR tubes. Anhydrous ether, pentane, toluene, THF, benzene, and CH_2Cl_2 were sparged with nitrogen and passed through activated alumina prior to use. Chloroform-d and C_6D_6 were stored over molecular sieves. 3-methyl-2-butenal (Aldrich) was dried over $MgSO_4$ and filtered. The following chemicals were purchased from Aldrich and used as received: Methyltriphenylphosphonium bromide, n-butyllithium

solutions, trans-2-butenal (crotonaldehyde), crotyl chloride, triphenylphosphine, Oxone, cinnamaldehyde, (E,E,E)-1,6-diphenyl-1,3,5-hexatriene, $B(C_6F_5)_3$, and (E)-2-nonenal. Sodium sulfide nonahydrate and potassium t-butoxide were purchased from Strem and used as received. Dibromodifluoromethane was purchased from Fluka and used as received. Catalysts **1** $(Mo(NAr)(C_3H_6)(pyr)(OHIPT))^{14}$, **6** $(Mo(NAr)(CHCMe_2Ph)(pyr)(OHMT))^{17}$, **7** $(Mo(NAr')(CHCMe_2Ph)(pyr)(OHMT))^{17}$, **8** $(W(NAr)(C_3H_6)(pyr)(OHIPT))^{10b}$, and **9** $W(NAr')(C_3H_6)(pyr)(OHIPT)^{10d}$ were synthesized according to reported procedures. Catalyst precursor complexes $Mo(NAr)(CHCMe_2Ph)(Me_2pyr)(OTPP)^{15}$, $Mo(NAr)(CHCMe_3)(OTf)_2(dme)^{16}$, $W(NAr)(CHCMe_2Ph)(pyr)_2(dme)^{33}$, $W(NAr')(CHCMe_2Ph)(pyr)_2(dme)^{10d}$ and $Mo(NAr')(CHCMe_2Ph)(pyr)_2(bpy)^{17}$ were synthesized according to reported procedures. The ligands $HOHMT^{34}$ and $HOHIPT^{35}$ were synthesized according to reported procedures. $ZnCl_2(dioxane)^{36}$ was synthesized according to a reported procedure. $Li(Me_2pyr)$ was prepared by addition of 1.1 equivalents of n-BuLi to an ether solution of 2,5-dimethylpyrrole (Aldrich) and isolation of the resulting white solid by filtration and washing with ether. NMR spectra were obtained on Varian spectrometers operating at either 300 MHz or 500 MHz. NMR chemical shifts are reported as ppm relative to tetramethylsilane, and are referenced to the residual proton or ^{13}C signal of the solvent (^1H $CDCl_3$: 7.27 ppm, ^1H C_6D_6: 7.16 ppm, ^{13}C $CDCl_3$: 77.16 ppm, ^{13}C C_6D_6, 128.06 ppm).

Experimental details for metal complex preparation

$Mo(NAr)(CH_2)(Me_2pyr)(OTPP)$ (2)

In a 100-mL Schlenk bomb in glovebox was placed a stir bar, 576 mg Mo(NAr)(CHCMe_2Ph)(Me_2Pyr)(OTPP) (0.644 mmol, 1.0 equiv) and 30 mL pentane (starting material did not fully dissolve). The bomb was sealed, brought out of box, and the contents were freeze-pump-thawed three times. The solution was exposed to 1 atm ethylene while stirring for 3 h. A light red powder came out of solution. The bomb was brought into box and the contents quickly filtered and washed with cold pentane to obtain 395 mg light red powder product (79% yield). ^1H NMR (C_6D_6, 20°C): δ [ppm] 11.77 (d, 1H, methylidene, J_{HH} = 4 Hz), 11.58 (d, 1H, methylidene, J_{HH} = 4 Hz), 7.33-7.21 (8H, aryl), 7.02-6.83 (16 H, aryl), 6.11 (s, 2H, Me_2pyr aryl), 3.33 (sept, 2H, i-Pr methines, J_{HH} = 7 Hz), 2.03 (s, 6H, Me_2pyr methyls), 1.10 (d, 6H, i-Pr methyls, J_{HH} = 7 Hz), 1.014 (d, 6H, i-Pr methyls, J_{HH} = 7 Hz). $^{13}C\{^1H\}$ NMR (C_6D_6, 20°C): δ [ppm] 273.55,

159.29, 154.37, 146.27, 142.14, 141.80, 137.99, 134.24, 132.17, 131.69, 130.29, 130.23, 129.85, 128.53, 128.35, 128.13, 127.97, 127.73, 127.03, 126.76, 126.61, 122.88, 109.08, 102.30, 28.74, 24.94, 24.50, 23.14, 16.64. Anal. Calcd for $C_{49}H_{48}MoN_2O$: C, 75.76; H, 6.23; N, 3.61. Found: C, 75.59; H, 6.35; N, 3.55.

Mo(NAr)(CHCMe₃)(Me₂pyr)₂ (3)

To a 100-mL round-bottom flask in the glovebox were added a stir bar, 2.00 g Mo(NAr)(CHCMe₃)(OTf)₂(dme) (2.74 mmol, 1.00 equiv), and 70 mL ether. The contents of the flask were stirred to dissolve and chilled to -25 °C for 1 h. To the flask was added 559 mg Li(Me₂Pyr) (5.48 mmol, 2.00 equiv). The flask was capped and the contents stirred and allowed to warm to RT over 2.5 h. All solvent was removed *in vacuo* and 25 mL toluene added. After stirring at RT for 1 h, the mixture was filtered through Celite to remove triflate salts. The filtrate was evacuated to dryness, pentane was added, the mixture was chilled, and filtration yielded 850 mg yellow product (59% yield). ^{1}H NMR (C₆D₆, 20°C): δ [ppm] 13.53 (s, ^{1}H, C*H*CMe₃), 6.93 (s, 3H, NAr aryls), 5.99 (br s, 4H, Me₂Pyr aryls), 3.49 (sept, 2H, *i*-Pr methines, J$_{HH}$ = 7 Hz), 2.19 (br s, 12H, Me₂Pyr methyls), 1.22 (s, 9H, CHC*Me₃*), 1.13 (d, 12H, *i*-Pr methyls, J$_{HH}$ = 7 Hz). ^{13}C{^{1}H} NMR (C₆D₆, 20°C): 318.55, 318.40, 151.74, 147.12, 127.58, 123.79, 51.44, 32.82, 27.64, 24.90, 23.84, 18.59. Anal. Calcd For $C_{29}H_{43}MoN_3$: C, 65.76; H, 8.18; N, 7.93. Found: C, 65.14; H, 8.12; N, 7.96.

Mo(NAr)(CHCMe₃)(Me₂pyr)(OHMT) (4)

In the glovebox, a 100-mL Schlenk bomb was charged with a stir bar, 400 mg **3** (0.755 mmol, 1.0 equiv), 250 mg HOHMT (0.755 mmol, 1.0 equiv), and 25 mL benzene. The bomb was sealed, brought out of glovebox, and allowed to stir in an oil bath at 65 °C for 22 h. All solvent was removed on Schlenk line and bomb brought back into glovebox. Isolation from pentane gave 421 mg orange powder product in 2 crops (73% yield). ^{1}H NMR (C₆D₆, 20°C): δ [ppm] 11.46 (s, 1H,C*H*CMe₃), 7.00-6.83 (10H, Aryl from NAr, OHMT), 6.10 (br s, 1H, Me₂pyr aryl), 5.90 (br s, 1H, Me₂pyr aryl), 3.20 (br, overlaps with next, 1H, *i*-Pr methine), 3.13 (br, overlaps with previous, 1H, *i*-Pr methine), 2.29 (br s, 3H, Me₂Pyr), 2.22 (s, 6H, OHMT methyls), 2.21 (s, 6H, OHMT methyls), 2.10 (s, 6H, OHMT methyls), 1.91 (br s, 3H, Me₂Pyr), 1.30 (br, 3H, *i*-Pr methyls), 1.09 (s, 9H, CHC*Me₃*), 1.08 (br, 6H, *i*-Pr methyls), 0.70 (br, 3H, *i*-Pr methyls). ^{13}C{^{1}H} NMR (C₆D₆, 20°C): 296.62, 159.72, 153.72, 150.42, 144.95, 136.83, 136.74, 136.67,

136.62, 134.91, 133.35, 131.98, 131.06, 129.51, 128.83, 123.78, 122.68, 122.31, 109.56, 108.80, 49.91, 31.48, 29.18, 27.70, 24.63, 23.92, 23.72, 23.15, 22.74, 21.56, 21.34, 20.49, 18.43, 15.89. Anal. Calcd for $C_{47}H_{60}MoN_2O$: C, 73.80; H, 7.91; N, 3.66. Found: C, 73.63; H, 7.86; N, 3.53.

Observation of Mo(NAr)(CHCHC(CH$_3$)$_2$)(pyr)(OHIPT) (1a)

In the glovebox, a 50-mL round-bottom flask was charged with a stir bar, 200 mg **1** (mixture of 89% metallacycle and 11% methylidene) (0.229 mmol, 1.0 equiv), and 5 mL toluene. While stirring, 397 µL 4-methyl-1,3-pentadiene solution (6.24 M in ether/toluene) (2.29 mmol, 10.0 equiv) was added. The flask was capped and the contents stirred at RT for 1 h. All solvent was evaporated *in vacuo* to get a dark oil. Attempts to recrystallize or otherwise isolate product from oil with pentane and TMS were unsuccessful, but the vinylalkylidene peaks were clearly visible in the crude NMR spectrum. Selected peaks from ^{1}H NMR (C$_6$D$_6$, 20°C): δ [ppm] 13.09 (d, 1H, C*H*CHC(CH$_3$)$_2$, J$_{HH}$ = 10 Hz), 7.70 (d, 1H, CHC*H*C(CH$_3$)$_2$, J$_{HH}$ = 10 Hz), 1.52 (s, 3H, CHCHC(C*H$_3$*)$_2$), 1.51 (s, 3H, CHCHC(C*H$_3$*)$_2$).

Observation of mixture of Mo(NAr)(CHCHC(CH$_3$)$_2$)(Me$_2$yr)(OTPP) (2a) and Mo(NAr)(CHCHCH$_2$)(Me$_2$pyr)(OTPP) (2b)

In the glovebox, a 50-mL round-bottom flask was charged with a stir bar, 150 mg **2** (0.193 mmol, 1.0 equiv), and 6 mL toluene. While stirring, 310 µL 4-methyl-1,3-pentadiene solution (6.24 M in ether/toluene) was added (1.93 mmol, 10.0 equiv). The flask was capped and the contents stirred at RT for 1 h. All solvent was removed *in vacuo* to get a dark oil. Recrystallization from tetramethylsilane gave red powder, which was a mixture of [Mo](CHCHC(CH$_3$)$_2$) and [Mo](CHCHCH$_2$). Selected resonances from ^{1}H NMR of [Mo](CHCHC(CH$_3$)$_2$) (C$_6$D$_6$, 20°C): δ [ppm] 12.37 (d, 1H, C*H*CHC(CH$_3$)$_2$ J$_{HH}$ = 10 Hz), 7.79 (d, 1H, CHC*H*C(CH$_3$)$_2$, J$_{HH}$ = 10 Hz), 1.52 (s, 3H, CHCHC(C*H$_3$*)$_2$), 1.41 (s, 3H, CHCHC(C*H$_3$*)$_2$). Selected peaks from ^{1}H NMR of [Mo](CHCHCH$_2$) (C$_6$D$_6$, 20 °C): δ [ppm] 11.42 (d, ^{1}H, C*H*CHCH$_2$, J$_{HH}$ = 10 Hz), 7.72 (dd, 1H, CHC*H*CH$_2$, J$_{HH}$ = 10 Hz, 14 Hz), 5.52 (m, 2H, CHCHC*H$_2$*).

Mo(NAr)(CHCHC(CH$_3$)$_2$)(Me$_2$pyr)(OHMT) (4a)

To a 50-mL round-bottom flask in the glovebox were added a stir bar, 363 mg **8** (0.475 mmol, 1.0 equiv), and 10 mL pentane. While stirring, to the flask was added 380 µL 4-methyl-

1,3-pentadiene solution (6.24 M in ether/toluene) (2.37 mmol, 5.0 equiv). The flask was capped and the contents stirred at RT for 4 h. After this time, all solvent was removed *in vacuo* and ~8 mL pentane was added to the flask. The contents were stirred and then chilled for 2 h, after which time filtration gave 215 mg of orange-red powder product (59% yield). Crystals for X-ray structure determination were grown in ether at -25 °C. ^{1}H NMR (C$_6$D$_6$, 20 °C): δ [ppm] 12.92 (d, 1H, C*H*CHC(CH$_3$)$_2$, J_{HH} = 10 Hz), 7.72 (d, 1H, CHC*H*C(CH$_3$)$_2$, J_{HH} = 10 Hz), 7.00-6.84 (10H, aryls of NAr and OHMT), 5.93 (br s, 2H, Me$_2$Pyr aryls), 3.24 (sept, 2H, *i*-Pr methines, J_{HH} = 7 Hz), 2.27 (s, 6H, OHMT methyls), 2.18 (s, 6H, OHMT methyls), 2.15 (s, 6H, OHMT methyls), 2.01 (s, 6H, *Me*$_2$Pyr), 1.58 (s, 3H, CH-CH=C(C*H*$_3$)$_2$), 1.52 (s, 3H, CH-CH=C(C*H*$_3$)$_2$), 1.15 (d, 6H, *i*-Pr methyls, J_{HH} = 7 Hz), 1.03 (d, 6H, *i*-Pr methyls, J_{HH} = 7 Hz). ^{13}C{^{1}H} NMR (C$_6$D$_6$, 20 °C): 276.25, 159.57, 152.76, 147.63, 136.64, 136.58, 136.34, 136.09, 135.98, 134.92, 131.80, 130.55, 129.01, 128.84, 126.91, 123.15, 122.23, 108.86, 28.53. 24.34, 23.83, 23.69, 21.37, 21.22, 20.72, 18.82, 16.37. Anal. Calcd For C$_{47}$H$_{58}$MoN$_2$O: C, 73.99; H, 7.66; N, 3.67. Found: C, 73.98; H, 7.71; N, 3.57.

Observation of Mo(NAr)(CHCHCHCH$_3$)(Me$_2$pyr)(OHMT) (4b)

In a 50-ml round-bottom flask in the glovebox were placed a stir bar, 195 mg **4** (0.255 mmol, 1.0 equiv) and 340 μL trans-1,3-pentadiene (6.5 M solution with some toluene and dioxane) (2.21 mmol, 8.7 equiv), and ~8 mL pentane. The flask was capped and the contents stirred at RT for 4 h. The solvent was then removed on the Schlenk line to give a red/brown solid. Recrystallization from pentane and filtration gave microcrystalline red product with some small alkylidene impurities (70 mg, 37% yield). ^{1}H NMR (C$_6$D$_6$, 20°C, 500 MHz): δ [ppm] 12.08 (d, 1H C*H*CH=CHCH$_3$, J_{HH} = 9 Hz), 7.73 (dd, 1H, CHC*H*=CHCH$_3$, J_{HH} = 14 Hz, 9 Hz), 7.00-6.83 (10H, aryl), 5.99 (br s, 2H, Me$_2$Pyr aryl), 4.73 (m, 1H, CHCH=C*H*CH$_3$), 3.31 (sept, 2H, *i*-Pr methines J_{HH} = 7 Hz), 2.19 (s, 3H aryl methyl), 2.17 (s, 3H, aryl methyl), 2.16 (s, 3H, aryl methyl), 2.00 (s, 3H, aryl methyl), 1.51 (dd, 3H, CHCH=CHC*H*$_3$, J_{HH} = 7 Hz, 2 Hz), 1.15 (d, 6H, *i*-Pr methyls, J_{HH} = 7 Hz), 1.06 (d, 6H, *i*-Pr methyls, J_{HH} = 7 Hz).

Mo(NAr′)(CHCMe$_2$Ph)(pyr)(OHIPT) (5)

In a 100-mL Schlenk bomb in the glovebox were placed 159 mg Mo(NAr′)(CHCMe$_2$Ph)(pyr)$_2$(bpy) (0.250 mmol, 2.0 equiv), 56 mg ZnCl$_2$(dioxane)(0.250 mmol, 2.0 equiv), 62.3 mg HOHIPT (0.125 mmol, 1.0 equiv), and 25 mL toluene. The bomb was

sealed, brought out of the glovebox, and sonicated for 14 h (water bath reached approximately 50 °C). The bomb was brought back into the glovebox, the contents filtered through Celite, and the filter cake washed with toluene. The filtrate was placed into a Schlenk bomb and the solvent removed *in vacuo*. The residue was taken up in pentane and filtered through Celite (washing through with pentane). The filtrate was dried in vacuo to obtain ~50 mg (45% yield) foam product. ^{1}H NMR (C_6D_6, 20 °C, 500 MHz): δ [ppm] 12.49 (s, 1H, C*H*CMe$_2$Ph), 7.26-6.84 (12 H, aryl), 6.70 (app s, 3H, aryl), 6.30 (m, 2H, Pyr aryl), 6.15 (m, 2H, Pyr aryl), 3.08 (sept, 2H, OHIPT *i*-Pr methines, J_{HH} = 7 Hz), 2.90 (overlapping sept, 4H, OHIPT *i*-Pr methines), 2.02 (s, 6H, NAr' methyls), 1.44 (s, 3H, CHC*Me*$_2$Ph), 1.35 (d, 6H, *i*-Pr methyls, J_{HH} = 7 Hz), 1.32 (d, 6H, *i*-Pr methyls, J_{HH} = 7 Hz), 1.23 (d, 6H, *i*-Pr methyls, J_{HH} = 7 Hz), 1.21 (s, 3H, CHC*Me*$_2$Ph), 1.20 (d, 6H, *i*-Pr methyls, J_{HH} = 7 Hz), 1.10 (d, 6H, *i*-Pr methyls, J_{HH} = 7 z), 1.05 (d, 6H, *i*-Pr methyls, J_{HH} = 7 Hz). ^{13}C{^{1}H} NMR (C_6D_6, 20 °C, 125 MHz): δ [ppm] 293.64, 159.21, 156.05, 148.34, 148.05, 147.45, 135.34, 134.58, 133.08, 131.76, 131.63, 126.55, 126.46, 126.39, 122.01, 121.78, 120.98, 110.24, 54.94, 34.78, 31.43, 31.22, 30.92, 30.20, 29.20, 25.74, 24.91, 24.45, 24.37, 24.20, 23.39, 19.27. Anal. Calcd For $C_{58}H_{74}MoN_2O$: C, 76.45; H, 8.19; N, 3.07. Found: C, 76.29; H, 8.14; N, 3.06.

W(NAr)(CHCMe$_2$Ph)(pyr)(OHMT) (10)

In a 100-mL Schlenk bomb in the glovebox were combined a stir bar, 300 mg W(NAr)(CHCMe$_2$Ph)(pyr)$_2$(DME) (0.42 mmol, 1.0 equiv), 139 mg HOHMT (0.42 mmol, 1.0 equiv), and ~12 mL benzene. The bomb was sealed, brought out of box, and stirred in a 60 °C oil bath for 15 h. After this time, the solvent was removed and the residue dried on the Schlenk line. The residue was brought into the box and ether was added to dissolve. Chilling this ether solution gave a powder which, when filtered off, proved to be undesirable material by ^{1}H NMR. The filtrate was dried to a residue; the ^{1}H NMR spectrum of this residue showed mostly product, but some trace starting material and some impurity peaks in the DME region (~2-3 ppm). This residue was recrystallized from pentane and tetramethylsilane to give yellow powder, which was recrystallized again from pentane to give analytically pure product. Yield of pure product: ~70 mg (~20% yield). 41% crude yield of mostly pure product was obtainable in another attempt. ^{1}H NMR (C_6D_6, 20°C, 500 MHz): δ [ppm] 9.03 (s, 1H, C*H*CMe$_2$Ph), 7.25-6.75 (15 H, aryl), 6.64 (m, 2H, pyr aryl), 6.36 (m, 2H, pyr aryl), 2.11 (s, 6H, OHMT methyl), 2.10 (s, 6H, OHMT

methyl), 1.97 (s, 6H, OHMT methyl), 1.47 (s, 3H, CHCMe_2Ph), 1.46 (s, 3H, CHCMe_2Ph), 1.14 (d, 6H, i-Pr methines, J_{HH} = 7 Hz), 1.03 (d, 6H, i-Pr methines, J_{HH} = 7 Hz). $^{13}C\{^1H\}$ NMR (C_6D_6, 20°C, 125 MHz): δ [ppm] 261.94, 157.58, 152.04, 151.10, 144.78, 137.16, 136.79, 136.59, 135.17, 134.19, 132.46, 130.03, 129.11, 128.96, 126.34, 126.14, 123.85, 122.71, 111.50, 53.03, 32.95, 32.40, 28.34, 24.14, 23.51, 21.10, 20.87, 20.48. Anal. Calcd For $C_{50}H_{58}N_2OW$: C, 67.72; H, 6.59; N, 3.16. Found: C, 67.68; H, 6.59; N, 3.11.

W(NAr')(CHCMe₂Ph)(pyr)(OHMT) (11)

In a 100-mL Schlenk bomb in the glovebox were combined a stir bar, 264 mg W(NAr')(CHCMe₂Ph)(pyr)₂(DME) (0.403 mmol, 1.0 equiv), 133 mg HOHMT (0.403 mmol, 1.0 equiv), and ~12 mL benzene. The bomb was sealed, brought out of box, and stirred at RT for 13 h. After this time, the solvent was removed and the residue dried on the Schlenk line. The residue was brought into the box and ether was added to dissolve. Chilling this ether solution gave a powder which, when filtered off, proved to be undesirable material by ^1H NMR. The filtrate was dried to a residue; the ^1H NMR spectrum of this residue showed mostly product, but some trace starting material and some impurity peaks in the DME region (~2-3 ppm). This residue was recrystallized from pentane, but the obtained greenish solid contained high levels of impurities. The mother liquor was removed and concentrated to furnish bright yellow powdery product. The product was washed with tetramethylsilane. Yield of pure product ~60 mg (~18% yield). 70% crude yield of mostly pure product was obtainable in another attempt. ^1H NMR (C_6D_6, 20°C, 500 MHz): δ [ppm] 8.83 (s, 1H, CHCMe₂Ph), 7.24-6.73 (15 H, Aryl), 6.70 (m, 2H, pyr aryl), 6.42 (m, 2H, pyr aryl), 2.08 (s, 6H, NAr' methyls), 2.04 (s, 6H, OHMT methyls), 2.02 (s, 6H, OHMT methyls), 1.94 (s, 6H, OHMT methyls), 1.44 (s, 3H, CHCMe_2Ph), 1.39 (s, 3H, CHCMe_2Ph). $^{13}C\{^1H\}$ NMR (C_6D_6, 20°C, 125 MHz): δ [ppm] 260.29, 157.41, 154.68, 150.92, 137.26, 136.62, 136.47, 134.91, 134.21, 133.81, 132.37, 129.71, 129.19, 128.77, 127.49, 126.40, 126.00, 125.18, 123.74, 111.65, 52.14, 32.62, 31.82, 21.03, 20.84, 20.40, 19.04. Anal. Calcd For $C_{46}H_{50}N_2OW$: C, 66.51; H, 6.07; N, 3.37. Found: C, 66.22; H, 5.94; N, 3.26.

Experimental details for substrate preparation

4-methyl-1,3-pentadiene (A)

The following was based on a literature procedure.[11] A 1-L Schlenk round-bottom flask was equipped with a 250-mL addition funnel and stir bar. The setup was flame-dried under nitrogen. To the flask was added 500 mL anhydrous ether and 100 g methyltriphenylphosphonium bromide (280 mmol, 1.6 eq.) under nitrogen. While stirring, 186 mL 1.4 M n-butyllithium solution in toluene (260 mmol, 1.5 eq.) was transferred to the addition funnel via cannula. The n-butyllithium solution was added dropwise over 2 h while stirring. The solution turned yellow. The addition funnel was replaced with a septum under nitrogen. 16.8 mL 3-methyl-2-butenal (174 mmol, 1.0 eq.) was added by syringe dropwise over 15 min. The solution filled with sludgy solid and was allowed to stir overnight at RT. The sludgy solution was filtered through Celite to remove triphenylphosphine oxide; solids on frit were extracted with ether and toluene. The combined filtrate was distilled through a Vigreaux column and water-cooled condenser. Eight fractions were collected: the first three between 25 °C and 35 °C, the next four between 60 °C and 80 °C (bp of product: 74-76 °C), and the last at 100 °C. ^{1}H NMR showed that the product was most prevalent in fractions 4-7. These fractions were combined, dried over sodium/benzophenone ketyl overnight, and distilled under nitrogen. The major fraction was collected at 76 °C. This fraction was still a mixture of ether, toluene, hexane, and product. Molarity of product in mixture: 3.5 M. Yield: 5.3 g (14%) ^{1}H NMR (C_6D_6, 20°C, 500 MHz): δ [ppm] 6.58 (dt, 1H, $CH_2CHCHC(CH_3)_2$, $J_{HH,d}$ = 17 Hz, , $J_{HH,t}$ = 11 Hz), 5.88 (dm, 1H, $CH_2CHCHC(CH_3)_2$, J_{HH} = 11 Hz), 5.10 (dm, 1H, $CH_2CHCHC(CH_3)_2$, J_{HH} = 17 Hz), 4.98 (dm, 1H, $CH_2CHCHC(CH_3)_2$, J_{HH} = 11 Hz). 1.59 (s, 3H, $CH_2CHCHC(CH_3)_2$), 1.54 (s, 3H, $CH_2CHCHC(CH_3)_2$). ^{1}H NMR data in $CDCl_3$ matched that of a literature report.[12]

(E)-1,3-pentadiene (B)

The following was based on a literature procedure.[11] A 1-L Schlenk round-bottom flask was equipped with 250-ml addition funnel and stir bar. The setup was flame-dried under nitrogen. To the flask was added 500 mL anhydrous 1,4-dioxane and 100 g methyltriphenylphosphonium bromide (280 mmol, 1.6 eq.) under nitrogen. While stirring, 186 mL 1.4 M n-butyllithium solution in toluene (260 mmol, 1.5 eq.) was transferred to the addition

funnel via cannula. The *n*-butyllithium solution was added dropwise to the 1-L flask over 2 h while stirring. The solution turned yellow. The addition funnel was replaced with a septum under nitrogen. 14.4 mL trans-2-butenal (174 mmol, 1.0 eq.) was added by syringe dropwise over 15 min. The solution filled with sludgy solid and was allowed to stir overnight at RT. The sludgy solution was filtered through Celite to remove triphenylphosphine oxide; solids on frit were extracted with ether and toluene. The filtrate was cooled in an acetone/dry ice bath throughout the filtration in order to avoid product evaporation. The combined filtrate was distilled through a Vigreaux column and water-cooled condenser. Two low-boiling fractions were collected between 25 °C and 45 °C; ^{1}H NMR showed that these were predominantly product. The fractions were combined, dried over CaH_2, and vacuum transferred. The solution was freeze-pump-thawed three times, brought into the box, and stored over molecular sieves. This solution was predominantly product, but also contained small amounts of toluene, 1,4-dioxane, and pentane. Molarity of product: 6.5 M. Yield: 6.97 g (39%). ^{1}H NMR (C_6D_6, 20°C, 500 MHz): δ [ppm] 6.28 (dt, 1H, CH_2CHCHCHCH$_3$, $J_{HH,d}$ = 17 Hz, $J_{HH,t}$ = 10 Hz), 6.00 (m, 1H, CH_2CHCHCHCH$_3$), 5.50 (apparent sextet, 1H, $CH_2CHCHCH$CH$_3$), 5.04 (d, 1H, CH_2CHCHCHCH$_3$, J_{HH} = 17 Hz), 4.91 (d, 1H, CH_2CHCHCHCH$_3$, J_{HH} = 10 Hz) 1.53 (d, 3H, $CH_2CHCHCHCH_3$, J_{HH} = 7 Hz) ^{1}H NMR data matched that of a literature report.[13]

(E)-1-phenylbutadiene (C)

The following was based on a literature procedure.[11] A 2-neck, 2-L round-bottom flask was equipped with a stir bar and a 250-mL addition funnel. The setup was flame-dried under nitrogen. Under nitrogen, 125 g methyltriphenylphosphonium bromide (350 mmol, 1.6 equiv) and 900 mL anhydrous ether were added to the flask. To the addition funnel was added 131 mL 2.5 M *n*-BuLi (328 mmol, 1.5 equiv). The contents of the addition funnel were added dropwise to the flask while stirring over 1 h, after which time the yellow mixture was stirred at RT for 1.5 h. Next, 27.5 mL cinnamaldehyde (219 mmol, 1.0 equiv) was added to the flask slowly over 15 min. The solution filled with solid as the addition proceeded; the mixture was allowed to stir for 2.5 h after the addition was complete. The sludgy solution was filtered through Celite to remove triphenylphosphine oxide; solids on frit were extracted with ether and toluene. The red filtrate was concentrated down to give an orange liquid and a red solid. ^{1}H NMR spectroscopy showed that the product was predominantly in the orange liquid. The orange liquid was loaded onto a

silica column and run with pentane as the eluent. The first substance to elute was the product. The product-containing fractions were concentrated down to ~8 mL, dried over CaH_2, freeze-pump-thawed three times, brought into the box, filtered, and stored over sieves. The product solution was a mixture with pentane. Molarity of product solution: 3.00 M. Yield: 8 mL (11% yield). ^1H NMR (C_6D_6, 20°C, 300 MHz): δ [ppm] 7.30-7.00 (5H, aryl), 6.68 (m, 2H, PhC*H*CHCHCH$_2$), 6.39 (m, PhCHC*H*C*H*CH$_2$), 5.19 (d, 1H, PhCHCHCHC*H*$_2$, J$_{HH}$ = 17 Hz), 5.05 (d, 1H, PhCHCHCHC*H*$_2$, J$_{HH}$ = 10 Hz). ^1H NMR data in $CDCl_3$ matched that of a literature report.[18]

(*E*)-1,3-decadiene (D)

The following was based on a literature procedure.[11] A 1-L Schlenk round-bottom flask was equipped with 250-ml addition funnel and stir bar. The setup was flame-dried under nitrogen. To the flask was added 550 mL anhydrous ether and 100 g methyltriphenylphosphonium bromide (280 mmol, 1.6 eq.) under nitrogen. While stirring, 104 mL 2.5 M *n*-butyllithium solution in hexanes (260 mmol, 1.5 eq.) was transferred to the addition funnel via cannula. The *n*-butyllithium solution was added dropwise over 40 min while stirring. The solution turned yellow and was allowed to stir for 1 h at RT. The addition funnel was replaced with a septum under nitrogen. 16.8 mL 3-methyl-2-butenal (174 mmol, 1.0 eq.) was added by syringe dropwise over 15 min. The solution filled with sludgy solid and was allowed to sit overnight (stirring was impossible due to solid formation) at RT. The sludgy solution was filtered through Celite to remove triphenylphosphine oxide; solids on frit were extracted with ether and hexanes. The filtrate was concentrated; excess solid was filtered off along the way as necessary. Obtained ~ 30 mL yellow solution, which was run on a silica column with 1% ether in pentane as eluent. The first substance to elute was the product. The product-containing fractions were concentrated (to a solution containing pentane), dried over CaH_2, freeze-pump-thawed three times, brought into the box, filtered, and stored over sieves. Molarity of product solution: 2.12 M. Yield ~12 mL (15% yield). ^1H NMR (C_6D_6, 20°C, 500 MHz): δ [ppm]] 6.33 (dt, 1H, CH$_2$C*H*CHCHCH$_2$R, J$_{HH,d}$ = 17 Hz, J$_{HH,t}$ = 10 Hz), 6.06 (m, 1H, CH$_2$CHC*H*CHCH$_2$R), 5.60 (m, 1H, CH$_2$CHCHC*H*CH$_2$R), 5.08 (d, 1H, C*H*$_2$CHCHCHCH$_2$R, J$_{HH}$ = 17 Hz), 4.94 (d, 1H, C*H*$_2$CHCHCHCH$_2$R, J$_{HH}$ = 10 Hz), 1.97 (m, 2H, CH$_2$CHCHCHC*H*$_2$R), 1.32-0.83 (11H, alkyl) ^1H NMR data in $CDCl_3$ matched that of a literature report.[19]

Experimental details for synthesis/identification of triene products

(Z)-2,7-dimethyl-2,4,6-octatriene (A-Z)

In the glovebox, a 20-mL vial was charged with 100 mg solid **1** (0.116 mmol, 3.4 mol%), 0.928 mL **A** solution (3.21 mmol), and a stir bar. The vial was sealed and the contents stirred at RT. The product mixture was quenched by exposure to air after 28 h of reaction time. The mixture was loaded onto a silica column and run with pentane as the eluent; the product was the first substance to elute. Product-containing fractions were concentrated to give a viscous liquid. Note: **A-Z** is moderately air-sensitive; any manipulations should be carried out quickly and the product should be stored in the dark under nitrogen. ^1H NMR (C_6D_6, 20 °C, 500 MHz): δ [ppm] 6.51 (m, 2H, $(CH_3)_2CHCHCHCH(CH_3)_2$), 6.22 (m, 2H, $(CH_3)_2CHCHCHCH(CH_3)_2$), 1.85 (s, 6H, methyls), 1.79 (s, 6H, methyls). ^1H NMR ($CDCl_3$, 20 °C, 500 MHz): δ [ppm] 6.31 (m, 2H, $(CH_3)_2CHCHCHCH(CH_3)_2$), 6.09 (m, 2H, $(CH_3)_2CHCHCHCH(CH_3)_2$), 1.70 (s, 6H, methyls), 1.63 (s, 6H, methyls). $^{13}C\{^1H\}$ NMR ($CDCl_3$, 20°C, 125 MHz): δ [ppm] 135.88, 123.18, 120.77, 26.59, 18.24. GC/MS: m/z = 136.

Observation of (E)-2,7-dimethyl-2,4,6-octatriene (A-E)

This product was identified in the product mixtures of homocoupling reactions. ^1H NMR (C_6D_6, 20 °C, 500 MHz): δ [ppm] 6.45 (m, 2H, $(CH_3)_2CHCHCHCH(CH_3)_2$), 6.00 (m, 2H, $(CH_3)_2CHCHCHCH(CH_3)_2$), methyl signals difficult to pick out of the mixture. See Figure 9 for the information on the NMR assignment process.

(E,Z,E)-2,4,6-octatriene (B-Z)

In the glovebox, a sealable Schlenk tube was charged with 107 mg **8** (0.111 mmol, 2.3 mol%), 0.739 mL **B** solution (4.81 mmol), and a stir bar. The tube was sealed, brought out of the glovebox, and stirred at RT for 16 h. After this time, the reaction mixture was exposed to air. The mixture was loaded onto a silica column and run with pentane as the eluent; the product was the first substance to elute. Product-containing fractions were carefully concentrated to give a small amount of product-containing solution with benzene and pentane. Note: **B-Z** is moderately air-sensitive; any manipulations should be carried out quickly and the product should be stored in the dark under nitrogen. ^1H NMR (C_6D_6, 20 °C, 500 MHz): δ [ppm] 6.54 (m, 2H, $CH_3CHCHCHCHCHCH_3$), 5.90 (m, 2H, $CH_3CHCHCHCHCHCH_3$), 5.54 (m, 2H,

CH₃C*H*CHCHCHCHC*H*CH₃), 1.61 (dd, 6H, C*H₃*CHCHCHCHCHC*H₃* J_{HH} = 7 Hz, 2 Hz). ¹³C{¹H} NMR (CDCl₃, 20°C, 125 MHz): δ [ppm] 128.50, 127.47, 127.34, 18.51. GC/MS: m/z = 108. ¹H NMR data in CDCl₃ was consistent with that of a literature report.[21] See Figure 10.

(*E,E*)-dicrotyl sulfide

This procedure was based on a literature report.[24] Into a 250-mL round-bottom flask were placed 13.68 g sodium sulfide nonahydrate (57.0 mmol, 1.0 equiv), 175 mL methanol, and a stir bar. The mixture was stirred until all solid dissolved. To the flask was added 11.3 mL (*E*)-crotyl chloride (125 mmol, 2.2 equiv). The reaction mixture was stirred for 17 h at RT, after which it was concentrated to a salty suspension. The suspension was filtered through a frit to remove NaCl, and the salts were washed with dichloromethane and ether. The filtrate was concentrated down to a yellow biphasic solution, and the bottom (aqueous) layer was removed by pipet to leave the product-containing layer. Layers from two of these reactions were combined and distilled (major fraction at 55 °C at 7 torr) to give 6.68 g (40% yield across two reactions) of product (with some isomeric impurities). ¹H NMR (CDCl₃, 20 °C, 500 MHz): δ [ppm] 5.56-5.38 (m, 4H, CH₃C*H*C*H*CH₂SCH₂C*H*C*H*CH₃), 3.03 (d, 4H, CH₃CHCHC*H₂*SC*H₂*CHCHCH₃, J_{HH} = 7 Hz), 1.70 (d, 4H, C*H₃*CHCHCH₂SCH₂CHCHC*H₃*, J_{HH} = 7 Hz). GC/MS: m/z = 142. ¹H NMR data was consistent with a literature report.[28]

(*E,E*)-dicrotyl sulfone

This procedure was based on some literature reports.[16,26,27] 3.10 g of the (*E,E*)-dicrotyl sulfide (3.5 mL, 21.8 mmol, 1.0 equiv) from above was added to 100 mL methanol in a 500-mL round-bottom flask with stir bar. This mixture was cooled to 0 °C in an ice bath. To this flask was slowly added 33.55 g Oxone (KHSO₅/0.5 KHSO₄/0.5 K₂SO₄) (109 mmol, 5.0 equiv) dissolved in 200 mL water. The resulting cloudy slurry was allowed to stir and warm to RT overnight. The solution was then concentrated by rotary evaporation and filtered to remove bulk salts. The solid from the filtration was washed with CH₂Cl₂. The filtrate was extracted with 3 x 100 mL CH₂Cl₂, and the organic layer was subsequently washed with 150 mL water and 150 mL brine. The organic layer was then dried over MgSO₄, filtered, and concentrated down to ~3 g of crude liquid. ¹H NMR showed product, but with significant impurities. This crude liquid was combined with ~2.5 g crude liquid from an identical reaction. The combined products were placed under Schlenk line vacuum to remove solvent and subsequently loaded onto a silica

column. The column was carefully and slowly run using 3:1 hexanes:ethyl acetate as the solvent system. TLC analysis to track the products required high spot loading and development of the TLC plates in an iodine chamber. Three evenly spaced spots were seen in the crude. The first of these to elute was found to be the product. All pure-product-containing fractions were combined and concentrated by rotary evaporation to obtain a small amount of liquid. This liquid was placed under Schlenk line vacuum to remove residual solvent. ^{1}H NMR showed product with some very small impurities. Yield: 650 mg across both syntheses (9% yield). ^{1}H NMR (CDCl$_3$, 20 °C, 500 MHz): δ [ppm] 5.83 (m, 2H, CH$_3$CHCHCH$_2$SO$_2$CH$_2$CHCHCH$_3$), 5.53 (m, 2H, CH$_3$CHCHCH$_2$SO$_2$CH$_2$CHCHCH$_3$), 3.61 (d, 4H, CH$_3$CHCHCH$_2$SO$_2$CH$_2$CHCHCH$_3$), J$_{HH}$ = 7 Hz), 1.79 (d, 6H, CH$_3$CHCHCH$_2$SO$_2$CH$_2$CHCHCH$_3$, J$_{HH}$ = 7 Hz). GC/MS: m/z = 174 (Note: parent ion peak very small, but visible. Predominant peak is crotyl fragment at m/z = 55). ^{1}H NMR data was consistent with a literature report.[37]

(E,E,E)-2,4,6-octatriene (B-E)

This synthesis was based on some literature reports.[24,25] In a 50-mL round-bottom flask were placed a stir bar, 3.5 g KOH/Al$_2$O$_3$, and ~8 mL CH$_2$Cl$_2$. This mixture was cooled to 0 °C in an ice bath, and to it was added 300 mg (E,E)-dicrotyl sulfone (1.72 mmol, 1.0 equiv) dissolved in ~2 mL CH$_2$Cl$_2$ while stirring. This mixture was capped with a septum and allowed to stir for 15 min at 0 °C, after which time 1.44 g CF$_2$Br$_2$ (6.88 mmol, 4.0 equiv) was injected. It is helpful to pre-cool the syringe, as CF$_2$Br$_2$ is quite volatile (bp 22.8 °C). The resulting was allowed to stir at 0 °C for 2.5 h, after which time it was filtered through a pad of Celite (washing through with CH$_2$Cl$_2$ and pentane) and concentrated down to ~1.5 mL of a yellow liquid. This liquid was run through a flash plug of silica with pentane as the eluent. A 100-mL portion was collected from the column, and this was concentrated down to obtain pure product with trace pentane. Note: B-E is moderately air-sensitive; any manipulations should be carried out quickly and the product should be stored in the dark under nitrogen. ^{1}H NMR (C$_6$D$_6$, 20 °C, 500 MHz): δ [ppm] 6.13-6.02 (overlapping m, 4H, CH$_3$CHCHCHCHCHCH$_3$), 5.53 (m, 2H, CH$_3$CHCHCHCHCHCHCH$_3$), 1.60 (dd, 6H, CH$_3$CHCHCHCHCHCHCH$_3$ J$_{HH}$ = 7 Hz, 2 Hz). ^{13}C{^{1}H} NMR (CDCl$_3$, 20°C, 125 MHz): δ [ppm] 131.98, 130.68, 128.88, 18.39. GC/MS: m/z = 108. ^{1}H NMR data was consistent with a literature report.[22] See Figure 11.

Observation of (E,Z,E)-1,6-diphenyl-2,4,6-hexatriene (C-Z)

This product was identified in the product mixtures of homocoupling reactions. ^{1}H NMR (C$_6$D$_6$, 20°C, 500 MHz): δ [ppm] 7.37 (m, 2H, PhCHC*H*CHCHCH*C*HPh), 6.50 (d, 2H, PhC*H*CHCHCHCHC*H*Ph, J$_{HH}$ = 17 Hz), 6.18 (m, 2H, PhCHCHC*HC*HCHCHPh). ^{1}H NMR in CDCl$_3$ matched that of a literature report.[29] See Figure 12.

Observation of (E,E,E)-1,6-diphenyl-2,4,6-hexatriene (C-E)

This product was identified by taking the ^{1}H NMR spectrum of a pure sample purchased from Sigma Aldrich. ^{1}H NMR (C$_6$D$_6$, 20°C, 500 MHz): δ [ppm] 6.82 (m, 2H, PhCHC*H*CHCHC*H*CHPh), 6.50 (d, 2H, PhC*H*CHCHCHCHC*H*Ph, J$_{HH}$ = 17 Hz), 6.37 (m, 2H, PhCHCHC*HC*HCHCHPh). See Figure 13.

Observation of (E,Z,E)-7,9,11-octadecatriene (D-Z)

This product was identified in the product mixtures of some homocoupling reactions and assigned with the aid of comparison with the ^{1}H NMR spectrum of **B-Z** (See Figure 14). ^{1}H NMR (C$_6$D$_6$, 20°C, 500 MHz): δ [ppm] 6.67 (m, 2H, RCH$_2$CHC*H*CHCHC*H*CHCH$_2$R), 6.00 (m, 2H, RCH$_2$CHCHC*HC*HCHCHCH$_2$R), 5.66 (m, 2H, RCH$_2$C*H*CHCHCHCHC*H*CH$_2$R), 2.05 (m, 4H, RC*H*$_2$CHCHCHCHCHCHC*H*$_2$R), 1.38-0.82 (22H, alkyl).

Observation of (E,E,E)-7,9,11-octadecatriene (D-E)

This product was identified in the product mixtures of some homocoupling reactions and assigned with the aid of comparison with the 1H NMR spectrum of **B-E** (See Figure 15). ^{1}H NMR (C$_6$D$_6$, 20°C, 500 MHz): δ [ppm] 6.19-6.10 (overlapping m, 4H, RCH$_2$CHC*HC*HC*HC*HCHCH$_2$ R), 5.72-5.56 (between these values) (m, 2H, RCH$_2$C*HCHCHCHCHC*HCH$_2$ R), 2.05 (m, 4H, RC*H*$_2$CHCHCHCHCHCHC*H*$_2$ R), 1.38-0.82 (22H, alkyl).

Experimental details for metathesis homocoupling reactions

In reading the tables, please note that all conversions, yields and Z content numbers are based on NMR integration of spectra of the product mixture. Conversion is based on disappearance of the substrate. The yield is defined as [(Z product + E product)/ (Z product + E product + side products + remaining substrate)] x 100%. The Z content is defined as the [Z

product/ (Z product + E product)] x 100%. Side product formation was quantified by comparison to an internal standard (4,4′-di-t-butylbiphenyl).

General procedure for closed-vessel homocoupling reactions

In the glovebox, a J. Young tube was charged with 0.01 mmol solid catalyst (5 mol%, ~ 10 mg), 0.75 mL C_6D_6, and 0.20 mmol liquid substrate solution (in cases of detectable side product formation, some 4,4′-di-t-butylbiphenyl was added as an internal standard). The tube was sealed, shaken to mix, and allowed to sit at RT. ^{1}H NMR spectra were taken periodically to monitor the reaction.

General procedure for open-vessel homocoupling reactions

In the glovebox, a small vial was charged with a stir bar, 0.01 mmol solid catalyst (5 mol%, ~10 mg), 1.5 mL C_6D_6, and 0.20 mmol liquid substrate solution (in cases of detectable side product formation, some 4,4′-di-t-butylbiphenyl was added as an internal standard). This mixture was then stirred at room temperature with the cap on loosely to allow for the escape of generated ethylene. Aliquots were taken for ^{1}H NMR analysis periodically to monitor the reaction.

Procedure for obtaining an isolated yield of pure product from the homocoupling of C

In the glovebox, a 20-mL vial was charged with a stir bar, 4 mL C_6D_6, 1.0 mL 3.00 M C solution (3.00 mmol, 1 equiv) and 130 mg 1 (.150 mmol, 5 mol%). This mixture was stirred at RT with the vial cap on loosely for 24 h, after which time a ^{1}H NMR aliquot was taken (spectrum showed >98% conv., >98% Z). The mixture was brought out of the glovebox, quenched with 8 drops MeOH, and the volatiles were removed by rotary evaporation. A silica dry-load of the residue was made with ~2 g silica. This was run in a silica column with pentane as the eluent. A bright blue product spot (under UV) was observed in the TLC analysis of the fractions. 308 mg white/yellow material was isolated (88% yield); ^{1}H NMR analysis showed it to be pure homocoupling product, but the composition was ~3:1 C-Z:C-E. As negligible C-E was present in the original reaction mixture (prior to workup), it was concluded that some isomerization[32] (but little to no decomposition) of the C-Z product must have occurred during workup.

Experimental details for crystal structure acquisition and refinement

Mo(NAr)(CHCHC(CH₃)₂)(Me₂pyr)(OHMT) (4a)

The crystal structure acquisition and refinement were carried out with assistance from Dr. Peter Müller and Dr. Michael Takase. Low-temperature diffraction data (φ- and ω-scans) were collected on a Siemens Platform three-circle diffractometer coupled to a Bruker-AXS Smart Apex CCD detector with graphite-monochromated Mo Kα radiation (λ=0.71073 Å) for the structure of compound **4a**. The structure was solved by direct methods using SHELXS[38] and refined against F_2 on all data by full-matrix least squares with SHELXL-97[39] following established refinement strategies.[40]

All non-hydrogen atoms were refined anisotropically. All hydrogen atoms (except H1 and H2, which have been taken from the difference Fourier synthesis and refined semi-freely with the help of distance restraints) were included into the model at geometrically calculated positions and refined using a riding model. The isotropic displacement parameters of all hydrogen atoms were fixed to 1.2 times the U value of the atoms they are linked to (1.5 times for methyl groups). Mo(NAr)(CHCHC(CH₃)₂)(Pyr)(OHMT) crystallized in space group P2(1)/n with one molecule in the asymmetric unit.

Crystal data and structure refinement for 4a

Identification code	11139_0m	
Empirical formula	$C_{47}H_{58}MoN_2O$	
Formula weight	762.89	
Temperature	100(2) K	
Wavelength	0.71073 Å	
Crystal system	Monoclinic	
Space group	P2₁/n	
Unit cell dimensions	a = 10.7915(9) Å	$\alpha = 90°$
	b = 18.6255(15) Å	$\beta = 90.8240(10)°$
	c = 20.4579(16) Å	$\gamma = 90°$
Volume	4111.6(6) Å^3	
Z	4	

Density (calculated)	1.232 Mg/m^3
Absorption coefficient	0.355 mm^{-1}
F(000)	1616
Crystal size	0.25 x 0.20 x 0.20 mm^3
Theta range for data collection	1.48 to $30.32°$
Index ranges	$-15 \leq h \leq 15, -26 \leq k \leq 26, -28 \leq l \leq 29$
Reflections collected	113555
Independent reflections	12346 [R(int) = 0.0480]
Completeness to theta = $30.32°$	99.9%
Absorption correction	Semi-empirical from equivalents
Max. and min. transmission	0.9324 and 0.9165
Refinement method	Full-matrix least-squares on F^2
Data / restraints / parameters	12346 / 2 / 480
Goodness-of-fit on F^2	1.042
Final R indices [I>2sigma(I)]	$R_1 = 0.0291, wR_2 = 0.0697$
R indices (all data)	$R_1 = 0.0372, wR_2 = 0.0749$
Largest diff. peak and hole	0.946 and -0.483 e Å^{-3}

REFERENCES

[1] Schrock, R. R. *Chem. Rev.* **2009**, *109*, 3211.

[2] a) Schrock, R. R.; Crowe, W. E.; Bazan, G. C.; DiMare, M.; O'Regan, M. B.; Schofield, M. H. *Organometallics* **1991**, *10*, 1832; b) Johnson, L. K.; Grubbs, R. H.; Ziller, W. J. *J. Am. Chem. Soc.* **1993**, *115*, 8130; c) de la Mata, F. J.; Grubbs, R. H. *Organometallics* **1996**, *15*, 577.

[3] (a) Schrock, R. R.; Luo, S.; Lee, J. C.; Zanetti, N. C.; Davis, W. M. *J. Am. Chem. Soc.* **1996**, *118*, 3883. (b) Fox, H. H.; Lee, J.-K.; Park, L. Y.; Schrock, R. R. *Organometallics* **1993**, *12*, 759. (c) Fox, H. H.;Wolf,M.O.;O' Dell, R.; Lin, B. L.; Schrock, R. R.; Wrighton, M. S. *J. Am. Chem. Soc.***1994**, *116*, 2827. (d) Anders,U.; Nuyken,O.; Buchmeiser,M. R.; Wurst, K. *Angew. Chem., Int. Ed.* **2002**, *41*, 4044. (e) Anders, U.; Nuyken, O.; Buchmeiser, M. R.; Wurst, K. *Macromolecules* **2002**, *35*, 9029. (f) Buchmeiser, M. R. *Monatsh. Chem.* **2003**, *134*, 327.

[4] Funk, T. W.; Efskind, J.; Grubbs, R. H. *Org. Lett.* **2005**, *7*, 187.

[5] Dewi, P.; Randl, S.; Blechert, S. *Tet. Lett.* **2005**, *46*, 577.

[6] Trnka, T. M.; Day, M. W.; Grubbs, R. H. *Organometallics* **2001**, 20, 3845.

[7] Lee, H.-Y.; Kim, B. G.; Snapper, M. L. *Org. Lett.* **2003**, *5*, 1855.

[8] Royer, F.; Vilain, C.; Elkaim, L.; Grimaud, L. *Org. Lett.* **2003**, *5*, 2007.

[9] Woerlee, E. F. G.; Bosma, R. H. A.; van Eijl, J. M. M.; Mol, J. C. Applied Catalysis 1984, 10, 219.

[10] (a) Ibrahem, I; Yu, M.; Schrock, R. R.; Hoveyda, A. H. *J. Am. Chem. Soc.* **2009**, *131*, 3844. (b) Flook, M. M.; Jiang, A. J.; Schrock, R. R.; Müller, P.; Hoveyda, A. H. *J. Am. Chem. Soc.* **2009**, *131*, 7962. (c) Flook, M. M.; Gerber, L. C. H.; Debelouchina, G. T.; Schrock, R. R. *Macromolecules* **2010**, *43*, 7515. (d) Jiang, A. J.; Zhao, Y.; Schrock, R. R.; Hoveyda, A. H. *J. Am. Chem. Soc.* **2009**, *131*, 16630. (e) Marinescu, S. C.; Schrock, R. R.; Müller, P.; Takase, M. K.; Hoveyda, A. H. *Organometallics* **2011**, *30*, 1780. (f) Meek, S. J.; O'Brien, R. V.; Llaveria, J.; Schrock, R. R.; Hoveyda, A. H. *Nature* **2011**, *471*, 461. (g) Yu, M.; Wang, C.; Kyle, A. F.; Jakubec, P.; Dixon, D. J.; Schrock, R. R.; Hoveyda, A. H. *Nature* **2011**, *479*, 88. (h) Peryshkov, D. V.; Schrock, R. R.; Takase, M. K.; Müller, P.; Hoveyda, A. H. *J. Am. Chem. Soc.* **2011**, *133*, 20754. (i) Yu, M.; Ibrahem, I.; Hasegawa, M.; Schrock, R. R.; Hoveyda, A. H. *J. Am. Chem. Soc.* **2012**, *134*, 2788.

[11] Mariano, P. S.; Bay, E.; Watson, D. G.; Rose, T.; Bracken, C. *J. Org. Chem.* **1980**, *45*, 1753.

[12] Werstiuk, N. H.; Timmins, G.; Ma, J.; Wildman, T. A. *Can. J. Chem.* **1992**, *70*, 1971.

[13] Olivella, S.; Sole, A.; Lledo, A.; Ji, Y.; Verdaguer, X.; Suau, R.; Riera, A. *J. Am. Chem. Soc.* **2008**, *130*, 16898.

[14] Schrock, R. R.; Jiang, A. J.; Marinescu, S. C.; Simpson, J. H.; Müller, P. *Organometallics*, **2010**, *29*, 5241.

[15] Lee, Y.-J.; Schrock, R. R.; Hoveyda, A. H. *J. Am. Chem. Soc.* **2009**, *131*, 10652.

[16] Schrock, R. R.; Murdzek, J. S.; Bazan, G. C.; Robbins, J.; DiMare, M.; O'Regan, M. *J. Am. Chem. Soc.* **1990**, *112*, 3875.

[17] Lichtscheidl, A. G.; Ng, V. W. L.; Müller, P.; Takase, M. K.; Schrock, R. R.; Malcolmson, S. J.; Meek, S. J.; Li, B.; Kiesewetter, E. T.; Hoveyda, A. H. *Organometallics* **2012**, *31*, 4558.

[18] Mundal, D. A.; Lutz, K. E.; Thomson, R. J. *Org. Lett.* **2009**, *11*, 465.

[19] Wu, J. Y.; Moreau, B.; Ritter, T. *J. Am. Chem. Soc.* **2009**, *131*, 12915.

[20] Amoroso, D.; Snelgrove, J. L.; Conrad, J. C.; Drouin S. D.; Yap, G. P. A.; Fogg D. E. *Adv. Synth. Catal.* **2002**, *344*, 757.

[21] Baldwin, J. E.; Reddy, V. P. *J. Org. Chem.* **1988**, *53*, 1129.

[22] Schuster, D. I.; Wang, L.; van der Veen, J. M. *J. Am. Chem. Soc.* **1985**, *107*, 7045.

[23] Jacobson, B. M.; Arvanitis, G. M.; Eliasen, C. A.; Mitelman, R. *J. Org. Chem.* **1985**, *50*, 194.

[24] Cao, X.-P.; Chan, T.-L.; Chow, H.-F.; Tu, J. *J. Chem. Soc. Chem. Commun.* **1995**, 1297.

[25] Chan, T.-L.; Fong, S.; Li, Y.; Man, T.-O.; Poon, C.-D. *J. Chem. Soc. Chem. Commun.* **1994**, 1771.

[26] McCarthy, J. R.; Matthews, D. P.; Paolini, J. P. *Org. Synth.* **1995**, *72*, 209.

[27] Trost, B. M.; Curran, D. P. *Tet. Lett.* **1981**, *22*, 1287.

[28] Martinetz, D.; Hiller, A. *Zeitschrift fur Chimie*, **1978**, *18*, 61.

[29] Sonoda, Y.; Suzuki, Y. *J. Chem. Soc. Perkin Trans. 2* **1996**, 401.

[30] Marinescu, S. C.; King, A. J.; Schrock, R. R.; Singh, R.; Muller, P; Takase, M. K. *Organometallics* **2010**, *29*, 6816 and references therein.

[31] Jiang, A. J.; Simpson, J. H.; Müller, P.; Schrock, R. R. *J. Am. Chem. Soc.* **2009**, *131*, 7770.

[32] Saltiel, J.; Wang, S.; Watkins, L. P.; Ko, D.-H. *J. Phys. Chem. A* **2000**, *104*, 11443.

[33] Krieckmann, T; Arndt, S.; Schrock, R. R.; Müller, P. *Organometallics* **2007**, *26*, 5702.

[34] Dickie, D. A.; MacIntosh, I. S.; Ino, D. D.; He, Q.; Labeodan, O. A.; Jennings, M. C.; Schatte, G.; Walsby, C. J.; Clyburne, J. A. C. *Can. J. Chem.* **2008**, *86*, 20.

[35] (a) Schiemenz, B.; Power, P. P. *Organometallics* **1996**, *15*, 958 (b) Stanciu, C.; Olmstead, M. M.; Phillips, A. D.; Stender, M.; Power, P. P. *Eur. J. Inorg. Chem.* **2003**, 3495.

[36] Hatch, L. F.; Everett, G. D. *J. Org. Chem.* **1968**, *33*, 2551.

[37] Foa, M.; Venturi, M. T. *Gazz. Chim. Ital.* **1975**, *105*, 1199.

[38] Sheldrick, G. M. *Acta Cryst.* **1990**, A46, 467.

[39] Sheldrick, G. M. *Acta Cryst.* **2008**, A64, 112.

[40] Müller, P. *Crystallography Reviews* **2009**, *15*, 57.

Chapter 3

Heteroatom-Substituted Alkylidene Complexes of Molybdenum

INTRODUCTION

High-oxidation-state Mo and W imido alkylidene complexes have been studied for many years, and hundreds of derivatives are now known. The vast majority of these have substituents on the alkylidene that are either hydrogen or carbon-based.[1] Consequently, despite the breadth of research in this area, relatively few high-oxidation-state alkylidene complexes with heteroatom substituents exist. A small number of complexes in which there are Si or Ge substituents on the alkylidene have been reported,[1a,2] as have some Fischer-carbene-like W(VI) siloxy examples.[3] The most relevant Schrock-type examples come in the form of Re(VII) alkylidyne alkylidene bis-alkoxide complexes reported in the mid-1990s.[4] The report by Toreki *et. al.*[4a] is of particular note; within it there are examples of complexes in which the alkylidenes are substituted with alkoxy, amido, sulfide, and siloxy groups. (Figure 1).

ER = OEt, Fc, SPh, N(pyrrolidinone)
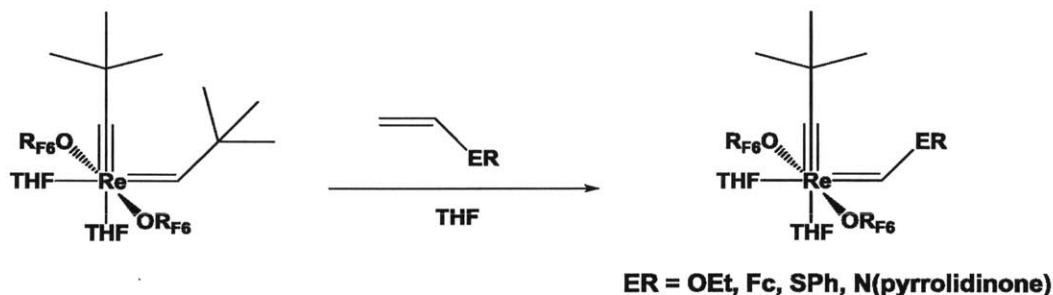
Figure 1: High-oxidation-state Re heteroatom-substituted alkylidenes

These complexes were studied from a fundamental perspective, but their metathesis properties were not reported to any substantial extent. Furthermore, no Mo or W analogues have been synthesized. As such, there is much interest in the stability and reactivity of Mo and W heteroatom-substituted alkylidenes, especially in light of the many advances in Schrock catalysts in recent years.

A broader look at heteroatom-substituted alkylidenes reveals some examples that are relevant from a metathesis perspective, but there remains a relative lack of exploration in the area. For instance, Grubbs and coworkers have described the synthesis of heteroatom-substituted Ru bis-triphenylphosphine dichloride (or bis-trifluoroacetato) complexes (Grubbs I-type complexes), with the heteroatom being N, O, or S.[5] More recently, this theme was expanded to include Grubbs-II-type complexes with similar alkylidene substituents.[6] The complexes in these reports were active for the ring-opening metathesis polymerization of norbornene.

112

Heteroatom-substituted alkylidenes are presumably intermediates in metathesis of heteroatom-substituted olefins. Nearly all reports of heteroatom-substituted olefin metathesis involve Ru-based catalysts, and while there has been reasonable success in some areas (especially with vinyl ethers),[7] there remain many unmet challenges.[8] Mo- and W-based catalysts may be able to overcome these challenges, and they bring enhanced opportunities for reactivity and selectivity as well. Recent prominent examples include Z-selective cross-metathesis of vinyl ethers[9] and (separately) vinylboronates[10] from reports by Hoveyda and coworkers. While the results are impressive, no attempt is made to probe for the existence of heteroatom-substituted alkylidene intermediates in any of the above reports.

As olefin metathesis advances to include heteroatom-substituted substrates, it becomes more important to determine what types of heteroatom-substituted alkylidene complexes can be formed and to investigate their reactivity with ordinary olefins. With this in mind, we undertook an effort to explore the synthesis, fundamental properties, and basic metathesis reactivity of heteroatom-substituted alkylidenes in a monoalkoxide pyrrolide (MAP) framework. Part I of this chapter focuses on the exploratory synthesis and characterization of several MAP heteroatom-substituted alkylidene complexes, including NMR analysis, X-ray crystallographic studies and some comparisons of structural/electronic features. In some cases, the alkylidene complexes showed unusual temperature-dependent fluxional behavior, and investigations in this area can be found in Part II. Finally, Part III contains examinations of the behavior of the new complexes in olefin metathesis. These studies give us substantial insight into the basic organometallic chemistry of the systems and open up new, potentially synthetically useful avenues in olefin metathesis.

RESULTS AND DISCUSSION

I. Synthesis of heteroatom-substituted MAP alkylidene complexes

It was decided that the investigation of heteroatom-substituted alkylidenes would be undertaken from a purely synthetic point of view to begin. As the relative reactivity of the heteroatom-substituted terminal olefins with metal alkylidene complexes was not fully known, using a very reactive alkylidene starting point (such as a Mo methylidene) would be prudent. Furthermore, an alkylidene exchange reaction in which the only by-product is ethylene is synthetically desirable. The MAP methylidene complex $Mo(NAr)(CH_2)(Me_2pyr)(OTPP)$ (**1a**) (Ar = 2,6-

diisopropylphenyl; Me$_2$pyr = 2,5-dimethylpyrrolide; TPP = 2,3,5,6-tetraphenylphenyl) was chosen as a starting point for the studies of heteroatom-substituted alkylidenes: its ligand framework is representative of the MAP catalyst family, and the tetraphenylphenoxide ligand is known to form highly crystalline complexes. Thus, the chances of a metathesis reaction occurring to give the desired heteroatom substituted alkylidene were relatively high (due to the reactivity of methylidenes), as were the chances of the resulting compound being isolable.

I-A. Preparation of precursors

A general route for the synthesis of heteroatom-substituted alkylidene complexes is shown in Scheme 1. It should be noted that in some cases, it is possible to bypass the formation of **1a** and simply form the target complex by direct reaction of the heteroatom-substituted olefin with **1**.
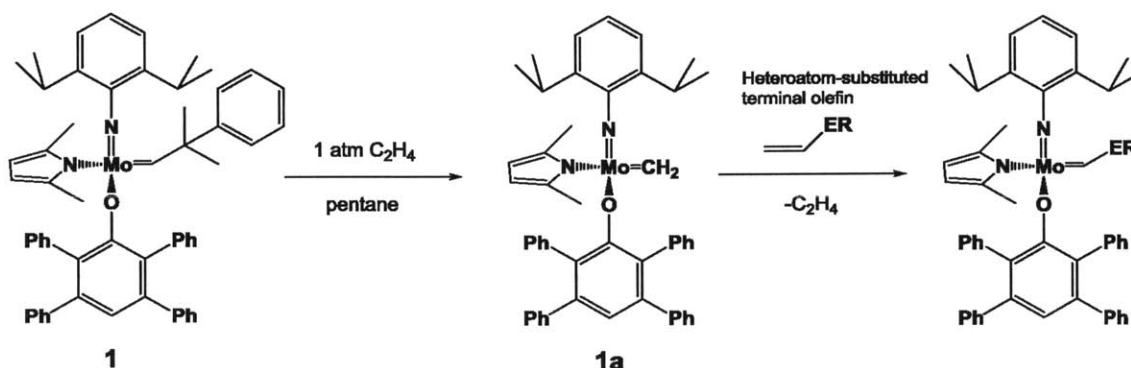
Scheme 1: Strategy for synthesis of heteroatom-substituted alkylidenes

Compound **1** is isolable in high yield according to a reported procedure.[11] Furthermore, although the HOTPP ligand has been reported,[12] a more detailed, improved synthesis is reported in Chapter 4. Formation of the methylidene **1a** is described in Chapter 2. Thus, the precursors to heteroatom-substituted alkylidenes were relatively easy to prepare on a reasonable scale.

I-B. An oxygen-substituted alkylidene

Given the prior success of vinyl ether cross-metathesis with Mo MAP species,[9] pursuit of an oxygen-substituted alkylidene complex seemed a logical place to start. While oxygen-substituted alkylidenes are not strictly necessary intermediates in the cross-metathesis mechanism, they are likely found in reaction mixtures when there is excess vinyl ether present. Initial NMR-scale studies in which propyl vinyl ether was added to **1** showed the formation of a

single new alkylidene species. The scaled-up reaction to obtain an isolable complex is shown in Scheme 2.
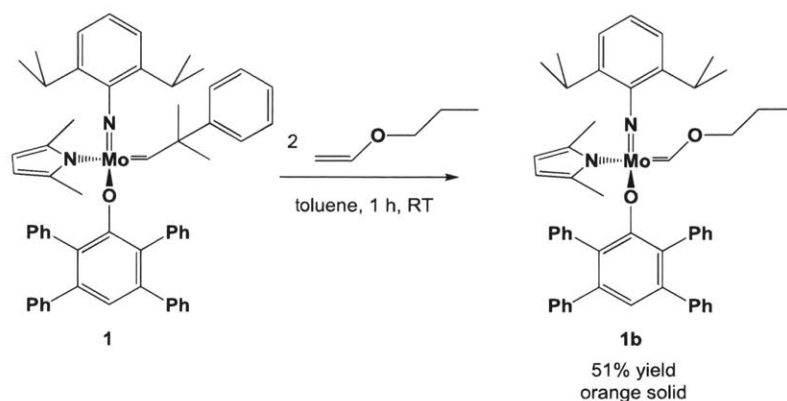
Scheme 2: Synthesis of Mo(NAr)(CHOPr)(Me$_2$pyr)(OTPP) (1b)

1 was treated with 2 equivalents of propyl vinyl ether in toluene and this mixture was stirred for 1 h. Removal of the solvent *in vacuo*, followed by successive additions of pentane and further solvent removals, led to the isolation of the product, Mo(NAr)(CHOPr)(Me$_2$pyr)(OTPP) (**1b**), as an orange solid in 51% yield.

The ^{1}H NMR spectrum of **1b** in C$_6$D$_6$ showed a lone singlet in the alkylidene region at 10.57 ppm. At this point, it was still unknown if the alkylidene was *syn* (substituent oriented toward the imido group) or *anti*. The $^1J_{CH}$ value for the alkylidene proton (coupling to the alkylidene carbon) was 140 Hz, which is in the *anti* range for conventional Mo and W MAPs and bisalkoxide alkylidene complexes.[13] However, the previously mentioned report on Re alkylidyne alkylidene complexes[4a] included ^{1}H NMR data for the *syn* and *anti* isomers of Re(C-*t*-Bu)(CHOEt)(OC(CF$_3$)$_2$CH$_3$)$_2$(THF)$_2$: the *syn* alkylidene had a similar $^1J_{CH}$ value of 135 Hz while the *anti* isomer had a much higher $^1J_{CH}$ value of 163 Hz. These precedents, along with the *syn* configuration seen in the X-ray crystal structure of **1b**, led to the conclusion that **1b** is observed as a *syn* isomer only.

Crystals of **1b** grown from ether and pentane were used to obtain an X-ray crystal structure, which is shown in Figure 2.

115

Figure 2: Thermal ellipsoid drawing of 1b (50% probability ellipsoids). Selected distances (Å) and angles (deg): Mo(1)-C(1) = 1.921(3), C(1)-O(2) = 1.343(4), Mo(1)-C(1)-O(2) = 142.7(3), Mo(1)-C(1)-H(1): 109(2), C(1)-O(2)-C(2): 118.1(3).

As previously mentioned, the structure clearly shows a *syn* alkylidene configuration. Not surprisingly, the bond angles about the alkylidene carbon are indicative of the commonly seen α agostic interaction between the alkylidene C-H bond and the metal (Mo1-C1-O2 = 142.7°). The Mo=C bond measures 1.92 Å, which is slightly longer than the alkylidene bond in the analogous neophylidene compound (1.88 Å).[11] Natural Bond Orbital (NBO) calculations using the atom positions from the crystal structure were run by Dr. Stefan Kilyanek as part of this study (Figure 3).
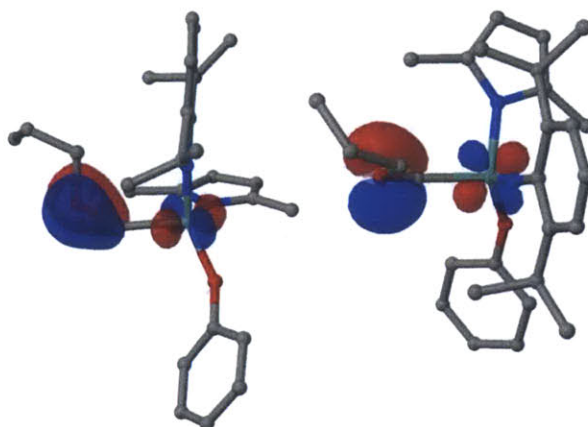
Figure 3: NLMO of the O lone pair (0.02 isovalue) showing an O lone pair overlapping with the Mo=C π antibonding orbital in 1b. H atoms and the OTPP phenyl rings have been omitted for clarity. Calculations and figure done by Dr. Stefan Kilyanek.

116

These calculations reveal that the O lone pair donates electron density into the Mo=C π* orbital: the Natural Localized Molecular Orbital (NLMO) of the lone pair contains a 7.0% contribution from the alkylidene carbon and a 3.4% contribution from Mo (98% d character). This donation could explain the longer bond distance, as population of the π* orbital gives the bond less double bond character and more single bond character. Aside from this conjugation, the structural and electronic features of **1b** appear typical for MAP species.

I-C. A chelating nitrogen-substituted alkylidene

Following the lead of previous studies of nitrogen-substituted alkylidenes,[4a,5,6] the next step was to probe the reaction of the methylidene complex **1a** with the commercially available nitrogen-substituted olefin *N*-vinylpyrrolidinone (NVP). NMR-scale studies showed clean formation of a new alkylidene species, so the reaction was scaled up as shown in Scheme 3.
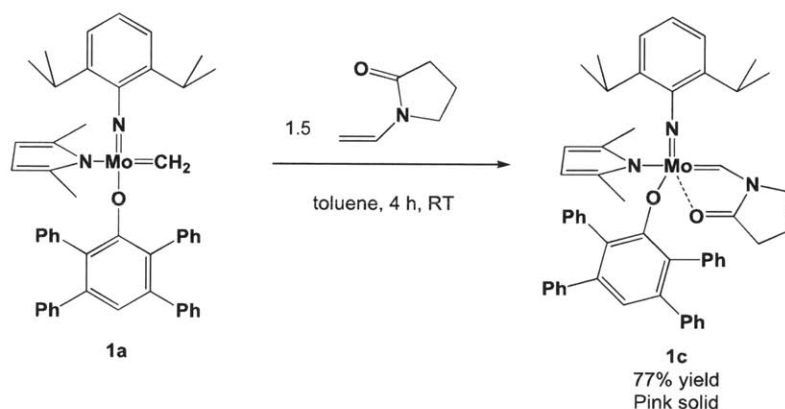
Scheme 3: Synthesis of Mo(NAr)[(CHN(CH₂)₃CO)](Me₂pyr)(OTPP) (1c)

Mo(NAr)[(CHN(CH$_2$)$_3$CO)](Me$_2$pyr)(OTPP) (**1c**) was synthesized via the addition of 1.5 equivalents of NVP to **1a** in toluene. After 4 h, the solvent was removed and pentane was added. Filtration gave a 77% yield of pink solid **1c.** It should be noted that **1c** can also be synthesized from the neophylidene precursor **1**, but much more reaction time is required for full conversion.

The $^1J_{CH}$ value for the alkylidene resonance of **1c** was 166 Hz, which is indicative of an *anti* alkylidene. The proposed structure involved coordination of the oxygen from the pyrrolidinone moiety in a position trans to the imido group, forcing the *anti* alkylidene orientation. An analogous five-coordinate rhenium heteroatom-substituted complex was reported to show a similar alkylidene coupling constant (173 Hz).[4a]

The X-ray crystal structure of **1c** (crystals were grown from dichloromethane/pentane) confirms this *anti*, chelating configuration of the alkylidene (Figure 4).
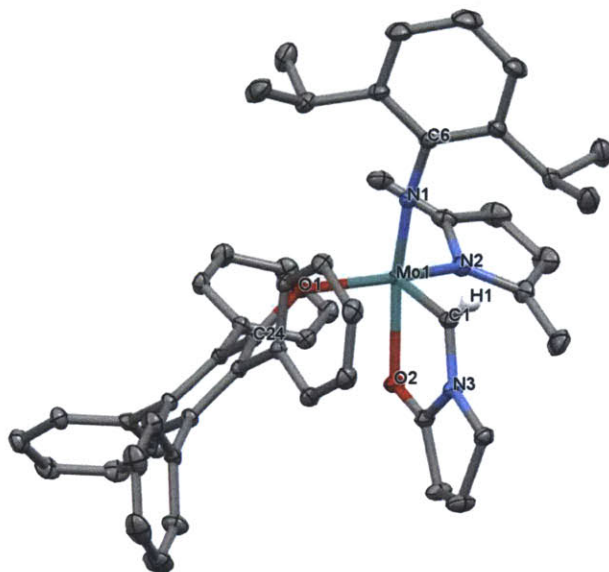
Figure 4: Thermal ellipsoid drawing of 1c (50% probability ellipsoids). Selected distances (Å) and angles (deg): Mo(1)-C(1) = 1.9578(11), Mo(1)-O(2) = 2.2080(8), H(1)-C(1)-Mo(1) = 129.5, C(1)-Mo(1)-O(2) = 75.08(4)

The Mo1-O2 distance (2.208 Å) is clearly indicative of a bonding interaction. The bond angles and distances of **1c** are somewhat distorted from those expected for a MAP complex, but this can be attributed to the unusual five-coordinate structure.

I-D. A four-coordinate nitrogen substituted alkylidene complex

While the structure of **1c** was interesting and unusual, we still wanted to prepare a nitrogen-substituted alkylidene complex with a standard four-coordinate MAP structure. To this end, the commercially available olefin *N*-vinylcarbazole (NVC) was added to the methylidene complex **1a** in an NMR-scale reaction. When a new alkylidene was cleanly formed, the reaction was scaled up as shown in Scheme 4.

118
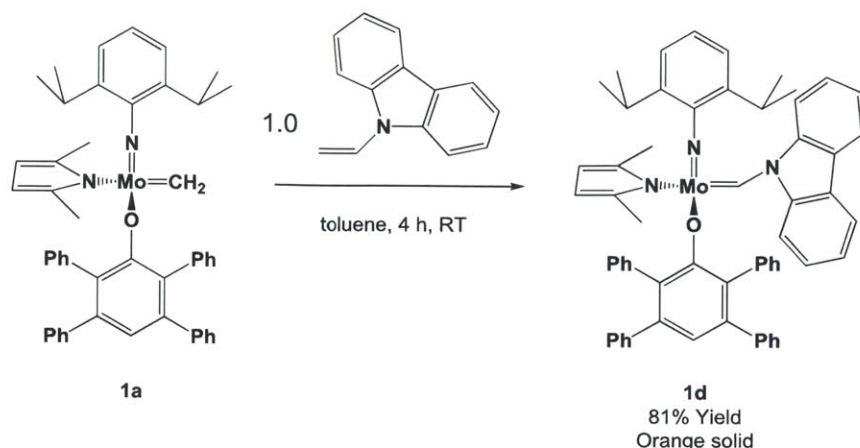
Scheme 4: Synthesis of Mo(NAr)(CHCarbaz)(Me$_2$pyr)(OTPP) (1d)

Mo(NAr)(CHCarbaz)(Me$_2$pyr)(OTPP) (**1d**) (Carbaz = *N*-carbazolyl) was synthesized via addition of 1.0 equivalents of NVC to **1a** in toluene. After 4 h, the solvent was removed and pentane was added. Filtration gave an 81% yield of orange solid **1d**. The ^{1}H NMR spectrum of **1d** showed a clean singlet in the alkylidene region with $^1J_{CH}$ = 134 Hz, which is within the range of *syn* alkylidenes for this system.

X-ray-quality crystals of **1d** were grown from toluene and pentane, and the obtained structure is shown below in Figure 5.
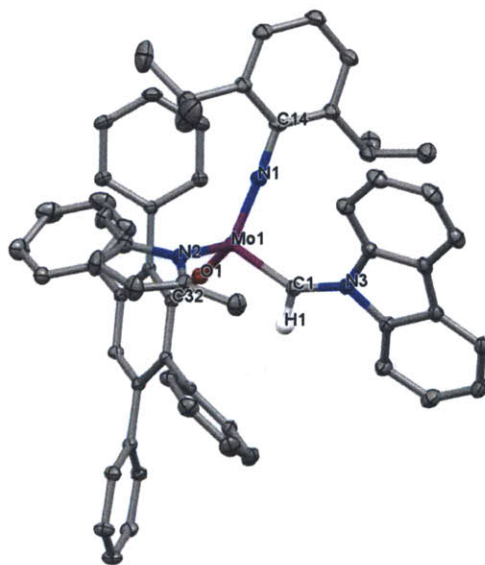
Figure 5: Thermal ellipsoid drawing of 1d (50% probability ellipsoids). Selected distances (Å) and angles (deg): Mo(1)-C(1) = 1.9140(13), C(1)-N(3) = 1.3797(16), Mo(1)-C(1)-N(3) = 143.60, Mo(1)-C(1)-H(1) = 108.2.

The *syn* alkylidene configuration matches the prediction based on the alkylidene coupling constant. Furthermore, the α agostic interaction of the alkylidene C-H bond is clearly visible

from the angles about C1. Otherwise, the slightly distorted tetrahedral structure that is typical of MAP complexes predominates.

I-E. A boron-substituted alkylidene

Boron-substituted olefins have been studied in metathesis processes before, both for Ru systems[8] and for Mo systems.[10] Perhaps the most common boron substrate of this type is vinylboronic acid pinacol ester (vinylBpin). Addition of 2.0 equivalents of vinylBpin to **1a** in an NMR-scale reaction showed that two new clean alkylidene species were formed. The signals for these species were broad and are thought to arise from a rapidly exchanging mixture of *syn* and *anti* Mo(NAr)(CHBpin)(Me$_2$pyr)(OTPP) (**1e**). The reaction to form **1e** was scaled up as shown in Scheme 5.
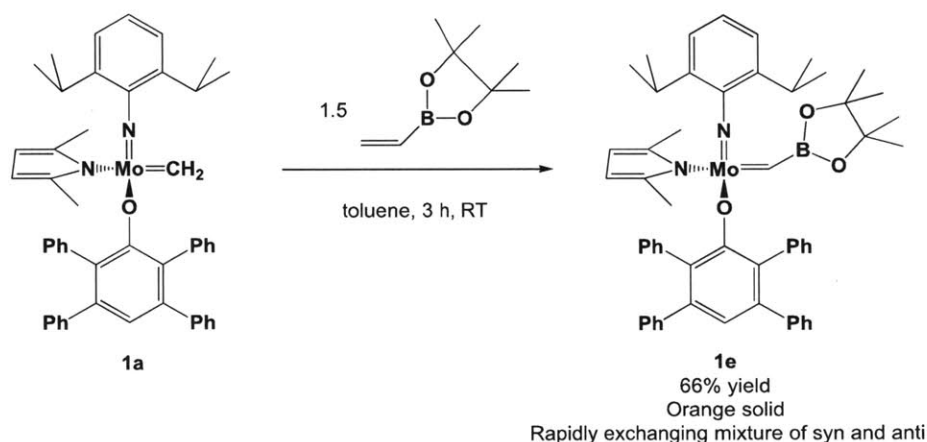
Scheme 5: Synthesis of Mo(NAr)(CHBpin)(Me$_2$pyr)(OTPP) (1e)

1.5 equivalents of vinylBpin were added to **1a** in toluene. After 3 h, the solvent was removed *in vacuo* and pentane was added to the residue. Filtration gave a 66% yield of orange solid **1e** (135 mg). The ^{1}H NMR spectrum of **1e** showed two broad peaks (2:1 integration ratio) in the alkylidene region at room temperature. Furthermore, the pyrrolide and isopropyl methine regions showed corresponding pairs of broad peaks in 2:1 ratios. Variable temperature NMR studies led to the conclusion that the peaks arise from the *syn* and *anti* isomers of **6**, which rapidly exchange at room temperature (details in Part II).

The X-ray crystal structure of **1e** (crystals were grown from toluene/pentane) is shown in Figure 6.
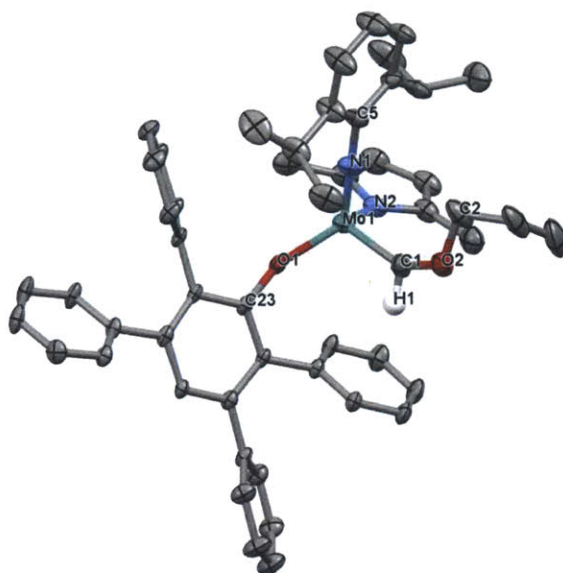
Figure 6: Thermal ellipsoid drawing of 1e (50% probability ellipsoids). Selected distances (Å) and angles (deg): Mo(1)-C(1) = 1.8811(11), C(1)-B(1) = 1.5511(16), Mo(1)-O(2) = 2.837, Mo(1)-C(1)-B(1) = 106.24(7), Mo(1)-C(1)-H(1) = 130.54 (1.01)

The *anti* alkylidene configuration is rare among four-coordinate complexes; this structure represents the only structurally characterized 14e Mo or W *anti* alkylidene. The Mo1-O2 distance of 2.837 Å is too long to suggest any electronic interaction between the two atoms. NBO calculations run by Dr. Stefan Kilyanek reveal that the empty p orbital on B is conjugated with the Mo=C π orbital, but the contribution from the B orbital (99% p) is only 3.7% of the Mo=C π NLMO (Figure 7).
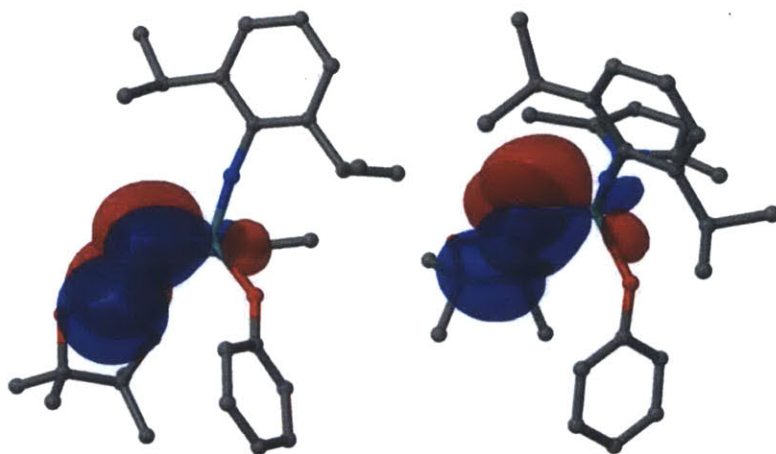
Figure 7: Overlap of the filled Mo=C π bond and the empty B p orbital in 1e (preorthogonalized NBOs at the 0.02 isovalue). H atoms and OTPP phenyl rings have been omitted for clarity. Calculations and figure done by Dr. Stefan Kilyanek.

121

Conjugation to the empty B p orbital should decrease the double-bond character of the Mo=C alkylidene bond, allowing it to rotate more freely. This interaction could help to explain the fluxional *syn/anti* interconversion displayed by **1e**.

I-F. A silicon-substituted alkylidene

There are some previous examples of high-oxidation-state silicon-substituted Mo and W alkylidenes.[2] However, these are limited to a few imido alkylidene bis-alkoxide complexes. Furthermore, silicon-substituted olefins are potentially useful substrates for olefin metathesis, so we chose to pursue the first Si-substituted alkylidene MAP complex (Scheme 6).
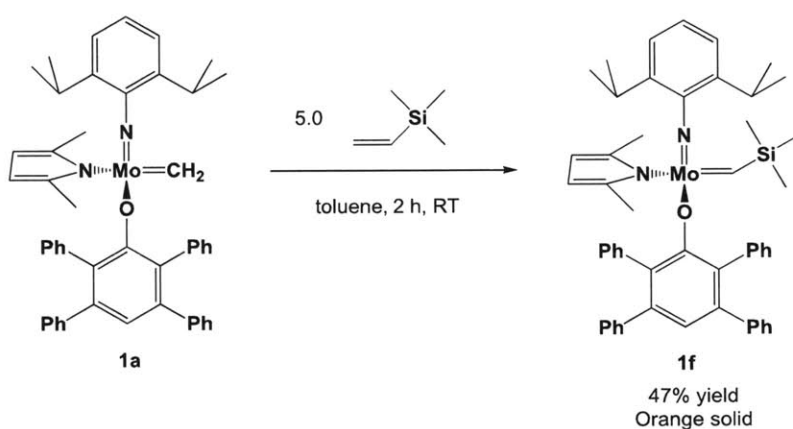
Scheme 6: Synthesis of Mo(NAr)(CHTMS)(Me₂pyr)(OTPP) (1f)

Trimethylvinylsilane (1.5 equivalents) was added to **1a** in toluene. After 2 h, the solvent was removed *in vacuo*. Trituration with pentane and filtration gave a 47% yield of orange solid Mo(NAr)(CHTMS)(Me₂pyr)(OTPP) **1f** (TMS = trimethylsilyl). (Note: The synthesis of this complex from **1** and trimethylvinylsilane appeared to be complete within ~8 h on an NMR-tube scale, but an attempt to scale up this reaction resulted in major decomposition.) The ^{1}H NMR spectrum of **1f** shows a single sharp alkylidene resonance at 12.55 ppm in C_6D_6. Furthermore, the alkylidene $^1J_{CH}$ of 114 Hz signifies that only the *syn* isomer exists in solution, in contrast with some previous bisalkoxide examples of the type M(NAr)(CHTMS)(OAr)₂, in which the *syn* and *anti* isomers interconverted rapidly at room temperature.[2a,b]

The X-ray crystal structure of **1f** (crystals grown in toluene and pentane) is shown in Figure 8.
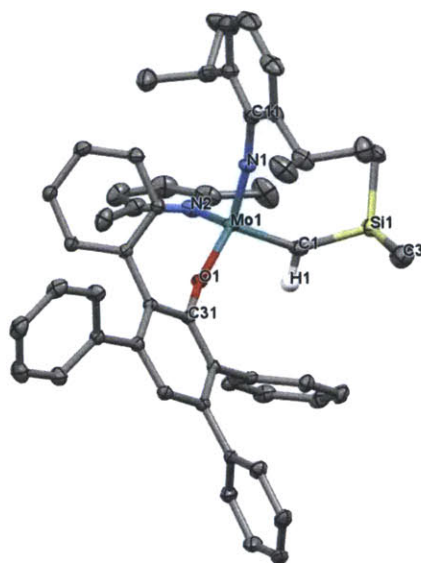
Figure 8: Thermal ellipsoid drawing of 1f (50% probability ellipsoids). Selected distances (Å) and angles (deg): Mo(1)-C(1) = 1.875(2), C(1)-Si(1) = 1.862(1), Mo(1)-C(1)-Si(1) = 139.96(8), Mo(1)-C(1)-H(1) = 102(1).

The observed *syn* configuration matches that expected from the ^{1}H NMR spectrum. The structure is otherwise unremarkable and quite similar to that of **1**.[11]

I-G. A sulfur-substituted alkylidene

Sulfur-substituted alkylidenes were previously unknown in Schrock-type systems. Addition of 2 equivalents of phenyl vinyl sulfide to **1** in a J. Young tube in C_6D_6 led to complete conversion to a new alkylidene within 18 h. The reaction was scaled up in order to isolate $Mo(NAr)(CHSPh)(Me_2pyr)(OTPP)$ (**1g**, Scheme 7).
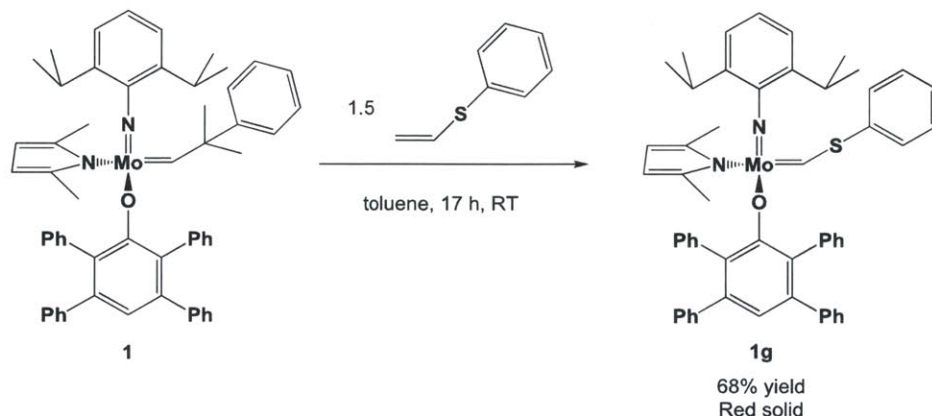
Scheme 7: Synthesis of Mo(NAr)(CHSPh)(Me₂pyr)(OTPP) (1g)

Phenyl vinyl sulfide (1.5 equivalents) was added to **1** in toluene and stirred for 17 h, after which time the solvent was removed *in vacuo*. Trituration with pentane and filtration gave a 68%

yield of red solid **1g**. (Note: The synthesis of this complex from **1a** also appeared clean on the NMR scale.) The ^{1}H NMR spectrum of **1g** shows a single sharp alkylidene resonance at 11.48 ppm in C_6D_6. The alkylidene $^1J_{CH}$ (146 Hz) seems fairly large for a *syn* isomer, but when compared to the values for the similar complex Re(Ct-Bu)(OC(CF$_3$)$_2$Me)$_2$(THF)$_2$(CHSPh)[4a] (*syn* J_{CH} = 143 Hz, *anti* J_{CH} = 184 Hz), it seems reasonable.

The X-ray crystal structure of **1g** (crystals were grown in toluene and pentane) is shown in Figure 9.
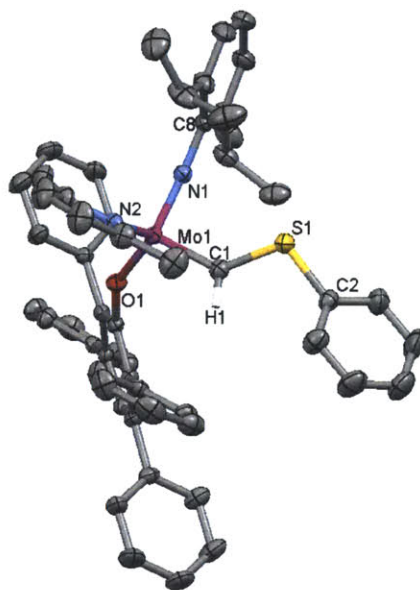
Figure 9: Thermal ellipsoid drawing of 1g (50% probability ellipsoids). Selected distances (Å) and angles (deg): Mo(1)-C(1) = 1.9112(15), C(1)-S(1) = 1.7179(16), Mo(1)-C(1)-S(1): 130.20(09), Mo(1)-C(1)-H(1) = 114.9, C(1)-S(1)-C(2) = 105.99(08).

The *syn* configuration of the alkylidene in the structure matches the assignment from the ^{1}H NMR spectrum. Furthermore, the α agostic interaction of the alkylidene C-H bond is clearly visible from the angles about C1.

NBO calculations run by Dr. Stefan Kilyanek reveal some interaction between the lone pair on the S atom and the Mo=C alkylidene bond: the NLMO of the S lone pair contains a 5.1% contribution from the alkylidene carbon and a 4.7% contribution from Mo (98% d character). This interaction may be responsible for the slightly elongated Mo=C bond (1.91 Å) with respect to the analogous bond in the neophylidene complex **1** (1.88 Å).

I-H. A phosphorus-substituted alkylidene

High-oxidation-state P-substituted alkylidene complexes of Mo and W were completely unprecedented, so we decided to synthesize and isolate a MAP alkylidene derived from diphenylvinylphosphine. Initial NMR-scale reactions suggested that the target could be synthesized from diphenylvinylphosphine and either **1** or **1a**, but scaled-up attempts at synthesis from **1** led to major decomposition (similar to the case of **1f**). Therefore, the scaled-up reaction was undertaken using **1a** as the starting material.

Diphenylvinylphosphine (1.0 equivalent) was added to **1a** in toluene. After 2 h, the solvent was removed *in vacuo* and pentane was added. Addition of tetramethylsilane was necessary to obtain a powdery solid, and filtration gave a 65% yield of Mo(NAr)(CHPPh$_2$)(Me$_2$pyr)(OTPP) (**1h**), but the ^{1}H NMR spectrum showed ~0.05 equivalents of free phosphine in the powder as well. The ^{1}H NMR spectrum of **1h** shows a tall, slightly broad alkylidene resonance at 12.31 ppm and a shorter, broader alkylidene resonance at 12.64 ppm in C$_6$D$_6$. The tall resonance has a $^1J_{CH}$ of 130 Hz, leading to its assignment as the *syn* isomer and the assignment of the shorter, broader isomer as the *anti*. The ratio of *syn:anti* is ~5:1. (Note: for a more detailed analysis of *syn:anti* isomerism in this complex, see Part II of this chapter).

In an attempt to isolate a pure complex (free from extra phosphine), the following synthesis of the acetonitrile adduct Mo(NAr)(CHPPh$_2$)(Me$_2$pyr)(OTPP)(MeCN) (**1h-MeCN**) was undertaken (Scheme 8). The synthetic details are similar to those above, only acetonitrile was added in place of tetramethylsilane. **1h-MeCN** can be isolated as a light orange solid, clearly different in color from **1h**.
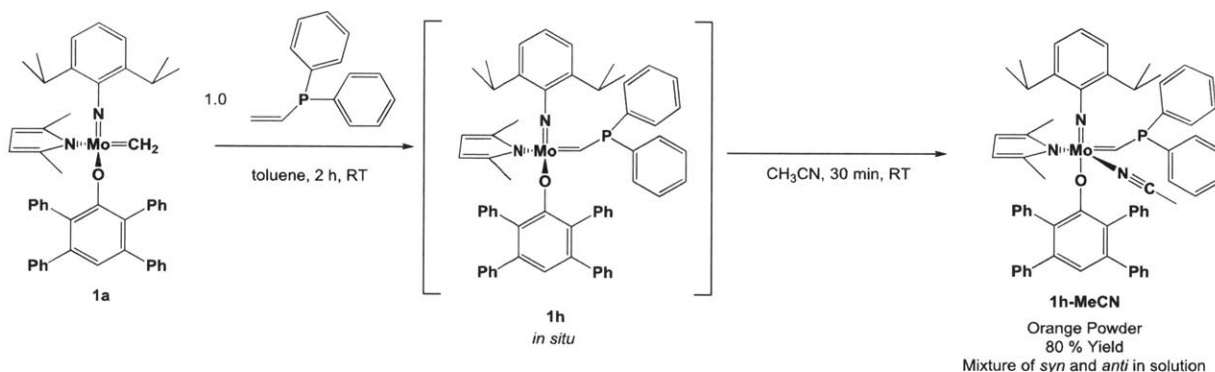
Scheme 8: Synthesis of Mo(NAr)(CHPPh$_2$)(Me$_2$pyr)(OTPP)(MeCN) (1h-MeCN)

The ^{1}H NMR spectrum of **1h-MeCN** is identical to that of **1h** at room temperature in C$_6$D$_6$, save for the presence of free MeCN in the spectrum of **1h-MeCN**. This led to the

conclusion that acetonitrile is not bound at room temperature in C_6D_6. Variable-temperature NMR studies (found in Part II) lent further evidence to this claim.

A later attempt at isolation of pure **1h** was successful through addition of exactly 1 equivalent of diphenylvinylphosphine and multiple washes with pentane. As stated before, **1h** is a red solid, and no spectral characteristics were different in this completely pure sample than in the sample containing a small amount of free phosphine. **1h** and **1h-MeCN** were resistant to characterization by elemental analysis; seemingly pure samples of **1h** would turn out poorly, and removing excess acetonitrile from **1h-MeCN** always led to either incomplete drying or decomposition. One elemental analysis result is given in the Experimental section. The synthesis of pure **1h** is shown in Scheme 9.
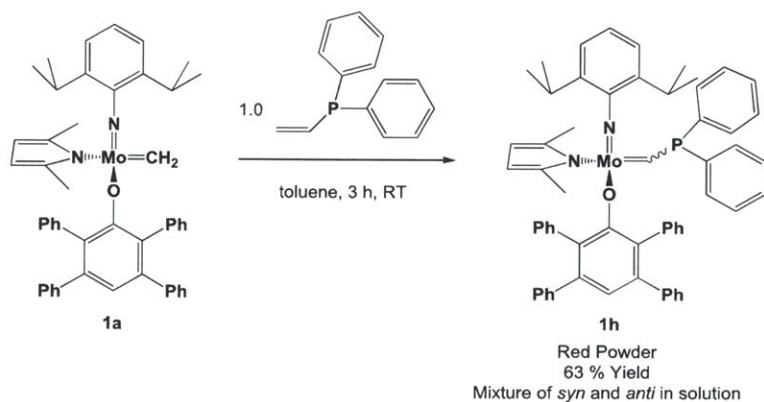
Scheme 9: Synthesis of Mo(NAr)(CHPPh₂)(Me₂pyr)(OTPP) (1h)

X-ray-quality crystals of **1h-MeCN** were grown in dichloromethane and ether. The structure is displayed in Figure 10.
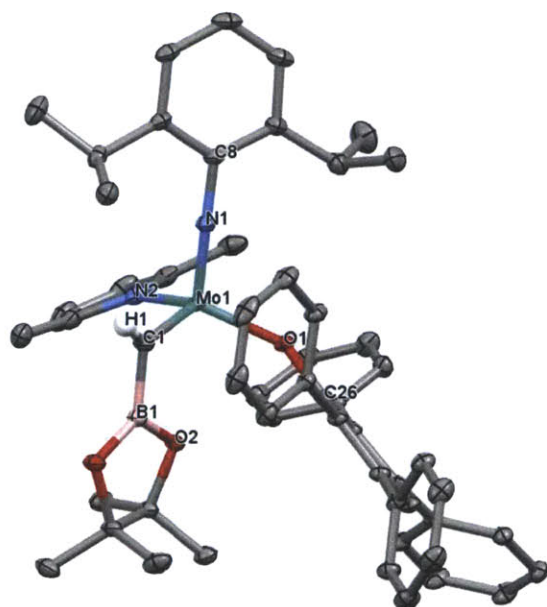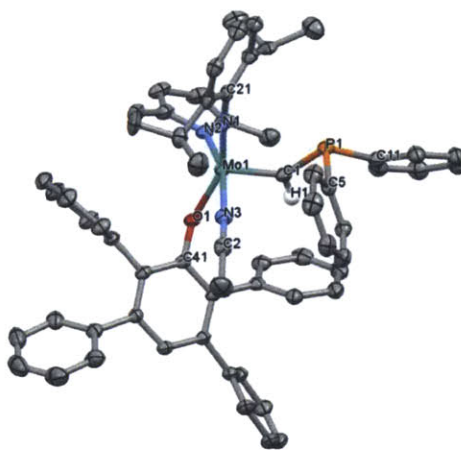

Figure 10: Thermal ellipsoid drawing of 1h-MeCN (50% probability ellipsoids). Selected distances (Å) and angles (deg): Mo(1)-C(1) = 1.904(2), C(1)-P(1) = 1.812, Mo(1)-C(1)-P(1) = 126.1(1), Mo(1)-C(1)-H(1) = 114(1).

126

The structure shows the acetonitrile adduct of the *syn* isomer. The complex is close to a square pyramid with the alkylidene ligand in the apical position. Further analysis of *syn/anti* isomerism and adduct formation can be found in Part II of this chapter.

NBO Calculations by Dr. Stefan Kilyanek reveal little to no contribution of the phosphorus lone pair to the Mo=C π bond. This is reasonable given that heavier main-group elements have a low propensity for forming multiple bonds to carbon because their lone pairs are largely of unhybridized s character.[14]

II. Fluxional and temperature-dependent behavior

As previously mentioned, some of the newly synthesized heteroatom-substituted alkylidene species showed evidence for both *syn* and *anti* isomers in their room temperature ^{1}H NMR spectra. In order to confirm this and to investigate the behavior of these species over a range of temperatures, variable-temperature ^{1}H NMR studies were carried out in toluene-d_8.

II-A. *Syn/anti* exchange in Mo(NAr)(CHBpin)(Me$_2$pyr)(OTPP) (1e)

The room-temperature ^{1}H NMR spectrum of **1e** in C$_6$D$_6$ showed two broad peaks in the alkylidene region. These peaks were postulated to arise from the rapidly exchanging *syn* and *anti* alkylidene isomers. In order to investigate this phenomenon, a sample of **1e** was dissolved in toluene-d_8 and the ^{1}H NMR spectra over a wide range of temperatures were observed. The comparison of these spectra can be found in Figure 11.

127
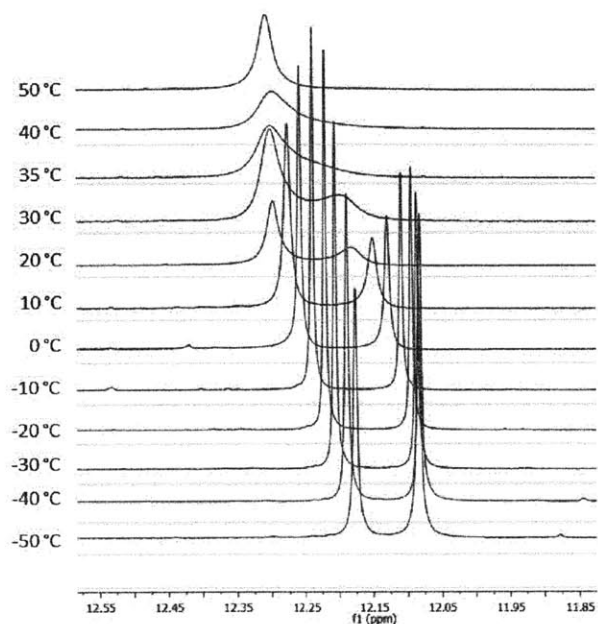
Figure 11: Temperature-dependent ¹H NMR spectra of 1e (toluene-d_8, 500 MHz) in the alkylidene region

The two broad peaks coalesce into one peak at around 35 °C, and at 50 °C, there is only one broad singlet that represents the average of the two isomers as the exchange process has become faster than the NMR time scale. Upon cooling the sample, the same two-peak spectrum can be recovered at room temperature. Cooling the sample results in a gradual sharpening of the two peaks; below -10 °C or so they appear as sharp singlets. Warming to room temperature after cooling yields the same broad signals as before, signifying that the variable-temperature behavior is fully reversible.

Full lineshape exchange simulation of the spectra using gNMR[15] gave calculated rates of *syn/anti* exchange at various temperatures, as shown in Table 1.

T (K)	T (°C)	Exch. Rate (1/s)	1/T (K⁻¹)	ln(rate/T)
303	30	44.8	0.0033	-1.91
293	20	27.8	0.00341	-2.36
283	10	12.6	0.00353	-3.11
273	0	8.4	0.00366	-3.48
263	-10	4	0.0038	-4.19
253	-20	2.5	0.00395	-4.62
243	-30	0.9	0.00412	-5.6

Table 1: Calculated *syn/anti* exchange rates for 1e and parameters for Eyring analysis

An Eyring analysis using the parameters from Table 1 revealed that the $\Delta H^{\ddagger} = 8.7(3)$ kcal/mol and $\Delta S^{\ddagger} = 0.02$ kcal/(mol K) for the *syn/anti* exchange process. The plot and full analysis can be found in the Experimental section.

Unfortunately, despite many attempts at many temperatures, the $^1J_{CH}$ values for each of the two alkylidene signals could not be determined. Thus, we do not know which is *syn* and which is *anti*. However, the exchange $\Delta H^{\ddagger}$ of 8.7 kcal/mol is consistent with the relatively rapid exchange observed at room temperature, and the near-zero $\Delta S^{\ddagger}$ is indicative of a unimolecular process. Furthermore, the fact that **1e** crystallized as the *anti* isomer strengthens the claim that *syn* and *anti* are both readily accessible in the system. This is likely due to a weakening of the Mo=C π-bond by conjugation of the π system with the empty B p orbital (See Section I-E).

II-B. *Syn/anti* isomerism and MeCN adduct formation in Mo(NAr)(CHPPh$_2$) (Me$_2$pyr)(OTPP) (1h)

As discussed in Part I, the room-temperature ^1H NMR spectrum of **1h** contains two alkylidene signals: a tall, slightly broad alkylidene resonance at 12.31 ppm and a shorter, broader alkylidene resonance at 12.64 ppm in C$_6$D$_6$. These appear in a ratio of ~5:1, and the taller of the two was assigned as the *syn* isomer ($^1J_{CH} = 130$ Hz). In order to confirm that these peaks arise from the two exchanging isomers, a series of ^1H NMR spectra of **9a** in toluene-d_8 were taken. The comparison of these spectra can be found in Figure 12.
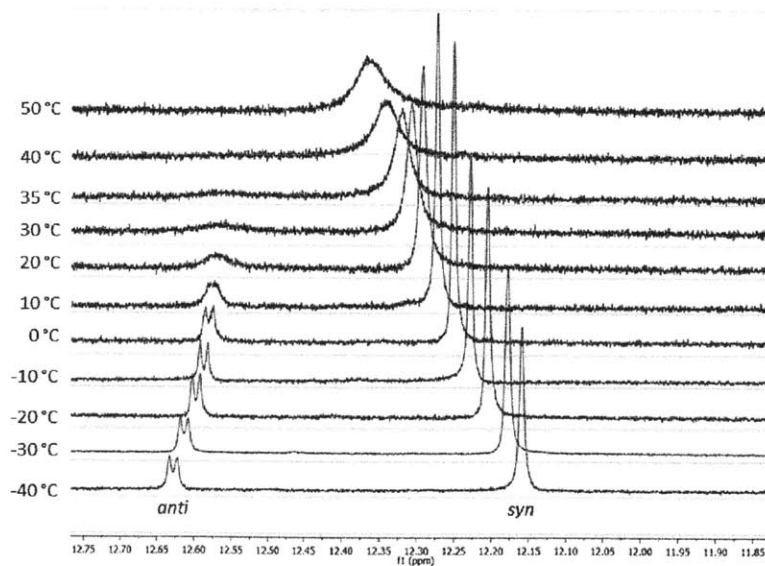
Figure 12: Temperature-dependent ^1H NMR spectra of 1h (toluene-d_8, 500 MHZ) in the alkylidene region

129

Upon heating the sample, the signals begin to coalesce, and by 40 °C, they appear as a single broad peak. This signifies the fast exchange limit for alkylidene rotation has been reached. Cooling to room temperature produces the same spectrum as seen initially. Cooling further induces peak sharpening as the exchange becomes slower. At or below 0 °C, the signals are fairly sharp, and one can see that the downfield signal is a doublet due to coupling with phosphorus ($^2J_{PH} = 5$ Hz). At first, there was confusion as to why one isomer but not the other would show coupling to phosphorus, but inspection of the literature revealed that $^2J_{PH}$ values are highly variable and very small or negative values are not uncommon.[16] The behavior upon cooling is reversible, as the room temperature spectrum can be observed again after warming. Overall, the behavior is consistent of an exchanging *syn/anti* alkylidene system.

The acetonitrile-containing **1h-MeCN** (an orange solid) appears identical to **1h** (a red solid) in solution at room temperature by ^1H NMR (in C_6D_6 or toluene-d_8), save for the presence of free acetonitrile in **1h-MeCN**. This leads to the conclusion that MeCN is not bound to the metal in solution in **1h-MeCN** at RT. When a solution of **1h-MeCN** in toluene-d_8 is monitored by ^1H NMR spectroscopy over a range of temperatures, an interesting phenomenon occurs (Figure 13).
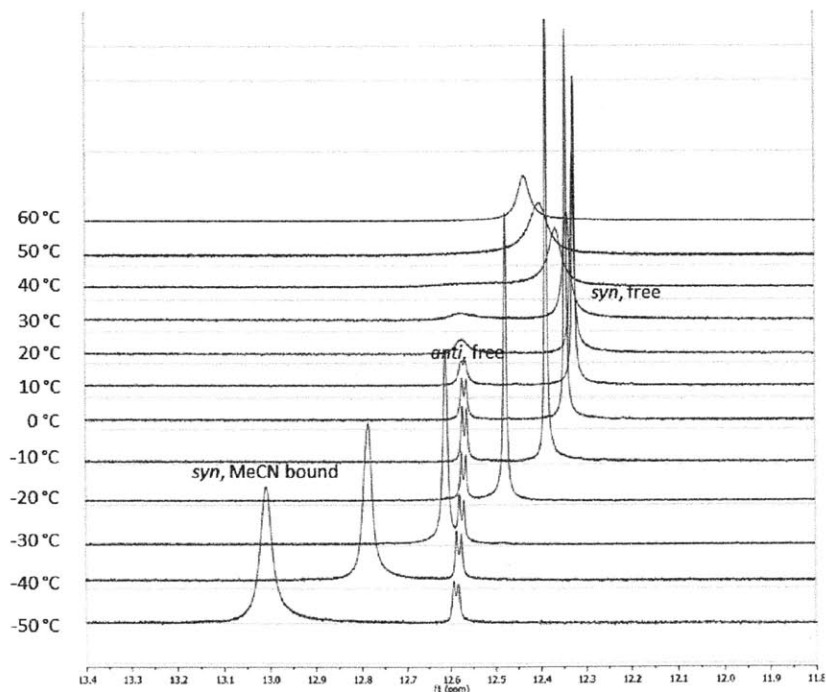
Figure 13: Temperature-dependent ^1H NMR spectra of 1h-MeCN (toluene-d_8, 500 MHz) in the alkylidene region (in the presence of ~1.5 equiv MeCN).

At room temperature and above, the behavior is the same as for **1h** (coalescence, fully reversible, etc.). However, upon cooling, the *syn* signal undergoes a drastic shift from ~12.3 ppm to ~13.0 ppm between 20 °C to -50 °C. The *anti* signal, on the other hand, remains unchanged throughout the cooling process. As the only difference between the spectra in Figure 12 and Figure 13 is the presence of MeCN in solution in the latter case, we attribute this shift to a binding of MeCN to the metal at temperatures below 20 °C. It is interesting to note that MeCN appears to bind to only the *syn* isomer. This observation matches with the fact that the crystal structure obtained for **1h-MeCN** is an adduct of the *syn* isomer. All variable-temperature behavior is reversible within the temperature range studied.

III. Olefin metathesis reactivity of heteroatom-substituted alkylidenes

Once the stability and basic features of the heteroatom-substituted alkylidene complexes **1b-1h** had been established, the question was whether or not these complexes would behave like other high-oxidation-state Mo alkylidenes in the context of olefin metathesis. It was postulated that the presence of a heteroatom substituent may render the alkylidene more electronically similar to a Fischer carbene and thus decrease or even shut off its metathesis reactivity. Section III-A below describes the behavior and performance of the complexes in terminal olefin homocoupling reactions. Following this, Section III-B details comparative kinetic studies of reactions of the complexes with internal olefins.

III-A. Homocoupling of 1-octene

In order to test the basic metathesis ability of complexes **1b-1h**, the conversion of 1-octene to *E/Z* 7-tetradecene using 5 mol% catalyst was monitored over time (Scheme 10). The reactions were run in a closed system (sealed J. Young NMR tube) in C_6D_6. The parent neophylidene complex **1** was included in the trials to provide a facile comparison to a regular MAP system. The results are shown in Table 2.

131
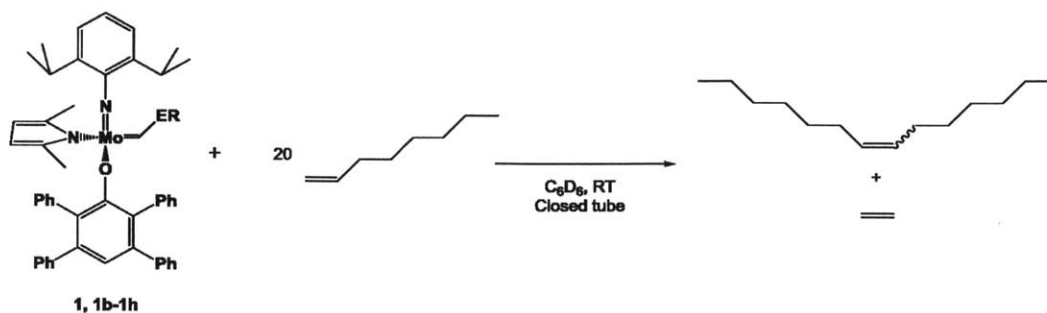
Scheme 10: Homocoupling of 1-octene with 1 and 1b-1h (5 mol% catalyst)

Catalyst	Substituent	0.5 h	1 h	2 h	10 h	24 h
1	CMe₂Ph	47	48	48	51	58
1b	OPr	47	47	47	49	55
1c	Pyrrol	0	0	3	12	18
1d	Carbaz	50	50	50	53	56
1e	Bpin	47	47	47	49	57
1f	TMS	55	54	54	54	56
1g	SPh	53	54	54	58	57
1h	PPh₂	48	48	49	53	56
1h-MeCN	PPh₂	49	49	50	57	56

Table 2: Percent conversion for metathesis homocoupling of 1-octene by 1 and 1b–1h (5 mol %) in C₆D₆ at 22 °C (closed system)

All reactions reach equilibrium (~50% *E/Z* 7-tetradecene) in 0.5 h except the one involving **1c** (in the equilibrium cases, conversion was limited by buildup of ethylene in the system). The identity of the substituent on the alkylidene does not seem to affect metathesis activity as observable in this experiment. The slow initiation by **1c** is no surprise, given the relatively strong binding of the pyrrolidinone carbonyl group to the metal.

Although the catalytic ability of the above complexes appeared to be similar, there were visible differences in catalyst resting state during the course of the reaction. In the homocoupling system described in Scheme 10, there can be three possible alkylidene species present: the starting complex, a heptylidene (present after alkylidene exchange with 1-octene), or a methylidene (present after a homocoupling step or after alkylidene exchange). Also possible are a range of metallacycles with different substituents. Observations of homocoupling reaction mixtures showed no evidence for methylidenes or metallacycles, so attention was focused on the ratio of starting alkylidene to heptylidene (Scheme 11).
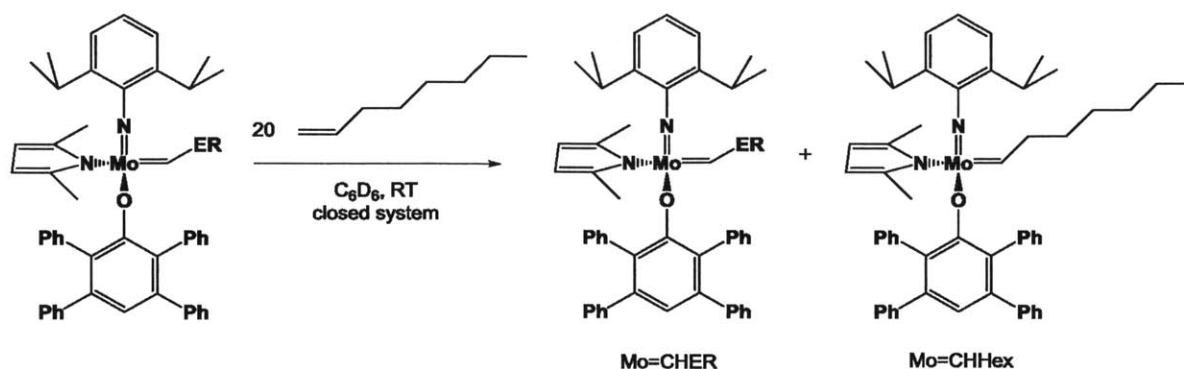
Scheme 11: Mo=CHER and Mo=CHHex catalyst resting states in homocoupling reactions of 1-octene

The catalyst resting states were investigated by monitoring of the alkylidene region of the ^{1}H NMR spectra of the homocoupling reaction mixtures. The observed ratios of starting alkylidene to heptylidene are shown in Table 3.

Catalyst	Substituent	0.5 h	1 h	2 h	10 h	24 h
1	CMe$_2$Ph	0:100	0:100	0:100	0:100	0:100
1b	OPr	13:87	14:86	14:86	15:85	18:82
1c	Pyrrol	100:0	100:0	100:0	100:0	100:0
1d	Carbaz	77:23	78:22	79:21	79:21	86:14
1e	Bpin	60:40	60:40	57:43	63:37	53:47
1f	TMS	100:0	100:0	100:0	100:0	100:0
1g	SPh	100:0	100:0	100:0	100:0	100:0
1h	PPh$_2$	77:23	74:26	70:30	70:30	n/a
1h-MeCN	PPh$_2$	78:22	72:28	68:32	60:40	n/a

Table 3: Ratios of Mo=CHER:Mo=CHHex observed in 1-octene homocoupling reactions (5 mol % catalyst)

All complexes except **1c**, **1f**, and **1g** formed some observable and relatively constant amount of heptylidene (Mo=CHHex) over a period of 10 h. The ratios at 24 h are less informative because the amount of total alkylidene remaining at this point may be small (see Table 4). Because **1f** and **1g** carry out metathesis homocoupling rapidly, we ascribe the lack of observable heptylidene to a thermodynamic preference for the heteroatom-substituted alkylidene species in these cases. For **1c**, the slow rate of homocoupling (see Table 2) and lack of observable heptylidene lead to the conclusion that initial alkylidene exchange from this complex is very slow. It is interesting to note that the neophylidene **1** (the representative regular MAP species) was not observable because the resting state lies completely on the heptylidene side in that case.

133

Throughout the catalyst resting state studies, all alkylidene species gradually disappeared with time. This process is likely related to catalyst resting state, as decomposition presumably proceeds from some alkylidene species faster than from others. To determine the relative long-term stability of the catalysts in homocoupling conditions, the total alkylidene concentration (Mo=CHER + Mo=CHHex) was monitored in the ^{1}H NMR spectra of the homocoupling reaction mixtures (reaction setup in Scheme 11) by integration of the alkylidene signals with respect to an internal standard (4,4'-di-t-butylbiphenyl). The results are displayed in the form of percent total alkylidene remaining, with the amount present after 0.5 h defined as 100% (Table 4).

Catalyst	Substituent	0.5 h	1 h	2 h	10 h	24 h
1	CMe$_2$Ph	100	82	82	55	12
1b	OPr	100	95	95	53	18
1c	Pyrrol	100	100	100	100	100
1d	Carbaz	100	96	91	68	37
1e	Bpin	100	100	100	66	18
1f	TMS	100	91	86	72	63
1g	SPh	100	96	92	60	36
1h	PPh$_2$	100	98	92	34	0
1h-MeCN	PPh$_2$/MeCN	100	93	83	30	0

Table 4: Percent total alkylidene remaining in 1-octene homocoupling reactions (5 mol% catalyst).

All complexes except 1c, which is essentially inert, decomposed to a substantial degree after 24 h. However, many of the heteroatom-substituted complexes showed less decomposition than did the parent complex 1 at various time points. In fact, complexes 1b-1h each had higher a total alkylidene concentration than 1 after 1 h. If we view the results from Table 3 and Table 4 together, it becomes apparent that there is a correlation between catalyst longevity and preferred resting state: complexes that prefer to stay in their starting alkylidene states decompose more slowly. For example, 1f and 1g are visible only as starting alkylidenes, and they also have the highest concentration of alkylidene remaining after 24 h (barring the special case of 1c). Conversely, 1 and 1b show both the highest proportions of heptylidene in their resting states and the highest rates of decomposition. It should be noted that these trends do not explain the high levels of decomposition seen after 10 h and 24 h for 1h and 1h-MeCN; another pathway may be operative in these cases.

The above studies prove that MAP complexes with a variety of heteroatom substituents can be as active for simple metathesis as are traditional MAP catalysts. While the coupling

experiments did not distinguish between the overall activities of the various catalysts, other differences were readily apparent. For instance, the observed resting states of the catalysts during the reactions varied substantially, and this variation appeared to have substantial effects on the rate of catalyst decomposition.

III-B. Kinetic studies of reactions with (Z)-4-octene

In order to systematically compare the olefin metathesis reactivity of **1** and **1b-1g** in a simple system, the experiment shown in Scheme 12 was devised.

rate = k[Mo][C4O]

⇓

rate = k$_{obs}$[Mo]

C$_6$D$_6$, RT
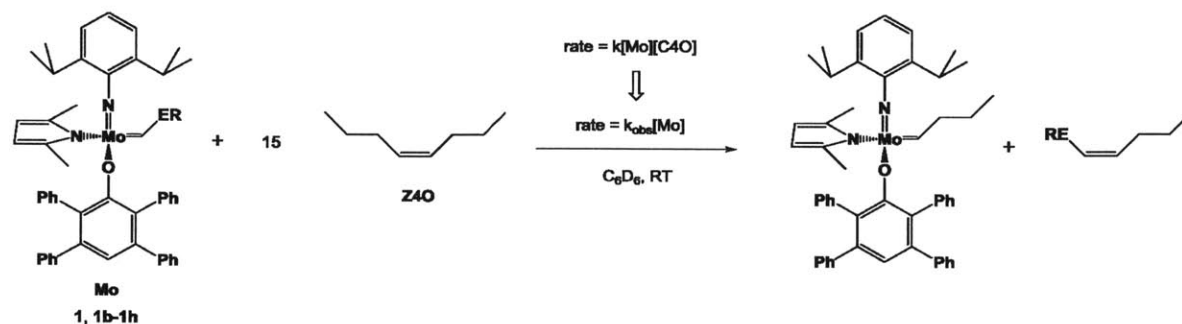
Scheme 12: Kinetic studies of reactions between 1 and 1b-1h with Z-4-octene (Z4O) in a pseudo-first-order regime

The above experiment was chosen for its relative simplicity. The excess of Z-4-octene (Z4O) creates a pseudo-first-order environment in the otherwise second-order reaction system. Furthermore, metathesis of the product butylidene with Z4O would be a fully degenerate process, meaning the concentration of all species would remain unaffected. Finally, the lack of terminal olefins in the system prevents the formation of ethylene, which averts catalyst trapping and ethenolysis. The disappearance of the starting Mo complex and the appearance of butylidene was monitored versus an internal standard by ^{1}H NMR spectroscopy.

In practice, the kinetic studies were less informative than was originally hoped, as compounds **1**, **1c**, **1d**, **1f**, **1g**, **1h**, and **1h-MeCN** showed no reaction after a few hours and little (~5%) to no conversion to butylidene even after 2 days. The exact reasons for this are unknown, but compounds **1**, **1d**, **1h**, and **1h-MeCN** possess bulky alkylidene substituents that may preclude formation of the trisubstituted metallacycle necessary for metathesis with Z4O. Compounds **1c**, **1f**, and **1g** seemingly show a thermodynamic preference to rest in their starting state even when presented with an excess of terminal olefin (see 1-octene studies in Section III-A). There is no reason to believe that this preference would change in the presence of internal olefin.

135

The two systems that produced interpretable kinetic data were those involving **1b** and **1e**. The full kinetic analyses of these two systems can be found in the Experimental Section. The studies yielded first-order rate constants of $1.2 \times 10^{-3} \ M^{-1}s^{-1}$ for **1b** and $9.9 \times 10^{-5} \ M^{-1}s^{-1}$ for **1e**. Compound **1e** reacts with *cis*-4-octene about ten times faster than **1b** does, perhaps because the steric bulk of **1b** is less than that of **1e**. However, it is difficult to disentangle the steric differences from possible electronic effects with regard to reaction rate.

CONCLUSIONS

We have shown that a wide variety of heteroatom-substituted alkylidene complexes are isolable and stable within the Mo MAP imido framework. These complexes can be synthesized by alkylidene exchange from neophylidene or methylidene precursors. Some of the heteroatom-substituted alkylidene complexes show interesting *syn/anti* exchange behavior, which has been investigated by variable-temperature NMR. The exchange behavior and some of the structural features of the complexes can be attributed to the electronic effects of the heteroatom substituents.

Overall, it seems that the presence of the heteroatom substituent on the alkylidene does little to help or hinder the metathesis reactivity of the complexes with terminal olefins. There are no major differences in the catalytic activity for homocoupling of 1-octene for any of the complexes (except in the special case of the five-coordinate **1c**). There are, however, significant differences in the preferred resting state of the catalysts, which are currently ascribed to differing thermodynamic preferences for the heteroatom-substituted alkylidene over a straight-chain alkylidene. The differences in preferred resting state appear to affect the overall stability of the catalysts under metathesis conditions, with catalysts that prefer their starting alkylidene forms being more resistant to decomposition. Steric factors play a large role in reactivity of the complexes as well, as evidenced by the difficulty faced by many of the complexes in reacting with internal olefins such as Z-4-octene.

The studies in this chapter represent an advance in the scope of alkylidene chemistry and provide hope for future olefin metathesis reactions involving heteroatom-substituted olefins. The investigated complexes retained the structural and functional characteristics of Schrock-type alkylidenes without regard to substituent identity. While further work would be needed to isolate

the electronic effects of heteroatom substituents in metathesis, it is clear that the MAP framework can provide a solid basis for metathesis of even the more exotic substrates.

EXPERIMENTAL

General comments

All manipulations of air- and moisture-sensitive materials were performed in oven-dried (175 °C) or flame-dried glassware on a dual-manifold Schlenk line or a Vacuum Atmospheres glovebox with nitrogen atmosphere. NMR measurements of air- and moisture-sensitive materials were carried out in Teflon-valve-sealed J. Young-type NMR tubes. Anhydrous ether, pentane, toluene, THF, benzene, CH_2Cl_2, and acetonitrile were sparged with nitrogen and passed through activated alumina prior to use. Chloroform-d, C_6D_6, and toluene-d_8 were stored over molecular sieves in the glovebox. N-vinylpyrrolidinone, trimethylvinylsilane, phenyl vinyl sulfide, dimethylphenylphosphine, N-vinylcarbazole, Z-4-octene, and 1-octene were purchased from commercial sources, degassed and stored over molecular sieves in the glovebox. Vinylboronic acid pinacol ester was purchased from Aldrich, run through a plug of silica, degassed, and stored over sieves in the glovebox. Propyl vinyl ether was purchased from Aldrich, degassed, dried over CaH_2, filtered, and stored in the glovebox. $Mo(NAr)(CHCMe_2Ph)(Me_2pyr)(OTPP)$[11] (1) and $Mo(NAr)(CH_2)(Me_2pyr)(OTPP)$[17] (1a) were synthesized according to reported procedures. NMR spectra were obtained on Varian spectrometers operating at either 300 MHz or 500 MHz. NMR chemical shifts are reported as ppm relative to tetramethylsilane, and are referenced to the residual proton or ^{13}C signal of the solvent (^1H $CDCl_3$: 7.27 ppm, ^1H C_6D_6: 7.16 ppm, ^1H toluene-d_8: 2.08 (methyl) ^{13}C $CDCl_3$: 77.16 ppm, ^{13}C C_6D_6, 128.06 ppm).

Experimental procedures for synthesis of compounds

Mo(NAr)(CHOPr)(Me₂pyr)(OTPP) (1b)

In the glovebox, a 50-mL round-bottom flask was charged with a stir bar, 10 mL toluene, 170 mg 1 (0.190 mmol, 1.0 equiv.), and 43 μL propyl vinyl ether (0.380 mmol, 2.0 equiv.). The flask was capped and the contents stirred for 1 h at RT, after which time the solvent was removed *in vacuo*. Pentane was added (10 mL) and the solvent was removed *in vacuo* again. Pentane was again added (10 mL) and the red slurry was stirred and filtered to obtain 81 mg pure

orange solid product (51% yield). ^{1}H NMR (C$_6$D$_6$, 20 °C): δ [ppm] 10.573 (s, 1H, C*H*OCH$_2$CH$_2$CH$_3$, J$_{CH}$ = 140 Hz, *syn* isomer), 7.32-6.83 (24H, aryl), 6.17 (s, 2H, Me$_2$pyr aryl), 3.63 (m, 2H, CHOC*H$_2$*CH$_2$CH$_3$), 3.31 (sept, 2H, NAr methines, J$_{HH}$ = 7 Hz), 2.11 (s, 6H, Me$_2$pyr methyls), 1.27 (m, 2H, CHOCH$_2$C*H$_2$*CH$_3$), 1.08 (d, 6H, NAr methyls, J$_{HH}$ = 7 Hz), 1.07 (d, 6H, NAr methyls, J$_{HH}$ = 7 Hz), 0.54 (t, 3H, CHOCH$_2$CH$_2$C*H$_3$*). ^{13}C{^{1}H} NMR (C$_6$D$_6$, 20 °C): δ [ppm] 286.29, 159.67, 154.05, 147.72, 142.26, 142.09, 138.42, 131.75, 130.81, 130.22, 128.58, 127.73, 127.03, 126.64, 126.16, 123.01, 109.05, 79.60, 28.51, 24.04, 23.41, 22.85, 16.66, 10.19. Anal. Calcd for C$_{52}$H$_{54}$MoN$_2$O$_2$: C, 74.80; H, 6.52; N, 3.36. Found: C, 74.88; H, 6.56; N, 3.36.

Mo(NAr)[(CHN(CH$_2$)$_3$CO)](Me$_2$pyr)(OTPP) (1c)

In the glovebox, a 50-mL round-bottom flask was charged with a stir bar, 10 mL toluene, 200 mg 1a (0.257 mmol, 1.0 equiv.), and 41 µL *N*-vinylpyrrolidinone (0.386 mmol, 1.5 equiv.). The flask was capped and the contents stirred for 4 h at RT, after which time the solvent was removed *in vacuo*. Pentane was added and the solvent was removed *in vacuo* again. Pentane was again added and the red slurry was stirred and filtered to obtain 171 mg pure red/pink solid product (77% yield). ^{1}H NMR (C$_6$D$_6$, 20°C): δ [ppm] 10.42 (s, 1H, C*H*N(CO)CH$_2$CH$_2$CH$_2$, J$_{CH}$ = 166 Hz, *anti* isomer), 7.90 (br s, 2H, CHN(CO)CH$_2$CH$_2$C*H$_2$*), 7.30-6.60 (24H, aryl, includes a very broad signal), 6.09 (s, 2H, Me$_2$pyr aryl), 3.95 (sept, 2H, NAr methines, J$_{HH}$ = 7 Hz), 2.49 (m, 2H, CHN(CO)CH$_2$C*H$_2$*CH$_2$), 2.01 (t, 2H, CHN(CO)C*H$_2$*CH$_2$CH$_2$, J$_{HH}$ = 8 Hz), 1.83 (s, 6H, Me$_2$pyr methyls), 1.23 (d, 6H, NAr methyls, J$_{HH}$ = 7 Hz), 1.15 (d, 6H, NAr methyls, J$_{HH}$ = 7 Hz). ^{13}C{^{1}H} NMR (C$_6$D$_6$, 20 °C): δ [ppm] 255.78, 175.09, 161.93, 150.74, 149.22, 143.01, 138.80, 136.28, 131.10, 130.30, 128.78, 126.28, 124.66, 123.21, 108.12, 47.11, 28.14, 27.54, 25.10, 23.19, 21.44, 16.41. Anal. Calcd for C$_{53}$H$_{53}$MoN$_3$O$_2$: C, 74.02; H, 6.21; N, 4.89. Found: C, 74.05; H, 6.28; N, 4.76.

Mo(NAr)(CHCarbaz)(Me$_2$pyr)(OTPP) (1d)

In the glovebox, a 50-mL round-bottom flask was charged with a stir bar, 10 mL toluene, 165 mg 1a (0.213 mmol, 1.0 equiv.), and 41 mg *N*-vinylcarbazole (0.213 mmol, 1.0 equiv.). The flask was capped and the contents stirred for 4 h at RT, after which time the solvent was removed *in vacuo*. Pentane was added (10 mL) and the solvent was removed *in vacuo* again. Pentane was again added (10 mL) and the red slurry was stirred and filtered to obtain 163 mg pure orange solid product (81% yield). ^{1}H NMR (C$_6$D$_6$, 20°C): δ [ppm] 11.57 (s, 1H, C*H*Carbaz,

J_{CH} = 134 Hz, *anti* isomer), 7.70 (d, 2H, carbazole aryls, J_{HH} = 7 Hz), 7.60 (d, 2H, carbazole aryls, J_{HH} = 7 Hz), 7.45 (s, 1H, OTPP *para* H), 7.24-6.73 (23H, aryl), 6.23 (s, 2H, Me$_2$pyr aryl), 3.42 (sept, 2H, NAr methines, J_{HH} = 7 Hz), 2.03 (br s, 6H, Me$_2$pyr methyls), 1.05-0.40 (br, 6H, NAr methyls). $^{13}C\{^1H\}$ NMR (C$_6$D$_6$, 20°C): δ [ppm] 245.05, 159.21, 154.43, 142.35, 141.81, 139.49, 137.99, 131.83, 130.75, 130.29, 128.73, 127.23, 127.10, 126.87, 126.28, 125.01, 123.16, 122.73, 119.99, 112.80, 109.64, 28.23, 23.93, 23.52, 16.80. Anal. Calcd for C$_{61}$H$_{55}$MoN$_3$O: C, 77.77; H, 5.88; N, 4.46. Found: C, 77.47; H, 6.15; N, 4.20.

Mo(NAr)(CHBpin)(Me$_2$pyr)(OTPP) (1e)

In the glovebox, a 50-mL round-bottom flask was charged with a stir bar, 10 mL toluene, 175 mg **1a** (0.225 mmol, 1.0 equiv.), and 57.3 μL vinylboronic acid pinacol ester (0.338 mmol, 1.5 equiv.). The flask was capped and the contents stirred for 3 h at RT, after which time the solvent was removed *in vacuo*. Pentane (10 mL) was added and the solvent was removed *in vacuo* again. Pentane was again added (10 mL) and the red slurry was stirred and filtered to obtain 135 mg pure pale orange solid product (66% yield). This product can also be synthesized using the same procedure from the neophylidene complex **1** and 2 equivalents of vinylboronic acid pinacol ester in 83% yield. The ^{1}H NMR showed a 2:1 mixture of rapidly exchanging isomers A and B, but it is not known which is the *syn* and which the *anti*. ^{1}H NMR (C$_6$D$_6$, 20 °C): δ [ppm] 12.37 (br s, 1H, C*H*Bpin, isomer A), 12.25 (br s, 1H, C*H*Bpin, isomer B), 7.40-6.92 (24H, aryl, isomers A and B), 6.07 (br s, 2H, Me$_2$pyr aryl, isomer A), 6.01 (br s, 2H, Me$_2$pyr aryl, isomer B), 3.96 (br s, 2H, NAr methines, isomer B), 3.17 (br s, 2H, NAr methines, isomer A), 1.99 (br s, 6H, Me$_2$pyr methyls, isomer A), 1.90 (br s, 6H, Me$_2$pyr methyls, isomer B), 1.20-0.70 (br, 24H, NAr methyls and Bpin methyls, isomers A and B). $^{13}C\{^1H\}$ NMR (C$_6$D$_6$, 20°C) (Mixture of two isomers): δ [ppm] 282.80, 276.09, 159.30, 158.83, 155.15, 154.02, 147.42, 146.47, 142.52, 142.31, 142.06, 138.12, 134.67, 133.58, 131.91, 131.45, 130.17, 128.57, 127.35, 126.83, 126.59, 125.40, 123.28, 122.72, 122.55, 109.19, 108.74, 84.52, 83.08, 82.97, 28.69, 28.46, 25.28, 25.00, 24.62, 24.38, 23.52, 23.40, 16.48, 16.27. Anal. Calcd for C$_{55}$H$_{59}$MoBN$_2$O$_3$: C, 73.17; H, 6.59; N, 3.10. Found: C, 72.82; H, 6.81; N, 2.93.

Mo(NAr)(CHTMS)(Me$_2$pyr)(OTPP) (1f)

In the glovebox, a 50-mL round-bottom flask was charged with a stir bar, 10 mL toluene, 166 mg **1a** (0.214 mmol, 1.0 equiv.), and 157 μL trimethylvinylsilane (1.07 mmol, 5.0 equiv.).

The flask was capped and the contents stirred for 2 h at RT, after which time the solvent was removed *in vacuo*. Pentane was added (10 mL) and the solvent was removed *in vacuo* again. Pentane was again added (5 mL) and the red slurry was stirred and filtered to obtain 86 mg pure orange solid product (47% yield). ^{1}H NMR (C_6D_6, 20°C): δ [ppm] 12.55 (s, 1H, C*H*SiMe$_3$ $^1J_{CH}$ = 114 Hz, *syn* isomer), 7.35-6.75 (24H, aryls), 6.08 (s, 2H, Me$_2$pyr aryls), 3.27 (sept, 2H, NAr methines, $^3J_{HH}$ = 7 Hz), 1.95 (s, 6H, Me$_2$pyr methyls), 1.08 (d, 12H, NAr methyls, $^3J_{HH}$ = 7 Hz), 0.01 (s, 9H, CHSi*Me$_3$*). ^{13}C{^{1}H} NMR (C_6D_6, 20°C): δ [ppm] 297.34, 159.36, 154.35, 146.19, 142.43, 141.94, 138.16, 134.52, 131.94, 131.05, 130.20, 128.64, 128.35, 128.10, 127.97, 127.77, 127.35, 126.88, 126.69, 123.29, 109.28, 28.26, 24.53, 23.78, 16.98, 1.02. Anal. Calcd for $C_{52}H_{56}MoN_2OSi$: C, 73.56; H, 6.65; N, 3.30. Found: C, 73.24; H, 6.66; N, 3.21.

Mo(NAr)(CHSPh)(Me₂pyr)(OTPP) (1g)

In the glovebox, a 50-mL round-bottom flask was charged with a stir bar, 10 mL toluene, 200 mg **1** (0.223 mmol, 1.0 equiv.), and 58.3 µL phenyl vinyl sulfide (0.446 mmol, 2.0 equiv.). The flask was capped and the contents stirred for 19 h at RT, after which time the solvent was removed *in vacuo*. Pentane was added (10 mL) and the solvent was removed *in vacuo* again. Pentane was again added (10 mL) and the red slurry was stirred and filtered to obtain 133 mg pure pink solid product (68% yield). ^{1}H NMR (C_6D_6, 20°C): δ [ppm] 11.48 (s, 1H, C*H*SPh,$^1J_{CH}$ = 146, *syn* isomer), 7.35-6.70 (29H, aryls), 6.15 (s, 2H, Me$_2$pyr aryls), 3.44 (sept, 2H, NAr methines, $^3J_{HH}$ = 7 Hz), 2.16 (s, 6H, Me$_2$pyr aryls), 1.19 (d, 6H, NAr methyls, $^3J_{HH}$ = 7 Hz), 1.18 (d, 6H, NAr methyls, $^3J_{HH}$ = 7 Hz). ^{13}C{^{1}H} NMR (C_6D_6, 20°C): δ [ppm] 269.78, 159.47, 153.64, 147.98, 142.28, 141.93, 140.53, 138.24, 135.74, 131.62, 130.20, 128.91, 128.79, 128.77, 128.35, 128.14, 127.96, 127.38, 127.18, 126.76, 126.72, 123.15, 109.37, 28.81, 24.11, 23.74, 16.80. Anal. Calcd for $C_{55}H_{52}MoN_2OS$: C, 74.64; H, 5.92; N, 3.17. Found: C, 74.46; H, 5.89; N, 2.99.

Mo(NAr)(CHPPh₂)(Me₂pyr)(OTPP) and MeCN adduct (1h/1h-MeCN)

In the glovebox, a 50-mL round-bottom flask was charged with a stir bar, 8 mL toluene, 119 mg **1a** (0.153 mmol, 1.0 equiv.), and 31 µL diphenylvinylphosphine (0.153 mmol, 1.0 equiv.). The flask was capped and the contents stirred for 3 h at RT, after which time the solvent was removed *in vacuo*. Pentane was added (10 mL) and the solvent was removed *in vacuo* again. Pentane was again added (10 mL) and the red slurry was stirred and filtered to obtain 92 mg pure

red solid product (63% yield). This species is present in solution as a ~5:1 mixture of *syn* and *anti* alkylidene isomers. ^{1}H NMR (C_6D_6, 20°C): δ [ppm] 12.65 (br d, 1H, *anti*, C*H*PPh$_2$ $^2J_{PH}$ = 5 Hz at -20 °C), 12.31 (br s, 1H, *syn*, C*H*PPh$_2$, $^1J_{CH}$ = 130 Hz, *syn* isomer), 7.42-6.68 (34H, both isomers, aryl), 6.09 (br s, 2H, *anti*, Me$_2$pyr aryls), 6.03 (br s, 2H, *syn*, Me$_2$pyr aryls), 4.25 (br sept, 2H, *anti*, NAr methines), 3.41 (br sept, 2H, *syn*, NAr methines), 1.96 (br s, 6H, *syn*, Me$_2$pyr methyls), 1.85 (br s, 6H, *anti*, Me$_2$pyr methyls), 1.30-1.18 (overlapping d, 12H, *anti*, NAr methyls), 1.10-1.02 (overlapping d, 12H, *syn*, NAr methyls). ^{13}C{^{1}H} NMR (C_6D_6, 20°C): δ [ppm] (mixture of two isomers) 276.59, 276.19, 160.01, 153.93, 146.97, 142.44, 142.09, 141.99, 141.06, 140.93, 140.21, 140.09, 138.31, 137.90, 137.59, 134.69, 134.06, 133.90, 133.67, 133.52, 132.88, 132.72, 132.38, 132.07, 131.80, 130.96, 130.28, 130.20, 129.33, 128.81, 128.63, 128.54, 128.35, 128.15, 127.97, 127.30, 127.08, 126.72, 125.71, 123.02, 109.57, 106.53, 28.95, 28.64, 25.63, 24.04, 23.09, 17.12. The acetonitrile adduct of this species can also be obtained as an orange powder in 79% yield by adding acetonitrile in place of pentane in the workup. This was done to aid in the elemental analysis process, which proved difficult with the parent species. The ^{1}H NMR spectrum of the acetonitrile adduct looks identical to that of the parent species in C_6D_6, which signifies that the acetonitrile is not bound in solution. Elemental analysis was obtained for the acetonitrile adduct with one additional equivalent of acetonitrile, as drying led to inconsistent removal of acetonitrile and decomposition. Elemental analysis (still low on carbon) for Mo(NAr)(CHPPh$_2$)(Me$_2$pyr)(OTPP)(MeCN)·MeCN follows: Anal. Calcd for $C_{65}H_{63}MoN_4OP$: C, 74.84; H, 6.09; N, 5.37. Found: C, 72.48; H, 6.07; N, 5.36.

Experimental Procedures for Olefin Metathesis Reactions

General procedure for 1-octene homocoupling experiments

In a 2-mL vial in the glovebox was placed 0.010 mmol solid catalyst (8-10 mg, 1.0 equiv., 5 mol%), ~5 mg 4,4'-di-*t*-butylbiphenyl (as internal standard), and 0.75 mL C_6D_6. This solution was transferred to a J. Young NMR tube. To the tube was added 31 µL 1-octene (0.200 mmol, 20.0 equiv), after which the tube was sealed, shaken, and allowed to sit at room temperature. ^{1}H NMR spectra were taken after 0.5 h, 1 h, 2 h, 10 h, and 24 h. The conversion of 1-octene to 7-tetradecene, the ratio of observable alkylidene species, and the total remaining alkylidene species were monitored against the internal standard. The heptylidene ^{1}H NMR signal was observed as a broad signal at ~11.36 ppm in C_6D_6.

Details of Kinetic and Exchange Analyses

Eyring analysis of *syn/anti* interconversion for 1e

The exchange rates in the below table (Table 1) were obtained by using gNMR[15] for full-lineshape-iteration modeling of the exchange process based on the broadness and shape of the alkylidene peaks in the ^{1}H NMR spectra at different temperatures.

T (K)	T (°C)	Exch. Rate (1/s)	1/T (K^1)	ln(rate/T)
303	30	44.8	0.0033	-1.91
293	20	27.8	0.00341	-2.36
283	10	12.6	0.00353	-3.11
273	0	8.4	0.00366	-3.48
263	-10	4	0.0038	-4.19
253	-20	2.5	0.00395	-4.62
243	-30.	0.9	0.00412	-5.6

Table 5: Calculated *syn/anti* exchange rates for 1e and parameters for Eyring analysis

An Eyring analysis using the data in Table 5 was carried out, as shown in Figure 14: Eyring plot and important values for *syn/anti* exchange in 1e and the following paragraphs. Note that the values in the rightmost two columns were used as the x and y values for the plot.
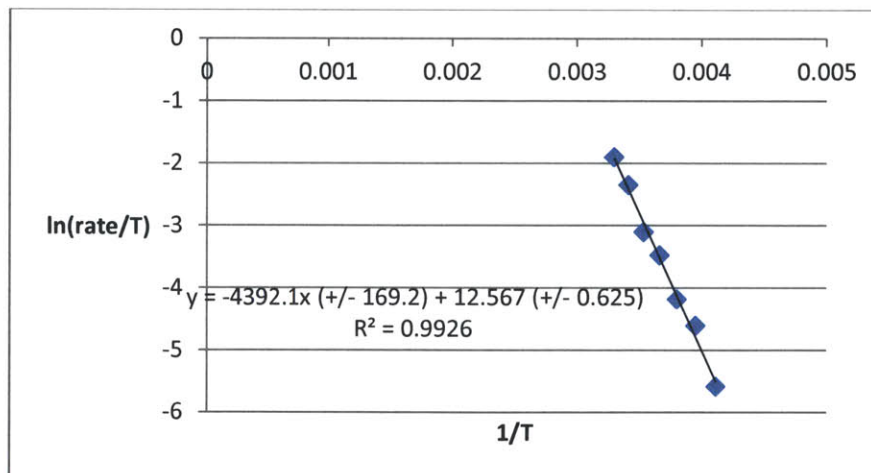
Slope	-4390
Standard error in slope	169
Intercept	12.6
Standard error in intercept	0.625

Figure 14: Eyring plot and important values for *syn/anti* exchange in 1e

142

The linear form of the Eyring equation is as follows:

$$\ln \frac{k}{T} = \frac{-\Delta H^{\ddagger}}{R} \cdot \frac{1}{T} + \ln \frac{k_B}{h} + \frac{\Delta S^{\ddagger}}{R}$$

This means that in a plot of ln(k/T) vs. 1/T, the slope = $-\Delta H^{\ddagger}/R$, and the y-intercept = ln(k_b/h) + $\Delta S^{\ddagger}$/R. Note that we use the exchange rate calculated from full lineshape iteration at each given temperature in place of "k" in the equation. Some useful constants: R = 8.314 J/(mol*K), ln(k_b/h) = 23.76.

From above:

Slope = $-\Delta H^{\ddagger}$/R = -4390. Thus, $\Delta H^{\ddagger}$ = 4390*R = 4390*8.314 = 36500 J/mol = 36.5 kJ/mol

$\Delta H^{\ddagger}$ = 8.72 kcal/mol +/- 0.3 kcal/mol. (same analysis applied to standard error)

y-intercept = 12.6 = ln(k_b/h) + $\Delta S^{\ddagger}$/R = 23.76 + $\Delta S^{\ddagger}$/8.314.

$\Delta S^{\ddagger}$ = (y-intercept – 23.76)*R = (12.6-23.76)*8.314 = -92.8 J/mol*K = -.0928 kJ/mol

$\Delta S^{\ddagger}$ = -0.0222 kcal/mol +/- 0.0460 kcal/mol. (same analysis applied to standard error)

General procedure for kinetics experiments with Z-4-octene

In a 2-mL vial in the glovebox was placed 0.010 mmol solid catalyst (8-10 mg, 1.0 equiv.), ~5 mg 4,4'-di-t-butylbiphenyl (as internal standard), and 0.75 mL C_6D_6. This solution was transferred to a J. Young NMR tube. To the tube was added 23 μL Z-4-octene (0.150 mmol, 20.0 equiv.), after which the tube was sealed, shaken, and allowed to sit at room temperature. ^{1}H NMR spectra were taken at various time points. The conversion of starting alkylidene species to butylidene was monitored against the internal standard. The butylidene ^{1}H NMR signal was observed as a triplet ($^3J_{HH}$ = 6.5 Hz) at 11.36 ppm in C_6D_6. In the tables and plots to follow, [Mo] refers to the concentration (judged by ^{1}H NMR) of the starting Mo complex at the given time point, while $[Mo]_0$ refers to the original concentration. The plots of ln($[Mo]$/$[Mo]_0$) were constructed in the linear, pseudo-first-order regions of the data collected.
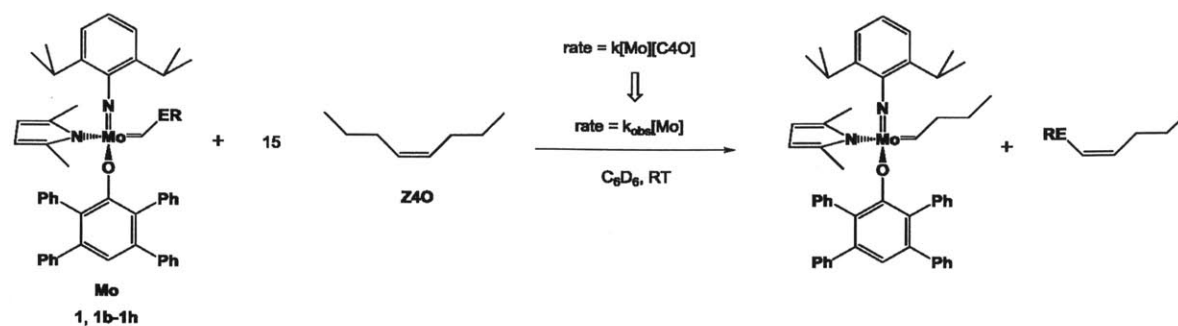
Scheme 13: Kinetic studies of reactions between 1 and 1b-1h with Z-4-octene (Z4O) in a pseudo-first-order regime

Kinetic analysis of reaction between 1b and Z-4-octene

The data collected from the reaction between **1b** and 15 equivalents of Z4O was compiled into Table 6 and plotted in Figure 15 below. Note that the values from the central two columns of the table were used for the plot.

Time (h)	Time (sec)	ln([Mo]/[Mo]$_0$) (1b)	% 1b Remaining
0.184	661	-0.208	81.2
0.369	1330	-0.406	66.6
0.456	1640	-0.493	61.1
0.542	1950	-0.608	54.4
0.744	2680	-0.794	45.2
0.831	2990	-0.853	42.6
1.04	3760	-1.02	36.1
1.18	4260	-1.08	34.1

Table 6: Conversion data from reaction between 1b and 15 equivalents Z4O

144
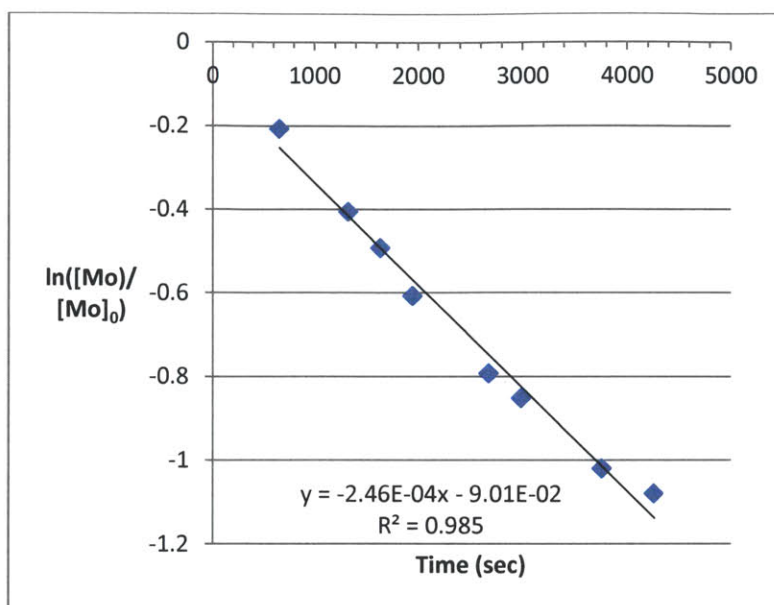
Slope	-2.46E-04
Standard error in slope	1.26E-05
[C4O]	0.200 M

Figure 15: Pseudo-first-order kinetic plot of ln([Mo]/[Mo]$_0$) vs. time for 1b along with important values

Rate = k[Mo][C4O]. When [C4O] >> [Mo], we have pseudo first-order conditions, so Rate = k_{obs}[Mo]. The slope of the ln([Mo]/[Mo]$_0$) graph is $-k_{obs}$.

From above:

Slope = -2.46E-04 = $-k_{obs}$. Thus, k_{obs} = 2.46E-04 s^{-1} = k[C4O]. From above, k = k_{obs}/[C4O] = 2.46E-04 s^{-1}/0.200 M

Second order rate constant: **k = 1.23E-03 M^{-1}s^{-1} +/- 6.30E-05 M^{-1}s^{-1}** (same analysis applied to standard error)

Kinetic analysis of reaction between 1e and *Z*-4-octene

The data collected from the reaction between **1e** and 15 equivalents of Z4O was compiled into Table 7 and plotted in Figure 16 below.

145

Time (h)	Time(sec)	$\ln([Mo]/[Mo]_0)$ (1e)	% 1e Remaining
0.675	2430	-0.0154	98.5
0.972	3500	-0.0294	97.1
1.31	4720	-0.0484	95.3
2.26	8120	-0.106	89.9
3.61	13000	-0.165	84.8
7.72	27800	-0.502	60.5
10.3	37000	-0.779	45.9
22.9	82600	-1.57	20.9

Table 7: Conversion data from reaction between 1e and 15 equivalents Z4O
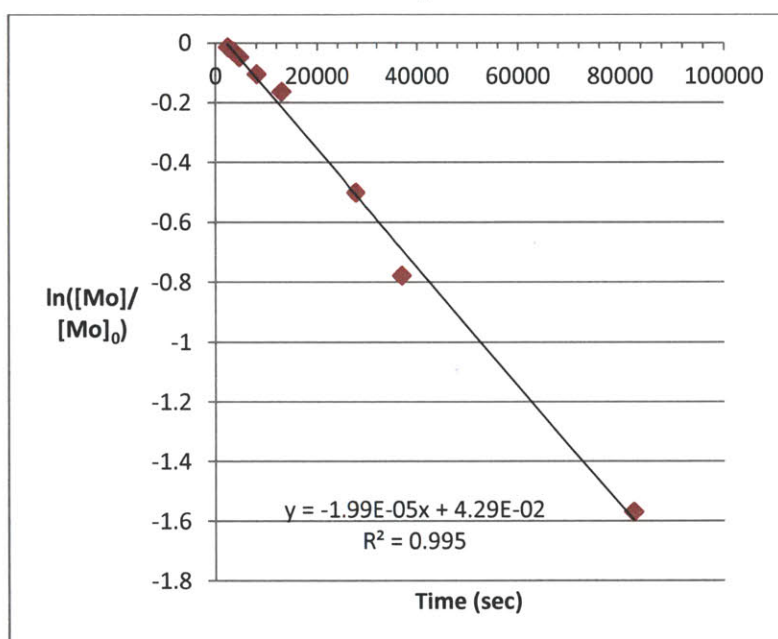
Slope	-1.99E-05
Standard error in slope	6.02E-07
[Z4O]	0.200 M

Figure 16: Pseudo-first-order kinetic plot of $\ln([Mo]/[Mo]_0)$ vs. time for 1e along with important values

Rate = k[Mo][Z4O]. When [Z4O] >> [Mo], we have pseudo first-order conditions, so rate = k_{obs}[Mo]. The slope of the $\ln([Mo]/[Mo]_0)$ graph is $-k_{obs}$.

From above:

Slope = -1.99E-05 = $-k_{obs}$. Thus, k_{obs} = 1.99E-05 s^{-1} = k[Z4O]. From above, k = k_{obs}/[Z4O] = 1.99E-05 s^{-1}/0.200 M

146

Second order rate constant: **k = 9.95E-05 M⁻¹s⁻¹ +/- 3.01E-06 M⁻¹s⁻¹** (same analysis applied to standard error)

Experimental Details for Crystal Structure Acquisition and Refinement

Mo(NAr)(CHOPr)(Me₂pyr)(OTPP) (1b)

The crystal structure acquisition and refinement were carried out with assistance from Dr. Peter Müller and Dr. Stacey Smith. X-ray quality crystals were grown from toluene and pentane. Low-temperature diffraction data (φ-and ω-scans) were collected on a Bruker-AXS X8 Kappa Duo diffractometer coupled to a Smart APEX2 CCD detector with Mo $K\alpha$ radiation ($\lambda = 0.71073$ Å) from an $I\mu S$ micro-source. Absorption and other corrections were applied using SADABS.[18] All structures were solved by direct methods using SHELXS[19] and refined against F_2 on all data by full-matrix least squares with SHELXL-97[20] using established refinement approaches.[21] The structure was refined as a racemic twin; the twin ratio refined freely and converged at 0.09(2). All non-hydrogen atoms were refined anisotropically. All hydrogen atoms (except H1, which was taken from the difference Fourier synthesis and refined semi-freely with the help of distance restraints) were included into the model at geometrically calculated positions and refined using a riding model. The isotropic displacement parameters of all hydrogen atoms were fixed to 1.2 times the U value of the atoms they are linked to (1.5 times for methyl groups). Mo(NAr)(CHOPr)(Me₂pyr)(OTPP) crystallized in space group Pn with two molecules in the asymmetric unit. In one of these molecules, the positions of the Mo center (Mo2), alkylidene ligand, and pyrrolide ligand are all part of a twofold disorder. In each molecule, the diisopropylphenylimido ligand is part of a twofold disorder. Furthermore, there is a disordered pentane solvent molecule present. Each of these disorders was refined with the help of 1,2- and 1,3-distance restraints. Due to the large amount of disorder in the overall structure, strong SIMU and DELU displacement parameter restraints were globally applied. Some of the larger thermal ellipsoids, such as those on the isopropyl groups, may be disordered further, but refinement of this further disorder may render the overall refinement unstable. It should be noted that the relatively large residual electron density near Mo1 was treated as a separate, disordered position for the Mo center in several refinement attempts. In each case, the refinement proved unstable. FLAT restraints on the pyrrolide and phenylimido rings were applied. The anisotropic

147

displacement parameters of certain disordered pairs of isopropyl methyl groups (C11, C11A) (C13, C13A) were considered to be equivalent.

Crystal data and structure refinement for 1b

Identification code	x12195
Empirical formula	$C_{54.50} H_{60} Mo N_2 O_2$
Formula weight	870.98
Temperature	100(2) K
Wavelength	0.71073 Å
Crystal system	Monoclinic
Space group	Pn
Unit cell dimensions	$a = 10.3886(10)$ Å $\quad \alpha = 90°$
	$b = 37.276(3)$ Å $\quad \beta = 93.108(2)°$
	$c = 12.6481(12)$ Å $\quad \gamma = 90°$
Volume	4890.8(8) Å^3
Z	4
Density (calculated)	1.183 Mg/m^3
Absorption coefficient	0.308 mm^{-1}
F(000)	1836
Crystal size	0.200 x 0.150 x 0.050 mm^3
Theta range for data collection	1.702 to 31.508°
Index ranges	$-15 \leq h \leq 15, -54 \leq k \leq 54, -18 \leq l \leq 18$
Reflections collected	222296
Independent reflections	32333 [R(int) = 0.0439]
Completeness to theta = 25.242°	99.8 %
Absorption correction	Semi-empirical from equivalents
Refinement method	Full-matrix least-squares on F^2
Data / restraints / parameters	32333 / 2462 / 1480
Goodness-of-fit on F^2	1.103
Final R indices [I>2sigma(I)]	$R_1 = 0.0518, wR_2 = 0.1421$

R indices (all data)	$R_1 = 0.0610$, $wR_2 = 0.1478$
Absolute structure parameter	0.09(3)
Extinction coefficient	n/a
Largest diff. peak and hole	1.970 and -0.674 e.Å^{-3}

Mo(NAr)[CHN(CH$_2$)$_3$CO](Me$_2$pyr)(OTPP) (1c)

The crystal structure acquisition and refinement were carried out with assistance from Dr. Peter Müller and Dr. Stacey Smith. X-ray-quality crystals were grown from dichloromethane/pentane. Low-temperature diffraction data (φ-and ω-scans) were collected on a Bruker-AXS X8 Kappa c Duo diffractometer coupled to a Smart APEX2 CCD detector with Mo $K\alpha$ radiation ($\lambda = 0.71073$ Å) from an $I\mu S$ micro-source. Absorption and other corrections were applied using SADABS.[18] All structures were solved by direct methods using SHELXS[19] and refined against F_2 on all data by full-matrix least squares with SHELXL-97[20] using established refinement approaches.[21] All hydrogen atoms (except H1, which was taken from the difference Fourier synthesis and refined semi-freely with the help of distance restraints) were included into the model at geometrically calculated positions and refined using a riding model. The isotropic displacement parameters of all hydrogen atoms were fixed to 1.2 times the U value of the atoms they are linked to (1.5 times for methyl groups).

Mo(NAr)(CHN(CH$_2$)$_3$CO)(Me$_2$pyr)(OTPP) crystallized in space group P2(1)/n with one molecule in the asymmetric unit. The methylene carbon atoms in the pyrrolidinone ring were modeled as a twofold disorder with the help of restraints on 1,2-distance, 1,3-distance, and anisotropic displacement parameters. A disordered dichloromethane solvent molecule was also present; this molecule was modeled as a threefold disorder with the help of restraints on 1,2-distance, 1,3-distance, and anisotropic displacement parameters. SIMU and DELU restraints were applied to all disordered atoms. Furthermore, an ISOR restraint was applied to the smallest part of the threefold disorder in order to achieve more well-behaved thermal ellipsoids. It is possible that the solvent molecule is in reality disordered over more than three positions, but attempts at disorders with further multiplicity were not pursued.

Crystal data and structure refinement for 1c

Identification code	x13004
Empirical formula	$C_{54} H_{55} Cl_2 Mo N_3 O_2$
Formula weight	944.85
Temperature	100(2) K
Wavelength	0.71073 Å
Crystal system	Monoclinic
Space group	$P2_1/n$
Unit cell dimensions	a = 11.5255(13) Å $\quad$ $\alpha = 90°$
	b = 18.411(2) Å $\quad$ $\beta = 102.283(2)°$
	c = 22.662(3) Å $\quad$ $\gamma = 90°$
Volume	4698.8(9) Å^3
Z	4
Density (calculated)	1.336 Mg/m^3
Absorption coefficient	0.437 mm^{-1}
F(000)	1968
Crystal size	0.36 x 0.21 x 0.15 mm^3
Theta range for data collection	1.44 to 33.21°
Index ranges	$-16 \le h \le 17, -28 \le k \le 28, -34 \le l \le 34$
Reflections collected	339648
Independent reflections	17827 [R(int) = 0.0398]
Completeness to theta = 33.21°	98.9 %
Absorption correction	Semi-empirical from equivalents
Max. and min. transmission	0.9365 and 0.8592
Refinement method	Full-matrix least-squares on F^2
Data / restraints / parameters	17827 / 136 / 624
Goodness-of-fit on F^2	1.025
Final R indices [I>2sigma(I)]	$R_1 = 0.0265$, $wR_2 = 0.0660$
R indices (all data)	$R_1 = 0.0326$, $wR_2 = 0.0699$
Largest diff. peak and hole	0.615 and -0.641 e.Å^{-3}

Mo(NAr)(CHCarbaz)(Me₂pyr)(OTPP) (1d)

The crystal structure acquisition and refinement were carried out with assistance from Dr. Peter Müller and Dr. Stacey Smith. X-ray-quality crystals were grown from toluene/pentane. Low-temperature diffraction data (φ-and ω-scans) were collected on a Bruker-AXS X8 Kappa Duo diffractometer coupled to a Smart APEX2 CCD detector with Mo $K\alpha$ radiation ($\lambda = 0.71073$ Å) from an $I\mu S$ micro-source. Absorption and other corrections were applied using SADABS.[18] All structures were solved by direct methods using SHELXS[19] and refined against F_2 on all data by full-matrix least squares with SHELXL-97[20] using established refinement approaches.[21] All non-hydrogen atoms were refined anisotropically. All hydrogen atoms (except H1, which was taken from the difference Fourier synthesis and refined semi-freely with the help of distance restraints) were included into the model at geometrically calculated positions and refined using a riding model. The isotropic displacement parameters of all hydrogen atoms were fixed to 1.2 times the U value of the atoms they are linked to (1.5 times for methyl groups). Mo(NAr)(CHCarbaz)(Me₂pyr)(OTPP) crystallized in space group P2(1)/n with one molecule in the asymmetric unit. Strong SIMU and DELU restraints were placed on the diisopropylphenylimido ligand, as this ligand may in reality be slightly disordered. Attempts to model the disorder were fruitless, so the restraints serve as an alternative.

Crystal data and structure refinement for 1d

Identification code	x13012	
Empirical formula	C₆₁ H₅₅ Mo N₃ O	
Formula weight	942.02	
Temperature	100(2) K	
Wavelength	0.71073 Å	
Crystal system	Monoclinic	
Space group	P2₁/n	
Unit cell dimensions	a = 18.861(3) Å	$\alpha = 90°$
	b = 14.440(2) Å	$\beta = 113.109(3)°$
	c = 19.221(3) Å	$\gamma = 90°$
Volume	4815.1(13) Å³	
Z	4	

151

Density (calculated)	$1.299\ \text{Mg/m}^3$
Absorption coefficient	$0.318\ \text{mm}^{-1}$
F(000)	1968
Crystal size	$0.15 \times 0.12 \times 0.07\ \text{mm}^3$
Theta range for data collection	1.28 to 31.69°
Index ranges	$-27 \le h \le 27, -21 \le k \le 21, -28 \le l \le 28$
Reflections collected	255051
Independent reflections	16219 [R(int) = 0.0421]
Completeness to theta = 31.69°	99.6 %
Absorption correction	Semi-empirical from equivalents
Max. and min. transmission	0.9781 and 0.9539
Refinement method	Full-matrix least-squares on F^2
Data / restraints / parameters	16219 / 101 / 605
Goodness-of-fit on F^2	1.051
Final R indices [I>2sigma(I)]	$R_1 = 0.0297, wR_2 = 0.0730$
R indices (all data)	$R_1 = 0.0370, wR_2 = 0.0776$
Largest diff. peak and hole	0.790 and $-0.659\ \text{e.Å}^{-3}$

Mo(NAr)(CHBpin)(Me₂pyr)(OTPP) (1e)

The crystal structure acquisition and refinement were carried out with assistance from Dr. Peter Müller and Dr. Stacey Smith. X-ray-quality crystals were grown from toluene/pentane. Low-temperature diffraction data (φ-and ω-scans) were collected on a Bruker-AXS X8 Kappa Duo diffractometer coupled to a Smart APEX2 CCD detector with Mo $K\alpha$ radiation (λ = 0.71073 Å) from an $I\mu S$ micro-source. Absorption and other corrections were applied using SADABS.[18] All structures were solved by direct methods using SHELXS[19] and refined against F_2 on all data by full-matrix least squares with SHELXL-97[20] using established refinement approaches.[21] All non-hydrogen atoms were refined anisotropically. All hydrogen atoms (except H1, which was taken from the difference Fourier synthesis and refined semi-freely with the help of distance restraints) were included into the model at geometrically calculated positions and refined using a riding model. The isotropic displacement parameters of all hydrogen atoms were fixed to 1.2

times the *U* value of the atoms they are linked to (1.5 times for methyl groups). Mo(NAr)(CHBpin)(Me$_2$pyr)(OTPP) crystallized in space group P$\bar{1}$ with one molecule in the asymmetric unit. There is a partially disordered pentane solvent molecule in the structure. Two atoms of this molecule were modeled as a twofold disorder with the help of 1,2- and 1,3-distance restraints. Strong SIMU and DELU restraints were also employed on this solvent molecule.

Crystal data and structure refinement for 1e

Identification code	x13018	
Empirical formula	C$_{60}$ H$_{71}$ B Mo N$_2$ O$_3$	
Formula weight	974.94	
Temperature	100(2) K	
Wavelength	0.71073 Å	
Crystal system	Triclinic	
Space group	P$\bar{1}$	
Unit cell dimensions	a = 11.221(2) Å	α = 79.245(4)°
	b = 14.951(3) Å	β = 80.120(4)°
	c = 15.986(3) Å	γ = 81.881(4)°
Volume	2579.2(9) Å^3	
Z	2	
Density (calculated)	1.255 Mg/m^3	
Absorption coefficient	0.301 mm^{-1}	
F(000)	1032	
Crystal size	0.25 x 0.17 x 0.12 mm^3	
Theta range for data collection	1.31 to 31.81°.	
Index ranges	-16 ≤ h ≤ 16, -22 ≤ k ≤ 22, -23 ≤ l ≤ 22	
Reflections collected	130820	
Independent reflections	17387 [R(int) = 0.0281]	
Completeness to theta = 31.81°	98.6 %	
Absorption correction	Semi-empirical from equivalents	
Max. and min. transmission	0.9648 and 0.9286	

Refinement method	Full-matrix least-squares on F^2
Data / restraints / parameters	17387 / 82 / 640
Goodness-of-fit on F^2	1.045
Final R indices [I>2sigma(I)]	$R_1 = 0.0273$, $wR_2 = 0.0704$
R indices (all data)	$R_1 = 0.0305$, $wR_2 = 0.0725$
Largest diff. peak and hole	0.990 and -0.634 e.Å^{-3}

Mo(NAr)(CHTMS)(Me₂pyr)(OTPP) (1f)

The crystal structure acquisition and refinement were carried out by Dr. Peter Müller and Dr. Stacey Smith. X-ray-quality crystals were grown from toluene/pentane. Low-temperature (100 K) x-ray diffraction data comprising φ- and ω- scans were collected using a Bruker-AXS X8 Kappa Duo diffractometer coupled to a Smart Apex II CCD detector with an $I\mu S$ source of Mo K_α radiation ($\lambda = 0.71073$ Å). The structure was solved by direct methods using SHELXS[19] and refined against F^2 on all data by full-matrix least squares with SHELXL-97[20] using established refinement strategies.[21] All non-hydrogen atoms were refined anisotropically. The positions of all hydrogen atoms except that on the alkylidene carbon (C1) were calculated geometrically and refined using a riding model. The position of the hydrogen atom attached to C1 was taken from the difference Fourier synthesis and subsequently refined semi-freely with the help of a distance restraint. The isotropic displacement parameters of all hydrogen atoms were constrained to 1.2 times the U_{eq} value of the atom to which they are bound (1.5 times for methyl groups).

The target molecule crystallized in the triclinic space group $P\bar{1}$ with one molecule in the asymmetric unit. One pentane solvent molecule co-crystallized with the target molecule and was disordered over two positions. One of the isopropyl groups (the one proximal to the disordered pentane molecule) on the $NC_6H_3(C_3H_7)_2$ ligand displayed rotational disorder and was modeled as a two-fold disorder. Rigid bond restraints and similarity restraints were employed for the displacement parameters of all atoms involved in disorders, and similarity restraints were used on the 1-2 and 1-3 distances for all equivalent disordered atoms. Additional isotropy restraints were employed for the displacement parameters of three of the four disordered methyl carbons (C18a, C19a, C19) of the isopropyl group. The somewhat larger displacement parameters of

these atoms suggest further rotational disorder, but no additional disordered components were included in the model due to the already low occupancy (15%) of the minor component.

Crystal data and structure refinement for 1f

Identification code	x13038
Empirical formula	$C_{57} H_{68} Mo N_2 O Si$
Formula weight	921.16
Temperature	100(2) K
Wavelength	0.71073 Å
Crystal system	Triclinic
Space group	$P\bar{1}$
Unit cell dimensions	a = 11.0930(9) Å α = 98.741(2)°
	b = 11.2523(10) Å β = 100.267(2)°
	c = 21.8352(19) Å γ = 107.259(2)°
Volume	2499.5(4) Å^3
Z	2
Density (calculated)	1.224 Mg/m^3
Absorption coefficient	0.326 mm^{-1}
F(000)	976
Crystal size	0.14 x 0.09 x 0.09 mm^3
Theta range for data collection	1.94 to 31.52°
Index ranges	$-16 \leq h \leq 16, -16 \leq k \leq 16, -32 \leq l \leq 32$
Reflections collected	129577
Independent reflections	16625 [R(int) = 0.0375]
Completeness to theta = 31.52°	99.7 %
Absorption correction	Semi-empirical from equivalents
Max. and min. transmission	0.9712 and 0.9557
Refinement method	Full-matrix least-squares on F^2
Data / restraints / parameters	16625 / 238 / 638
Goodness-of-fit on F^2	1.042

155

Final R indices [I>2sigma(I)]	$R_1 = 0.0321$, $wR_2 = 0.0786$
R indices (all data)	$R_1 = 0.0375$, $wR_2 = 0.0810$
Largest diff. peak and hole	0.700 and -0.385 e.Å^{-3}

Mo(NAr)(CHSPh)(Me₂pyr)(OTPP) (1g)

The crystal structure acquisition and refinement were carried out by Dr. Peter Müller and Dr. Stacey Smith. X-ray-quality crystals were grown from toluene/pentane. Low-temperature diffraction data(-123 °C, φ-and ω-scans) were collected on a Siemens Platform three-circle diffractometer coupled to a Smart APEX2 CCD detector with Mo Kα radiation ($\lambda = 0.71073$ Å) from an IμS micro-source. Absorption and other corrections were applied using SADABS.[18] All structures were solved by direct methods and Patterson methods using SHELXS[19] and refined against F2 on all data by full-matrix least squares with SHELXL-97[20] using established refinement approaches.[21] All hydrogen atoms were included into the model at geometrically calculated positions and refined using a riding model. The isotropic displacement parameters of all hydrogen atoms were fixed to 1.2 times the U value of the atoms they are linked to (1.5 times for methyl groups). Mo(NAr)(CHSPh)(Me₂pyr)(OTPP) crystallized in space group P2₁/n with one molecule in the asymmetric unit. One isopropyl group on the diisopropylphenylimido ligand was modeled as a twofold disorder, with the help of restraints on 1,2-distance, 1,3-distance, and anisotropic displacement parameters. Strong SIMU and DELU restraints were also applied to this disordered isopropyl group; it is possible that a threefold disorder may exist in the structure, but attempts to model it led to unstable refinements.

Crystal data and structure refinement for 1g

Identification code	13004
Empirical formula	C₅₅ H₅₂ Mo N₂ O S
Formula weight	884.99
Temperature	150(2) K
Wavelength	0.71073 Å
Crystal system	Monoclinic
Space group	P2₁/n
Unit cell dimensions	a = 14.0945(12) Å α = 90°

	$b = 20.0137(17)$ Å $\beta = 105.9870(10)°$
	$c = 16.7996(14)$ Å $\gamma = 90°$
Volume	$4555.6(7)$ Å^3
Z	4
Density (calculated)	1.290 Mg/m^3
Absorption coefficient	0.375 mm^{-1}
F(000)	1848
Crystal size	$0.23 \times 0.20 \times 0.17$ mm^3
Theta range for data collection	1.62 to $30.49°$
Index ranges	$-20 \leq h \leq 20, -28 \leq k \leq 28, -23 \leq l \leq 23$
Reflections collected	127110
Independent reflections	13885 [R(int) = 0.0402]
Completeness to theta = $30.49°$	$100.0\ \%$
Absorption correction	Semi-empirical from equivalents
Max. and min. transmission	0.9390 and 0.9187
Refinement method	Full-matrix least-squares on F^2
Data / restraints / parameters	13885 / 100 / 568
Goodness-of-fit on F^2	1.031
Final R indices [I>2sigma(I)]	$R_1 = 0.0316, wR_2 = 0.0773$
R indices (all data)	$R_1 = 0.0400, wR_2 = 0.0832$
Largest diff. peak and hole	1.141 and -0.584 e.Å^{-3}

Mo(NAr)(CHPPh₂)(Me₂pyr)(OTPP)(MeCN) (1h-MeCN)

The crystal structure acquisition and refinement were carried out by Dr. Peter Müller and Dr. Stacey Smith. X-ray quality crystals were grown from dichloromethane/ether. Low-temperature (100 K) x-ray diffraction data comprising φ- and ω- scans were collected using a Bruker-AXS X8 Kappa Duo diffractometer coupled to a Smart Apex II CCD detector with an IμS source of Mo K_α radiation ($\lambda = 0.71073$ Å). The structure was solved by direct methods using SHELXS[19] and refined against F^2 on all data by full-matrix least squares with SHELXL-97[20] using established refinement strategies.[21] All non-hydrogen atoms were refined anisotropically.

The positions of all hydrogen atoms except that on the alkylidene carbon (C1) were calculated geometrically and refined using a riding model. The position of the hydrogen atom attached to C1 was taken from the difference Fourier synthesis and subsequently refined semi-freely with the help of a distance restraint. The isotropic displacement parameters of all hydrogen atoms were constrained to 1.2 times the U_{eq} value of the atom to which they are bound (1.5 times for methyl groups).

The target molecule crystallized in the monoclinic space group $P2_1/n$ with one molecule in the asymmetric unit. One of the ligands [NC$_6$H$_3$(C$_3$H$_7$)$_2$] was disordered over two positions. Two dichloromethane solvent molecules also crystallized with the target molecule, both displaying disorder. One was disordered over three independent positions and the other over two independent positions. Due to the proximity of an inversion center to the two-fold disordered dichloromethane, the second component was generated by the inversion, requiring the occupancy of each of component to be set at 0.5 instead of being allowed to refine freely. As only one of the disordered components was thus contained in the asymmetric unit, a non-integer value appeared for the element carbon in the empirical formula, and the ratio of dichloromethane to the target molecule was actually 1.5 instead of 2. For all atoms involved in disorders, rigid bond restraints and similarity restraints were employed on the displacement parameters, and similarity restraints were used for the 1-2 and 1-3 distances for all equivalent atoms.

Crystal data and structure refinement for 1h-MeCN

Identification code	x13033	
Empirical formula	C$_{64.50}$ H$_{63}$ Cl$_3$ Mo N$_3$ O P	
Formula weight	1129.44	
Temperature	100(2) K	
Wavelength	0.71073 Å	
Crystal system	Monoclinic	
Space group	P2$_1$/n	
Unit cell dimensions	a = 12.6179(19) Å	α = 90°
	b = 20.931(3) Å	β = 98.621(3)°
	c = 21.512(3) Å	γ = 90°
Volume	5617.3(15) Å^3	

Z	4
Density (calculated)	1.336 Mg/m^3
Absorption coefficient	0.450 mm^{-1}
F(000)	2348
Crystal size	$0.69 \times 0.37 \times 0.28$ mm^3
Theta range for data collection	1.36 to $31.53°$
Index ranges	$-18 \leq h \leq 18, -30 \leq k \leq 30, -31 \leq l \leq 30$
Reflections collected	232005
Independent reflections	18676 [R(int) = 0.0335]
Completeness to theta = $31.53°$	99.6 %
Absorption correction	Semi-empirical from equivalents
Max. and min. transmission	0.8852 and 0.7472
Refinement method	Full-matrix least-squares on F^2
Data / restraints / parameters	18676 / 605 / 859
Goodness-of-fit on F^2	1.108
Final R indices [I>2sigma(I)]	$R_1 = 0.0468, wR_2 = 0.1189$
R indices (all data)	$R_1 = 0.0553, wR_2 = 0.1250$
Largest diff. peak and hole	1.800 and -1.037 $e.Å^{-3}$

Details for Computational Studies

Computational studies and figures derived therefrom were made by Dr. Stefan Kilyanek. The bonding characteristics and molecular orbitals of compounds **1** and **1b-1h** were examined by population analyses using density functional theory (DFT). Single point calculations were performed on the geometries obtained from X-ray diffraction studies of **1** and **1b-1h** using the B3LYP functional[22] as implemented in the computational package ORCA 2.9.1.[23] Main group atoms were represented by the 6-31G* basis set.[24] Mo was represented by the LANLDZ basis set and effective core potential.[25] Further orbital analysis was performed using the NBO method.[26] All images were rendered using the Jmol visualization package.[27]

159

REFERENCES

[1] (a) Schrock, R. R. *Chem. Rev.* **2002**, *102*, 145. (b) Schrock, R. R. *Chem. Rev.* **2009**, *109*, 3211.

[2] (a) Schrock, R. R.; Murdzek, J. S.; Bazan, G. C.; Robbins, J.; DiMare, M.; O'Regan, M. *J. Am. Chem. Soc.* **1990**, *112*, 3875. (b) Schrock, R. R.; DePue, R. T.; Feldman, J.; Yap, K. B.; Yang, D. C.; Davis, W. M.; Park, L. Y.; DiMare, M.; Schofield, M.; Anhaus, J.; Walborsky, E.; Evitt, E.; Krüger, C.; Betz, P. *Organometallics* **1990**, *9*, 2262. (c) Barinova, Y. P.; Bochkarev, A. L.; Begantsova, Y. E.; Bochkarev, L. N.; Kurskii, Y. A.; Fukin, G. K.; Cherkasov, A. V.; Abakumov, G. A. *Russ. J. Gen. Chem.* **2010**, *80*, 1945. (d) Barinova, Y. P.; Begantsova, Y. E.; Stolyarova, N. E.; Grigorieva, I. K.; Cherkasov, A. V.; Fukin, G. K.; Kurskii, Y. A.; Bochkarev, L. N.; Abakumov, G. A. *Inorg. Chim. Acta* **2012**, *363*, 2313. (e) Bochkarev, A. L.; Basova, G. V.; Grigorieva, I. K.; Stolyarova, N. E.; Malysheva, I. P.; Fukin, G. K.; Baranov, E. V.; Kurskii, Y. A.; Bochkarev, L. N.; Abakumov, G. A. *J. Organomet. Chem.* **2010**, *695*, 692. (f) Barinova, Y. P.; Bochkarev, A. L.; Kurskii, Y. A.; Abakumov, G. A. *Russ. J. Gen. Chem.* **2012**, *82*, 17.

[3] Cross, J. L.; Crane, T. W.; White, P. S.; Templeton, J. L. *Organometallics* **2003**, *22*, 548.

[4] (a) Toreki, R.; Vaughan, G. A.; Schrock, R. R.; Davis, W. M. *J. Am. Chem. Soc.* **1993**, *115*, 127. (b) Lapointe, A. M.; Schrock, R. R. *Organometallics* **1995**, *14*, 1875.

[5] Wu, Z.; Nguyen, S. T.; Grubbs, R. H.; Ziller, J. W. *J. Am. Chem. Soc.* **1995**, *117*, 5503.

[6] Louie, J.; Grubbs, R. H. *Organometallics* **2002**, *21*, 2153.

[7] (a) Khan, R. K. M.; O' Brien, R. V.; Torker, S.; Li, B.; Hoveyda, A. H. *J. Am. Chem. Soc.* **2012**, *134*, 12774. (b) Katayama, H.; Urushima, H.; Nishioka, T.; Wada, C.; Nagao, M.; Ozawa, F. *Angew. Chem., Int. Ed.* **2000**, *39*, 4513. (c) Weeresakare, G. M.; Liu, Z.; Rainier, J. D. *Org. Lett.* **2004**, *6*, 1625. (d) Liu, Z.; Rainier, J. D. *Org. Lett.* **2005**, *7*, 131.

[8] Van de Weghe, P.; Bisseret, P.; Blanchard, N.; Eustache, J. *J. Organomet. Chem.* **2006**, *691*, 5078.

[9] (a) Meek, S. J.; O' Brien, R. V.; Llaveria, J.; Schrock, R. R.; Hoveyda, A. H. *Nature* **2011**, *471*, 461. (b) Yu, M.; Ibrahem, I.; Hasegawa, M.; Schrock, R. R.; Hoveyda, A. H. *J. Am. Chem. Soc.* **2012**, *134*, 2788.

[10] Kiesewetter, E. T.; O' Brien, R. V.; Yu, E. C.; Meek, S. J.; Schrock, R. R.; Hoveyda, A. H. *J. Am. Chem. Soc.* **2013**, *135*, 6026.

[11] Lee, Y.-J.; Schrock, R. R.; Hoveyda, A. H. *J. Am. Chem. Soc.* **2009**, *131*, 10652.

[12] Yates, P.; Hyre, J. E. *J. Org. Chem.* **1962**, *27*, 4101.

[13] Oskam, J. H.; Schrock, R. R. *J. Am. Chem. Soc.* **1993**, *115*, 11831.

[14] Epeotis, N. D.; Cherry, W. *J. Am. Chem. Soc.* **1976**, *98*, 4365.

[15] Budzelaar, P. H. M. gNMR; University of Manitoba: Canada.

[16] Harris, R. K.; Woplin, J. R. *J. Magnetic Res.* **1972**, *7*, 291.

[17] (a) Townsend, E. M.; Schrock, R. R.; Hoveyda, A. H. *J. Am. Chem. Soc.* **2012**, *134*, 11334. (b) Chapter 2 of this work

[18] Sheldrick, G. M. SADABS; University of Göttingen: Germany, 1996.

[19] Sheldrick, G. M. *Acta Cryst.* **1990**, A46, 467.

[20] Sheldrick, G. M. *Acta Cryst.* **2008**, A64, 112.

[21] Müller, P. Crystallography Reviews **2009**, 15, 57.

[22] ORCA keyword B3LYP/G . (a) Becke, A. D. *J. Chem. Phys.* **1993**, *98*, 5648. (b) Becke, A. D. *Phys. Rev. A*, **1988**, *38*, 3098. (c) Lee, C.; Yang, W.; Parr, R. G. *Phys. Rev. B*, **1988**, *37*, 785. (d) Vosko, S. H.; Wilk, L.; Nusair, M. *Can. J. Phys.* **1980**, *58*, 1200. (e) Miehlich, B.; Savin, A.; Stoll, H.; Preuss, H. *Chem. Phys. Lett.* **1989**, *157*, 200.

[23] a) Neese, F. *WIREs Comput Mol Sci* **2012**, *2*, 73. ORCA *An Ab Initio, DFT and Semiempirical electronic structure package v2.9.1* Juanary 2012 b) 2 e⁻ integrals were calculated using the libint2 library, LIBINT: A library for the evaluation of molecular integrals of many-body operators over Gaussian functions, Version 2.0.3 Edward F. Valeev, http://libint.valeyev.net/ .

[24] (a) Hehre, W.J.; Ditchfield, R.; Pople, J. A.; *J. Chem. Phys.* **1972**, *56*, 2257 (b) Dill, J. D.; Pople, J. A. *J. Chem. Phys.* **1975**, *62*, 2921. (c) Francl, M. M.; Pietro, W. J.; Hehre, W. J.; Binkley, J. S.; Gordon, M. S.; DeFrees, D. J.; Pople, J. A. *J. Chem. Phys.* **1982**, *77*, 3654.

[25] Hay, P. J.; Wadt, W. R. J. *J. Chem. Phys.* **1985**, *82*, 299.

[26] Glendening, E. D.; Badenhoop, J. K.; Reed, A. E.; Carpenter, J. E.; Bohmann, J. A.; Morales, C. M.; Weinhold, F. NBO 5.9; Theoretical Chemistry Institute, University of Wisconsin: Madison, WI, 2009; http://www.chem.wisc.edu/nbo5.

[27] Jmol: an open-source Java viewer for chemical structures in 3D. http://www.jmol.org/

161

Chapter 4

Molybdenum and Tungsten Olefin Metathesis Catalysts Bearing Thiolate Ligands

INTRODUCTION

Mo and W (VI) imido alkylidene complexes are powerful and versatile catalysts for olefin metathesis processes. The wide variety of additional anionic ligands (X and Y in Figure 1) that can be installed in these complexes is partially responsible for the depth and breadth of research in the area.[1] Differences in ligand steric profile and electronic donor ability are used as tools for catalyst design and mechanistic studies. As such, general principles relating to the effects of ligand identity on complex behavior are exceedingly important.
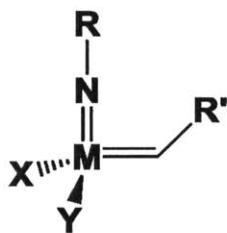
Figure 1: General structure of a Mo or W (VI) imido alkylidene complex X, Y = monoanionic ligands.

The first generation of efficient molecular imido alkylidene catalysts featured two alkoxide ligands (X and Y = OR).[2] A vast improvement in the activity of bisalkoxide catalysts could be seen with the use of electron-withdrawing alkoxide ligands, leading to the conclusion that an electron-poor environment at the metal center accelerates metathesis reactivity.[3] However, monoaryloxide pyrrolide (MAP) imido alkylidenes were often shown to be substantially more active than bisalkoxides, despite the fact that pyrrolides are more electron-donating than alkoxides.[1a] Clearly, the electronic trends for these catalysts are not as straightforward as previously believed.

Detailed density functional theory (DFT) calculations have been carried out by Eisenstein and coworkers to probe the reactivity trends of catalysts with different donor ligands.[4] It was found that the two key steps in the catalytic cycle are olefin coordination and metallacycle breakup (cycloreversion), and that the donor properties of X and Y can have large effects on the favorability of these steps (Scheme 1).

olefin coordination

TBP olefin complex: the more donating ligand X goes axial. If Y is too donating, this is slow to form.

cyclization

TBP metallacyclobutane: if X and Y are withdrawing, this intermediate is more stable.

cycloreversion and olefin decoordination
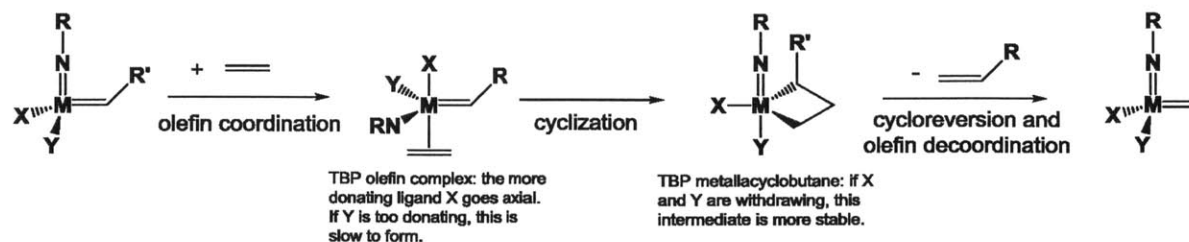
Scheme 1: Mechanism of olefin metathesis by M(NR)(CHR')(X)(Y) complexes

If X and Y are too electron-donating, the olefin coordination step is slow because the necessary trigonal pyramid is disfavored. However, if the ligands are extremely electron-withdrawing, the electron-poor metal will be slow to release olefin from the metallacyclobutane

intermediate, which decreases the catalytic turnover rate. According to the calculations, the ideal scenario involves an asymmetric ligand environment in which X and Y are "donor" and "acceptor" ligands, respectively.[4] The donor can remain in the apical position of the trigonal pyramid in the TBP olefin complex, while also providing electron density to encourage the breakup of the metallacycle in the subsequent step. This theory can explain why MAP complexes have met with so much catalytic success: the pyrrolide plays the role of the donor (X in Scheme 1) while the less-donating alkoxide serves as the acceptor (Y) in order to strike an advantageous balance.

While MAPs (and in some cases bisalkoxides) are currently the most successful Mo and W metathesis catalysts, it is plausible that for some metal-ligand combinations, other donors may provide even better results. It is known that W catalysts are generally slower than their Mo counterparts, and that metallacycle breakup in W MAP complexes is slower than for Mo MAPs.[5] Therefore, it would be interesting to observe the effect of a stronger donor ligand in a M(NR)(CHR')(X)(Y) framework.

To this end, we chose to replace alkoxides with thiolate ligands in existing complexes. Thiolates are generally regarded as stronger sigma donors that exhibit bonding interactions with more covalent character.[6] A small number of imido alkylidene thiolate complexes have been prepared previously.[7] These complexes, while isolable, were not tested for general olefin metathesis reactivity (only enyne metathesis reactivity was explored). With a more systematic approach, we can further explore the previously detailed trends and perhaps identify an even better combination of ligands. W catalysts in particular may benefit from a stronger donor to destabilize their metallacycle forms.

Side-by-side comparisons between alkoxide-containing catalysts and their thiolate analogues will be the most useful. Part I will describe the synthesis of four such catalyst pairs, including three MAP/monothiolate pyrrolide (MTP) pairs and one bisalkoxide/bisthiolate pair. Part II will discuss the side-by-side comparisons of these catalysts in metathesis homocoupling and ring-opening metathesis polymerization (ROMP) processes. Both reactivity and selectivity will be examined in order to both gain more fundamental knowledge about ligand effects in our systems and to potentially find better catalysts in the process.

RESULTS AND DISCUSSION

I. Catalyst synthesis

The eight catalysts chosen for the comparison studies are shown in Figure 2.
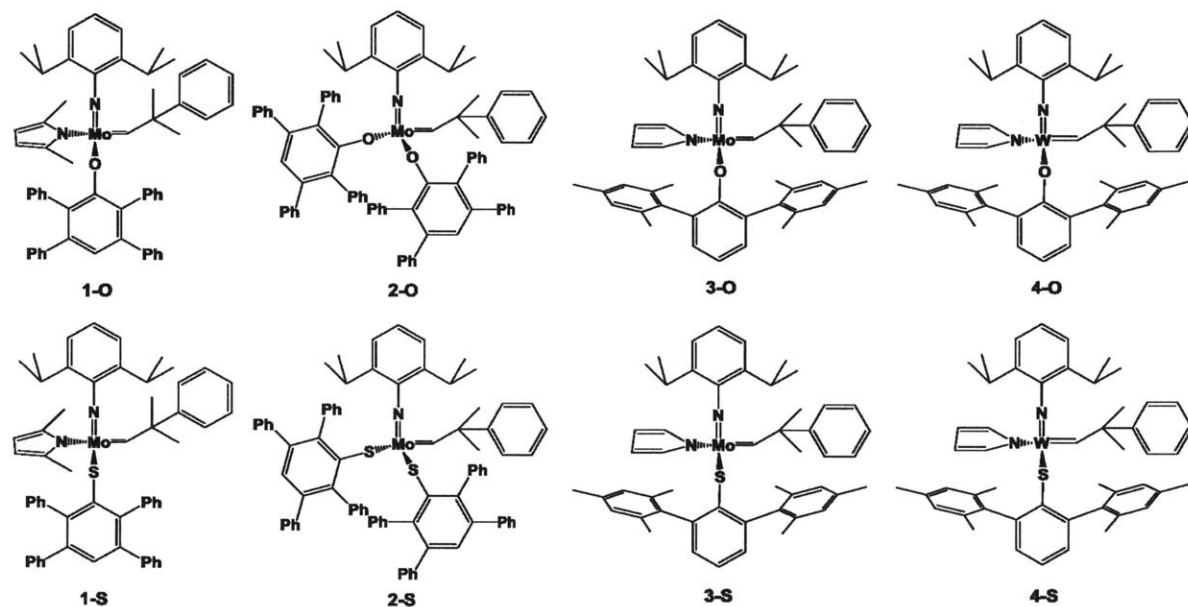
Figure 2: Mo and W alkoxide and thiolate alkylidene complexes

The top row of Figure 2 shows four alkoxide-bearing catalysts, three of which are previously reported MAP complexes (**1-O**,[8] **3-O**,[9] and **4-O**[10]) while the fourth is a new bisaryloxide (**2-O**). The bottom row contains the direct thiolate analogues (**1-S, 2-S, 3-S,** and **4-S**), which are all previously unreported. The complexes were synthesized by addition of the appropriate oxygen- and sulfur-based ligands to metal precursors of the type $M(NAr)(CHCMe_2Ph)X_2$ or $M(NAr)(CHCMe_2Ph)X_2L_2$ (Ar = 2,6-diisopropylphenyl; X = pyrrolide (pyr), 2,5-dimethylpyrrolide (Me_2pyr), or OTf; L_2 = 1,2-dimethoxyethane (dme) or 2,2'-bipyridine (bipy)). The synthesis of the necessary alkoxide and thiolate ligands is detailed in Section I-A below. Section I-B will focus on the isolation and characterization of the catalytic Mo and W complexes.

I-A. Ligand Synthesis

In all, four alkoxide or thiolate ligands were necessary for the completion of the catalyst series shown in Figure 2. The HOHMT ligand (HMT = 2,6-bis(2,4,6-trimethylphenyl)phenyl),

165

which is featured in **3-O** and **4-O**, was synthesized by lithiation of the iodide precursor IHMT followed by quenching with nitrobenzene according to a literature procedure.[11] A similar procedure (also reported in the literature)[12] employing sulfur as a quenching agent and LiAlH$_4$ as a reductant yielded the HSHMT ligand, which was used to make complexes **3-S** and **4-S**. The synthetic routes to these ligands are shown in Scheme 2.
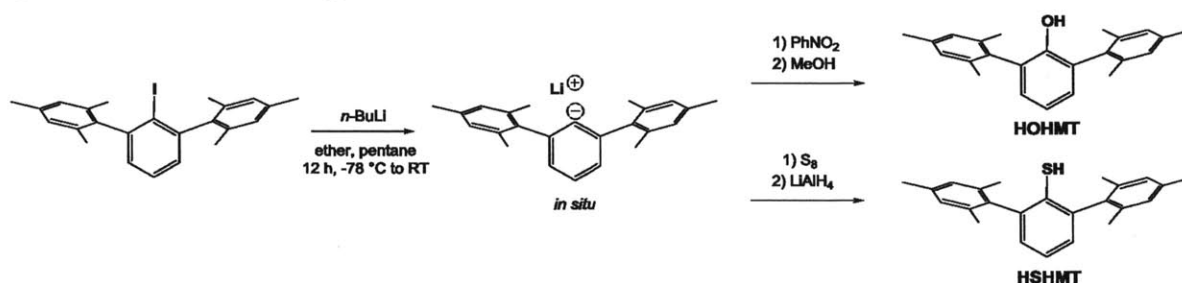
Scheme 2: Synthesis of HOHMT and HSHMT

    Complexes **1-O** and **2-O** require the use of the ligand HOTPP (TPP = 2,3,5,6-tetraphenylphenyl), and **1-S** and **2-S** are similarly derived from the thiol HSTPP. A synthesis of HOTPP has been reported previously in the literature,[13] but an improved synthetic route was utilized to obtain the ligand for these studies. A synthetic route to the previously unreported HSTPP was devised using HOTPP as the starting material. The route involving both TPP-based ligands is shown in Scheme 3.
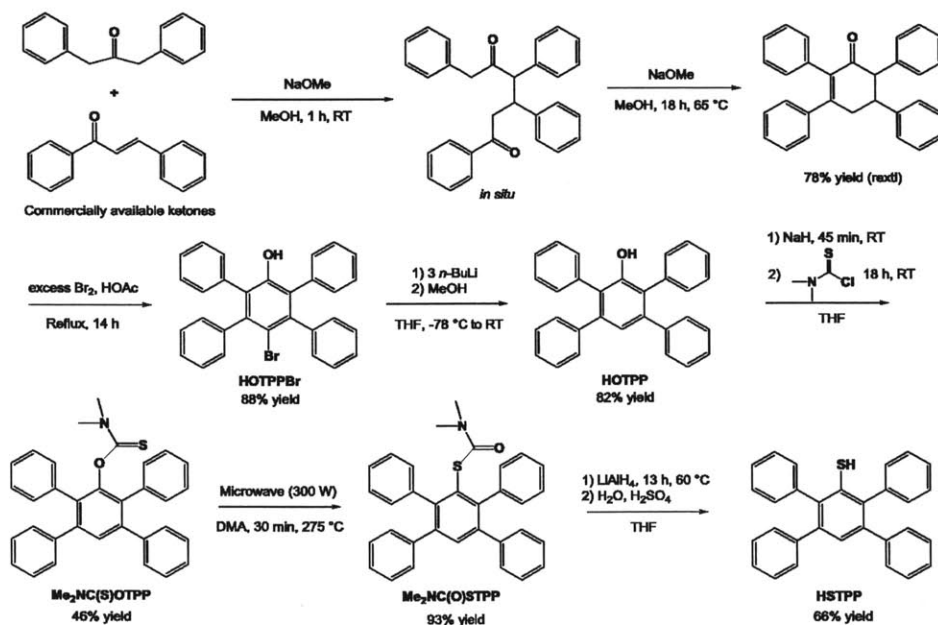
Scheme 3: Synthetic route to HOTPP and HSTPP

The synthesis, which was based on a previous report,[13] began from the commercially available ketones 1,3-diphenyl-2-propanone and 1,3-diphenyl-2-propenone. Condensation of these reagents under basic conditions in refluxing methanol afforded 2,3,5,6-tetraphenylcyclohexenone in 78% yield. Oxidation of this product with bromine led to both formation of the phenol functionality and bromination in the *para* position (HOTPPBr, 88% yield). HOTPP was obtained in 82% yield by debromination with *n*-butyllithium.

Conversion of the alcohol functionality of HOTPP to a thiol group required a three-step, protection/rearrangement/deprotection strategy commonly referred to as the Newman-Kwart rearrangement.[14] Deprotonation of the alcohol with sodium hydride and protection with *N,N*-dimethylthiocarbamoyl chloride led to the product $Me_2NC(S)OTPP$ in 46% yield. The rearrangement step, which requires high temperatures to occur, was carried out using a microwave reactor (30 min, 300 W, 275 °C) and led to pure $Me_2NC(O)STPP$ in nearly quantitative yield (93%). Finally, removal of the thiocarbamate group with $LiAlH_4$ and acid afforded the desired thiol ligand HSTPP in 66% yield after recrystallization. The protection and deprotection steps were based on a literature synthesis of a related thiophenol,[15] and the microwave step was also inspired by a previous report.[16]

I-B. Complex synthesis

The metal complexes pictured in Figure 2 were synthesized through addition of the above alcohol or thiol ligands (or, in one case, a lithium alkoxide) to imido alkylidene bispyrrolide or bistriflate precursors. Complexes **1-O**,[8] **3-O**,[9] and **4-O**[10] were synthesized from alcohol ligands and bispyrrolides according to literature procedures. The synthesis of the bisalkoxide catalyst **2-O** is shown in Scheme 4.

Scheme 4: Synthesis of $Mo(NAr)(CHCMe_2Ph)(OTPP)_2$ (2-O)

167
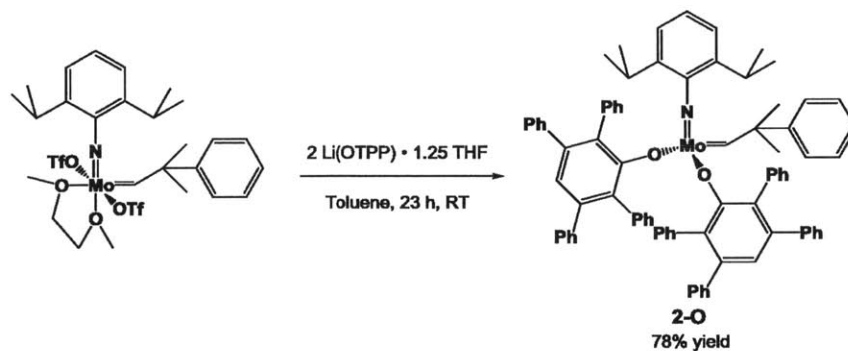
Treatment of Mo(NAr)(CHCMe$_2$Ph)(OTf$_2$)(dme) with 2 equivalents of Li(OTPP) · 1.25 THF in toluene at room temperature cleanly gave product **2-O**, which could be isolated as an orange solid in 78% yield.

With the four alkoxide catalysts in hand, the next efforts were devoted to the isolation of the analogous thiolate complexes: **1-S**, **2-S**, **3-S**, and **4-S**.

Compound **1-S** was obtained via protonolysis of one dimethylpyrrolide ligand from Mo(NAr)(CHCMe$_2$Ph)(Me$_2$pyr)$_2$ with HSTPP. Partial oversubstitution to form mixtures including the bisthiolate complex **2-S** was common in nonpolar or ethereal solvents. Attempts using 1 equivalent of HSTPP in toluene or ether led to mixtures comprised of ~60% **1-S**, ~25% **2-S**, and ~15% Mo(NAr)(CHCMe$_2$Ph)(Me$_2$pyr)$_2$. Improved results were seen when the reaction was run in a 4:1 mixture of MeCN:benzene, and finally the synthesis pictured in Scheme 5 was devised.
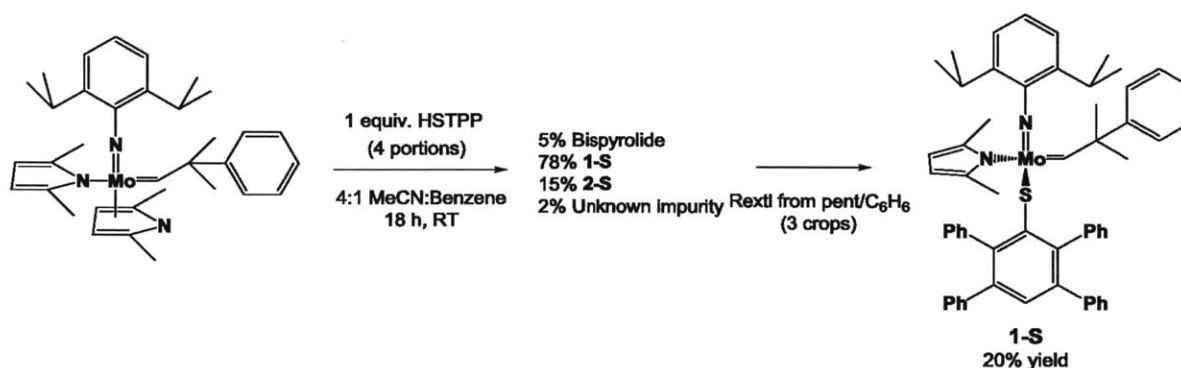
Scheme 5: Synthesis of Mo(NAr)(CHCMe$_2$Ph)(Me$_2$pyr)(STPP) (1-S)

One equivalent of HSTPP was split into four equal portions, which were added to a solution of Mo(NAr)(CHCMe$_2$Ph)(Me$_2$pyr)$_2$ in 4:1 MeCN:benzene over a period of 4 h (Note: the starting materials were not soluble in neat MeCN). This strategy was adopted in an attempt to discourage bisthiolate formation by limiting the available amount of HSTPP in solution at a given time. After the additions were complete, the solution was stirred for 18 h, after which time a mixture containing 78% **1-S** was observable by ^{1}H NMR. Evaporation of solvent, trituration of the residue with ether, and recrystallization from benzene and pentane led to a 20% yield of pure **1-S**.

X-ray-quality crystals of **1-S** were grown from toluene and pentane, and the structure obtained therefrom is shown in Figure 3.
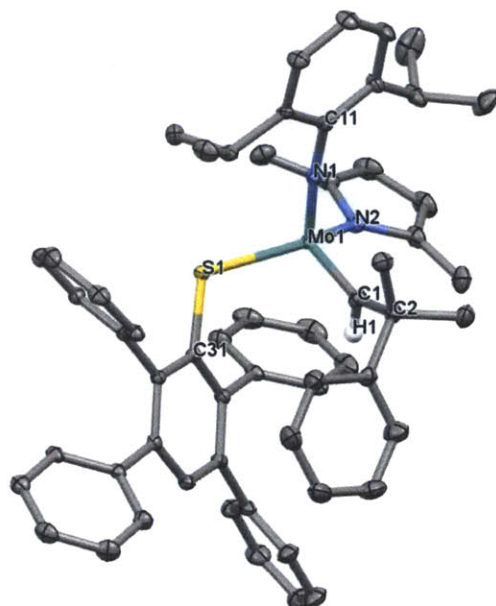
Figure 3: Thermal ellipsoid drawing of 1-S (50% probability ellipsoids). Selected distances (Å) and angles (deg): Mo(1)-C(1) = 1.870(2), Mo(1)-N(1) = 1.726(2), Mo(1)-N(2) = 2.052(2), Mo(1)-S(1) = 2.371(1), Mo(1)-S(1)-C(31) = 112.7.

The geometry about the metal forms a slightly distorted tetrahedron: all angles are between 100 and 110 degrees with the exception of S1-Mo1-N2 at 126.9(1). The Mo-N bond lengths in **1-S** are slightly longer than those found in the previously reported structure of **1-O** (Mo-imido = 1.719 (4); Mo-pyrrolide = 2.048(4)),[8] which can be interpreted as a sign of greater sigma donor ability of STPP when compared to OTPP. The Mo-S-C angle is 112.7 degrees, signifying the lack of pi-donation from the sulfur atom to the metal; in contrast, the Mo-O-C angle in **1-O** measures 157.2 degrees. The alkylidene is in the *syn* configuration, just as it is in **1-O.** A noticeable feature of the structure is the apparent abundance of open space near the metal that arises from the bent conformation of the thiolate ligand.

The synthesis of **2-S** proceeded naturally from the efforts toward **1-S**: two equivalents of HSTPP were added to Mo(NAr)(CHCMe$_2$Ph)(Me$_2$pyr)$_2$ as shown in Scheme 6.
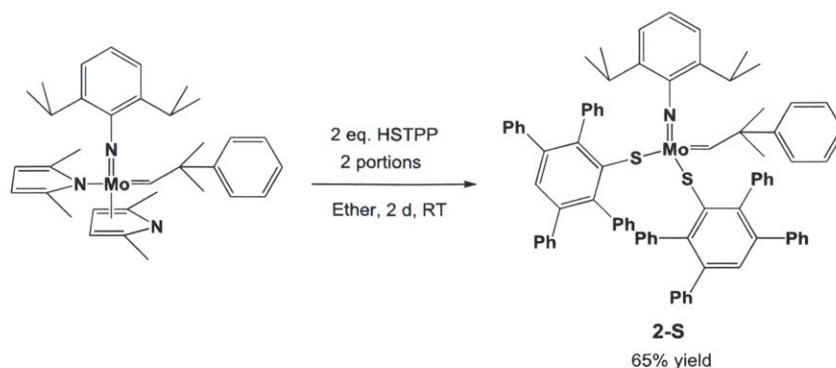
Scheme 6: Synthesis of Mo(NAr)(CHCMe₂Ph)(STPP)₂ (2-S)

The thiolate ligand was added in two portions (20 h apart) and the reaction was allowed to run for two days. The ligand substitution steps appear to occur quickly, so it is likely that a substantially shorter reaction time would be equally effective. **2-S** was obtained as a bright orange solid in 65% yield after evaporation of the solvent and washing of the crude product with diethyl ether.

X-ray-quality crystals of **2-S** were grown from toluene and diethyl ether, and a drawing of the structure is shown below in Figure 4.
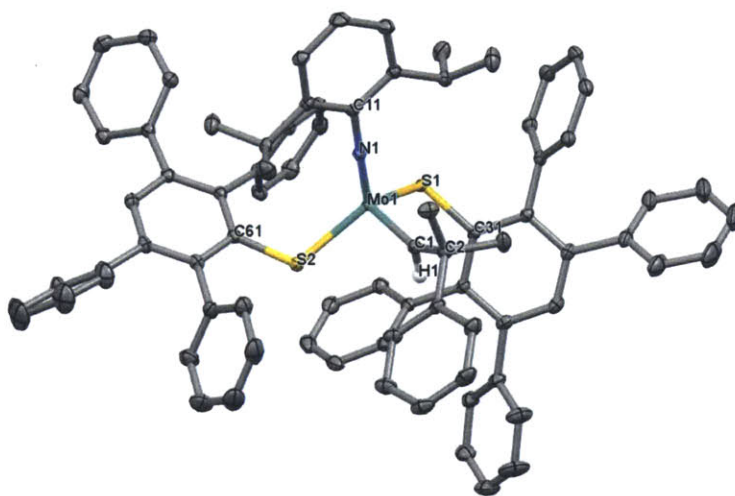
Figure 4: Thermal ellipsoid drawing of 2-S (50% probability ellipsoids). Selected distances (Å) and angles (deg): Mo(1)-C(1) = 1.877(1), Mo(1)-N(1) = 1.731(1), Mo(1)-S(1) = 2.394(1), Mo(1)-S(2): 2.371(1), Mo(1)-S(1)-C(31) = 109.0(1), Mo(1)-S(2)-C(61) = 116.1.

The alkylidene adopts the *syn* configuration in **2-S**. The thiolate angles in the structure of **2-S** are similarly bent to that found in **1-S**. The other angles and Mo-ligand bonds are also quite similar to those in the structure of **1-S**. Interestingly, the bond lengths and angles about S1 are slightly different than those about S2 despite the fact that the two thiolate ligands are chemically

equivalent in theory. It is postulated that crystal packing effects are responsible for this difference.

Complex **3-S** was synthesized by single substitution of HSHMT on Mo(NAr)(CHCMe$_2$Ph)(pyr)$_2$ as displayed in Scheme 7. The protonolysis reaction led cleanly to the MTP as the sole alkylidene product (unlike in the case of **1-S**). Evaporation of the solvent led to isolation of pure **3-S** as a foam in 65% yield. The J$_{CH}$ for the alkylidene signal was 110 Hz, strongly suggesting a *syn* alkylidene configuration.
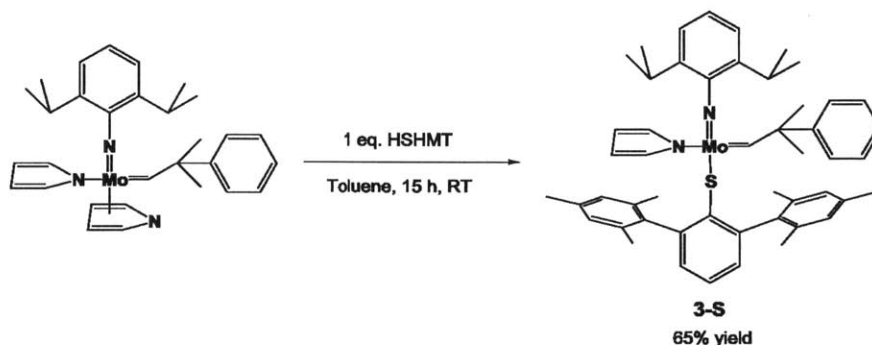
Scheme 7: Synthesis of Mo(NAr)(CHCMe$_2$Ph)(pyr)(SHMT) (3-S)

The final thiolate complex in the series is **4-S**, which was synthesized according to Scheme 8.
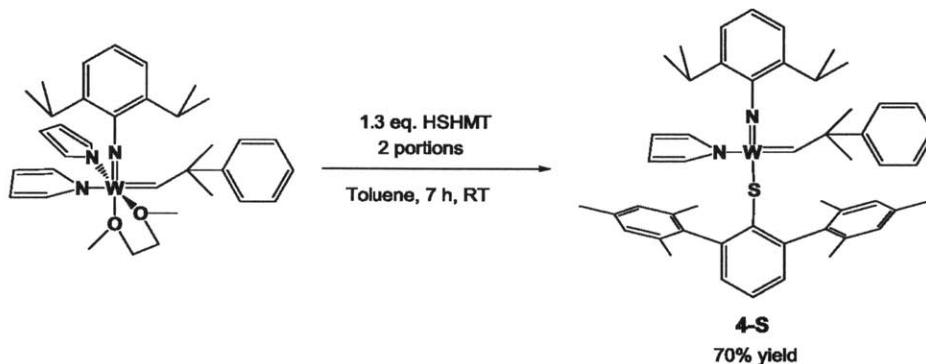
Scheme 8: Synthesis of W(NAr)(CHCMe$_2$Ph)(pyr)(SHMT) (4-S)

Addition of 1 equivalent of HSHMT to W(NAr)(CHCMe$_2$Ph)(pyr)$_2$(dme) led to 76% conversion to **4-S** after 4 h, so 0.3 additional equivalents were added and the mixture was stirred at RT for an additional 3 h. After this time, the ^{1}H NMR showed complete conversion to MTP, so the solvent was evaporated and a foam was isolated. Two recrystallizations of this material (impurities precipitated while product remained in solution) were necessary to obtain analytically

171

pure **4-S** as a yellow foam in 70% yield. This purification procedure was similar to that required to obtain pure **4-O** as detailed elsewhere.[10] The J_{CH} for the alkylidene signal in the ^{1}H NMR measured 100 Hz, which strongly indicates that the alkylidene is the *syn* isomer. A single, sharp alkylidene peak was observed in the ^{1}H NMR for each of the thiolate complexes; they appear not to undergo *syn/anti* interconversion on the NMR timescale.

II. Comparisons of olefin metathesis reactivity and selectivity

With the eight alkoxide/thiolate catalysts in hand, systematic evaluations of their activity and selectivity in olefin metathesis reactions were in order. Direct comparisons between the alkoxide/thiolate analogue pairs are especially interesting, and an overall assessment of the usefulness of thiolates as ligands is also valuable. Section II-A will focus on catalytic metathesis homocoupling of 1-octene, which is a common benchmark reaction for catalysts of this type. Section II-B details some studies on the ROMP of 2,3-dicarbomethoxynorbornadiene (DCMNBD). Finally, Section II-C contains experiments involving the ROMP of dicyclopentadiene (DCPD) that were carried out by Dr. Benjamin Autenrieth.

II-A. Homocoupling of 1-octene

The catalytic trials involving homocoupling of 1-octene to (*Z/E*)-7-tetradecene were carried out with 1 mol% catalyst in a 0.4 M solution of 1-octene in C_6D_6 at room temperature (Scheme 9).
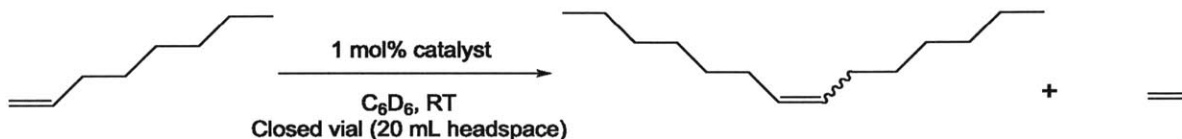
Scheme 9: Homocoupling of 1-octene with alkoxide and thiolate catalysts

The reaction vessel had ~20 mL of headspace and was opened only when aliquots were taken. The results of these homocoupling trials, including both conversion and % *Z* product, are shown in Table 1.

Catalyst	Time (h)	% Conversion	% Z product
1-O	0.25/1/6/24	56/60/67/68	19/19/18/18
1-S	0.25/1/6/24	0/2/6/22	n.d./n.d./40/44
2-O	0.25/1/6/24	0/0/13/46	n.d./n.d./21/19
2-S	0.25/1/6/24	0/0/1/3	n.d./n.d./n.d./n.d.
3-O	0.25/1/6/24	64/62/67/78	19/21/23/24
3-S	0.25/1/6/24	0/0/7/19	n.d./n.d./52/54
4-O	0.25/1/6/24	34/52/66/72	86/75/46/43
4-S	0.25/1/6/24	0/1/4/14	n.d/n.d./69/62

Table 1: Homocoupling of 1-octene with alkoxide and thiolate catalysts

The most striking feature of the results is that the thiolate catalysts were noticeably slower to homocouple 1-octene than their alkoxide counterparts in each case. It may be that the higher sigma donor ability of the thiolates is rendering the metal less likely to bind an olefin substrate, either due to the specific factors discussed in Scheme 1 or to a decrease in electrophilicity at the metal. Another interesting observation is that the alkoxide catalysts furnished product mixtures with approximately thermodynamic ratios of $Z:E$ internal olefins (~1:4), while the thiolate catalysts were able to maintain a moderate level of Z selectivity (40%-60% Z after 24 h). Prior studies have shown that some MAP catalysts show decent initial kinetic Z selectivity in homocoupling, but the selectivity will erode over time due to secondary metathesis isomerization.[10a,17] It is postulated that the alkoxide catalysts in Table 1 operate under a similar regime; their relatively high reactivity allows them to metathesize internal double bonds and enforce thermodynamic control in the system. The thiolate catalysts, on the other hand, appear to be less reactive overall, which may mean that they are slower to attack internal double bonds and that the initial kinetic Z selectivity is conserved to some degree.

II-B. ROMP of 2,3-dicarbomethoxynorbornadiene (DCMNBD)

ROMP processes are particularly useful probes of metathesis activity because no ethylene is generated and the product polymer is resistant to secondary metathesis. The catalytic trials involving the ROMP of DCMNBD were carried out with 2 mol% catalyst in a 0.12 M solution of DCMNBD in $CDCl_3$ at room temperature (Scheme 10).
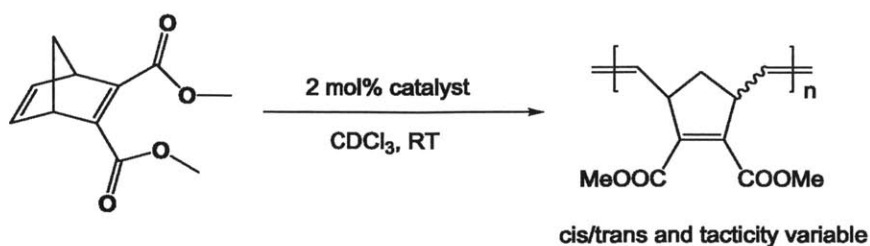
Scheme 10: ROMP of DCMNBD with alkoxide and thiolate catalysts

The results of the polymerization trials, including conversion, *cis/trans* content, and tacticity data, are shown in Table 2.

Catalyst	Time (h)	% Conversion	Polymer Composition
1-O	0.25/1/24	0/7/75	43% *cis*, syndio 7% *cis*, iso 50% *trans*, syndio
1-S	0.25/1/24	0/0/27	45% *cis*, syndio 11% *cis*, iso 44% *trans*, syndio
2-O	0.25/1/24	0/2/97	27% *cis*, syndio 20% *cis*, iso 53% *trans*, syndio
2-S	0.25/1/24	0/0/25	45% *cis*, syndio 10% *cis*, iso 45% *trans*, syndio
3-O	0.25/1/24	100/100/100	100% *cis*, syndio
3-S	0.25/1/24	2/20/97	64% *cis*, syndio 4% *cis*, iso 32% *trans*, syndio
4-O	0.25/1/24	100/100/100	100% *cis*, syndio
4-S	0.25/1/24	0/3/66	69% *cis*, syndio 4% *cis*, iso 27% *trans*, syndio

Table 2: ROMP of DCMNBD with alkoxide and thiolate catalysts

The thiolate catalysts in Table 2 show slower rates of conversion than their respective alkoxide counterparts. This trend matches the observations from the homocoupling experiments in Table 1, strengthening the argument that the increased electron donation from thiolates serves to decrease the overall reactivity of the complexes.

174

Catalyst **3-O** has been previously shown (and confirmed in Table 2) to rapidly polymerize DCMNBD to pure *cis*, syndiotactic polymer.[9] The *cis* selectivity of MAPs such as **3-O** arise from the steric mismatch between the large aryloxide and the smaller imido group, while the syndioselectivity is a result of the propensity for metallacycles to both form and break up *trans* to the "donor" pyrrolide ligand within the complex's stereogenic-at-metal framework.[18] These ideas held true for the W MAP **4-O**, which also quickly and selectively polymerized DCMNBD. Substituting SHMT for OHMT in these complexes, however, led to drastically reduced selectivity: **3-S** and **4-S** produced polymer that was still primarily syndiotactic (~95%) but only 60-70% *cis*. It is postulated that the longer measure of the Mo-S bond and the bent conformation about S in the thiolate complexes forces the bulk of the HMT group out and away from the reaction site, resulting in less steric regulation of incoming monomer orientation than is achievable with the alkoxide catalysts. The slight loss of syndioselectivity could result from the thiolate competing with the pyrrolide for the "donor" ligand role in the propagation mechanism,[4] leading to an observable concentration of isotactic dyads in the polymer chain. The selectivity comparison of **1-O** and **2-O** with **1-S** and **2-S** is less clear, as all four of these catalysts produced ~1:1 *cis:trans* polymer with high but not exceptional syndioselectivity.

II-C. ROMP of Dicyclopentadiene (DCPD)

A further opportunity to collect data and observe trends on the catalytic characteristics of the alkoxide and thiolate catalysts arose through a collaboration with Dr. Benjamin Autenrieth. Dr. Autenrieth, when provided with samples of each of the eight catalysts in question, carried out trials involving the ROMP of DCPD with 1 mol% catalyst in a 0.2 M solution of DCPD in CH_2Cl_2 (Scheme 11).

cis/trans and tacticity variable
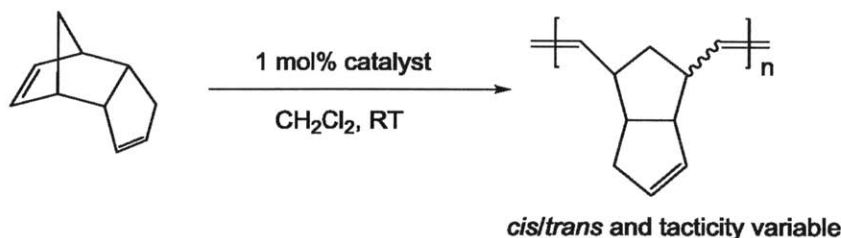
Scheme 11: ROMP of DCPD with alkoxide and thiolate catalysts

The results of the polymerization trials, including reactivity, *cis* selectivity, and tacticity data, are shown in Table 3.

Catalyst	Time*	% Conversion	% cis	Tacticity
1-O	< 2 min	100	50	atactic
1-S	15 min	< 30	n.d.**	n.d.**
2-O	3 min	70	n.d.**	n.d.**
2-S	15 min	< 30	n.d.**	n.d.**
3-O	< 2 min	100	80	90% syndio
3-S	20 min	100	45	atactic
4-O	5 min	100	100	100% syndio
4-S	30 min	100	50	atactic

Table 3: ROMP of DCPD with alkoxide and thiolate catalysts Reactions performed by Dr. Benjamin Autenrieth. *time elapsed until reaction stopped **polymer precipitated from solution and was unable to be analyzed.

As with the DCMNBD polymerizations, the fastest and most selective results for ROMP of DCPD were obtained with the OHMT MAP catalysts **3-O** and **4-O**. The principles behind the success of these catalysts are likely similar to those discussed previously, as DCPD is structurally related to DCMNBD. The thiolate analogues **3-S** and **4-S** also were able to achieve full conversion of DCPD, but the polymerization rate was substantially slower and the resulting polymer was atactic. The characteristics of thiolate complexes in the previous reactions match with those observed here.

The bisalkoxide complex **2-O** effected 70% conversion to polymer within 3 minutes, but the product was insoluble and unable to be analyzed. A similar result, but with a slower reaction rate, was found for the bisthiolate **2-S** and the MTP **1-S**. The reasons for the formation of intractable polymer are unknown. One explanation could be that the remaining cyclopentene rings present on the polymer product are being opened and crosslinked to other chains. Alternatively, initiation could be very slow, leading to the formation of a small number of polymer chains with very high molecular weight. This second possibility is more plausible given the relative unreactivity of thiolate complexes observed thus far.

CONCLUSIONS

Mo and W imido alkylidene complexes bearing thiolate ligands are stable and active catalysts for olefin metathesis. Four such complexes, including monothiolate pyrrolides (MTPs) **1-S**, **3-S**, and **4-S** along with the bisthiolate **2-S** have been synthesized and characterized here. The synthesis of the thiolate complexes followed published routes to alkoxide complexes. When compared to alcohols, thiols appear to be more prone to oversubstitution of metal bispyrrolides and thus can form bisthiolates rather than MTPs under some circumstances. X-ray

crystallographic studies reveal that the metal-thiolate bonds are longer and adopt much more bent confirmations than the analogous metal-alkoxide bonds in MAPs.

The metathesis reactivity of the thiolate complexes (**1-S**, **2-S**, **3-S**, and **4-S**) can be compared with that of the alkoxide analogues (**1-O**, **2-O**, **3-O**, and **4-O**). In 1-octene homocoupling reactions, the thiolate catalysts are substantially slower than the alkoxide catalysts. The thiolate catalysts manage to achieve higher Z-selectivity for homocoupling, perhaps due to a decreased likelihood of engaging in secondary metathesis isomerization of internal olefin products. The reactivity trend is mirrored in the results from ROMP reactions of DCMNBD and DCPD: thiolate-bearing catalysts are almost universally slower than alkoxide complexes. Furthermore, the stereoselectivity and tacticity control of the thiolates is proven to be markedly poorer than for alkoxides.

The principles of ligand effects on metathesis activity[4] outlined in the introduction hold true: substitution of a stronger donor ligand (thiolate) into the "acceptor" role previously occupied by an alkoxide resulted in a noticeable decrease in reaction rate across the board. Even in the case of W MAP complexes, where breakup of the metallacycle is known to be relatively slow,[5] the additional sigma donation presumably provided by the thiolate ligand does not increase overall activity. The steric differences between alkoxides and thiolates also have some effect on the catalytic results. The MTP complexes are unable to maintain the high selectivity of MAPs in ROMP, likely due to the fact that the longer bond length and bent bond conformation of thiolates decreases the ligand's steric control at the active site.

The systematic comparisons above have served to strengthen the steric and electronic model of ligand effects on metathesis capability in high-oxidation-state Mo and W imido alkylidenes. Although none of the newly synthesized thiolate-based catalysts offered meaningful improvement over existing catalysts, knowledge of their synthesis and characteristics is nevertheless important if we are to fully understand the system and make reasonable predictions regarding the consequences of future modifications.

EXPERIMENTAL

General Comments

All manipulations of air- and moisture-sensitive materials were performed in oven-dried (175 °C) or flame-dried glassware on a dual-manifold Schlenk line or a Vacuum Atmospheres

glovebox with nitrogen atmosphere. NMR measurements of air- and moisture-sensitive materials were carried out in Teflon-valve-sealed J. Young-type NMR tubes. Anhydrous ether, pentane, toluene, THF, benzene, and CH_2Cl_2 were sparged with nitrogen and passed through activated alumina prior to use. Chloroform-d and C_6D_6 were stored over molecular sieves. The following chemicals were purchased from Aldrich and used as received: sulfur, $LiAlH_4$, n-butyllithium, (E)-1,3-diphenyl-2-propenone, 1,3-diphenyl-2-propanone, NaOMe in MeOH, bromine, acetic acid, sodium hydride, N,N-dimethylthiocarbamoyl chloride, N,N-dimethylacetamide, benzaldehyde, and sulfuric acid. 1-octene was purchased from Aldrich, dried over calcium hydride, degassed by three freeze-pump-thaw cycles, and filtered in the glovebox before use. Dicyclopentadiene (DCPD, 95% endo) was purchased from Aldrich, distilled, and degassed before use by Dr. Benjamin Autenrieth. The following substances were prepared according to literature procedures: **1-O** $(Mo(NAr)(CHCMe_2Ph)(Me_2pyr)(OTPP))$,[8] **3-O** $(Mo(NAr)(CHCMe_2Ph)(pyr)(OHMT)$,[9] **4-O** $W(NAr)(CHCMe_2Ph)(pyr)(OHMT)$,[10] HOHMT,[11] HSHMT,[12] $Mo(NAr)(CHCMe_2Ph)(OTf_2)(dme)$,[19] $Mo(NAr)(CHCMe_2Ph)(Me_2pyr)_2$,[20] $Mo(NAr)(CHCMe_2Ph)(pyr)_2$,[21] $W(NAr)(CHCMe_2Ph)(pyr)_2(dme)$,[22] and 2,3-dicarbomethoxynorbornadiene (DCMNBD)[23] Li(OTPP) was isolated as Li(OTPP) · 1.25 THF by addition of n-BuLi to a solution of HOTPP in THF at RT, followed by concentration, addition of pentane, and filtration (washing with pentane). NMR spectra were obtained on Varian spectrometers operating at either 300 MHz or 500 MHz. NMR chemical shifts are reported as ppm relative to tetramethylsilane, and are referenced to the residual proton or ^{13}C signal of the solvent (^1H CDCl$_3$: 7.27 ppm, ^1H C$_6$D$_6$: 7.16 ppm, ^{13}C CDCl$_3$: 77.16 ppm, ^{13}C C$_6$D$_6$, 128.06 ppm).

Experimental details for synthesis of ligands

2,3,5,6-tetraphenyl-2-cyclohexenone

This procedure was based on a literature report.[13] A 500-mL round-bottom flask was charged with a stir bar, 25.98 g 1,3-diphenyl-2-propanone (123.5 mmol, 1.0 equiv.), 25.62 g (E)-1,3-diphenyl-2-propenone (123.5 mmol, 1.0 equiv.), and 75 mL 25 wt.% NaOMe in MeOH. This yellow solution was refluxed for 16 h, over which time the solution became a suspension of white sludge. The mixture was allowed to cool in an ice bath and filtered to obtain crude white solid, which contained some impurity by ^1H NMR. This solid was recrystallized from hot

benzene/petroleum ether to give white crystals. Filtration and washing with petroleum ether yielded 38.49 g product (78% yield). ^{1}H NMR (CDCl$_3$, 20°C, 500 MHz): δ [ppm] 7.12-6.91 (20H, aryl), 4.01 (d, 1H, CH next to carbonyl, J$_{HH}$ = 11 Hz), 3.77 (m, 1H, CH farther from carbonyl), 3.11 (m, 2H, CH$_2$ *para* to carbonyl). ^{13}C{^{1}H} NMR (CDCl$_3$, 20°C) δ [ppm]: 197.99, 155.63, 142.26, 140.39, 138.42, 137.77, 135.53, 131.25, 129.34, 128.58, 128.45, 128.23, 128.18, 128.10, 127.70, 127.64, 126.99, 126.85, 126.69, 59.44, 47.32, 40.82. HRMS Calcd [M + H]$^+$: 401.18, Found [M + H]$^+$: 401.1898.

4-bromo-2,3,5,6-tetraphenylphenol (HOTPPBr)

This procedure was based on a literature report.[13] A 1-L round-bottom flask was charged with 42.1 g 2,3,5,6-tetraphenyl-2-cyclohexenone (105.1 mmol, 1.0 equiv.), a stir bar, and 500 mL glacial acetic acid. While stirring, 16.0 mL bromine (310.7 mmol, 2.95 equiv) was added by syringe. The resulting solution was heated to 75 °C for 15 h, after which time the color was light orange. The mixture was allowed to cool to room temperature and 500 mL water was added. Filtration gave a light yellow crude solid. This solid was washed on the frit with MeOH and then diethyl ether to give 44.14 g pure white product (88% yield). ^{1}H NMR (CDCl$_3$, 20°C, 500 MHz): 7.24-6.79 (20H, aryls), 5.00 (s, 1H, O*H*). ^{13}C{^{1}H} NMR (CDCl$_3$, 20°C) δ [ppm]: 149.49, 142.61, 140.95, 135.65, 130.75, 130.40, 129.15, 128.37, 127.57, 126.99, 116.56. HRMS Calcd [M + H]$^+$: 479.08, Found [M + H]$^+$: 479.0839.

2,3,5,6-tetraphenylphenol (HOTPP)

An oven-dried 1-L Schlenk flask with stir bar was cooled under nitrogen and charged with 20.0 g 4-bromo-2,3,5,6-tetraphenylphenol (HOTPPBr, 41.9 mmol, 1.0 equiv.) along with 600 mL anhydrous THF. This mixture was chilled in a dry ice/acetone bath (-78 °C). Next, 50.3 mL *n*-butyllithium solution (2.5 M in hexanes, 125.6 mmol, 3.0 equiv.) was slowly injected into the flask via syringe while stirring in the cooling bath. The mixture was allowed to stir and warm to room temperature over 2 days, after which time the reaction was quenched with 30 mL methanol. The solution was dried *in vacuo* to yield a crude solid. This solid was dissolved in 300 mL CH$_2$Cl$_2$ and washed with 300 mL water. The aqueous layer was extracted with 2 x 150 mL CH$_2$Cl$_2$. The combined organic layer was washed with 2 x 300 mL water and 2 x 200 mL brine. The organic layer was dried over MgSO$_4$, filtered, and dried *in vacuo* to yield a crude solid material. This solid was washed with diethyl ether on a frit to give 13.75 g pure white product

(82% yield). ^{1}H NMR (C$_6$D$_6$, 20°C, 500 MHz): δ [ppm] 7.32 (s, 1H, central aryl H), 7.23 (m, 8H, aryl), 7.04-6.91 (12H, aryl), 5.23 (s, 1H, OH). ^{13}C{^{1}H} NMR (CDCl$_3$, 20°C) δ [ppm]: 150.36, 141.62, 141.06, 135.90, 131.24, 129.89, 128.61, 127.84, 127.40, 126.65, 126.23, 124.26. HRMS Calcd [M + H]$^+$: 399.17, Found [M + H]$^+$: 399.1733.

O-(2,3,5,6-tetraphenyl)phenyl-*N,N*-dimethylthiocarbamate (Me$_2$NC(S)OTPP)

This procedure was discovered with the assistance of a literature report of a related compound.[15] Into an oven-dried 250-mL Schlenk flask were placed a stir bar and 5.0 g HOTPP (12.55 mmol, 1.0 equiv.). To this flask was added 150 mL anhydrous THF under N$_2$. A separate flask was charged with 2.02 g *N,N*-dimethylthiocarbamoyl chloride (16.31 mmol, 1.3 equiv.) and 10 mL anhydrous THF. The large flask was cooled in an ice bath (0 °C) and to it was added 600 mg NaH (60% mineral oil dispersion, 15.06 mmol, 1.3 equiv) in four portions under N$_2$ flow. The resulting mixture was stirred for 30 min in the ice bath, after which time the *N,N*-dimethylthiocarbamoyl chloride solution was injected in dropwise via syringe. This mixture was allowed to stir at RT overnight under N$_2$. After this time, a sample showed the reaction to be ~65% complete. An additional 407 mg NaH (60% mineral oil dispersion, 10.2 mmol, 0.81 equiv) was added in portions, followed by 1.45 g more *N,N*-dimethylthiocarbamoyl chloride (11.70 mmol, 0.93 equiv.) in the same manner as before. After stirring for 18 h at room temperature, TLC analysis still showed incomplete conversion. Still more NaH dispersion (156 mg) and *N,N*-dimethylthiocarbamoyl chloride (621 mg) were added and the solution was heated to 45 °C for 2 h, after which time a ^{1}H NMR aliquot showed ~75% conversion to product. Water was added to the flask, and the mixture was transferred to a larger flask. The THF was removed by rotary evaporation and a solid precipitated. This solid was washed on a frit with water and dried, and a silica column was run using gradient elution ranging from 3:1 hexanes:CH$_2$Cl$_2$ to 1:3 hexanes:CH$_2$Cl$_2$. The first substance to elute was HOTPP, followed by pure product (2.74 g, 46% yield.) ^{1}H NMR (C$_6$D$_6$, 20°C, 500 MHz) δ [ppm]: 7.62 (s, 1H, *para*-H), 7.85-7.20 (br, 4H, aryl), 7.24 (m, 4H, aryl), 7.07-6.89 (overlapping m, 12H, aryl), 2.52 (s, 3H, N*Me*$_2$), 2.26 (s, 3H, N*Me*$_2$). ^{13}C{^{1}H} NMR (C$_6$D$_6$, 20°C) δ [ppm]: 186.87, 150.26, 142.57, 141.27, 137.18, 134.59, 130.35, 128.11, 127.07, 126.89, 42.40, 37.48. HRMS Calcd [M + H]$^+$: 486.1886, Found [M + H]$^+$: 486.1885.

S-(2,3,5,6-tetraphenyl)phenyl-*N*,*N*-dimethylthiocarbamate (Me₂NC(O)STPP)

This procedure was discovered with the assistance of a literature report of a related compound.[16] 500 mg of Me₂NC(S)OTPP (1.03 mmol) was placed into a 10-mL microwave pressure tube with 5 mL anhydrous *N*,*N*-dimethylacetamide. The tube was set up in a microwave reactor and heated for 30 minutes at 275 °C (300 W power, 2 min ramp time, 200 PSI pressure, 20 min cooling time). This procedure was repeated for four more similarly prepared tubes for a total of 2.5 g material. The resulting mixtures were combined on a frit and washed with lots of water. The solid was dissolved in dichloromethane, dried over MgSO₄, filtered, and dried *in vacuo* to obtain 2.32 g pure product (93% yield). ^{1}H NMR (C₆D₆, 20°C, 500 MHz) δ [ppm]: 7.69 (s, 1H, *para*-H), 7.46 (br, 4H, aryl), 7.20 (m, 4H, aryl), 7.07-6.89 (overlapping m, 12H, aryl), 2.29 (br s, 3H, N*Me₂*), 2.04 (br s, 3H, N*Me₂*). ^{13}C{^{1}H} NMR (C₆D₆, 20°C) δ [ppm]:166.67, 146.76, 142.45, 141.95, 141.33, 134.02, 131.32, 130.25, 127.96, 127.45, 126.84, 126.73, 36.39 (one methyl signal because of interconversion). HRMS Calcd [M + H]⁺: 486.1886, Found [M + H]⁺: 486.1896. Thanks to Gregory Gutierrez for help with the microwave reaction.

2,3,5,6-tetraphenylthiophenol (HSTPP)

This procedure was discovered with the assistance of a literature report of a related compound.[15] In the glovebox, a 100-mL bomb was charged with a stir bar, 782 mg LiAlH₄ (20.6 mmol, 5.0 equiv.) and 15 mL THF. To the bomb was added 2.0 g Me₂NC(O)STPP (4.12 mmol, 1.0 equiv.) and 55 mL THF. The bomb was sealed, brought out of the glovebox, and stirred in an oil bath at 60 °C for 13 h. After this time, the bomb was allowed to cool to room temperature and water was added slowly to quench excess LiAlH₄. The resulting mixture was poured into a slurry of ice, water, and H₂SO₄. The slurry was stirred until the ice melted, and then filtered through a frit. The solid was washed with lots of water and dissolved in dichloromethane. This solution was dried over MgSO₄, filtered, and the resulting solid was recrystallized from hot toluene and hexanes to afford 1.13 g pure product (66% yield). ^{1}H NMR (C₆D₆, 20°C, 500 MHz) δ [ppm]: 7.43 (s, 1H, *para*-H), 7.24 (m, 4H, aryl), 7.19 (m, 4H, aryl), 7.00 (m, 8H, aryl), 6.92 (m, 4H, aryl), 3.62 (s, 1H, S*H*). ^{13}C{^{1}H} NMR (C₆D₆, 20°C) δ [ppm]: 142.02, 141.92, 140.56, 138.27, 135.11, 131.14, 130.06, 129.08, 128.73, 128.00, 127.61, 126.79. HRMS Calcd [M + NH₄]⁺: 432.18, Found [M + H]⁺: 432.1789.

181

Experimental details for preparation of metal complexes

Mo(NAr)(CHCMe₂Ph)(OTPP)₂ (2-O)

In the glovebox, a 100-mL round-bottom flask was charged with a stir bar, 10 mL toluene, 250 mg Mo(NAr)(CHCMe₂Ph)(OTf)₂(dme) (mixture with 12% $ArNH_3^+(OTf)^-$, 0.30 mmol, 1.0 equiv.), and 317 mg Li(OTPP) · 1.25 THF (0.641 mmol, 2.14 equiv.). The flask was capped and stirred at RT for 23 h, after which time the mixture was filtered through Celite and the solvent was removed from the filtrate. Pentane was added and subsequently removed *in vacuo*. Another pentane addition and filtration led to the isolation of pure product as an orange solid (281 mg, 78% yield). ¹H NMR (C₆D₆, 20°C, 500 MHz) δ [ppm]: 11.48 (s, 1H, C*H*CMe₂Ph), 7.34-7.08 (aryl, 17H), 7.03-6.86 (aryl, 33H), 2.90 (sept, 2H, *i*-Pr methines) J_{HH} = 7 Hz), 1.33 (s, 6H, CHC*Me*₂Ph), 0.91 (d, 12H, *i*-Pr methyls, J_{HH} = 7 Hz). ¹³C{¹H} NMR (C₆D₆, 20°C) δ [ppm]: 284.07, 162.44, 154.27, 150.31, 147.06, 142.83, 142.25, 137.71, 132.74, 131.55, 130.38, 130.22, 130.12, 128.51, 127.07, 126.62, 126.43, 126.05, 126.01, 123.56, 55.16, 31.71, 28.48, 24.62. Anal. Calcd for C₈₂H₇₁MoNO₂: C, 82.18; H, 5.97; N, 1.17. Found: C, 81.84; H, 6.30; N, 1.10.

Mo(NAr)(CHCMe₂Ph)(Me₂pyr)(STPP) (1-S)

In the glovebox, a 50-mL round-bottom flask was charged with a stir bar, 275 mg Mo(NAr)(CHCMe₂Ph)(Me₂pyr)₂ (0.465 mmol, 1.0 equiv), 20 mL acetonitrile, and 5 mL benzene. This mixture was stirred at RT and to it was added 183 mg HSTPP (0.442 mmol, 0.95 equiv.) in four portions (one every 75 minutes). After the additions, the flask was capped and the mixture stirred for 18 h at RT. The resulting mixture was filtered to give 256 mg of an orange solid, which was washed with acetonitrile. A ¹H NMR spectrum of this solid showed it to be 86% product and 14% 2-S. The solid was triturated with diethyl ether and filtered (¹H NMR showed 95% pure product)), and then recrystallized from benzene and pentane. Three crops were obtained for a total of 88 mg pure product (20% yield). ¹H NMR (C₆D₆, 20°C, 500 MHz) δ [ppm]: 11.82 (s, 1H, C*H*CMe₂Ph), 7.52 (s, 1H, *para*-H on STPP). 7.39 (m, 2H, aryl), 7.30-6.85 (15H, aryl), 6.81 (m, 2H, aryl), 5.71 (s, 2H, Me₂pyr aryls), 3.25 (br d, 2H, *i*-Pr methines), 2.04 (br s, 6H, Me₂pyr methyls), 1.51 (s, 6H, CHC*Me*₂Ph), 1.20-0.65 (br d and sharp d, 12H *i*-Pr methyls). ¹³C{¹H} NMR (C₆D₆, 20°C) δ [ppm]: 290.64, 153.60, 148.47, 145.67, 142.98, 142.61,

142.22, 140.42, 137.89, 132.31, 132.11, 131.94, 130.04, 129.33, 128.78, 128.57, 128.03, 127.81, 127.78, 127.13, 126.64, 126.60, 125.76, 125.70, 123.03, 108.76, 55.05, 32.40, 30.21, 28.52, 26-21 (broad signals). Anal. Calcd for $C_{58}H_{58}MoN_2S$: C, 76.43; H, 6.74; N, 3.02. Found: C, 76.83; H, 6.37; N, 3.05.

Mo(NAr)(CHCMe$_2$Ph)(STPP)$_2$ (2-S)

In the glovebox, a 50-mL round-bottom flask was charged with 275 mg Mo(NAr)(CHCMe$_2$Ph)(Me$_2$pyr)$_2$ (0.465 mmol, 1 equiv.), 193 mg HSTPP (0.465 mmol, 1.0 equiv.), 15 mL diethyl ether, and a stir bar. This flask was capped and the mixture stirred at RT for 20 h. The solvent was removed *in vacuo* (^{1}H NMR showed mixture of starting material, 1-S, and product). Toluene (10 mL) was added to the residue, along with another equivalent of HSTPP (193 mg). This mixture was capped and stirred at RT for 18 h, after which time the solvent was removed and the residue triturated with ether. Filtration gave 370 mg pure orange solid product (65% yield). Note: Addition of two equivalents of HSTPP at the beginning of the reaction, rather than the portionwise addition described here, is a logical alternative. ^{1}H NMR (C$_6$D$_6$, 20°C, 500 MHz) δ [ppm]: 12.72 (s, 1H, CHCMe$_2$Ph), 7.35-6.90 (50H, aryl, many overlapping signals), 3.48 (sept, 2H, *i*-Pr methines, J$_{HH}$ = 7 Hz), 1.25 (br s, 6H, CHCMe_2Ph), 0.96 (d, 12 H, *i*-Pr methyls, J$_{HH}$ = 7 Hz). ^{13}C{^{1}H} NMR (C$_6$D$_6$, 20°C) δ [ppm]: 153.78, 149.23, 146.51, 142.77, 141.91 (br), 133.05, 131.15, 130.66, 130.06, 129.84, 128.72, 128.50, 126.38, 126.29, 125.96, 123.26, 56.64, 29.71 (br), 27.91, 23.88. Anal. Calcd for $C_{82}H_{71}MoNS_2$: C, 80.04; H, 5.82; N, 1.14. Found: C, 79.74; H, 5.77; N, 0.98.

Mo(NAr)(CHCMe$_2$Ph)(pyr)(SHMT) (3-S)

In the glovebox, a 50-mL round bottom flask was charged with 330 mg Mo(NAr)(CHCMe$_2$Ph)(pyr)$_2$ (0.616 mmol, 1.0 equiv), 214 mg HSHMT (0.616 mmol, 1.0 equiv), a stir bar, and 15 mL toluene. This mixture was capped and allowed to stir at RT for 15 h, after which time the solvent was removed *in vacuo* and pentane was added to the residue. Removal of solvent from this solution resulted in 329 mg of pure foam product (65% yield) Recrystallization for elemental analysis was carried out using pentane. ^{1}H NMR (C$_6$D$_6$, 20°C, 500 MHz) δ [ppm]: 11.06 (s, 1H, CHCMe$_2$Ph, ^{1}J$_{CH}$ = 110 Hz), 7.28 (m, 2H, aryl), 7.13 (m, 2H, aryl), 7.05-6.95 (m, 2H, aryl), 6.91-6.87 (overlapping, 5H, aryl), 6.79 (s, 2H, HMT aryls), 6.72 (s, 2H, HMT aryls), 6.50 (m, 2H, pyr aryls), 6.26 (m, 2H, pyr aryls), 3.25 (sept, 2H, *i*-Pr

183

methines, J_{HH} = 7 Hz), 2.22 (s, 6H, HMT methyls), 2.21 (s, 6H, HMT methyls), 2.10 (s, 6H, HMT methyls), 1.51 (s, 3H, CHCMe_2Ph), 1.47 (s, 3H, CHCMe_2Ph), 1.02 (d, 6H, i-Pr methyls, J_{HH} = 7 Hz), 0.98 (d, 6H, i-Pr methyls, J_{HH} = 7 Hz). ^{13}C{^{1}H} NMR (C$_6$D$_6$, 20°C) δ [ppm]: 281.35, 153.88, 147.96, 147.80, 144.44, 139.61, 139.31, 137.30, 136.25, 135.97, 130.71, 129.95, 129.86, 129.43, 129.34, 129.13, 128.93, 128.67, 128.60, 127.19, 126.69, 126.24, 123.08, 109.56, 55.73, 31.16, 30.49, 28.53, 24.16, 23.34, 21.59, 21.52, 20.94. Anal. Calcd for C$_{50}$H$_{58}$MoN$_2$S: C, 73.68; H, 7.17; N, 3.31. Found: C, 73.38; H, 7.20; N, 3.44.

W(NAr)(CHCMe₂Ph)(pyr)(SHMT) (4-S)

In the glovebox, a 50-mL round-bottom flask was charged with 250 mg W(NAr)(CHCMe₂Ph)(pyr)₂(dme) (0.350 mmol, 1.0 equiv), 122 mg HSHMT (0.350 mmol, 1.0 equiv), a stir bar, and 15 mL toluene. This mixture was stirred at RT for 4 h, after which time the solvent was removed under vacuum to yield a foam. The ^{1}H NMR spectrum of the foam showed 76% conversion to product, so an additional 35 mg HSHMT (0.100 mmol, 0.29 equiv) was added along with 12 mL toluene. This mixture was stirred for 3 h at RT, after which time the solvent was removed. The resulting residue was combined with pentane, pumped to a foam, and combined with diethyl ether for recrystallization. The solid that resulted from this recrystallization contained no alkylidene, so it was discarded. An attempted recrystallization from pentane also resulted in precipitation of an unwanted product, which was filtered off. The filtrate was dried *in vacuo* to a yellow foam that was analytically pure product (220 mg, 70% yield). This unusual workup procedure is similar to that found in the previously reported synthesis of 4-O.[10] ^{1}H NMR (C$_6$D$_6$, 20°C, 500 MHz) δ [ppm]: 8.40 (s, 1H, CHCMe₂Ph, $^2J_{WH}$ = 15 Hz, $^1J_{CH}$ = 100 Hz), 7.35 (m, 2H, aryl), 7.16 (m, 2H, aryl), 7.05-6.98 (m, 2H, aryl), 6.97-6.82 (overlapping, 5H, aryl), 6.78 (s, 2H, HMT aryls), 6.69 (s, 2H, HMT aryls), 6.44 (m, 2H, pyr aryls), 6.22 (m, 2H, pyr aryls), 3.20 (sept, 2H, i-Pr methines, J_{HH} = 7 Hz), 2.21 (s, 6H, HMT methyls), 2.19 (s, 6H, HMT methyls), 2.10 (s, 6H, HMT methyls), 1.52 (s, 3H, CHCMe_2Ph), 1.47 (s, 3H, CHCMe_2Ph), 1.05 (d, 6H, i-Pr methyls, J_{HH} = 7 Hz), 0.99 (d, 6H, i-Pr methyls, J_{HH} = 7 Hz). ^{13}C{^{1}H} NMR (C$_6$D$_6$, 20°C) δ [ppm]: 260.65, 152.03, 149.92, 146.25, 145.09, 139.12, 138.77, 137.47, 136.14, 136.05, 131.50, 130.17, 129.35, 128.98, 128.48, 127.69, 127.42, 126.42, 126.28, 122.69, 110.51, 54.16, 32.39, 32.00, 28.31, 24.14, 23.24, 21.67, 21.52, 20.97, 20.54. Anal. Calcd for C$_{50}$H$_{58}$WN$_2$S: C, 66.51; H, 6.47; N, 3.10. Found: C, 66.44; H, 6.53; N, 3.07.

Experimental details for catalytic olefin metathesis trials

General procedure for 1-octene homocoupling experiments

In the glovebox, a 4-mL vial was charged with ~5 mg 4,4'-di-t-butylbiphenyl (as internal standard), 0.5 mL C_6D_6, 63 µL 1-octene (0.400 mmol, 100 equiv), and a stir bar. A separate 2-mL vial was charged with 0.004 mmol catalyst (3-5 mg, 1.0 equiv.) and 0.45 mL C_6D_6. The contents of the small vial were added to the 4-mL vial. The 4-mL vial was then placed into a 20-mL vial on a stir plate. The 20-mL vial was capped and the reaction allowed to stir at RT. The 20-mL vial was opened only when aliquots were taken. Aliquots (~100 µL) were taken at the designated time points and immediately quenched with benzaldehyde (~2.5 µL). ^1H NMR samples of these aliquots were made by dilution with 2 mL $CDCl_3$. Conversion and % Z were determined by ^1H NMR in a method similar to that found in a previous report.[17] Note: the evaporation of 1-octene from the system was shown to be negligible for our purposes (< 5%) over a period of 24 h, so conversion could reasonably be obtained by monitoring disappearance of starting material.

General procedure for ROMP of DCMNBD

In the glovebox, a 4-mL vial was charged with a stir bar, 52 mg DCMNBD (0.25 mmol, 50.0 equiv.), and 1 mL $CDCl_3$. A second vial was charged with 0.005 mmol catalyst (3-6 mg, 1.0 equiv.) and 1 mL $CDCl_3$. The contents of the second vial were added to the first, the first vial was sealed, and the contents allowed to stir at RT. Aliquots (~200 µL) were taken at the designated time points and immediately quenched with benzaldehyde (~2.5 µL). Conversion and polymer composition were determined by ^1H NMR spectroscopy. Cis, syndiotactic polymer,[24] cis, isotactic polymer,[25] and trans syndiotactic polymer[26] were identified according to the data found in three separate literature reports. Key resonances for cis, syndiotactic polymer: ^1H NMR: 5.33 ppm (multiplet, olefinic protons); ^{13}C NMR: 38.06 (C7 from DCMNBD). Key resonances for cis, isotactic polymer: ^1H NMR: 5.41 ppm (multiplet, olefinic protons); ^{13}C NMR: 38.80 ppm (C7 from DCMNBD). Key resonances for trans, syndiotactic polymer: ^1H NMR: 5.47 ppm (multiplet, olefinic protons); ^{13}C NMR: 37.87 ppm (C7 from DCMNBD). Thanks to Dr. William Forrest for assistance with analysis of polymer structure.

General procedure for ROMP of DCPD

These reactions were run by Dr. Benjamin Autenrieth. In the glovebox, a vial was charged with a stir bar, ~3 mg catalyst (1.0 equiv), ~45 mg DCPD (100 equiv.), and enough dichloromethane to bring the concentration of DCPD to 0.2 M. This mixture was allowed to stir at RT. Aliquots were taken periodically and quenched with benzaldehyde. After 24 h, the mixture was quenched with excess methanol to precipitate the polymer. The aliquots were monitored by ^{1}H NMR for conversion, and the isolated polymer was analyzed for tacticity and stereoregularity by ^{13}C NMR. Key resonances for cis, syndiotactic polymer: ^{13}C NMR: 45.0-44.9 (bicyclic bridgehead carbon atoms in polymer). Key resonances for cis, isotactic polymer: ^{13}C NMR: 45.4-45.3 ppm (bicyclic bridgehead carbon atoms in polymer). Trans polymer shows characteristic resonances in the range of 47.5-46.0 ppm (olefinic carbon atoms in polymer backbone). Literature reports describe the possible structures of polyDCPD in more detail.[27]

Experimental Details for Crystal Structure Acquisition and Refinement

Mo(NAr)(CHCMe₂Ph)(Me₂pyr)(STPP) (1-S)

The crystal structure acquisition and refinement were carried out by Dr. Peter Müller. X-ray-quality crystals were grown from toluene/pentane. Low-temperature diffraction data (φ-and ω-scans) were collected on a Bruker-AXS X8 Kappa c Duo diffractometer coupled to a Smart APEX2 CCD detector with Mo K_α radiation (λ = 0.71073 Å) from an IμS micro-source. Absorption and other corrections were applied using SADABS.[28] All structures were solved by direct methods using SHELXS[29] and refined against F_2 on all data by full-matrix least squares with SHELXL-97[30] using established refinement approaches.[31] The structure was refined as a non-merohedral twin. The orientations of the two unit cells were obtained using TWINABS.[32] Deconvolution of the reflections was carried out using CELL_NOW,[33] resulting in both an HKLF4 format reflection file and an HKLF5 format reflection file. Refinement was undertaken using the HKLF4 format reflection file and converted to the HKLF5 format reflection file once the positions of all non-hydrogen atoms were stable. The twin ratio was refined freely and converged at 0.4136. All non-hydrogen atoms were refined anisotropically. All hydrogen atoms (except the alkylidene proton, which was taken from the difference Fourier synthesis and refined semi-freely with the help of distance restraints) were included into the model at geometrically

calculated positions and refined using a riding model. The isotropic displacement parameters of all hydrogen atoms were fixed to 1.2 times the U value of the atoms they are linked to (1.5 times for methyl groups). $Mo(NAr)(CHCMe_2Ph)(Me_2pyr)(STPP)$ crystallized in triclinic space group P$\bar{1}$ with one molecule in the asymmetric unit.

Crystal data and structure refinement for 1-S

Identification code	x13174_t5
Empirical formula	$C_{61} H_{61}$ Mo N_2 S
Formula weight	950.11
Temperature	100(2) K
Wavelength	0.71073 Å
Crystal system	Triclinic
Space group	P$\bar{1}$
Unit cell dimensions	$\alpha = 10.842(2)$ Å $\quad \alpha = 109.152(5)°$
	$\beta = 14.437(3)$ Å $\quad \beta = 103.201(6)°$
	$\gamma = 17.924(4)$ Å $\quad \gamma = 100.459(5)°$
Volume	2477.9(9) Å^3
Z	2
Density (calculated)	1.273 Mg/m^3
Absorption coefficient	0.348 mm^{-1}
F(000)	998
Crystal size	0.200 x 0.150 x 0.110 mm^3
Theta range for data collection	1.265 to 30.507°
Index ranges	$-15 \leq h \leq 14, -20 \leq k \leq 19, 0 \leq l \leq 25$
Reflections collected	14892
Independent reflections	14892 [R(int) = ?]
Completeness to theta = 25.242°	99.5 %
Absorption correction	Semi-empirical from equivalents
Refinement method	Full-matrix least-squares on F^2
Data / restraints / parameters	14892 / 74 / 603

Goodness-of-fit on F^2	1.045
Final R indices [I>2sigma(I)]	$R_1 = 0.0342$, $wR_2 = 0.0929$
R indices (all data)	$R_1 = 0.0367$, $wR_2 = 0.0948$
Extinction coefficient	n/a
Largest diff. peak and hole	0.755 and -0.776 e.Å^{-3}

Mo(NAr)(CHCMe₂Ph)(STPP)₂ (2-S)

The crystal structure acquisition and refinement were carried out by Dr. Peter Müller. X-ray-quality crystals were grown from toluene/pentane. Low-temperature diffraction data (φ-and ω-scans) were collected on a Bruker-AXS X8 Kappa c Duo diffractometer coupled to a Smart APEX2 CCD detector with Mo $K\alpha$ radiation ($\lambda = 0.71073$ Å) from an IμS micro-source. Absorption and other corrections were applied using SADABS.[28] All structures were solved by direct methods using SHELXS[29] and refined against F_2 on all data by full-matrix least squares with SHELXL-97[30] using established refinement approaches.[31] All non-hydrogen atoms were refined anisotropically. All hydrogen atoms (except the alkylidene proton, which was taken from the difference Fourier synthesis and refined semi-freely with the help of distance restraints) were included into the model at geometrically calculated positions and refined using a riding model. The isotropic displacement parameters of all hydrogen atoms were fixed to 1.2 times the U value of the atoms they are linked to (1.5 times for methyl groups). Mo(NAr)(CHCMe₂Ph)(STPP)₂ crystallized in triclinic space group P$\bar{1}$ with one molecule in the asymmetric unit. There is a phase transition in the crystal structure somewhere between 170 K and 150 K. The 173 K structure is not as good as the 100 K structure. The 100K structure was used to create Figure 4. Both phases are triclinic (P-1). At 173 K, Z = 4; at 100 K, Z = 2.

Crystal data and structure refinement for 2-S

Identification code	x13166_100k
Empirical formula	$C_{89} H_{79} Mo N S_2$
Formula weight	1322.59
Temperature	100(2) K
Wavelength	0.71073 Å
Crystal system	Triclinic

Space group	P$\bar{1}$	
Unit cell dimensions	α = 13.0976(13) Å	α = 69.510(2)°
	β = 16.8512(17) Å	β = 89.838(2)°
	γ = 17.6393(17) Å	γ = 74.329(2)°
Volume	3493.1(6) Å^3	
Z	2	
Density (calculated)	1.257 Mg/m^3	
Absorption coefficient	0.295 mm^{-1}	
F(000)	1388	
Crystal size	0.300 x 0.160 x 0.120 mm^3	
Theta range for data collection	1.239 to 30.999°	
Index ranges	$-18 \leq h \leq 18$, $-24 \leq k \leq 24$, $-24 \leq l \leq 25$	
Reflections collected	164747	
Independent reflections	22239 [R(int) = 0.0370]	
Completeness to theta = 25.242°	100.0 %	
Absorption correction	Semi-empirical from equivalents	
Refinement method	Full-matrix least-squares on F^2	
Data / restraints / parameters	22239 / 1 / 848	
Goodness-of-fit on F^2	1.042	
Final R indices [I>2sigma(I)]	R$_1$ = 0.0300, wR$_2$ = 0.0723	
R indices (all data)	R$_1$ = 0.0354, wR$_2$ = 0.0753	
Extinction coefficient	n/a	
Largest diff. peak and hole	0.608 and -0.410 e.Å^{-3}	

REFERENCES

[1] (a) Schrock, R. R. *Chem. Rev.* **2002**, *102*, 145. (b) Schrock, R. R. *Chem. Rev.* **2009**, *109*, 3211.

[2] Murdzek, J. S.; Schrock, R. R. *Organometallics* **1987**, *6*, 1373.

[3] Schrock, R. R.; DePue, R.; Feldman, J.; Schaverian, C. J.; Dewan, J. C.; Liu, A. H. *J. Am. Chem. Soc.* **1988**, *110*, 1423.

[4] Poater, A.; Solans-Monfort, X.; Clot, E.; Copéret, C.; Eisenstein, O. *J. Am. Chem. Soc.* **2007**, *129*, 8207.

[5] Schrock. R. R.; Jiang. A. J.; Marinescu, S. C.; Simpson, J. H.; Müller, P. *Organometallics* **2010**, *29*, 5241.

[6] Chisholm, M. H.; Davidson, E. R.; Huffman, J. C.; Quinlan, K. B. *J. Am. Chem. Soc.* **2001**, *123*, 9652.

[7] Marinescu, S. C. Molybdenum and Tungsen Alkylidene Species for Catalytic Enantio-, Z-, and E-Selective Olefin Metathesis Reactions. Ph.D. Thesis, Massachusetts Institute of Technology, Cambridge, MA, May 2011.

[8] Lee, Y.-J.; Schrock, R. R.; Hoveyda, A. H. *J. Am. Chem. Soc.* **2009**, *131*, 10652.

[9] Lichtscheidl, A. G.; Ng, V. W. L.; Müller, P.; Takase, M. K.; Schrock, R. R.; Malcolmson, S. J.; Meek, S. J.; Li, B.; Kiesewetter, E. T.; Hoveyda, A. H. *Organometallics* **2012**, *31*, 455

[10] (a) Townsend, E. M.; Schrock, R. R.; Hoveyda, A. H. *J. Am. Chem. Soc.* **2012**, *134*, 11334. (b) Chapter 2 of this work

[11] Dickie, D. A.; MacIntosh, I. S.; Ino, D. D.; He, Q.; Labeodan, O. A.; Jennings, M. C.; Schatte, G.; Walsby, C. J.; Clyburne, J. A. C. *Can. J. Chem.* **2008**, *86*, 20.

[12] Ellison, J. J.; Ruhlandt-Senge, K.; Power, P. P. *Angew. Chem. Int. Ed. Engl.* **1994**, *33*, 1178.

[13] Yates, P.; Hyre, J. E. *J. Org. Chem.* **1962**, *27*, 4101.

[14] Lloyd-Jones, G. C.; Moseley, J. D.; Renny, J. S. *Synthesis* **2008**, *5*, 0661.

[15] Bishop, P. T.; Dilworth, J. R.; Nicholson, T.; Zubieta, J. *J. Chem. Soc. Dalton Trans.* **1991**, 385.

[16] Moseley, J. D.; Lenden, P. *Tetrahedron* **2007**, *63*, 4120.

[17] Jiang, A. J.; Zhao, Y.; Schrock, R. R.; Hoveyda, A. H. *J. Am. Chem. Soc.* **2009**, *131*, 16630.

[18] Flook, M. M.; Gerber, L. C. H.; Debelouchina, G. T.; Schrock, R. R. *Macromolecules* **2010**, *43*, 7515.

[19] Schrock, R. R.; Murdzek, J. S.; Bazan, G. C.; Robbins, J.; DiMare, M.; O'Regan, M. *J. Am. Chem. Soc.* **1990**, *112*, 3875.

[20] Singh, R.; Czekelius, C.; Schrock, R. R.; Müller, P.; Hoveyda, A. H. *Organometallics* **2007**, *26*, 2528.

[21] Hock, A.; Schrock, R. R.; Hoveyda, A. H.; *J. Am. Chem. Soc.* **2006**, *128*, 16373.

[22] Krieckmann, T; Arndt, S.; Schrock, R. R.; Müller, P. *Organometallics* **2007**, *26*, 5702.

[23] Tabor, D. C.; White, F. H.; Collier, L. W.; Evans, S. A. *J. Org. Chem.* **1983**, *48*, 1638.

[24] Flook, M. M.; Jiang, A. J.; Schrock, R. R.; Müller, P.; Hoveyda, A. H. *J. Am. Chem. Soc.* **2009**, *131*, 7962.

[25] McConville, D. H.; Wolf, J. R.; Schrock, R. R. *J. Am. Chem. Soc.* **1993**, *115*, 4413.

[26] Bazan, G. C.; Khosravi, E.; Schrock, R. R.; Feast, W. J.; Gibson, V. C.; O'Regan, M. B.; Thomas, J. K.; Davis, W. M. *J. Am. Chem. Soc.* **1990**, *112*, 8378.

[27] (a) Hamilton, J. G.; Ivin, K. J.; Rooney, J. J. *J. Mol. Catal. A* **1988**, *36*, 115. (b) Autenrieth, B.; Schrock, R. R. Manuscript in preparation.

[28] Sheldrick, G. M. SADABS; University of Göttingen: Germany, 1996.

[29] Sheldrick, G. M. *Acta Cryst.* **1990**, A46, 467.

[30] Sheldrick, G. M. *Acta Cryst.* **2008**, A64, 112.

[31] Müller, P. Crystallography Reviews **2009**, 15, 57.

[32] Sheldrick, G. M. TWINABS; University of Göttingen: Germany, 1996.

[33] Sheldrick, G. M. *CELL_NOW*; University of Göttingen: Germany, 2004.

Dept. of Chemistry, MIT, 32 Vassar St., 6-417, Cambridge, MA 02139 • 603-781-0095 • townse@mit.edu

Erik Townsend

EDUCATION

Aug 2009 - present	**Massachusetts Institute of Technology**	**Cambridge, MA**

Ph.D. Candidate in Department of Chemistry, Inorganic Division

- Completed coursework focused in inorganic chemistry and organometallic chemistry
- Explored catalyst synthesis and reaction methodology for olefin metathesis
- Supervisor: Prof. Richard R. Schrock

Aug 2006 – May 2009	**Rensselaer Polytechnic Institute**	**Troy, NY**

B.S. Department of Chemistry, *Summa cum Laude*

- ACS-accredited chemistry curriculum
- GPA: 4.0/4.0
- Rensselaer Medal Scholarship recipient in 2006

EXPERIENCE

Nov 2009 - Present	**Massachusetts Institute of Technology**	**Cambridge, MA**

Research Assistant – Schrock Group

- Designed catalysts for olefin metathesis using synthetic organometallic techniques
- Investigated the efficacy of olefin metathesis catalysts on solid supports
- Optimized molecular catalyst structure for highly stereoselective and chemoselective products
- Synthesized and characterized over 30 new organic and organometallic compounds
- Collected and analyzed characterization data including NMR (1D and 2D), GC/MS, and X-ray crystal structures

Aug 2009 - May 2010	**Massachusetts Institute of Technology**	**Cambridge, MA**

Teaching Assistant – Inorganic and Physical Chemistry Laboratory

- Aided faculty and staff in the development and administration of laboratory courses in inorganic and physical chemistry
- Guided and oversaw approximately 60 undergraduate students as they performed the experiments in these courses
- Received Chemistry Department Award for Outstanding Teaching in 2010

Aug 2008 - Dec 2008   **Rensselaer Polytechnic Institute**   **Troy, NY**

Teaching Assistant – Physical and Quantum Chemistry

- Supported students in their understanding of difficult concepts during office hours
- Helped the instructor evaluate and interpret student responses on homework and exams

Jun 2008 - Aug 2008   **Massachusetts Institute of Technology**   **Cambridge, MA**

Undergraduate Researcher/Amgen Scholar – Cummins Group

- Synthesized ligands and transition metal complexes with the goal of carbon dioxide activation
- Presented research at the Amgen Scholars poster session

Feb 2008 - May 2009   **Rensselaer Polytechnic Institute**   **Troy, NY**

Undergraduate Researcher – Dinolfo Group

- Explored click chemistry as a basis for layer-by-layer synthesis of dye-sensitized solar cells
- Employed electrochemical methods to quantitate surface coverage

LEADERSHIP/AWARDS

President – MIT Chemistry Graduate Student Committee (2013 - present)

- Organized volunteers for numerous departmental sports, socials and advice forums

Treasurer – Faith Lutheran Church, Cambridge, MA (2012 - present)

- Elected to manage income and expenses for a congregation of approximately 100 active members
- Oversaw the creation and execution of a $100,000 non-profit operating budget

MIT Environmental Health and Safety Representative (2010 - present)

- Inspected Schrock laboratory regularly to assist lab members with university safety policies
- Led a group-wide cleanup of an overcrowded and outdated chemical stockroom

Member – American Chemical Society (2008 - present)

Eagle Scout Award – Boy Scouts of America (2006)

Salutatorian – Portsmouth Christian Academy, Dover, NH (2006)

PUBLICATIONS AND PRESENTATIONS

Townsend, E. M.; Kilyanek, S. M.; Schrock, R. R.; Smith, S. J.; Müller, P.; Hoveyda, A. H. Synthesis of High Oxidation State Molybdenum Imido Heteroatom-Substituted Alkylidene Complexes. *Organometallics* **2013**, *32*, 4612-4617.

Townsend, E. M.; Highly Z-selective and Chemoselective Olefin Metathesis of 1,3-Dienes: Catalytic Studies and Exploration of Unusual Intermediates. Presented at the 245th Annual Meeting of the American Chemical Society, New Orleans, LA, 2013.

Townsend, E. M.; Schrock, R. R.; Hoveyda, A. H. Z-Selective Metathesis Homocoupling of 1,3-Dienes by Molybdenum and Tungsten Monoaryloxide Pyrrolide (MAP) Complexes. *J. Am. Chem. Soc.* **2012**, *134*, 11334-11337.

Yuan, J.; Townsend, E. M.; Schrock, R. R.; Goldman, A. S.; Müller, P.; Takase, M. K. Preparation of Tungsten-Based Olefin Metathesis Catalysts Supported on Alumina. *Adv. Synth. Catal.* **2011**, *353*, 1985-1992.

Fox, A. R.; Silvia, J. S.; Townsend, E. M.; Cummins, C. C. Six-Coordinate Uranium Complexes Featuring a Bidentate Anilide Ligand. *C. R. Chim.* **2010**, *13*, 781-789.

ACKNOWLEDGMENTS

I feel blessed and thankful to have had the opportunity to spend five years learning and working at MIT among some of the best chemists in the world. My advisor, Professor Schrock, is chief among them. He exhibits passion and determination on a daily basis while still maintaining a positive and comfortable working environment for the group. The intensity and emotional investment he displays toward research mirrors my natural approach to many aspects of life. If I were to start over again and choose a group, I would unquestionably choose the Schrock group again. I would like to sincerely thank Dick for being an excellent advisor. Other members of the Chemistry faculty have aided me in various important ways. Professors Lippard and Nocera gave me a strong theoretical foundation through their excellent teaching, and Professor Dincă lent me an ear and a helpful word on several occasions as my Thesis Committee Chair. Professor Cummins played perhaps the most crucial role of all, as it was my enjoyable experience in his group in the summer of 2008 that solidified my desire to pursue inorganic chemistry.

The members of the Schrock Group with whom I have been privileged to work are also deserving of praise. I thank Annie Jiang for passing along her glovebox and her wisdom to me during my first year. Keith Wampler, Brian Hanna, and Smaranda Marinescu were also very patient with my numerous and pestering questions. Yu Zhao and Jian Yuan both were essential to my learning process, and I particularly thank Jian for collaborations on the work in Chapter 1. Alex Lichtscheidl provided me with valuable advice and useful compounds. I thank Maggie Flook for helping me realize that doing things one's own way is not only allowable, but necessary to maintain sanity. I thank Laura Gerber for being a dependable friend and for sharing my feelings about throwing phones off bridges. Daniel Kozera and Janna Börner made up quite a crew, and I will miss the time we spent together. A big thanks goes to Stefan Kilyanek, who shared my office for three years, helped me with uncountable chemistry problems, and really knows how to develop a shtick. Jon Axtell is as solid as they come. Hyangsoo Jeong, thank you for being my best friend. More recently, I have received help, advice, and laughs from Matt Cain, Jakub Hyvl, Jeremy John, and Graham Dobereiner. Jakub has been a great laboratory companion, and has taught me a lot about cooking and Central Europe. Graham is an excellent burrito buddy and geographical guesser. Special thanks to Will Forrest and Benjamin Autenrieth for their assistance with the polymerizations in Chapter 4.

Outside lab, there are many people who provided me with invaluable support. Dan Ziegler was an awesome friend and roommate, and I was sad to see him move away. I'd like to thank all members of CGSC and my intramural sports teams as well. My friends from Faith Lutheran Church (especially Sean Carraher and Tim Stein) have been excellent companions and supporters for many years. I also thank God for the opportunities that He continues to give me; I feel blessed and humbled by the blessings in all areas of my life.

Finally, I would like to thank my family for everything. Thanks to Nanny, Big Poppa, Grandma, and Grandpa for being constant forces for good in my life. Thanks to Dad for being patient, steadfast, caring, and diligent at all times. Thanks to Mom for supporting me through the bad times and for talking to me on my way in to work. Thanks to Kile for sharing my conviction and attitude on life: keep on laying down the law! Thanks to Nikolas for being the best brother anyone could have. This thesis and all of the work that went into it is dedicated to you all.